Spring 2020

Lateral-Torsional Instability and Biaxial Flexure of Continuous GFRP Beams Including Warping and Shear Deformations

Waverly G. Hampton
Old Dominion University, whamp001@aol.com

LATERAL-TORSIONAL INSTABILITY AND BIAXIAL FLEXURE OF CONTINUOUS GFRP BEAMS INCLUDING WARPING AND SHEAR DEFORMATIONS

By

Waverly G Hampton

B.S.C.E. August 1983, Old Dominion University

M.C.E. December 1999, Old Dominion University

A Dissertation Submitted to the Faculty of Old Dominion University in Partial Fulfillment of the Requirements for the Degree of

Doctor of Philosophy
Civil Engineering
Old Dominion University
May 2020

Approved by:

Zia Razzaq (Committee Chair)

Gene J. Hou (Member)

Mojtaba B. Sirjani (Member)

Shahin N. Amiri (Member)

ABSTRACT

LATERAL-TORSIONAL INSTABILITY AND BIAXIAL FLEXURE OF CONTINUOUS GFRP BEAMS INCLUDING WARPING AND SHEAR DEFORMATIONS

Waverly G Hampton

Old Dominion University, May 2020

PhD Advisor, Dr. Zia Razzaq

This dissertation presents an experimental and theoretical study of the lateral-torsional instability and biaxial flexure of Glass Fiber Reinforced Polymer (GFRP) beams including warping and shear deformation effects. The theoretical analysis is based on three simultaneous differential equations of equilibrium with new terms added to account for shear deformation effects. To solve these equations, algorithms based upon a central finite-difference approach are then developed. The experimental study is conducted on a series of single- and multi-span beams subjected to concentrated loads. The predicted beam behavior agreed well with that observed experimentally. The investigation revealed that the ASCE-LRFD Prestandard for pultruded GFRP beams can result in seriously unconservative buckling load predictions. The same is found for biaxially loaded beams which can develop very large induced warping normal stresses currently unaccounted for by the ACSE-LRFD Prestandard. A new lateral-torsional buckling load equation is presented which accounts for shear deformation effects.

ACKNOWLEDGEMENT

My deepest appreciation and sense of gratitude to my research advisor and committee chair, Dr. Zia Razzaq, Professor, Department of Civil and Environmental Engineering, ODU, for his continuous guidance, encouragement, and support throughout my studies at Old Dominion University.

Thanks to the Civil and Environmental Engineering Department and other Old Dominion University team members including the Batten Model Shop for their cooperation and patience.

Also, I would like to acknowledge my mother, Catherine Spratley, and Heavenly Father, the Creator of the heavens and earth.

TABLE OF CONTENTS

FIGURES

TABLES

CHAPTER 1

INTRODUCTION

1.1 Prelude

Pultruded Glass Fiber Reinforced Polymer (GFRP) structural products are gaining significance particularly in practical applications where humidity, corrosion, and magnetic interference become concerns. The GFRP products are also much lighter than steel, concrete, wood, and other traditional construction materials. Although structural design specifications based on traditional materials are fairly well-developed, those for pultruded GFRP products are still evolving.

A unified design standard for GFRP structural products is needed. To this end, the American Society of Civil Engineers (ASCE) has published a Load and Resistance Factor Design (LRFD) Prestandard for pultruded GFRP structural members. When evaluating failure modes for flexure design, the ASCE-LRFD Prestandard includes lateral-torsional buckling without shear deformation effects. However, shear effects which typically are considered negligible can be significant when analyzing GFRP beam behavior. This dissertation presents detailed analysis and results of an experimental investigation to study the effects of shear deformation on the lateral-torsional buckling of GFRP beams as well as biaxially bent beams which can also develop significant induced warping stresses.

Beams in practical structures can also be subjected to biaxial bending which creates induced torsional effects such as those associated with Saint Venant and warping stresses. For example, biaxial bending can result from a combination of vertical loads simultaneously with horizontal wind loads. The proposed ASCE-LRFD standard does not account for induced torsional effects for biaxial bending thereby resulting in unconservative stress estimates. The current dissertation also addresses this issue and probes into the warping effects.

The analysis is based on three simultaneous differential equations of equilibrium modified to include shear deformation effects, with applicable boundary conditions. Both single-span and multi-span GFRP beams are analyzed to predict lateral-torsional buckling loads and biaxial bending response. To this end, a fourth order central difference approach is used and algorithms developed to investigate beam behavior both with and without shear effects. The analysis verified with a series of laboratory experiments on single- and multi-span beams.

1.2 Literature Review

A brief review of the existing literature related to lateral-torsional buckling and biaxial bending of beams in general and key developments for GFRP beams in particular is presented in this section. The governing system of differential equations for lateral-torsional buckling of beams without shear deformation effects are summarized by Timoshenko and Gere [21] and Galambos [1]. A variety of solutions to these differential equations have been developed in the past by these authors as well as others such as Salvadori [23], Chen [7], Razzaq, and Galambos [22]. The American Institute of Steel Construction beam buckling equations are based on such analyses [8].

However, the magnitude of the shear strains, horizontal deflections, and torsional rotations which are incurred when using slender fiber reinforced plastic beams is such that premature elastic lateral-torsional failure may be the primary failure mode and must be considered during each analysis. To this end, Sirjani, Bondi, and Razzaq [9], and [10] have written articles on flexural torsional response of FRP I beams. Razzaq, Prabhakaran, and Sirjani [11] presented LRFD approaches for channels, and Sirjani, and Razzaq [12] presented an LRFD approach for I beams recognizing the need to have some guidelines and ultimately one design guide for pultruded members. Presently, the ASCE [13] is promoting a LRFD design guide for pultruded members which will be a valuable tool for predicting of failure mode for GFRP beams. However, lateral torsional buckling predictions do not include shear deformations.

Knorowski [14] wrote a thesis on the behavior of FRP beams subject to biaxial bending using finite difference. She uses the aforementioned equations of equilibrium by Galambos but does not include shear deflection. Peck [15] wrote a Master's project on the behavior and strength of three span FRP beams under a midspan point load. While the paper addresses Timoshenko beam deflection and gets excellent results, it does not include lateral-torsional buckling analysis in any detail. Weaver [18] presents an excellent finite element grid analysis approach concerning applied torsional loads, but it is of no significance concerning induced lateral-torsion.

A fourth order central difference approach proves expedient when solving the partial differential equations resulting from modification of the equations of equilibrium to include a shear deflection term as defined by Timoshenko.

1.3 Problem Statement

This dissertation deals with lateral-torsional instability and biaxial bending of GFRP beams including shear deformations. The study involves modifications in three simultaneous differential equations of equilibrium including Saint Venant and induced warping effects, and subsequent solutions based on a fourth-order central finite difference approach. Laboratory experiments are conducted on single, two, and three span GFRP beams subjected to in-plane gradually increasing quasi-static loading eventually resulting in lateral-torsional instability. An experiment is also conducted on a three-span beam under biaxial loading. Figure 1 (a) shows a typical GFRP I-section beam in the x, y, and z coordinate system**,** and subjected to concentrated loads, P_x and P_y. Figure 1 (b) shows the dimensions of the I-section. Figure 1 (c) shows the position of a typical section in the displaced position. In this figure, u and v are respectively, the vertical (in-plane) deflection v, the horizontal (out-of-plane) deflections u, and the angle of twist, ϕ.

The problems posed herein include the prediction of the behavior of GFRP beams, experimental verification of the theoretical results, a comparison of the results to those based on ASCE-LRFD Prestandard, and proposed new guidelines for GFRP beams.

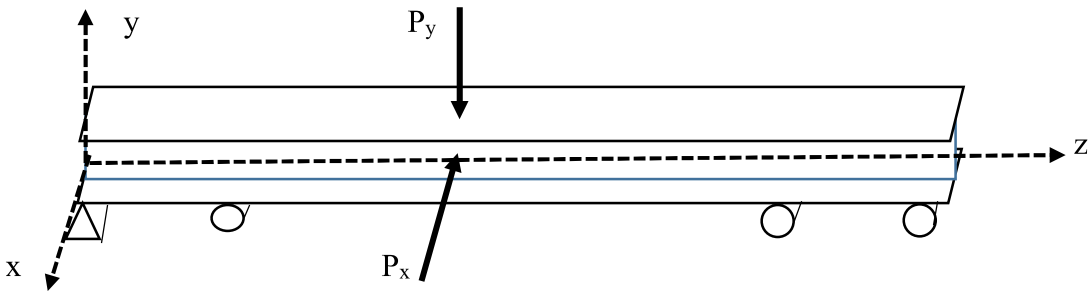

a. Continuous GFRP Beam with Biaxial Loading

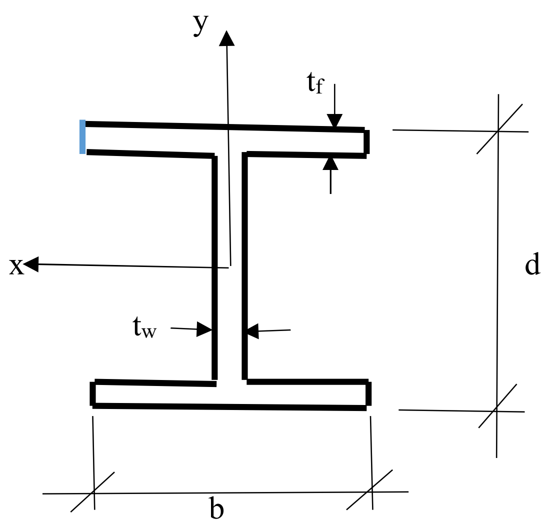

.b. Beam Cross Section

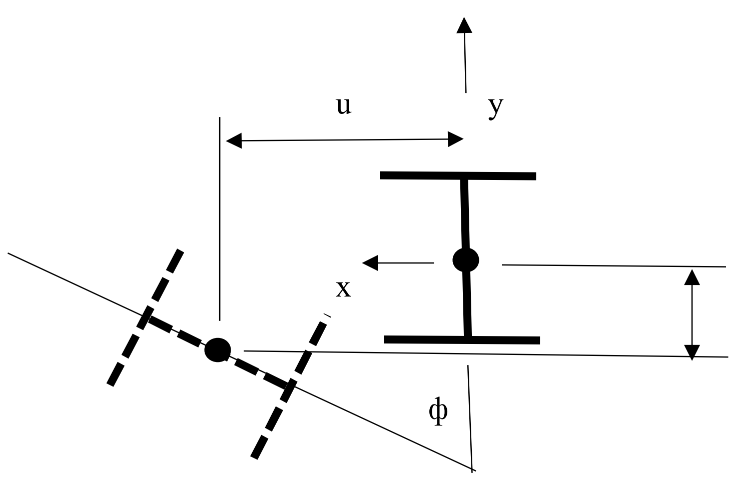

c. Cross Section in Deflections

Figure 1. Schematic of Problem

1.4 Objective and Scope

The main objective of this research is to conduct investigations, theoretical analyses and laboratory experiments, on GFRP continuous I beams. The specific objectives include:

1. To experimentally check the validity of the analysis including and not including shear deformation effects.

2. To compare the experimental beam failures and modes with those predicted using the ASCE-LRFD Prestandard and with lateral-torsional critical buckling loads predicted from analyses.

3. Propose generic design equations and check their validity analytically and experimentally foreach investigation.

Nine setups used for investigations are shown in Figures 2, 3, and 4.

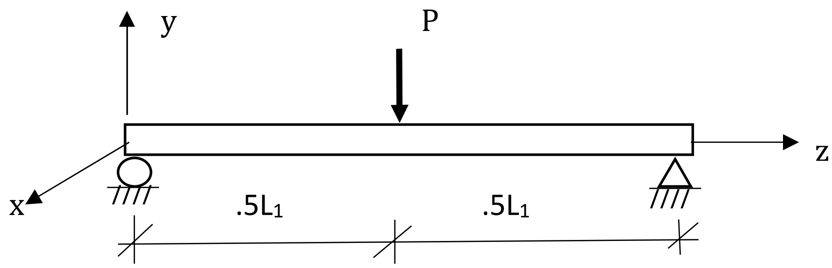

a. 4 in. x 4 in. x ¼ in. I Beam. Midspan Load

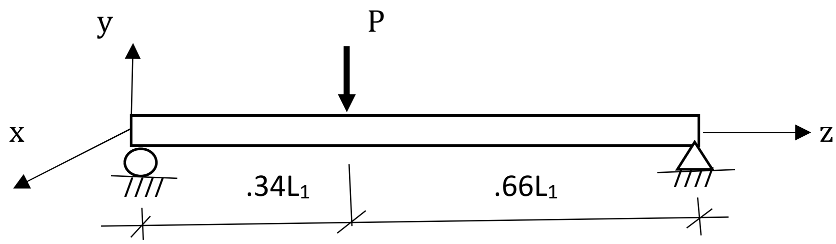

b. 3 in. x 3 in. x ¼ in. I Beam. Off Center Load

Figure 2. Single Span GFRP I Beams with Point Loads

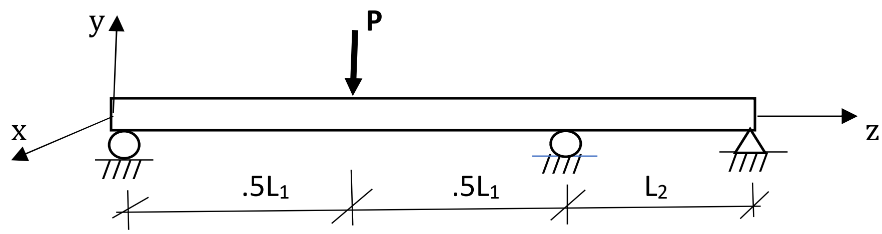

a. 4 in. x 4 in. x ¼ in. I Beam. Midspan Load. Long Span

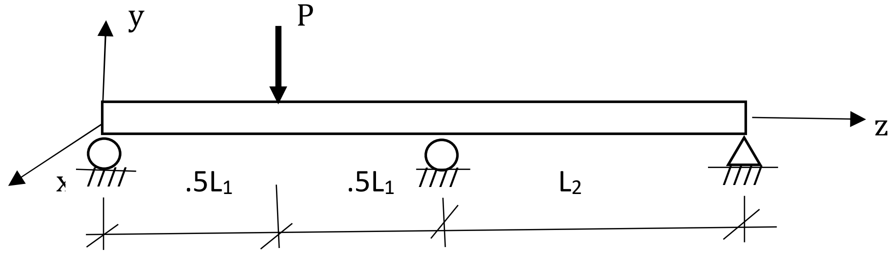

b. 3 in. x 3 in. x ¼ in. I Beam. Midspan. Near Equal Span

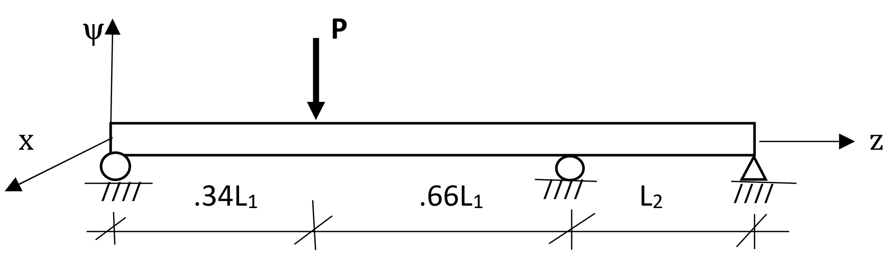

c. 3 in. x 3 in. x ¼ in. I Beam. Off Center Load

Figure 3. Two Span GFRP I Beams with Point Loads

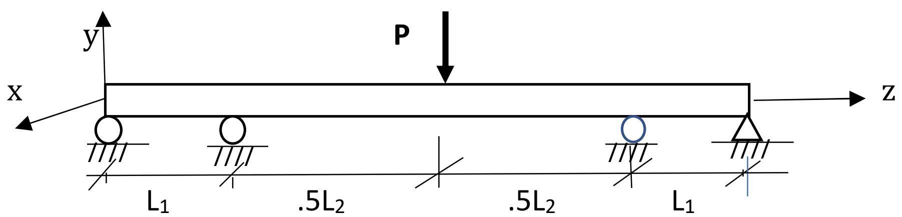

a. 4 in. x 4 in. x ¼ in. I Beam. Midspan Load. Center Span

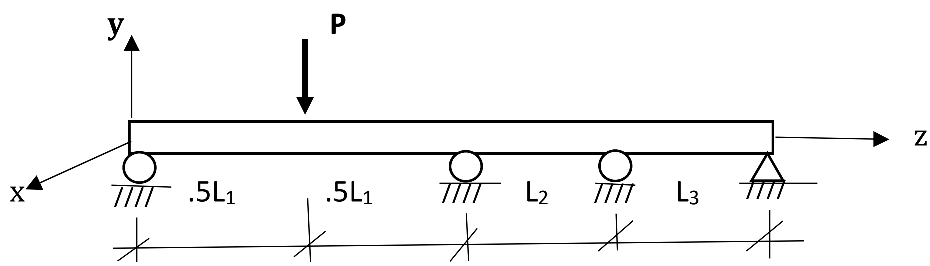

b. 3 in. x 3 in. x ¼ in. I Beam. Midspan. Outside Span

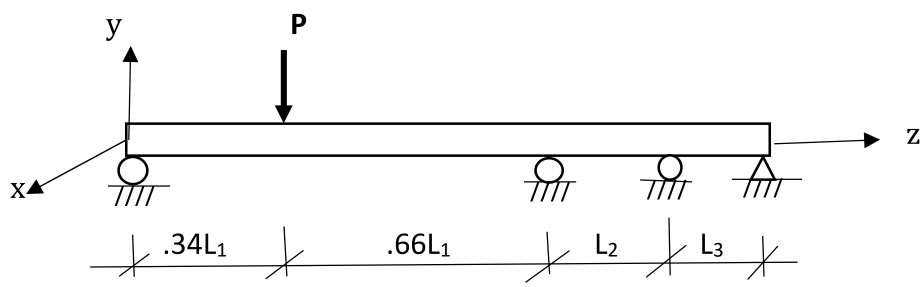

c. 3 in. x 3 in. x ¼ in. I Beam. Off Center

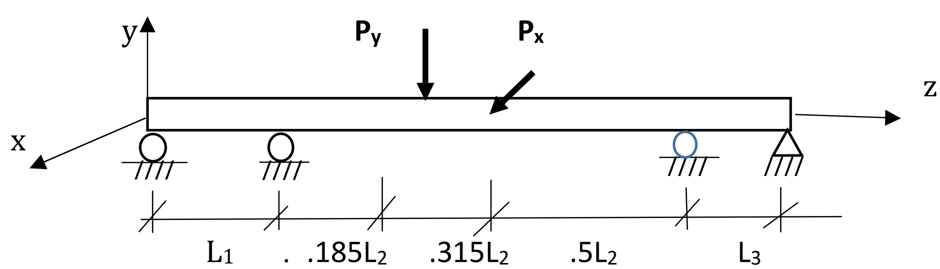

d. 4 in. x 4 in. x ¼ in. I Beam. Off Ctr. Biaxial

Figure 4. Three Span GFRP I Beams with Point Loads

Table 1 provides a list of investigations including span dimensions for each investigation shown in Figures 2, 3, and 4. Nine investigations are presented to insure a population size sufficient to define and evaluate the objectives without prejudice. To this end, beam lengths, cross sections, boundary conditions, and locations of loads are varied. 3 in. x 3 in. x ¼ in. and 4 in. x 4 in. x ¼ in. cross sections are used in our investigations; beams of one to three span are tested to evaluate pinned-pinned, pinned-fixed, and fixed-fixed end conditions on targeted spans; and loads are placed at center or off center of targeted spans. L_3

Table 1. Tabular Summary of Beam Test with Point Loads

Test No.	Beam Type	L_1 (in.)	L_2 (in.)	L_3 (in.)	Figure
1	Single Span	75.00			2a
2	Single Span	79.50			2b
3	Two Span	75.00	30.00		3a
4	Two Span	54.00	51.00		3b .
5	Two Span	79.50	25.50		3c
6	Three Span	15.00	75.00	15.00	4a
7	Three Span	54.00	25.50	25.50	4b
8	Three Span	79.50	15.00	10.50	4c .
9	Three Span	13.50	81.00	10.50	4d

1.5 Assumptions and Conditions

1. Angle of twist is of equal value for entire cross section. Cross sections do not remain planar.

2. Shear effects are not considered negligible

3. Material obeys Hooke's law in elastic range. Materials act homogeneous.

4. Shear stress distribution within plane of cross section is also distributed along adjacent axial planes.

5. For time being, there are no residual stresses in the FRP beam.

6. Beam or loading imperfections and eccentricities exists creating torsional loads as well.

7. Beam sections are thin walled.

8. Small deflection theory is valid.

9. Beam ends are simply supported.

10. Member end warping is unrestrained.

11. Fiberglass reinforced plastic beams are a layered product and will occasionally show imperfections such as delamination. Will look beyond these imperfections to categorize curves and determine critical buckling values from lab experiments consistent with moment versus deflection curve relationships discussed by Galambos.

CHAPTER 2

THEORY AND CURRENT PRACTICE

This chapter presents detailed theoretical formulations for the problems briefly outlined in Section 1.3 of this dissertation. The formulations are in the form of coupled simultaneous differential equations governing the translational and rotational response of GFRP members when subjected to uniaxial or biaxial loads. Finite difference based numerical solutions to the governing differential equations are then presented for each of the nine types of loading and support conditions shown in Figures 21 – 2b, 3a – 3c, and 4a – 4d. Relevant provisions of the ASCE-LRFD Prestandard are also summarized and used for numerical comparisons with the results obtained using the analysis presented here-in which accounts for shear deformations.

Governing equations for biaxial bending of simply supported beams loaded in-plane are[1]:

$$B_x v'' - \phi(M_y) = -M_x \qquad [1a]$$

$$B_y u'' - \phi(M_x) = -M_y \qquad [1b]$$

$$C_w\phi''' - (C_t + K)\phi' + u'(-M_x) - v'(M_y) - v/L (M_{y1} + M_{y2}) - u/L (M_{x1} + M_{x2}) = 0 \qquad [1c]$$

In these equations:

$B_x = EI_x$ or Modulus of Elasticity times the Moment of Inertia about x axis.

M_x = Moment about the x axis.

M_{x1} = Moment about X axis at right end of element

M_y = Moment about the y axis

M_{y1} = Moment about y axis at bottom of element

M_{y2} = Moment about y axis at top of element

v = vertical deflection

u = horizontal deflection.

ϕ = angle of twist.

$C_w = EI_w$ or Warping Constant, Modulus of Elasticity times Warping Moment of Inertia.

C_t = Saint Venant Torsional Stiffness.

K= $M_x\beta$ = cross sectional constant that equals zero for doubly symmetric cross sections. When dealing with long spans and slender members, shear deflection can be just as significant as deflection caused by bending concerning failure. As such, the shear moment, M_s, will be included for beams under bilateral bending. Use of this term will allow accurate determination of horizontal deflections and out of plane rotations. This is accomplished by replacing M_x in the above equations by M_{tx} where

$$M_{tx} = M_x + M_s \text{ and } M_s = Z_w P_s \qquad [2]$$

Timoshenko defined the shear moment to be placed on the conjugate beam as a point load and equal to

$$P_s = (\alpha EI_x/AG) P_2 \qquad [3]$$

where "α" is a numerical factor related to the cross section's ability to carry shear; A is the area of the cross section; G is the shear modulus; and P_2 is the point load located on the beam when including shear. P_1 is the point load on the beam when ignoring shear moment. Z_w is a factor discussed later in this section.

We cannot place the shear moment directly on the real beam because it is imaginary; however, we can place it on the conjugate beam and determine a relationship between the load P_1 without shear and the load P_2 with shear using the deflection values. From this relationship, we can define the moment relationships. This will be demonstrated for each investigation.

Next. The governing equations for biaxial bending and torsion are modified to include the shear moment, Ms, and take the following form:

$$B_x v'' - \phi (M_{ty}) = - M_{tx} \qquad [4a]$$

$$B_y u'' - \phi (M_{tx}) = - M_{ty} \qquad [4b]$$

$$C_w\phi''' - (C_t + K)\phi' + u'(- M_{tx}) - v' (M_{ty}) - v/L (M_{ty1} + M_{ty2}) - u/L (M_{tx1} + M_{tx2})$$

$$+ P(y_o/2) \phi_0 = 0 \qquad [4c]$$

The term $Py_o/2$ accounts for the load being placed on the top or bottom of the beam rather than at its centroid, and y_o is the distance from the centroid to the point of load.

The solution approach taken herein is a fourth order central difference approach. Though it is a finite difference approach, it is as accurate as any other finite element approach. Error is minimized by taking a forward difference approach and a backward difference approach and combining them. The following terms from a fourth order central difference approach: [16] will be used:

$f'(x_o) = (-f_2 + 8f_1 - 8f_{-1} + f_{-2}) /12h$ [5a]

$f''(x_o) = (-f_2 + 16f_1 -30f_o + 16f_{-1} - f_{-2}) /12h^2$ [5b]

$f'''(x_o)= (-f_3 + 8f_2 -13f_1+ 13f_{-1} - 8f_{-2} + f_{-3}) /8h^3$ [5c]

Shear moments and bending moments in the modified equilibrium equations may be determined from shear and bending moment diagrams. Thus, these terms are given loads and do not have to be differentiated. Unknowns to be differentiated are vertical and horizontal deflections and the out of plane rotations, u, v, and ϕ, respectively. Therefore, there are three equations and three unknowns related to each system of equations for each segment of the beam being differentiated. End boundary conditions and relationships between segments will be clearly defined by the global system of equations being solved linearly.

Central difference terms related to vertical deflection consist of

$v = vo$ [6a]

$v' = [-v_2 + 8v_1 - 8v_{-1} + v_{-2}]/12h$ [6b]

$v'' = [-v_2 + 16v_1 -30v_o + 16v_{-1} - v_{-2}]/12h^2$ [6c]

Difference terms related to the horizontal deflection consist of

$u = u_o$ [7a]

$u' = [-u_2 + 8u_1 - 8u_{-1} + u_{-2}]/12h$ [7b]

$u''=[-u_2 + 16u_1 - 30u_o + 16u_{-1} - u_{-2}]/12h^2$ [7c]

Difference terms related to the out of plane rotation are

$\phi = \phi_o$ [8a]

$\phi' = (-\phi_2 + 8\phi_1 - 8\phi_{-1} + \phi_{-2}) /12h$ [8b]

$\phi'' = (-\phi_2 + 16\phi_1 - 30\phi_0 + 16\phi_{-1} - \phi_{-2}) /12h^2$ [8c]

$\phi''' = (-\phi_3 + 8\phi_2 - 13\phi_1 + 13\phi_{-1} - 8\phi_{-2} + \phi_{-3}) / 8h^3$ [8d]

Next, these terms are substituted into our modified lateral-torsion equations to obtain

$B_x [-v_2 + 16v_1 -30v_o + 16v_{-1} - v_{-2}]/12h^2 - \phi_o (M_{ty}) = - M_{tx}$ [9a]

$B_y [-u_2 + 16u_1 - 30u_o + 16u_{-1} - u_{-2}]/12h^2 - \phi_o (M_{tx}) = - M_{ty}$ [9b]

$C_w(-\phi_3 + 8\phi_2 - 13\phi_1 + 13\phi_{-1} - 8\phi_{-2} + \phi_{-3}) / 8h^3 - (C_t + K) (-\phi_2 + 8\phi_1 - 8\phi_{-1} + \phi_{-2}) /12h + [-u_2 + 8u_1 - 8u_{-1} + u_{-2}]/12h (- M_{tx}) - [-v_2 + 8v_1 - 8v_{-1} + v_{-2}]/12h (M_{ty}) - v_o/L (M_{ty1} + M_{ty2}) - u_o/L (M_{tx1} + M_{tx2}) + P(y_o/2) \phi_0 = 0$ [9c]

Solving the above finite difference equations simultaneously using a stiffness matrix approach, vertical, horizontal, and lateral deflections along the beam are determined.

To solve for lateral-torsional buckling, replace the first two lower order equations with their fourth order equations and set the right side of each equation equal to zero. This also will be demonstrated for each investigation. LTB equations typically used by Galambos and ASCE in practice for solving P_{cr} are

$EI_y u^{IV} + M_x\phi'' + 2M'_x \phi' = 0$ [10a]

$EI_w \phi^{IV} - (GKt + M_x\beta_x) \phi'' - M'_x\beta_x \phi' - M_x u'' = 0$ [10b]

Because shear is included in the modified solution, equations are coupled and we will be including equilibrium equation for vertical deflection in our discussion. It is

$EI_x v^{IV} + M_{ty}\phi'' + 2M'_{tx} \phi' = M_{tx}$ [11]

Including additional terms into the third order lateral buckling equation and taking its fourth derivative, one obtains =

$C_w\phi^{IV} – (GK_t)\phi'' + u''(- M_{tx}) - u'(M'_{tx}) – u/L (M'_{tx1} + M'_{tx2}) – u'/L (M_{tx1} + M_{tx2})$

$+ P(y_o/2) \phi'_0 = 0$ [12]

Note: When considering shear, M_x in the equation becomes M_{tx} where $M_{tx} = M_s + M_x$

Given a point load on a simple beam, Timoshenko asked us to place a shear moment on the conjugate beam as a point load as shown in Figure 5. He further noted that a real point load is actually distributed over some small distance e and creates the moment point load. This point moment distributed over an eccentric distance e is in k-in. The resultant of the shear moment when placed on the conjugate beam is P_s given by:

$P_s – \alpha P_2 EI_x/AG$

P_2 is applied point load when including Timoshenko shear term. P_1 is applied point load when not including shear term. P_2 and P_1 can be solved using a central difference model and determining the buckling limit with and without shear being considered, respectively. Once have values P_1 and P_2, introduce factor SF where

$SF=P_2/P_1.$

Rather than setting up two central difference models to determine P_1 and P_2, propose calculate SF and use it with P_1 or P_2 as needed. P_1 and P_2 relationship changes with conjugate beam and loading.

Let M_{1xd} = Bending moment diagram without shear and

M_{2xd} = Bending moment diagram with shear. On the conjugate beam,

$M_{1xd} = M_{2xd} + M_s$.

For a single span beam with a point load in the middle,

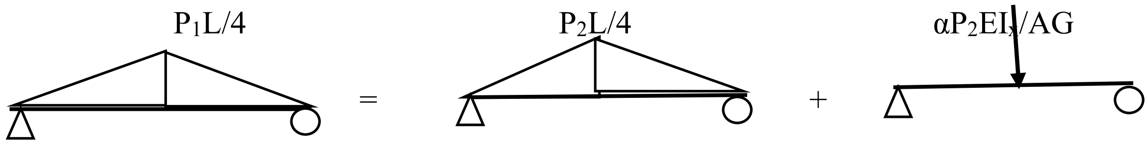

Figure 5. Moments on Conjugate Beam

$(½) P_1L/4 (L/2) + (½) P_1L/4 (L/2) = (½) P_2L/4 (L/2) + (½) P_2L/4 (L/2) + \alpha P_2EI_x/AG$ [14]

Where resultants are

$R_1 = (½) P_1L/4 (L/2)$ [15]

$R_2 = (½) P_1L/4 (L/2)$ [16]

$R_3 = (½) P_2L/4 (L/2)$ [17]

$R_4 = (½) P_2L/4 (L/2)$ [18]

Rearranging [14],

$SF = P_2 /P_1 = (L^2/8) / [(L^2/8) + \alpha EI_x/AG]$ [19]

Use of this factor will be demonstrated throughout.

Knowing the relationship between P_1 and P_2, we can define the value of M_s in the moment equation at midspan. Timoshenko defined the shear moment to be applied to the conjugate beam as $P_s = P_2(\alpha EI_x/AG)$ [20]

The moment at midspan of real beam can be shown to be

$M=P_1(L/4) = M_t = M_{bending} + M_{shear} = P_2(L/4 + Z_w(\alpha EI_x/AG))$ [21]

concerning moment without shear and moment with shear, respectively. Rearranging

$(L/4)/SF = (L/4 + Z_w(\alpha EI_x/AG))$; [22]

and $Z_w = (((L/4)/SF) – L/4)/ (\alpha EI_x/AG)$ [23]

2.1 Stability Analysis for Simply Supported Beam with Point Load Midspan

Numerical formulations for the critical buckling load and translational and rotational deflections are presented for Investigation 1 in this section. Numerical methods formulated are sine approximation and fourth order central difference. Critical buckling load as determined from the ASCE-LRFD Prestandard is also presented. Beam loading with boundary conditions, moments on conjugate beam, and shear deflection are defined in Figure 6.

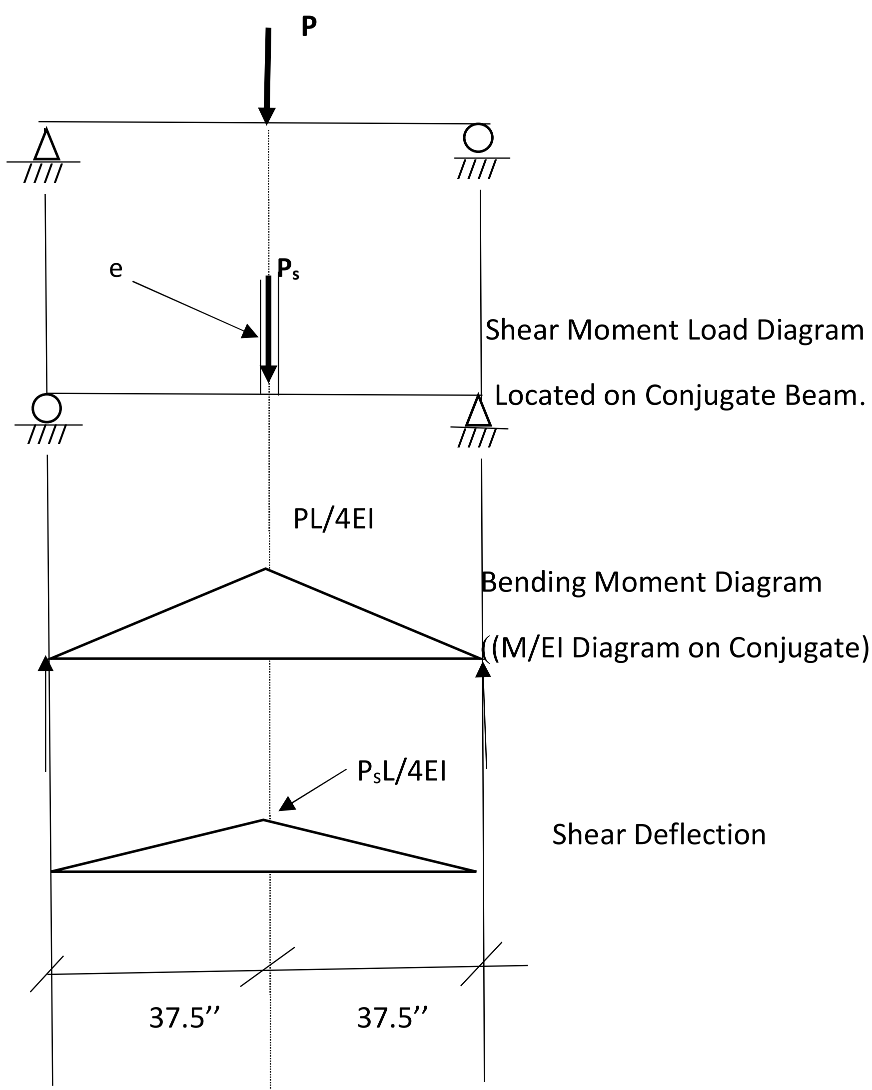

Figure 6. Investigation 1: Deflection Diagrams

2.1.1 Semi-analytic Solution Including Shear Deformation

When $M_y = 0$ and boundary conditions at ends are pinned-pinned, the equilibrium equations for the simple beam in Figure 4 are

$B_x v'' = - M_{tx}$ [24]

$B_y u'' - M_{tx}\,\phi = 0$ [25]

$C_w \phi''' - (C_t + \beta)\,\phi' - M_{tx}\,(u') = 0$ [26]

Where $M_{tx} = M_{bending} + Z_w P_2\,(\alpha EI_x/AG)$; without shear $M_{tx} = M_{bending} = M_x$.

Let

$\phi = A\sin(n\pi/L)z$ [27]

$v = B\sin(n\pi/L)z$ [28]

And $u = C\sin(n\pi/L)z$ [29]

For

$\phi = A\sin(n\pi/L)z$

$\phi' = (n\pi/L)\,A\cos(n\pi/L)z$ [30]

$\phi'' = -(n\pi/L)^2\,A\sin(n\pi/L)z$ [31]

$\phi''' = - (n\pi/L)^3\,A\cos(n\pi/L)z$ [32]

$v = B\sin(n\pi/L)z$

$v' = (n\pi/L)\,B\cos(n\pi/L)z$
[33]

$v'' = -(n\pi/L)^2\,B\sin(n\pi/L)z$ [34]

$u = C\sin(n\pi/L)z$

$u' = (n\pi/L)\,C\cos(n\pi/L)z$ [35]

$u'' = -(n\pi/L)^2\,C\sin(n\pi/L)z$ [36]

Substituting these terms into the aforementioned equilibirium equations we get

$-B_x\,(n\pi/L)^2\,B\sin(n\pi/L)z = M_{tx}$ [37]

$B_y(n\pi/L)^2\,C\sin(n\pi/L)z + M_{tx}\,A\sin(n\pi/L)z = 0$ [38]

$-C_w(n\pi/L)^3\,A\cos(n\pi/L)z - (C_t + \beta)\,(n\pi/L)\,A\cos(n\pi/L)z - M_{tx}\,((n\pi/L)\,C\cos(n\pi/L)z) = 0$ [39]

Simplify we get,

$-B_x\,(n\pi/L)^2\,B\sin(n\pi/L)z = M_{tx}$ [40]

$-B_y(n\pi/L)^2\,C - M_{tx}\,A = 0$ [41]

$-C_w(n\pi/L)^3\,A - (C_t + \beta)\,(n\pi/L)\,A - M_{tx}\,((n\pi/L)\,C = 0$ [42]

where M_{tx} is taken at a location z from the end of the beam. In our case, it will be midspan. Solving the determinant of the equations, we get the following lateral-torsional buckling equation:

$[-M_{cr}^2\,(n\pi/L)^3] + [B_y\,(n\pi/L)^4\,]\,[C_w\,(n\pi/L)^3 + C_t\,(n\pi/L)] = 0$ [43]

Solving the determinant and using the loads of the equations, we can now solve for ϕ, v, and u. This gives us the ability to plot a second finite element approach.

Note: The term $Py_o/2$ results in an end moment and can not be considered in a sine approximation.

Problem 2.1.1. Lab Investigation 1

Given: 4” x 4” x ¼” fiberglass reinforced plastic beam in Figure 4. L = 75”. E=2997 ksi.

I_x = 7.935 in.4. G = 450 ksi. I_y = 2.67 in.4. k_t = .0612. A = 2.85 in^2. I_w = 9.375 $in.^4$. SF = .92

Find: Buckling limit and vertical deflections with shear. Use Semi-analytic approach.

The equilibrium equations using sine approximation with pinned-pinned ends are

$-B_x\,(n\pi/L)^2\,B\sin(n\pi/L)z = M_{tx}$ [40]

$-B_y(n\pi/L)^2\,C - M_{tx}\,A = 0$ [41]

$-C_w(n\pi/L)^3\,A - (C_t\,)\,(n\pi/L)\,A - M_{tx}\,((n\pi/L)\,C = 0$ [42]

Simplifying for buckling calc where determinant equals zero, we get,

$B_x\,(n\pi/L)^2\,B = 0$

$-B_y(n\pi/L)^2\,C - M_{tx}\,A = 0$

$-C_w(n\pi/L)^3\,A - (C_t\,)\,(n\pi/L)\,A - M_{tx}\,((n\pi/L)\,C = 0$

Since M_{tx} is on right side and right side of equation [40] is zero, it becomes uncoupled. Solution to equations [41] and [42] for buckling determinant is

$$M_{tx} = [\ B_y\ (C_w(\pi/L)^4 + C_t\ (\pi/L)^2\ ]^{.5} \qquad [43]$$

Plugging in the given, we have

M_{tx} = 32.87 kip-in.

$M_{tx} = M_{xbending} + M_{shear}$; $P_2/P_1 = .92$

$M_{tx} = P_1L/4$ without shear, so P_1 = 1.76 kips

P_2 = .92 (1.76) = 1.62 kips. Load P_1, kips, M_{tx} (k-in.)

For vertical deflection calc, we can use determinant solution of

$$\frac{\begin{vmatrix} a_1 & d_1 & c_1 \\ a_2 & d_2 & c_2 \\ a_3 & d_3 & c_3 \end{vmatrix}}{\begin{vmatrix} a_1 & b_1 & c_1 \\ a_2 & b_2 & c_2 \\ a_3 & b_3 & c_3 \end{vmatrix}} = v_{w/s} \qquad [44]$$

where the column of d terms are load values substituted into the coefficient column for the unknown vertical deflections. Note that $d_2 = M_{tx}/\sin(n\pi z/L)$, and d_1 and d_3 equal zero. Plugging in values, the solution is

$$v_{w/s} = \frac{(M_{tx}{}^3(n\pi/L)/\sin(n\pi z/L)\ -\ (C_w(n\pi/L)^3\ +\ C_t(n\pi/L)B_y(n\pi/L)^2\ (M_{tx}/\sin(n\pi z/L)}{(M_{tx}{}^2(n\pi/L)^3(B_x)\ -\ C_w(n\pi/L)^3\ +\ C_t(n\pi/L)B_xB_y(n\pi/L)^4)} \qquad [45]$$

So, to find the vertical deflections with shear, we can use P_2 load values used in lab. Calculate P_1, then calculate M_{tx}. P_2 equals 1.55 kips at the buckling limit calculated using this approach. M_{tx} = 32.87 k-in. and vertical deflection are shown in Table 2.

Table 2. Vertical Deflection. Investigation I. Semi-Analytic, With Shear Load

Load P_2, kips	Load P_1, kips	M_{tx}, k-in.	Vert. Deflection, in.
0.0	0.0	0.0	0.0
.0141	.0159	.2984	.0071
.1292	.1461	2.739	.0657
.3149	.3559	6.674	.1598
.4913	.5563	10.412	.2493
.6858	.7752	14.536	.3480
.8787	.9932	18.623	.4458
1.0271	1.161	21.768	.5211
1.3618	1.539	28.861	.6909
1.6124	1.822	34.173	.8181
1.7509	1.979	37.108	
1.8316	2.070	38.818	

2.1.2 Semi-analytic Solution Without Shear Deformation

The semi-analytic approach without shear deformation is same as aforementioned semi-analytic approach with shear except $M_s = 0$. $M_{tx} = M_x = M_{bx}$. Lab values are P without shear values, P_1.

Problem 2.1.2. Lab Investigation 1

Given : 4"x 4" x ¼" fiberglass reinforced plastic beam in Figure 4. L = 75" . E = 2997 ksi.

I_x = 7.935 in.^{4}. G = 450 ksi. I_y = 2.67 in.^{4}. k_t = .0612. A = 2.85 in^2. I_w = 9.375 in. ^{4}.

Find: Buckling limit and vertical deflections without shear.

For vertical deflections without shear, we simply do not apply the shear moment to the beam. In other words M_s = 0.0 and $M_{tx} = M_{xbending}$. Procedure is exactly same as calculating critical load and vertical deflection outlined in previous problem which included shear. However, P loads from lab experiments are P_1 not P_2. Therefore, $M_{cr} = P_1L/4$ for this problem. See tabulated vertical deflection values for this problem in Table 3.

P_1 equals 1.75 kips at the buckling limit calculated using this approach. M_{tx} = 32.87 k-in. See Table 3.

Table 3. Vertical Deflection. Investigation 1. Semi-Analytic. W/o Shear

Load P_1, kips	M_{tx} or $M_{bending}$, k-in.	Vert. Deflection, in.
0.0	0.0	0.0
.0141	.2640	.0063
.1292	2.423	.0580
.3149	5.904	.1413
.4913	9.212	.2205
.6858	12.86	.3079
.8787	16.48	.3944
1.027	19.26	.4610
1.362	25.53	.6113
1.612	30.23	.7238
1.751	32.83	.7859
1.83	34.34	.8222

2.1.3 Central Difference Solution With Shear Deformation

For this approach, we use the three central difference governing equations previously developed to determine vertical, horizontal, and lateral deflection values along the beam. $M_x = M_{tx}$. For this approach, we follow the instructions of Timoshenko to the letter. We simply place the shear moment point load on the conjugate beam. The ends of the conjugate beam are pinned-pinned upon the length of an element or eccentricity, the shear moment M_s value varies from model to model. $P_s = P_2\ \alpha EI_x/(eAG)$ where e is the eccentricity or length of the element. With shear, $M_{tx} = M_{bending} + M_s$ on the conjugate beam.

Problem 2.1.3. Lab Investigation 1

Given: 4" x 4" x 1/4" fiberglass reinforced plastic beam in Figure 4. L = 75" . E=2997 ksi.

$I_x = 7.935$ in.^{4}. G = 450 ksi. $I_y = 2.67$ in. ^{4}. $K_t = .0612$. A= 2.85 in^2. $I_w = 9.375$ in. ^{6}.

Find: Buckling limit and vertical deflections with shear.

As shown in Galambos, the 4th order solution of the second order bending equilibrium equation including the angle of twist is:

$$EI_y u^{IV} + M_{tx} \phi'' + 2M'_{tx} \phi' = 0 \qquad [46]$$

And the 4th order solution of the third order equation of lateral deflection is

$$EI_w \phi^{IV} + Gk_t \phi'' - M_{tx} u'' - M'_{tx} u' - (M'_{tx1} + M'_{tx2}) u/L - (M_{tx1} + M_{tx2}) u'/L = 0 \qquad [47]$$

Both equations take into consideration that M'_{tx} is not zero for a beam with a point load. Symmetrical properties of I beam have also been taken into consideration. Next, we plug the 4th order central difference terms into the aforementioned lateral-torsion equations of equilibrium and we have

$$a_{17}u_3 + a_{16}u_2 + a_{15}u_1 + a_{14}u_0 + a_{13}u_{-1} + a_{12}u_{-2} + a_{11}u_{-3} + b_{15}\phi_2 + b_{14}\phi_1 + b_{13}\phi_0 + b_{12}\phi_{-1} + b_{11}\phi_{-2} = 0 \qquad [48]$$

$$a_{25}u_2 + a_{24}u_1 + a_{23}u_0 + a_{22}u_{-1} + a_{21}u_{-2} + b_{27}\phi_3 + b_{26}\phi_2 + b_{25}\phi_1 + b_{24}\phi_0 + b_{23}\phi_{-1} + b_{22}\phi_{-2} + b_{21}\phi_{-3} = 0 \qquad [49]$$

where a_{11} = $-EI_y/6h^4$; a_{12} = $2EI_y/h^4$; a_{13} = $-13EI_y/2h^4$; a_{14} = $28EI_y/3h^4$; a_{15} = $-13EI_y/2h^4$;

a_{16} = $2EI_y/h^4$; a_{17} = $-EI_y/6h^4$; b_{11} = $(-M_{tx}/12h^2 + M'_{tx}/6h)$; b_{12} = $(4M_{tx}/3h^2 -4 M'_{tx}/3h)$;

b_{13} = $-(5M_{tx}/2h^2$; b_{14} = $(4M_{tx}/3h^2 + 4 M'_{tx}/3h)$; and b_{15} = $-(M_{tx}/12h^2 + M'_{tx}/6h)$, and

a_{21} = $(M_{tx}/12h^2 - M'_{tx}/12h) – ((M_{tx1} +M_{tx2})/ 12hL)$;

a_{22} = $(-4M_{tx}/3h^2 + 2M'_{tx}/3h) + (2(M_{tx1} +M_{tx2})/ 3hL)$; a_{23} = $(5M_{tx}/2h^2 - ((M'_{tx1} +M'_{tx2})/ L)$;

a_{24} = $(-4M_{tx}/3h^2 - 2M'_{tx}/3h) - (2(M_{tx1} +M_{tx2})/ 3hL)$;

a_{25} = $(M_{tx}/12h^2 + M'_{tx}/12h) + ((M_{tx1} +M_{tx2})/ 12hL)$;

b_{21} = $-EI_y/6h^4$; b_{22} = $2EI_y/h^4 + GK_t/12h^2$; b_{23} = $-13EI_y/2h^4 - 4GK_t/3h^2$; b_{24} = $28EI_y/3h^4$;

b_{25} = $-13EI_y/2h^4 - 4GK_t/3h^2$; b_{26} = $2EI_y/h^4 + GK_t/12h^2$; and b_{27} = $-EI_y/6h^4$.

Next. We define h to be fraction of L. For this problem, L=75.0 in. and h=3.75 in. this gives us 21 locations. Boundary conditions are associated locations 1 and 21, and ghost boundary conditions are associated with locations 2,3,19, and 20. The term ghost is because we extend the columns out by two more imaginary locations beyond the boundary location. This allows us to modify equations to identify where supports are pinned or fixed. For example, the term a_{14} extended out two terms beyond the boundary gives us the two terms a_{12} and a_{11}. The modified term $^*a_{14}$ goes in the location a_{14}, and $^*a_{14} = a_{14} – a_{12}$; and $^*a_{15} = a_{15} – a_{11}$, if support is pinned. For fixed support, $^*a_{14} = a_{14} + a_{12}$; and $^*a_{15} = a_{15} + a_{11}$. b_{13}, a_{23}, b_{24}, b_{25} also need to be determined. Layout of K Matrix is demonstrated in Table 4.

Table 4. Central Difference Buckling K Matrix for Investigation 1

1		2		3		Location →					
u	ϕ	u	ϕ	u	ϕ						
0.0	0.0	0.0	0.0	0.0							→ Supports at locations 1 and 21
0.0	0.0	0.0									→ Zero out boundary
0.0	0.0	$*a_{14}$	b_{13}	$*a_{15}$	b_{14}	a_{16}	b_{15}	a_{17}	0.0	0.0	
0.0	0.0	a_{23}	b_{24}	a_{24}	b_{25}	a_{25}	b_{26}	0.0	b_{27}	0.0	
0.0	0.0	a_{13}	b_{12}	a_{14}	b_{13}	a_{15}	b_{14}	a_{16}	b_{15}	a_{17}	
0.0	0.0	a_{22}	b_{23}	a_{23}	b_{24}	a_{24}	b_{25}	a_{25}	b_{26}	0.0	
0.0	0.0	a_{12}	b_{11}	a_{13}	b_{12}	a_{14}	b_{13}	a_{15}	b_{14}	a_{16}	
0.0	0.0	a_{21}	b_{22}	a_{22}	b_{23}	a_{23}	b_{24}	a_{24}	b_{25}	a_{25}	
↓	↓										↘ Main diagonal

M_{tx} is the moment at the left end of an element because we are holding the element there. M_{tx1} is also the moment at the left end while M_{tx2} is the moment at the right end of an element. Signs are opposite, typically. M'_{tx} is equal to the slope of the moment. $M' = R_1$ or R_2.

$$R_1L - M_{tx1} - PL_2 + M_{tx2} = 0 \quad [50]$$

$$R_2L - M_{tx2} - PL_1 + M_{tx1} = 0 \quad [51]$$

Because we are dealing with a point load and discontinuity at its location, the slope is the same for each location to the left or right of the point load. Once values are assigned to all matrix locations including the shear moment location, we can solve the determinant of the matrix while increasing P_2 each time. When P_2 changes signs, we have crossed zero and reached the critical buckling limit. Value of P_{cr} with shear, P_2, for this problem is 1.83 kips.

The governing equations for deflections when considering lateral torsional buckling are:

$$B_x v'' - \phi M_{ty} = M_{tx}$$

$B_y\, u'' - \phi\, M_{tx} = M_{ty}$

$C_w\, \phi''' - (C_t + M_x\beta)\, \phi' - M_{tx}\, u' - M_{ty}\, v' - (M_{tx1} + M_{tx2})\, u/L - (M_{ty1} + M_{ty2})\, v/L + P(y_0/2)\, \phi = 0$

As we are solving these equations simultaneously using a fourth order central difference approach, we will be using the aforementioned central difference expressions. These terms are substituted into our modified lateral-torsion equations to obtain:

$B_x\, (-v_2 + 16v_1 - 30v_0 + 16\, v_{-1} - v_{-2}) - \phi_0\, M_{ty} = M_{tx}$

$B_y\, (-u_2 + 16u_1 - 30u_0 + 16\, u_{-1} - u_{-2}) - \phi_0\, M_{tx} = M_{ty}$

$C_w\, (- \Phi_3 + 8\phi_2 - 13\phi_1 + 13\phi_{-1} - 8\phi_{-2} + \phi_{-3})/8h^3 - (C_t + M_x\beta)\, (-\phi_2 + 8\phi_1 - 8\phi_{-1} + \phi_{-2})$

$- M_{tx}\, (-u_2 + 8u_1 - 8u_{-1} + u_{-2}) - M_{ty}\, (-v_2 + 8v_1 - 8v_{-1} + v_{-2})$

$- (M_{tx1} + M_{tx2})\, u_0/L - (M_{ty1} + M_{ty2})\, v_0/L + P(y_0/2)\, \phi_0 = 0$

Setting M_y to zero, we have,

$a_{11}v_{-2} + a_{12}v_{-1} + a_{13}v_0 + a_{14}v_1 + a_{15}v_2 = M_{tx}$ [52a]

where $a_{11} = -EI_x/12h^2$; $a_{12} = 4EI_x/3h^2$; $a_{13} = -5EI_x/2h^2$; $a_{14} = 4EI_x/3h^2$; $a_{15} = -EI_x/12h^2$;

$B_{21}u_{-2} + b_{22}u_{-1} + b_{23}u_0 + b_{24}u_1 + b_{25}u_2 + c_{21}\phi_0 = 0.0$ [52b]

Where $b_{21} = -EI_x/12h^2$; $b_{22} = 4EI_x/3h^2$; $b_{23} = -5EI_x/2h^2$; $b_{24} = 4EI_x/3h^2$; $b_{25} = -EI_x/12h^2$;

$c_{21} = - M_{tx}$

$b_{31}u_{-2} + b_{32}u_{-1} + b_{33}u_0 + b_{34}u_1 + b_{35}u_2 + c_{31}\phi_{-3} + c_{32}\phi_{-2} + c_{33}\phi_{-1} + c_{34}\phi_0 + c_{35}\phi_1 + c_{36}\phi_2 + c_{37}\phi_1 = 0.0$

[52c]

where $b_{31} = -M_{tx}/12h$; $b_{32} = 2M_{tx}/3h$; $b_{33} = -(M_{tx1} + M_{tx2})/L$; $b_{34} = -2M_{tx}/3h$; $b_{35} = M_{tx}/12h$;

$c_{31} = C_w/8h^3$; $c_{32} = - C_w/h^3 - C_t/12h$; $c_{33} = 13C_w/8h^3 + 2C_t/3h$; $c_{34} = Py_0/2$;

$c_{35} = -13C_w/8h^3 - 2C_t/3h$; $c_{36} = C_w/h^3 + C_t/12h$; $c_{37} = - C_w/8h^3$.

For the vertical deflection values, we use the same approach we just demonstrated for the buckling limit except we use the three governing equations and the load vector is not set to zero. [K] u = F. So we solve for the deflections using the inverse K matrix, u = $[K]^{-1}$ F. The vector u contains the unknowns v, u, and phi along the member. Central Difference K Matrix for deflection calcs is demonstrated in Table 5.

Table 5. Central Difference K Matrix for Deflection. Investigation 1

Location 1			**Location 2**			**Location 3**			**Location 4**		
V	**u**	**ϕ**	**v**	**u**	**ϕ**	**v**	**u**	**ϕ**	**v**	**u**	**ϕ**
~~0.0~~	~~0.0~~	~~0.0~~	~~0.0~~	~~0.0~~	~~0.0~~	~~0.0~~	~~0.0~~	~~0.0~~	~~0.0~~	~~0.0~~	~~0.0~~
~~0.0~~	~~0.0~~	~~0.0~~	~~0.0~~	~~0.0~~	~~0.0~~	~~0.0~~	~~0.0~~	~~0.0~~	~~0.0~~	~~0.0~~	~~0.0~~
~~0.0~~	~~0.0~~	~~0.0~~	~~0.0~~	~~0.0~~	~~0.0~~	~~0.0~~	~~0.0~~	~~0.0~~	~~0.0~~	~~0.0~~	~~0.0~~
0.0	0.0	0.0	*a_{13}	0.0	0.0	a_{14}	0.0	0.0	a_{15}	0.0	0.0
0.0	0.0	0.0	0.0	b_{33}	c_{34}	0.0	b_{34}	c_{35}	0.0	b_{35}	c_{36}
0.0	0.0	0.0	0.0	b_{23}	c_{21}	0.0	b_{24}	0.0	0.0	b_{25}	0.0
0.0	0.0	0.0	a_{12}	0.0	0.0	a_{13}	0.0	0.0	a_{14}	0.0	0.0
0.0	0.0	0.0	0.0	b_{32}	c_{33}	0.0	b_{33}	c_{34}	0.0	b_{34}	c_{35}
0.0	0.0	0.0	0.0	b_{22}	0.0	0.0	b_{23}	c_{21}	0.0	b_{24}	0.0

Main diagonal

Zero out boundaries

For this problem, we used h=1.5 inches and 51 locations. Vertical deflections were tabulated based upon given info and applied P_2 loads from laboratory. Values are shown in Table 6.

Table 6. Vertical Deflections. Investigation 1. Central Difference

	8" from support		18" from support		29" from support	
Load P, kips	**V_1w/s(in.)**	**V_1w/0(in.)**	**V_2w/s(in.)**	**V_2w/o(in.)**	**V_3w/s(in.)**	**V_3w/o(in.)**
0.00	0.00	0.00	0.00	0.00	0.00	0.00
.0141	.0020	.0018	.0037	.0034	.0054	.0048
.1292	.0180	.0165	.0340	.0311	.0491	.0442
.3149	.0438	.0403	.0830	.0758	.1196	.1077
.4913	.0684	.0628	.1294	.1183	.1866	.1680
.6858	.0955	.0877	.1807	.1652	.2604	.2346
.8787	.1223	.1124	.2315	.2116	.3337	.3006
1.0271	.1430	.1314	.2706	.2473	.3900	.3513
1.3618	.1896	.1742	.3588	.3279	.5171	.4658
1.6124	.2245	.2062	.4248	.3883	.6123	.5515
1.7509	.2438	.2240	.4613	.4216	.6649	.5988
1.8316	.2550	.2343	.4825	.4411	.6956	.6764
2.13	.2966	.2725	.5612	.5129	.8089	.7285

2.1.4 ASCE LRFD Method

The ASCE buckling limit equation was developed using the classical approach solution for a simple beam solution introduced by Galambos. The LTB equations used in the classical approach were

$$EI_y u^{IV} + M_{tx} \phi'' + 2M'_{tx} \phi' = 0 \quad [53]$$

And the 4th order solution of the third order equation of lateral deflection is

$$EI_w \phi^{IV} - (Gk_t + M_x \beta) \phi'' - M_x u'' - M'_x \beta_x \phi = 0 \quad [54]$$

The LRFD approach and equations used here-in may be found in the ASCE LRFD Design Guide for Pultruded Members.

$$M_n = C_b (\pi^2 E_{L f} I_y D_j/L_b^2 + \pi^4 E_{Lf} I_y C_w/L_b^4)^{.5} \quad [55]$$

where $D_j = Gk_t$; $C_w = I_w$; and $C_b = 12.5M_{max}/(2.5M_{max}+3M_A+4M_B+3M_C)$.

Problem 2.1.4. Lab Investigation 1

Given: 4” x 4” x ¼” fiberglass reinforced plastic beam in Figure 4. L = 75”. E_{LF}= 3194 ksi.

I_x = 7.935 in.^{4}. G = 450 ksi. I_y = 2.67 in.^{4}. k_t = .0612. A = 2.85 in^2. I_w = 9.375 in.^{4}.

Find: Buckling limit.

The ASCE-LRFD equation for lateral-torsional buckling moment of an I-shaped cross section is

$$M_n = C_b\,(\pi^2 E_{Lf} I_y D_j/L_b^2 + \pi^4 E_{Lf} I_y C_w/L_b^4)^{.5} \qquad [56]$$

where L_b is the braced length,

C_w is the warping constant,

E_{LF} is the Modulus Elasticity of the longitudinal flange,

$D_j = Gk_t$ and is the torsional rigidity, and

$$Cb = 12.5M_{max}/(2.5M_{max}+3M_A+4M_B+3M_C). \qquad [57]$$

and is the moment modification factor. M_A, M_B and M_C are moments at locations .25L, .5L, and .75L, respectively. See Figure 7.

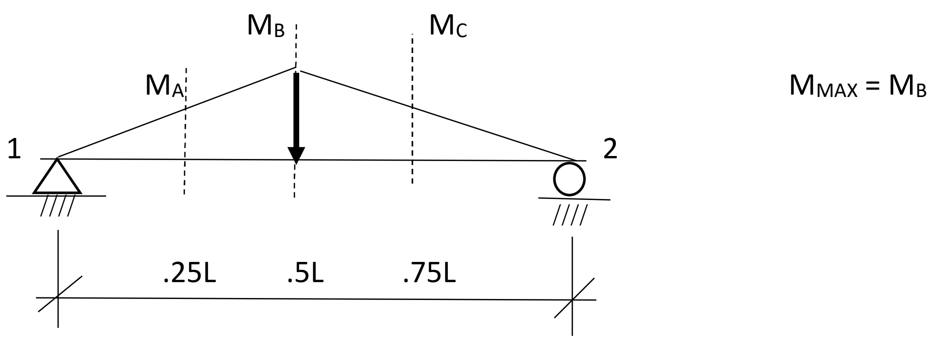

Figure 7. Moment Diagram for Investigation 1

Location of M_{max} varies with location of point load and equilibrium conditions. For this problem, $M_{max} = M_B = PL/4$. Plugging in moment values, $C_b = 1.32$. Plugging in given values and C_b, M_n=43.02 k-in. Knowing the relationship between the critical moment and critical load, P_1, without shear moment; we can calculate the critical load, P_1.

$P_1 = 4M_n/L = 2.29$ kips.

Now. We must find relationship of P_1, the critical load without shear moment, and P_2, the critical load with shear moment.

P_1 is associated with the moments on the conjugate beam when P_s is not present. P_2 is associated with the moments on the conjugate beam when P_s is present. The resultant of the moment diagram on the conjugate beam when considering and not considering shear moment is of equal value or

$$2(1/2)\,(P_1/L/4)\,(L/2) = 2(1/2)\,(P_2/L/4)\,(L/2) + P_2(\alpha EI_x/AG) \qquad [58]$$

Rearranged

$$P_2/P_1 = (L^2/8)/\,((L^2/8) + \alpha EI_x/AG) \qquad [59]$$

Solving we get $SF = P_2/P_1 = .92$

Thus,

$P_2 = .92P_1 = 2.11$ kips

Using the LRFD buckling limit equation, The buckling load with shear was determined to be 2.03 ksi.

Critical loads are summarized in Table 7 and will be compared to experimental load in Chapter 4. Deflections will be compared also.

2.1.5 Summary of Maximum Loads

Table 7. Summary Buckling Limits Theory

Section	Method	P_{cr}	
2.1.1	Semi-analytical Solution Including Shear Deformation	1.55	kips
2.1.2	Semi-analytical Solution Ignoring Shear Deformation	1.75	kips
2.1.3	Finite Difference Solution Including Shear Deformmation	1.83	kips
2.1.4	ASCE-LRFD Method	2.11	kips

2.2 Stability Analysis for Simply Supported Beam with Point Load Off Center

Numerical formulations for the critical buckling load and translational and rotational deflections are presented for Investigation 2 in this section. Numerical methods formulated include fourth order central difference. Critical buckling load as determined from the ASCE-LRFD Prestandard is also presented. Beam loading with boundary conditions and moments on conjugate beam are defined in Figure 8.

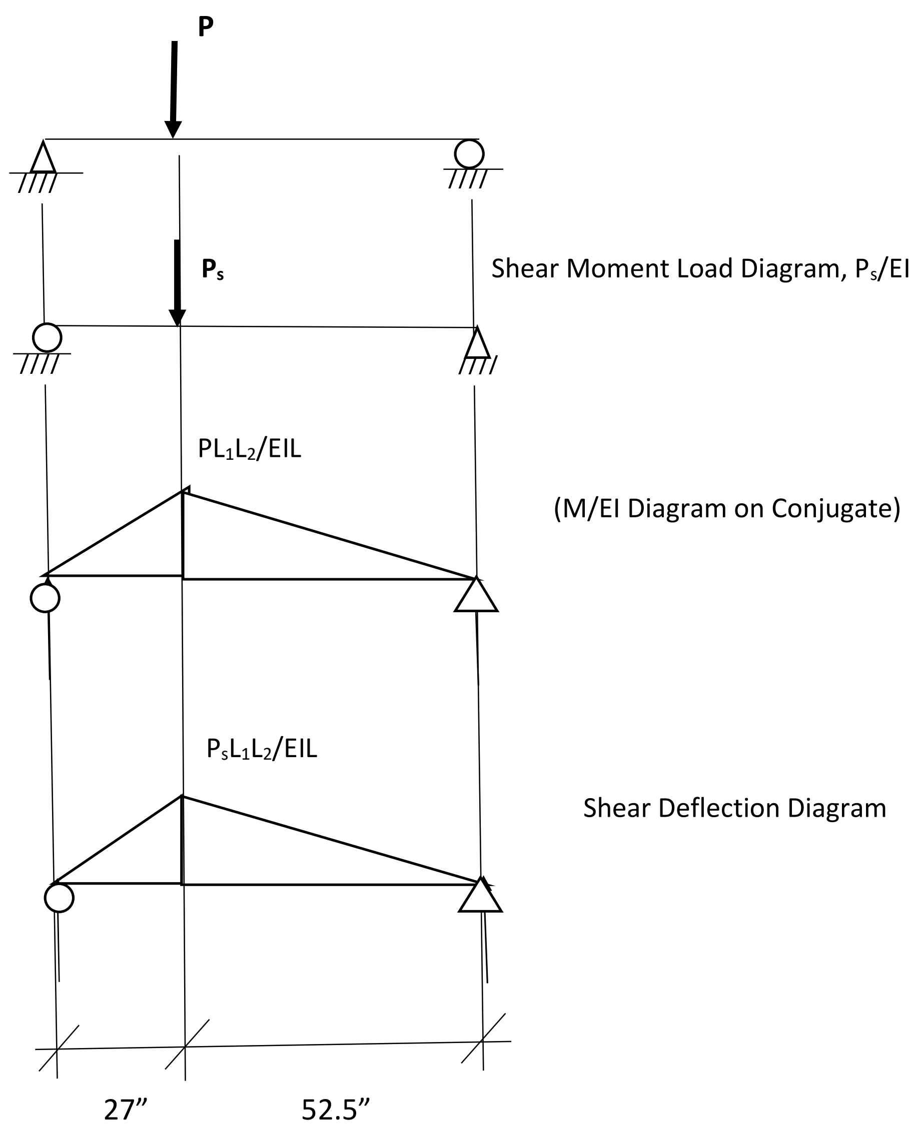

Figure 8. Investigation 2. Deflection Diagrams

2.2.1 Central Difference Solution With Shear Deformation

For this approach, use the three central difference governing equations previously developed to determine vertical, horizontal and lateral deflection values along the beam. $M_x = M_{tx}$. For this approach, follow the instructions of Timoshenko to the letter. Simply place the Shear moment point load on the conjugate beam. The ends of the conjugate beam are pinned-pinned. So, boundary conditions are set for pinned-pinned in the finite difference model. Depending up on the length of an element of eccentricity, the shear moment P_s value varies from model to model. $P_s = P_2\, \alpha EI_x/(eAG)$ where e is the eccentricity or length of the element. With shear, $M_{tx} = M_{bending} + P_s$ on the conjugate beam.

Problem 2.2.1. Lab Investigation 2

Given : 3" x 3" x 1/4 " fiberglass reinforced plastic beam in Figure 5. L=79.5" . E= 2997 ksi. I_x = 3.17 in.^{4} . G = 450 ksi. I_y = 1.13 in.^{4}. Kt = .046 . A = 2.13 in.^{2}. I_w = 2.13 in.^{6}

Find: Buckling limit and vertical deflections with shear.

As shown in Galambos, the 4th order solution of the second order bending equilibrium equation including the angle of twist is:

$$EI_y u^{IV} + M_{tx}\phi'' + 2M'_{tx}\phi' = 0 \qquad [46]$$

And the 4th order solution of the third order equation of lateral deflection is

$$EI_w \phi^{IV} + Gk_t \phi'' - M_{tx} u'' - M'_{tx} u' - (M'_{tx1} + M'_{tx2})\, u/L - (M_{tx1} + M_{tx2})\, u'/L = 0 \qquad [47]$$

Both equations take into consideration that M'_{tx} is not zero for a beam with a point load. Symmetrical properties of I beam have also been taken into consideration. Next, plug the 4th order central difference terms into the aforementioned lateral-torsion equations of equilibrium and obtain

$$a_{17}u_3 + a_{16}u_2 + a_{15}u_1 + a_{14}u_0 + a_{13}u_{-1} + a_{12}u_{-2} + a_{11}u_{-3} + b_{15}\phi_2 + b_{14}\phi_1 + b_{13}\phi_0 + b_{12}\phi_{-1} + b_{11}\phi_{-2} = 0 \qquad [48]$$

$$a_{25}u_2 + a_{24}u_1 + a_{23}u_0 + a_{22}u_{-1} + a_{21}u_{-2} + b_{27}\phi_3 + b_{26}\phi_2 + b_{25}\phi_1 + b_{24}\phi_0 + b_{23}\phi_{-1} + b_{22}\phi_{-2} + b_{21}\phi_{-3} = 0 \qquad [49]$$

where a_{11} = $-EI_y/6h^4$; a_{12} = $2EI_y/h^4$; a_{13} = $-13EI_y/2h^4$; a_{14} = $28EI_y/3h^4$; a_{15} = $-13EI_y/2h^4$;
a_{16} = $2EI_y/h^4$; a_{17} = $-EI_y/6h^4$; b_{11} = $(-M_{tx}/12h^2 + M'_{tx}/6h)$; b_{12} = $(4M_{tx}/3h^2 - 4\ M'_{tx}/3h)$;
b_{13} = $-(5M_{tx}/2h^2$; b_{14} = $(4M_{tx}/3h^2 + 4\ M'_{tx}/3h)$; and b_{15} = $-(M_{tx}/12h^2 + M'_{tx}/6h)$, and
a_{21} = $(M_{tx}/12h^2 - M'_{tx}/12h) - ((M_{tx1} + M_{tx2})/\ 12hL)$;
a_{22} = $(-4M_{tx}/3h^2 + 2M'_{tx}/3h) + (2(M_{tx1} + M_{tx2})/\ 3hL)$; a_{23} = $(5M_{tx}/2h^2 - ((M'_{tx1} + M'_{tx2})/\ L)$;
a_{24} = $(-4M_{tx}/3h^2 - 2M'_{tx}/3h) - (2(M_{tx1} + M_{tx2})/\ 3hL)$;
a_{25} = $(M_{tx}/12h^2 + M'_{tx}/12h) + ((M_{tx1} + M_{tx2})/\ 12hL)$;
b_{21} = $-EI_y/6h^4$; b_{22} = $2EI_y/h^4 + GK_t/12h^2$; b_{23} = $-13EI_y/2h^4 - 4GK_t/3h^2$; b_{24} = $28EI_y/3h^4$;
b_{25} = $-13EI_y/2h^4 - 4GK_t/3h^2$; b_{26} = $2EI_y/h^4 + GK_t/12h^2$; and b_{27} = $-EI_y/6h^4$.

Next. Define h to be a fraction of L. For this problem, L = 79.5 in. ; h=3.97in. ; and there are 21 location Boundary conditions are associated with locations 1 and 21, and ghost boundary conditions are associated with locations 2,3,19, and 20. The term ghost is because we extend the columns out by two more imaginary locations beyond the boundary location. This allows us to modify equations and identify whether supports are pinned or fixed. For example, the term a14 extended out two terms beyond the boundary gives us the two terms a_{12} and a_{11}. The modified term $*a_{14}$ goes in the location of term a_{14}, and $*a_{14} = a_{14} - a_{12}$; and $*a_{15} = a_{15} - a_{11}$, if support is pinned. For fixed support, $*a_{14} = a_{14} + a_{12}$; and $*a_{15} = a_{15} + a_{11}$. $*b_{13}$, $*a_{23}$, $*b_{24}$, and $*b_{25}$ also need to be determined. Layout of the K matrix is demonstrated in Table 8.

Table 8 Central Diff. K Matrix for Buckling. Investigation 2

1		2		3		Location →					
u	ϕ	u	ϕ	u	ϕ						
0.0	0.0	0.0	0.0	0.0							→ Supports at locations 1 and 21
0.0	0.0	0.0									→ Zero out boundary
0.0	0.0	$*a_{14}$	b_{13}	$*a_{15}$	b_{14}	a_{16}	b_{15}	a_{17}	0.0	0.0	
0.0	0.0	a_{23}	b_{24}	a_{24}	b_{25}	a_{25}	b_{26}	0.0	b_{27}	0.0	
0.0	0.0	a_{13}	b_{12}	a_{14}	b_{13}	a_{15}	b_{14}	a_{16}	b_{15}	a_{17}	
0.0	0.0	a_{22}	b_{23}	a_{23}	b_{24}	a_{24}	b_{25}	a_{25}	b_{26}	0.0	
0.0	0.0	a_{12}	b_{11}	a_{13}	b_{12}	a_{14}	b_{13}	a_{15}	b_{14}	a_{16}	
0.0	0.0	a_{21}	b_{22}	a_{22}	b_{23}	a_{23}	b_{24}	a_{24}	b_{25}	a_{25}	

Main diagonal

M_{tx} is the moment at the left end of an element because the element is being held there. M_{tx1} is also the moment at the left end while M_{tx2} is the moment at the right end of an element. Signs are opposite, typically. M'_{tx} is equal to the slope of the moment. $M' = R_1$ or R_2.

$$R_1L - M_{tx1} - PL_2 + M_{tx2} = 0 \quad [50]$$

$$R_2L - M_{tx2} - PL_1 + M_{tx1} = 0 \quad [51]$$

When dealing with a point load and discontinuity at its location, the slope is the same for each location to the left or right of the point load.

Once values are assigned to all matrix locations including the shear moment location, solve the determinant of the matrix while increasing P_2 each time. When the matrix determinant value changes signs, the determinant has crossed zero and P_2 has reached the critical buckling limit. Value of P_{cr} with shear, P_2, for this problem is .84 kips.

The governing equations for deflections when considering lateral torsional buckling are:

$B_x v'' - \phi M_{ty} = M_{tx}$

$B_y u'' - \phi M_{tx} = M_{ty}$

$C_w \phi''' - (C_t + M_x\beta)\phi' - M_{tx} u' - M_{ty} v' - (M_{tx1} + M_{tx2}) u/L - (M_{ty1} + M_{ty2}) v/L + P(y_0/2)\phi = 0$

Solve the modified equations of equilibrium simultaneously using a fourth order central difference approach and aforementioned central difference expressions. These terms are substituted into our modified lateral-torsion equations to obtain:

$B_x(-v_2 + 16v_1 - 30v_0 + 16v_{-1} - v_{-2}) - \phi_0 M_{ty} = M_{tx}$

$B_y(-u_2 + 16u_1 - 30u_0 + 16u_{-1} - u_{-2}) - \phi_0 M_{tx} = M_{ty}$

$C_w(-\Phi_3 + 8\phi_2 - 13\phi_1 + 13\phi_{-1} - 8\phi_{-2} + \phi_{-3})/8h^3 - (C_t + M_x\beta)(-\phi_2 + 8\phi_1 - 8\phi_{-1} + \phi_{-2})$

$- M_{tx}(-u_2 + 8u_1 - 8u_{-1} + u_{-2}) - M_{ty}(-v_2 + 8v_1 - 8v_{-1} + v_{-2})$

$- (M_{tx1} + M_{tx2}) u_0/L - (M_{ty1} + M_{ty2}) v_0/L + P(y_0/2)\phi_0 = 0$

Setting M_y to zero,

$a_{11}v_{-2} + a_{12}v_{-1} + a_{13}v_0 + a_{14}v_1 + a_{15}v_2 = M_{tx}$ [52a]

where $a_{11} = -EI_x/12h^2$; $a_{12} = 4EI_x/3h^2$; $a_{13} = -5EI_x/2h^2$; $a_{14} = 4EI_x/3h^2$; $a_{15} = -EI_x/12h^2$;

$B_{21}u_{-2} + b_{22}u_{-1} + b_{23}u_0 + b_{24}u_1 + b_{25}u_2 + c_{21}\phi_0 = 0.0$ [52b]

where $b_{21} = -EI_x/12h^2$; $b_{22} = 4EI_x/3h^2$; $b_{23} = -5EI_x/2h^2$; $b_{24} = 4EI_x/3h^2$; $b_{25} = -EI_x/12h^2$;

$c_{21} = -M_{tx}$

$b_{31}u_{-2} + b_{32}u_{-1} + b_{33}u_0 + b_{34}u_1 + b_{35}u_2 + c_{31}\phi_{-3} + c_{32}\phi_{-2} + c_{33}\phi_{-1} + c_{34}\phi_0 + c_{35}\phi_1 + c_{36}\phi_2 + c_{37}\phi_1 = 0.0$

[52c]

where $b_{31} = -M_{tx}/12h$; $b_{32} = 2M_{tx}/3h$; $b_{33} = -(M_{tx1} + M_{tx2})/L$; $b_{34} = -2M_{tx}/3h$; $b_{35} = M_{tx}/12h$;

$c_{31} = C_w/8h^3$; $c_{32} = -C_w/h^3 - C_t/12h$; $c_{33} = 13C_w/8h^3 + 2C_t/3h$; $c_{34} = Py_0/2$;

$c_{35} = -13C_w/8h^3 - 2C_t/3h$; $c_{36} = C_w/h^3 + C_t/12h$; $c_{37} = -C_w/8h^3$.

For the vertical deflection values, use the same approach just demonstrated for the buckling limit except use the three governing equations and the load vector is not set to zero. $[K]u = F$. So solve for the deflections using the inverse K matrix, $u = [K]^{-1} F$. The vector u contains the unknowns v, u, and phi along the member. K matrix is demonstrated in Table 9.

Table 9. Central Difference K Matrix for Deflection. Investigation 2

Location 1			**Location 2**			**Location 3**			**Location 4**		
V	**u**	**ϕ**	**v**	**u**	**ϕ**	**v**	**u**	**ϕ**	**v**	**u**	**ϕ**
0.0	0.0	0.0	0.0	0.0	0.0	0.0	0.0	0.0	0.0	0.0	0.0
0.0	0.0	0.0	0.0	0.0	0.0	0.0	0.0	0.0	0.0	0.0	0.0
0.0	0.0	0.0	0.0	0.0	0.0	0.0	0.0	0.0	0.0	0.0	0.0
0.0	0.0	0.0	*a_{13}	0.0	0.0	a_{14}	0.0	0.0	a_{15}	0.0	0.0
0.0	0.0	0.0	0.0	b_{33}	c_{34}	0.0	b_{34}	c_{35}	0.0	b_{35}	c_{36}
0.0	0.0	0.0	0.0	b_{23}	c_{21}	0.0	b_{24}	0.0	0.0	b_{25}	0.0
0.0	0.0	0.0	a_{12}	0.0	0.0	a_{13}	0.0	0.0	a_{14}	0.0	0.0
0.0	0.0	0.0	0.0	b_{32}	c_{33}	0.0	b_{33}	c_{34}	0.0	b_{34}	c_{35}
0.0	0.0	0.0	0.0	b_{22}	0.0	0.0	b_{23}	c_{21}	0.0	b_{24}	0.0

Main diagonal

Zero out boundaries

For this problem, we used h=1.5 inches and 54 locations. Vertical deflections were tabulated based upon given info and applied P_2 and P_1 loads from laboratory. Values are shown in Table 10.

Table 10. Vertical Deflections. Investigation 2. Central Difference

	6" from support	6" from support	21" from support	21" from support	36" from support	36" from support
Load P, kips	$v_{1w/s}$ (in.)	$v_{1w/o}$	$v_{2w/s}$	$v_{2w/o}$	$v_{3w/s}$	$v_{3w/o}$
0.00	0.00	0.00	0.00	0.00	0.00	0.00
.1826	.04672	.04426	.1455	.1369	.1811	.1719
.4244	.1086	.1029	.3383	.3182	.4209	.3996
.6514	.1667	.1579	.5192	.4885	.6461	.6133
.8653	.2214	.2097	.6897	.6488	.8582	.8146
1.072	.2744	.2600	.8549	.8042	1.064	1.010

2.2.2 Central Difference Solution Without Shear Deformation

For this approach, we use the three central difference governing equations previously developed to determine vertical, horizontal, and lateral deflection values along the beam. $M_x = M_{bending}$ and $P_s = 0$. The ends of conjugate beam are pinned-pinned. So, boundary conditions are set for pinned-pinned in the finite difference model.

Problem 2.2.2. Lab Investigation 2

Given: 3" x 3" x 1/4 " fiberglass reinforced plastic beam in Figure 5. L=79.5" . E= 2997 ksi.

I_x = 3.17 in. ^{4} . G = 450 ksi. I_y = 1.13 in. ^{4}. K_t = .046 . A = 2.13 in.^{2}. I_w = 2.13 in.^{6}

Find: Buckling limit and vertical deflections without shear.

For vertical deflections without shear, we simply do not apply the shear moment to the beam. In other words P_s = 0.0 and $M_{tx} = M_{xbending}$. Procedure is exactly same as calculating critical load and vertical deflection outlined in previous problem which included shear. However, P loads from lab experiments are P_1 not P_2. Therefore, $M_{cr} = P_1L_1L_2/L$ for this problem. See tabulated vertical deflection values for this problem in Table 6. P_1 equals .88 kips at the buckling limit calculated using this approach. M_{tx} = 15.69 k-in.

2.2.3 ASCE LRFD Method

The ASCE buckling limit equation was developed using the classical approach solution for a simple beam solution introduced by Galambos. The LTB equations used in the classical approach were

$$EI_y u^{IV} + M_{tx} \phi'' + 2M'_{tx} \phi' = 0 \quad [53]$$

And the 4th order solution of the third order equation of lateral deflection is

$$EI_w \phi^{IV} - (Gk_t + M_x \beta) \phi'' - M_x u'' - M'_x \beta_x \phi = 0 \quad [54]$$

The LRFD approach and equations used here-in may be found in the ASCE LRFD Design Guide for Pultruded Members.

$$M_n = C_b (\pi^2 E_{Lf} I_y D_j/L_b^2 + \pi^4 E_{Lf} I_y C_w/L_b^4)^{.5} \quad [55]$$

Where $D_j = Gk_t$; $C_w = I_w$; and $C_b = 12.5M_{max}/(2.5M_{max}+3M_A+4M_B+3M_C)$.

Problem 2.2.3. Lab Investigation 2

Given: 3” x 3” x ¼” fiberglass reinforced plastic beam in Figure 5. L=79.5”, E_{LF}=3194 ksi.

I_x=3.17in.4. G=450 ksi. I_y =1.13 in.^{4}. k_t = .046. A=2.13 in^2. I_w = 2.13 in. ^{6}.

Find: Buckling limit.

The ASCE-LRFD equation for lateral-torsional buckling moment of an I-shaped cross section is

$$M_n = C_b (\pi^2 E_{Lf} I_y D_j/L_b^2 + \pi^4 E_{Lf} I_y C_w/L_b^4)^{.5}$$

Where L_b is the braced length,

C_w is warping constant,

E_{LF} is the Modulus Elasticity of the longitudinal flange,

$D_j = GK_t$ and is the torsional rigidity, and

$C_b = 12.5M_{max}/(2.5M_{max}+3M_A+4M_B+3M_C)$

And is the moment modification factor.

M_A, M_B and M_C are moments at locations .25L, .5L, and .75L, respectively. See Figure 9. Location of M_{max} varies with location of point load and equilibrium conditions. For this problem, C_b = 1.41. $M_{max} = PL_1L_2/L$. Plugging in moment values, M_n=18.68 k-in. Knowing the relationship between the critical moment and critical load, P_1, without shear moment; we can calculate the critical load, P_1. $P_1 = ML/L_1L_2$ = 1.05 kips.

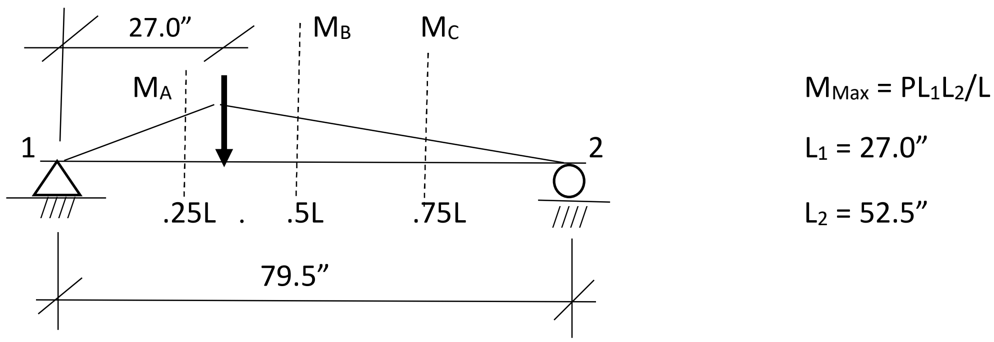

Figure 9. Moment Diagram for Investigation 2

Now. find the relationship of P_1, the critical load without shear moment, and P_2, the critical load with shear moment. P_1 is associated with the moments on the conjugate beam when M_s is not present. P_2 is associated with the moments on the conjugate beam when P_s is present. The resultants of the moments on the conjugate beam when considering and not considering shear moment are of the same value or

$$(½)(P_1L_1L_2/L)(L_1) + (½)(P_1L_1L_2/L)(L_2) = (½)(P_2L_1L_2/L)(L_1) + (½)(P_2L_1L_2/L)(L_2) + P_s$$

Rearranged

$$P_2/P_1 = [(½)(L_1L_2/L)(L_1) + (½)(L_1L_2/L)(L_2)] / [(½)(P_2L_1L_2/L)(L_1) + (½)(P_2L_1L_2/L)(L_2) + \alpha EI_x/AG]$$

Solving we get P_2/P_1 = .956 Therefore, P_2 = 1.00

2.2.4 Summary of Maximum Loads

Critical loads are summaraized in Table 11 and will be compared to experimental load in Chapter 4. Deflections will be compared also.

Table 11. Summary of Buckling Limits. Investigation 2

Section	Method	P_{cr}
2.2.1	Central Difference with Shear	.84 kips
2.2.2	Central Difference without Shear	.88 kips
2.2.3	ASCE-LRFD Buckling Limit	1.00 kips

2.3 Stability Analysis for Two Span Beam with Point Load Midspan. Longer Span.

Numerical formulations for the critical buckling load and translational and rotational deflections are presented for Investigation 3 in this section. Numerical methods formulated include fourth order central difference. Critical buckling load as determined from the ASCE-LRFD Prestandard is also presented. Beam loading with boundary conditions and moments on conjugate beam are defined in Figure 10.

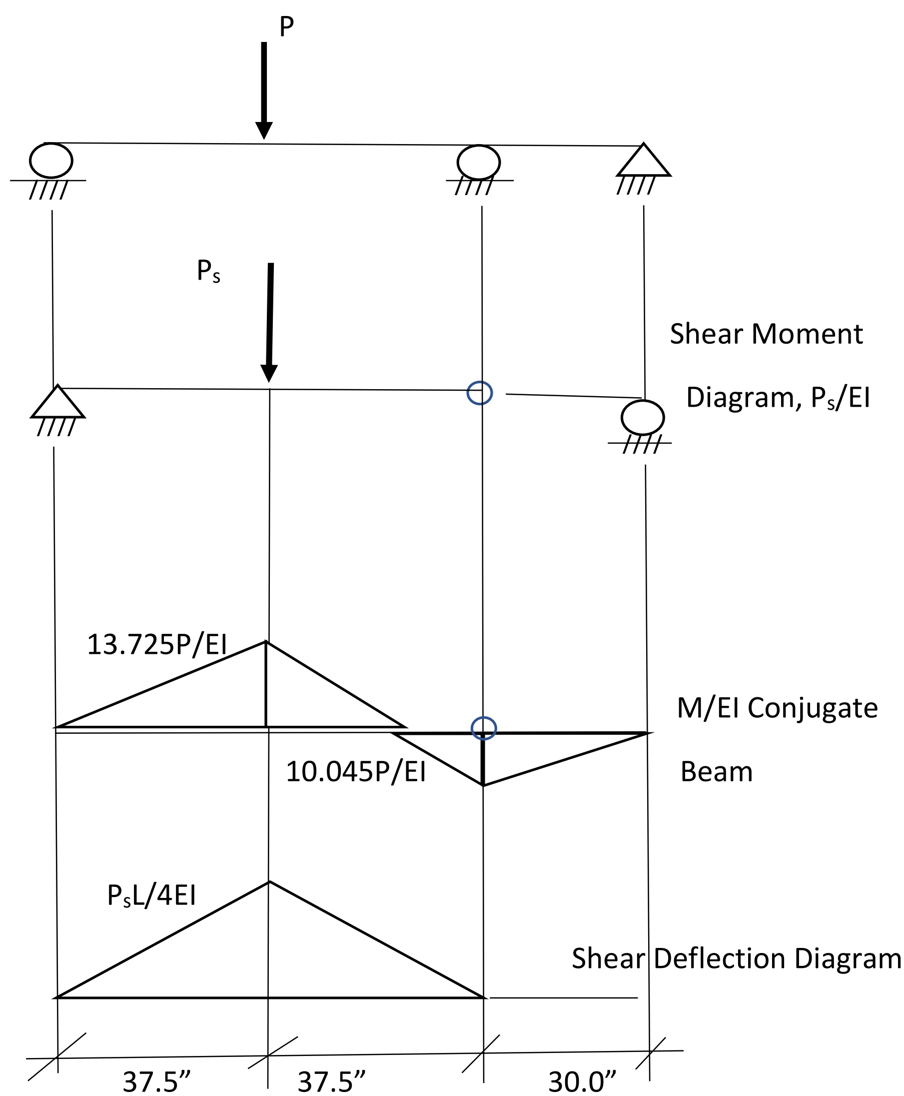

Figure 10. Investigation 3: Deflection Diagrams

2.3.1 Central Difference Solution With Shear Deformation

For this approach, use the three central difference governing equations previously developed to determine vertical, horizontal and lateral deflection values along the beam. $M_x = M_{tx}$. For this approach, follow the instructions of Timoshenko to the letter. Simply place the Shear moment point load on the conjugate beam. The ends of the conjugate beam are pinned-pinned. So, boundary conditions are set for pinned-pinned in the finite difference model. Depending up on the length of an element of eccentricity, the shear moment P_s value varies from model to model. $P_s = P_2\, \alpha EI_x/(eAG)$ where e is the eccentricity or length of the element. With shear, $M_{tx} = M_{bending} + P_s$ on the conjugate beam.

Problem 2.3.1. Lab Investigation 3

Given: 4"x4"x1/4" fiberglass reinforced plastic beam in Figure 6. L=75". E=2997ksi. I_x = 7.935 in.^{4}. G = 450 ksi . I_y = 2.67 in.^{4} . k_t =.0612. A = 2.85 in^2. I_w = 9.375 in. ^{6}.

Find: Buckling limit and vertical deflections with shear.

As shown in Galambos, the 4th order solution of the second order bending equilibrium equation including the angle of twist is:

$$EI_y u^{IV} + M_{tx} \phi'' + 2M'_{tx} \phi' = 0 \quad [46]$$

And the 4th order solution of the third order equation of lateral deflection is

$$EI_w \phi^{IV} + Gk_t \phi'' - M_{tx} u'' - M'_{tx} u' - (M'_{tx1} + M'_{tx2}) u/L - (M_{tx1} + M_{tx2}) u'/L = 0 \quad [47]$$

Both equations take into consideration that M'_{tx} is not zero for a beam with a point load. Symmetrical properties of I beam have also been taken into consideration. Next, plug the 4th order central difference terms into the aforementioned lateral-torsion equations of equilibrium and obtain

$$a_{17}u_3 + a_{16}u_2 + a_{15}u_1 + a_{14}u_0 + a_{13}u_{-1} + a_{12}u_{-2} + a_{11}u_{-3} + b_{15}\phi_2 + b_{14}\phi_1 + b_{13}\phi_0 + b_{12}\phi_{-1} + b_{11}\phi_{-2} = 0 \quad [48]$$

$$a_{25}u_2 + a_{24}u_1 + a_{23}u_0 + a_{22}u_{-1} + a_{21}u_{-2} + b_{27}\phi_3 + b_{26}\phi_2 + b_{25}\phi_1 + b_{24}\phi_0 + b_{23}\phi_{-1} + b_{22}\phi_{-2} + b_{21}\phi_{-3} = 0 \quad [49]$$

where $a_{11} = -EI_y/6h^4$; $a_{12} = 2EI_y/h^4$; $a_{13} = -13EI_y/2h^4$; $a_{14} = 28EI_y/3h^4$; $a_{15} = -13EI_y/2h^4$;

$a_{16} = 2EI_y/h^4$; $a_{17} = -EI_y/6h^4$; $b_{11} = (-M_{tx}/12h^2 + M'_{tx}/6h)$; $b_{12} = (4M_{tx}/3h^2 -4\ M'_{tx}/3h)$;

$b_{13} = -(5M_{tx}/2h^2$; $b_{14} = (4M_{tx}/3h^2 + 4\ M'_{tx}/3h)$; and $b_{15} = -(M_{tx}/12h^2 + M'_{tx}/6h)$, and

$a_{21} = (M_{tx}/12h^2 - M'_{tx}/12h) – ((M_{tx1} +M_{tx2})/ 12hL)$;

$a_{22} = (-4M_{tx}/3h^2 + 2M'_{tx}/3h) + (2(M_{tx1} +M_{tx2})/ 3hL)$; $a_{23} = (5M_{tx}/2h^2 - ((M'_{tx1} +M'_{tx2})/ L)$;

$a_{24} = (-4M_{tx}/3h^2 - 2M'_{tx}/3h) - (2(M_{tx1} +M_{tx2})/ 3hL)$;

$a_{25} = (M_{tx}/12h^2 + M'_{tx}/12h) + ((M_{tx1} +M_{tx2})/ 12hL)$;

$b_{21} = -EI_y/6h^4$; $b_{22} = 2EI_y/h^4 + GK_t/12h^2$; $b_{23} = -13EI_y/2h^4 - 4GK_t/3h^2$; $b_{24} = 28EI_y/3h^4$;

$b_{25} = -13EI_y/2h^4 - 4GK_t/3h^2$; $b_{26} = 2EI_y/h^4 + GK_t/12h^2$; and $b_{27} = -EI_y/6h^4$.

Next. Define h to be a fraction of L. For this problem, L=75.0 in. and h=3.75 in. This gives 21 locations. K matrix is shown in Table 12. Boundary conditions are associated with locations 1 and 21, and ghost boundary conditions are associated with locations 2,3, 19, and 20. The term ghost is because columns are extended out by two more imaginary locations beyond the boundary location. This allows modifying the equations to identify where supports are pinned or fixed. For example, the term a_{14} extended out two terms beyond the boundary gives the two terms a_{12} and a_{11}, The modified term $^*a_{14}$ in the location of term a_{14}, and $^*a_{14} = a_{14} - a_{12}$; and $^*a_{15} = a_{15} – a_{11}$, if support is pinned. For fixed support, $^*a_{14} = a_{14} + a_{12}$; and $^*a_{15} = a_{15} + a_{11}$ $^*b_{13}$, $^*a_{23}$, $^*b_{24}$, and $^*b_{25}$ also need to be determined.

Table 12. Central Diff. K Matrix for Buckling Limit. Investigation 3

1		2		3		Location →					
u	ϕ	u	ϕ	u	ϕ						
0.0	0.0	0.0	0.0	0.0							→ Supports at locations 1 and 21
0.0	0.0	0.0									→ Zero out boundary
0.0	0.0	$^*a_{14}$	b_{13}	$^*a_{15}$	b_{14}	a_{16}	b_{15}	a_{17}	0.0	0.0	
0.0	0.0	a_{23}	b_{24}	a_{24}	b_{25}	a_{25}	b_{26}	0.0	b_{27}	0.0	
0.0	0.0	a_{13}	b_{12}	a_{14}	b_{13}	a_{15}	b_{14}	a_{16}	b_{15}	a_{17}	
0.0	0.0	a_{22}	b_{23}	a_{23}	b_{24}	a_{24}	b_{25}	a_{25}	b_{26}	0.0	
0.0	0.0	a_{12}	b_{11}	a_{13}	b_{12}	a_{14}	b_{13}	a_{15}	b_{14}	a_{16}	
0.0	0.0	a_{21}	b_{22}	a_{22}	b_{23}	a_{23}	b_{24}	a_{24}	b_{25}	a_{25}	

Main diagonal

M_{tx} is the moment at the left end of an element because the element is being held there. M_{tx1} is also the moment at the left end while M_{tx2} is the moment at the right end of an element. Signs are opposite, typically. M'_{tx} is equal to the slope of the moment. $M' = R_1$ or R_2.

$$R_1L - M_{tx1} - PL_2 + M_{tx2} = 0 \quad [50]$$

$$R_2L - M_{tx2} - PL_1 + M_{tx1} = 0 \quad [51]$$

When dealing with a point load and discontinuity at its location, the slope is the same for each location to the left or right of the point load.

Once values are assigned to all matrix locations including the shear moment location, solve the determinant of the matrix while increasing P_2 each time. When the matrix determinant value changes signs, the determinant has crossed zero and P_2 has reached the critical buckling limit. Value of P_{cr} with shear, P_2, for this problem is 2.7 kips.

The governing equations for deflections when considering lateral torsional buckling are:

$B_x v'' - \phi M_{ty} = M_{tx}$

$B_y u'' - \phi M_{tx} = M_{ty}$

$C_w \phi''' - (C_t + M_x\beta)\phi' - M_{tx} u' - M_{ty} v' - (M_{tx1} + M_{tx2})u/L - (M_{ty1} + M_{ty2})v/L + P(y_0/2)\phi = 0$

Solve the modified equations of equilibrium simultaneously using a fourth order central difference approach and aforementioned central difference expressions. These terms are substituted into our modified lateral-torsion equations to obtain:

$B_x(-v_2 + 16v_1 - 30v_0 + 16v_{-1} - v_{-2}) - \phi_0 M_{ty} = M_{tx}$

$B_y(-u_2 + 16u_1 - 30u_0 + 16u_{-1} - u_{-2}) - \phi_0 M_{tx} = M_{ty}$

$C_w(-\Phi_3 + 8\phi_2 - 13\phi_1 + 13\phi_{-1} - 8\phi_{-2} + \phi_{-3})/8h^3 - (C_t + M_x\beta)(-\phi_2 + 8\phi_1 - 8\phi_{-1} + \phi_{-2})$

$- M_{tx}(-u_2 + 8u_1 - 8u_{-1} + u_{-2}) - M_{ty}(-v_2 + 8v_1 - 8v_{-1} + v_{-2})$

$-(M_{tx1} + M_{tx2})u_0/L - (M_{ty1} + M_{ty2})v_0/L + P(y_0/2)\phi_0 = 0$

Setting M_y to zero,

$a_{11}v_{-2} + a_{12}v_{-1} + a_{13}v_0 + a_{14}v_1 + a_{15}v_2 = M_{tx}$ [52a]

Where $a_{11} = -EI_x/12h^2$; $a_{12} = 4EI_x/3h^2$; $a_{13} = -5EI_x/2h^2$; $a_{14} = 4EI_x/3h^2$; $a_{15} = -EI_x/12h^2$;

$B_{21}u_{-2} + b_{22}u_{-1} + b_{23}u_0 + b_{24}u_1 + b_{25}u_2 + c_{21}\phi_0 = 0.0$ [52b]

Where $b_{21} = -EI_x/12h^2$; $b_{22} = 4EI_x/3h^2$; $b_{23} = -5EI_x/2h^2$; $b_{24} = 4EI_x/3h^2$; $b_{25} = -EI_x/12h^2$;

$c_{21} = -M_{tx}$

$b_{31}u_{-2} + b_{32}u_{-1} + b_{33}u_0 + b_{34}u_1 + b_{35}u_2 + c_{31}\phi_{-3} + c_{32}\phi_{-2} + c_{33}\phi_{-1} + c_{34}\phi_0 + c_{35}\phi_1 + c_{36}\phi_2 + c_{37}\phi_1 = 0.0$

[52c]

where $b_{31} = -M_{tx}/12h$; $b_{32} = 2M_{tx}/3h$; $b_{33} = -(M_{tx1} + M_{tx2})/L$; $b_{34} = -2M_{tx}/3h$; $b_{35} = M_{tx}/12h$;

$c_{31} = C_w/8h^3$; $c_{32} = -C_w/h^3 - C_t/12h$; $c_{33} = 13C_w/8h^3 + 2C_t/3h$; $c_{34} = Py_0/2$;

$c_{35} = -13C_w/8h^3 - 2C_t/3h$; $c_{36} = C_w/h^3 + C_t/12h$; $c_{37} = -C_w/8h^3$.

For the vertical deflection values, use the same approach, just demonstrated for the buckling limit except use the three governing equations and the load vector is not set to zero. [K]u = F. So solve for the deflections using the inverse K matrix, $u = [K]^{-1} F$. The vector u contains the unknowns v, u, and phi along the member. K matrix is demonstrated in Table 13.

Table 13. Central Difference K Matrix for Deflections. Investigation 3

Location 1			**Location 2**			**Location 3**			**Location 4**		
V	**u**	**ϕ**	**v**	**u**	**ϕ**	**v**	**u**	**ϕ**	**v**	**u**	**ϕ**
0.0	0.0	0.0	0.0	0.0	0.0	0.0	0.0	0.0	0.0	0.0	0.0
0.0	0.0	0.0	0.0	0.0	0.0	0.0	0.0	0.0	0.0	0.0	0.0
0.0	0.0	0.0	0.0	0.0	0.0	0.0	0.0	0.0	0.0	0.0	0.0
0.0	0.0	0.0	*a_{13}	0.0	0.0	a_{14}	0.0	0.0	a_{15}	0.0	0.0
0.0	0.0	0.0	0.0	b_{33}	c_{34}	0.0	b_{34}	c_{35}	0.0	b_{35}	c_{36}
0.0	0.0	0.0	0.0	b_{23}	c_{21}	0.0	b_{24}	0.0	0.0	b_{25}	0.0
0.0	0.0	0.0	a_{12}	0.0	0.0	a_{13}	0.0	0.0	a_{14}	0.0	0.0
0.0	0.0	0.0	0.0	b_{32}	c_{33}	0.0	b_{33}	c_{34}	0.0	b_{34}	c_{35}
0.0	0.0	0.0	0.0	b_{22}	0.0	0.0	b_{23}	c_{21}	0.0	b_{24}	0.0

Main diagonal

Zero out boundaries

For this problem, we used h=1.5 inches and 71 locations. Vertical deflections were tabulated based upon given info and applied P_2 loads from laboratory. See Table 14

Table 14. Vertical Deflections. Investigation 3. Central Difference

	32.5" from support	32.5" from support	29" from support	29" from support	4" from support	4" from support
Load P, kips	$v_{1w/s}$(in.)	$v_{1w/o}$	$v_{2w/s}$	$v_{2w/o}$	$v_{3w/s}$	$v_{3w/o}$
0.00	0.00	0.00	0.00	0.00	0.00	0.00
.3464	.0897	.0759	.0779	.0655	.0063	.005
.5803	.1502	.1272	.1306	.1098	.0106	.0084
.8144	.2108	.1786	.1833	.1541	.0149	.0118
1.047	.2710	.2296	.2356	.1980	.0192	.0152
1.245	.3222	.2729	.2801	.2355	.0228	.0181
1.418	.3671	.3109	.3190	.2682	.0259	.0206
1.617	.4187	.3546	.3639	.3060	.0296	.0235
1.794	.4644	.3933	.4036	.3393	.0328	.0261
2.028	.5250	.4446	.4563	.3836	.0371	.0295
2.326	.6022	.5101	.5234	.4400	.0426	.0338
2.656	.6876	.5824	.5976	.5025	.0486	.0386

2.3.2 Central Difference Solution Without Shear Deformation

For this approach, we use the three central difference governing equations previously developed to determine vertical, horizontal, and lateral deflection values along the beam. M_x=$M_{bending}$ and Ps=0. The ends of the conjugate beam are pinned-pinned. So, Boundary conditions are set for pinned-pinned in the finite difference model.

Problem 2.3.2. Lab Investigation 3

Given: 4"x4"x1/4" fiberglass reinforced plastic beam in Figure 6. L=75". E=2997ksi. I_x = 7.935 in.^{4}. G = 450 ksi . I_y = 2.67 in.^{4} . k_t =.0612. A = 2.85 in^2. I_w = 9.375 in. ^{6}.

Find: Buckling limit and vertical deflections without shear.

For vertical deflections without shear, we simply do not apply the shear moment to the beam. In other words $M_s = 0.0$ and $M_{tx} = M_{xbending}$. Procedure is exactly same as calculating critical load and vertical deflection outlined in previous problem which included shear. However, P loads from lab experiments are P_1 not P_2. Therefore, $M_{cr} = 13.73P_1$ for this problem. P_1 equals 3.2 kips at the buckling limit calculated using this approach M_{tx} = 43.97 k-in. and vertical deflections are shown in Table 14.

2.3.3 ASCE LRFD Method

The ASCE buckling limit equation was developed using the classical approach solution for a simple beam solution introduced by Galambos. The LTB equations used in the classical approach were

$$EI_y u^{IV} + M_{tx} \phi'' + 2M'_{tx} \phi' = 0 \qquad [53]$$

And the 4th order solution of the third order equation of lateral deflection is

$$EI_w \phi^{IV} - (Gk_t + M_x \beta) \phi'' - M_x u'' - M'_x \beta_x \phi = 0 \qquad [54]$$

The LRFD approach and equations used here-in may be found in the ASCE LRFD Design Guide for Pultruded Members.

$$M_n = C_b (\pi^2 E_{Lf} I_y D_j/L_b^2 + \pi^4 E_{Lf} I_y C_w/L_b^4)^{.5} \qquad [55]$$

where $D_j = Gk_t$; $C_w = I_w$; and $C_b = 12.5M_{max}/(2.5M_{max}+3M_A+4M_B+3M_C)$.

Problem 2.3.3. Lab Investigation 3

Given: 4”x4”x1/4” fiberglass reinforced plastic beam in Figure 6. L=75”. E=2997ksi. I_x = 7.935 in.^{4}. G = 450 ksi . I_y = 2.67 in.^{4} . k_t =.0612. A = 2.85 in^2. I_w = 9.375 in. ^{6}.

Find: Buckling limit.

The ASCE-LRFD equation for lateral-torsional buckling moment for an I-shaped cross section is

$$M_n = C_b (\pi^2 E_{Lf} I_y D_j/L_b^2 + \pi^4 E_{Lf} I_y C_w/L_b^4)^{.5}$$

where L_b is the braced length,

C_w is the warping constant,

E_{LF} is the Modulus Elasticity of the longitudinal flange,

$D_J = Gk_t$ and is the torsional rigidity, and

$C_b = 12.5M_{max}/(2.5M_{max}+3M_A+4M_B+3M_C)$

and is the moment modification factor.

M_A, M_B and M_C are moments at locations .25L, .5L, and .75L, respectively. See Figure 11.

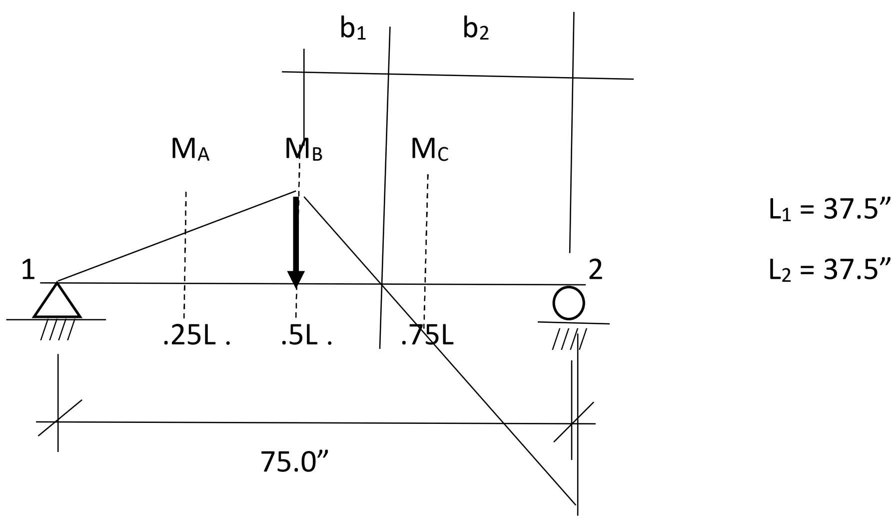

Figure 11. Moment Diagram for Investigation 3

Location of M_{max} varies with location of point load and equilibrium conditions. For this problem, $M_{max} = M_B = 13.73P$ and $M_2 = 10.04$. Plugging in moment values, $C_b = 1.46$. Plugging in given values and C_b, $M_n = 51.53$ k-in.

Knowing the relationship between the critical moment and critical load, P_1, without shear moment; we can calculate the critical load, P_1.

$P_1 = M_n/ 13.73 = 3.75$ kips

Now. We must find the relationship of P_1, the critical load without shear moment, and P_2, the critical load with shear moment.

P_1 is associated with the moments on the conjugate beam when M_s is not present. P_2 is associated with the moments on the conjugate beam when P_s is present. The resultant of the moments on the conjugate beam when considering and not considering shear moment is of the same value or:

$$.5\,(13.73P_1)L_1 + .5(13.73P_1)\,b_1 + .5(10.045P_1)\,b_2 = .5\,(13.73P_1)L_1 + .5(13.73P_1)\,b_1 + .5(10.045P_1)\,b_2 + P_s \qquad [62]$$

Rearranged and solved, we get $P_2/P_1 = .843$. Therefore, $P_2 = 3.16$ kips

2.3.4 Summary of Maximum Loads

Critical loads are summarized in Table 15 and will be compared to experimental load in Chapter 4. Deflections will be compared also

Table 15. Summary of Buckling Loads. Investigation 3

Section	Method	P_{cr}
2.3.1	Central Difference with Shear	2.7 kips
2.3.2	Central Difference without Shear	3.2 kips
2.3.3	ASCE_LRFD Buckling Limit	3.16 kips

2.4 Stability Analysis for Two Span Beam with Point Load Midspan. Spans Near Equal.

Numerical formulations for the critical buckling load and translational and rotational deflections are presented for Investigation 4 in this section. Numerical methods include fourth order central difference. Critical buckling load as determined from the ASCE-LRFD Prestandard is also presented. Beam loading with boundary conditions and moments on conjugate beam are defined in Figures 12.

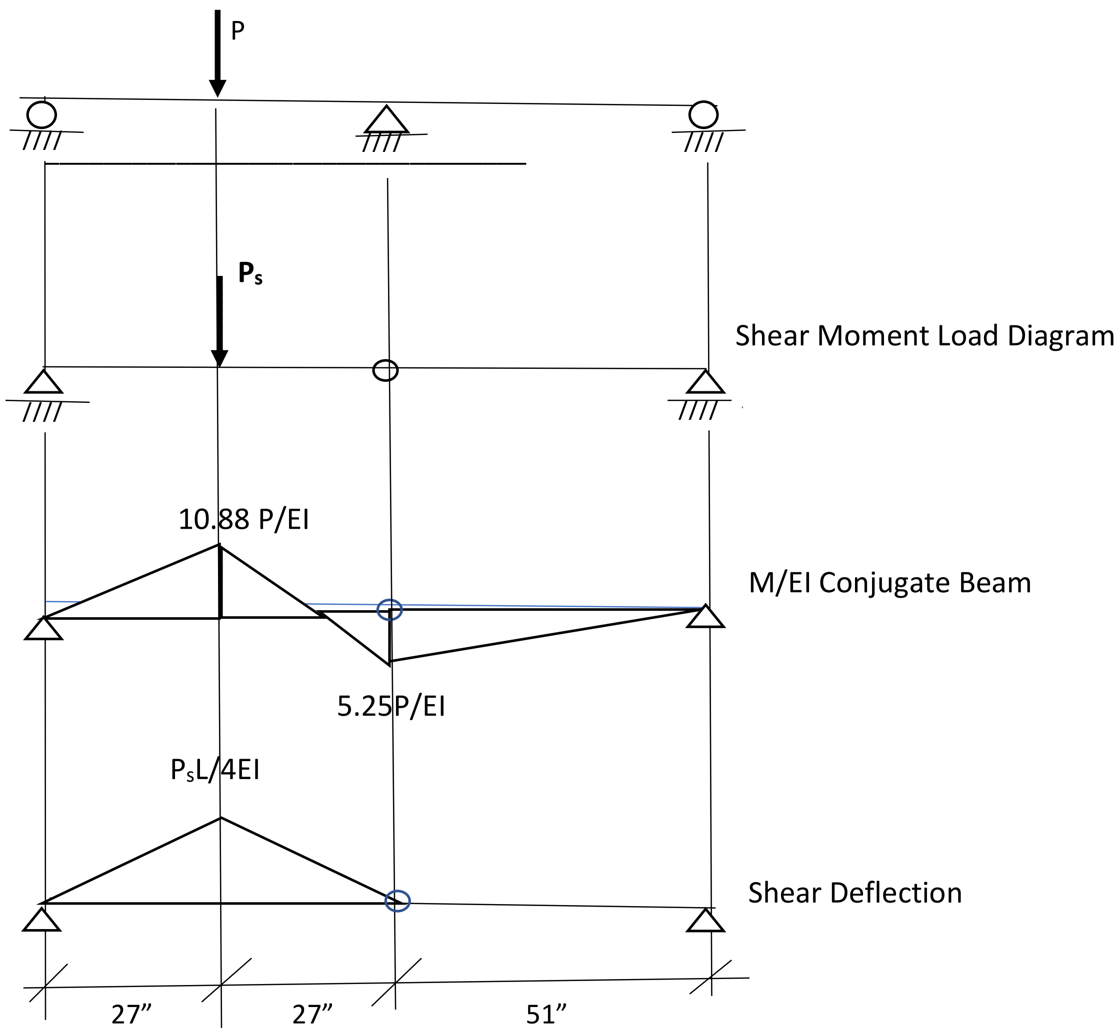

Figure 12. Investigation 4: Deflection Diagrams

2.4.1 Central Difference Solution With Shear Deformation

For this approach, use the three central difference governing equations previously developed to determine vertical, horizontal and lateral deflection values along the beam. $M_x = M_{tx}$. For this approach, follow the instructions of Timoshenko to the letter. Simply place the Shear moment point load on the conjugate beam. The ends of the conjugate beam are pinned-pinned. So, boundary conditions are set for pinned-pinned in the finite difference model. Depending up on the length of an element of eccentricity, the shear moment P_s value varies from model to model. $P_s = P_2\, \alpha EI_x/(eAG)$ where e is the eccentricity or length of the element. With shear, $M_{tx} = M_{bending} + P_s$ on the conjugate beam.

Problem 2.4.1. Lab Investigation 4

Given: 3”x3” x ¼” fiberglass reinforced plastic beam in Figure 7. L=54”. E=2997 ksi. Ix= 3.17in.^{4}. G = 450 ksi. I_y = 1.13 in.^{4}. k_t = .046. A = 2.13 in^2. I_w = 2.13 in.^{6}.

Find: Buckling limit and vertical deflections with shear.

As shown in Galambos, the 4th order solution of the second order bending equilibrium equation including the angle of twist is:

$$EI_y u^{IV} + M_{tx} \phi'' + 2M'_{tx} \phi' = 0 \quad [46]$$

And the 4th order solution of the third order equation of lateral deflection is

$$EI_w \phi^{IV} + Gk_t \phi'' - M_{tx} u'' - M'_{tx} u' - (M'_{tx1} + M'_{tx2})\, u/L - (M_{tx1} + M_{tx2})\, u'/L = 0 \quad [47]$$

Both equations take into consideration that M'_{tx} is not zero for a beam with a point load. Symmetrical properties of I beam have also been taken into consideration. Next, plug the 4th order central difference terms into the aforementioned lateral-torsion equations of equilibrium and obtain

$$a_{17}u_3 + a_{16}u_2 + a_{15}u_1 + a_{14}u_0 + a_{13}u_{-1} + a_{12}u_{-2} + a_{11}u_{-3} + b_{15}\phi_2 + b_{14}\phi_1 + b_{13}\phi_0 + b_{12}\phi_{-1} + b_{11}\phi_{-2} = 0$$

[48]

$$a_{25}u_2 + a_{24}u_1 + a_{23}u_0 + a_{22}u_{-1} + a_{21}u_{-2} + b_{27}\phi_3 + b_{26}\phi_2 + b_{25}\phi_1 + b_{24}\phi_0 + b_{23}\phi_{-1} + b_{22}\phi_{-2} + b_{21}\phi_{-3} = 0$$

[49]

where $a_{11} = -EI_y/6h^4$; $a_{12} = 2EI_y/h^4$; $a_{13} = -13EI_y/2h^4$; $a_{14} = 28EI_y/3h^4$; $a_{15} = -13EI_y/2h^4$;

$a_{16} = 2EI_y/h^4$; $a_{17} = -EI_y/6h^4$; $b_{11} = (-M_{tx}/12h^2 + M'_{tx}/6h)$; $b_{12} = (4M_{tx}/3h^2 -4\ M'_{tx}/3h)$;

$b_{13} = -(5M_{tx}/2h^2$; $b_{14} = (4M_{tx}/3h^2 + 4\ M'_{tx}/3h)$; and $b_{15} = -(M_{tx}/12h^2 + M'_{tx}/6h)$, and

$a_{21} = (M_{tx}/12h^2 - M'_{tx}/12h) – ((M_{tx1} +M_{tx2})/ 12hL)$;

$a_{22} = (-4M_{tx}/3h^2 + 2M'_{tx}/3h) + (2(M_{tx1} +M_{tx2})/ 3hL)$; $a_{23} = (5M_{tx}/2h^2 - ((M'_{tx1} +M'_{tx2})/ L)$;

$a_{24} = (-4M_{tx}/3h^2 - 2M'_{tx}/3h) - (2(M_{tx1} +M_{tx2})/ 3hL)$;

$a_{25} = (M_{tx}/12h^2 + M'_{tx}/12h) + ((M_{tx1} +M_{tx2})/ 12hL)$;

$b_{21} = -EI_y/6h^4$; $b_{22} = 2EI_y/h^4 + GK_t/12h^2$; $b_{23} = -13EI_y/2h^4 - 4GK_t/3h^2$; $b_{24} = 28EI_y/3h^4$;

$b_{25} = -13EI_y/2h^4 - 4GK_t/3h^2$; $b_{26} = 2EI_y/h^4 + GK_t/12h^2$; and $b_{27} = -EI_y/6h^4$.

Next. We define h to be a fraction of L. For this problem, L=54 in. and h=2.7 in. This gives us 21 locations. K matrix shown in table 16. Boundary conditions are associated locations 1 and 21, and ghost boundary conditions are associated with locations 2,3, 19, and 20. The term ghost is because columns extend out by two more imaginary locations beyond the boundary locations. This allows us to modify equations to identify whether supports are pinned or fixed. For example, the term a_{14} extended out two terms beyond the boundary gives us the two terms a_{12} and a_{11}. The modified term $*a_{14}$ goes in the location of term a_{14}, and $*a_{14} = a_{14} - a_{12}$; and $*a_{15} = a_{15} – a_{11}$, if support is pinned. For fixed support, $*a_{14} = a_{14} + a_{12}$; and $*a_{15} = a_{15} + a_{11}$. $*b_{13}$, $*a_{23}$, $*b_{24}$, and $*b_{25}$ also need to be determined.

Table 16. Central Difference K Matrix for Buckling Limit. Investigation 4

1		2		3		Location →					
u	ϕ	u	ϕ	u	ϕ						
0.0	0.0	0.0	0.0	0.0							→ Supports at locations 1 and 21
0.0	0.0	0.0									→ Zero out boundary
0.0	0.0	$*a_{14}$	b_{13}	$*a_{15}$	b_{14}	a_{16}	b_{15}	a_{17}	0.0	0.0	
0.0	0.0	a_{23}	b_{24}	a_{24}	b_{25}	a_{25}	b_{26}	0.0	b_{27}	0.0	
0.0	0.0	a_{13}	b_{12}	a_{14}	b_{13}	a_{15}	b_{14}	a_{16}	b_{15}	a_{17}	
0.0	0.0	a_{22}	b_{23}	a_{23}	b_{24}	a_{24}	b_{25}	a_{25}	b_{26}	0.0	
0.0	0.0	a_{12}	b_{11}	a_{13}	b_{12}	a_{14}	b_{13}	a_{15}	b_{14}	a_{16}	
0.0	0.0	a_{21}	b_{22}	a_{22}	b_{23}	a_{23}	b_{24}	a_{24}	b_{25}	a_{25}	
↓	↓										↘ Main diagonal

M_{tx} is the moment at the left end of an element because the element is being held there. M_{tx1} is also the moment at the left end while M_{tx2} is the moment at the right end of an element. Signs are opposite, typically. M'_{tx} is equal to the slope of the moment. $M' = R_1$ or R_2.

$$R_1L - M_{tx1} - PL_2 + M_{tx2} = 0 \quad [50]$$

$$R_2L - M_{tx2} - PL_1 + M_{tx1} = 0 \quad [51]$$

When dealing with a point load and discontinuity at its location, the slope is the same for each location to the left or right of the point load. Once values are assigned to all matrix locations including the shear moment location, solve the determinant of the matrix while increasing P_2 each time. When the matrix determinant value changes signs, the determinant has crossed zero and P_2 has reached the critical buckling limit. Value of P_{cr} with shear, P_2, for this problem is 2.3 kips.

The governing equations for deflections when considering lateral torsional buckling are:

$B_x v'' - \phi M_{ty} = M_{tx}$

$B_y u'' - \phi M_{tx} = M_{ty}$

$C_w \phi''' - (C_t + M_x\beta) \phi' - M_{tx} u' - M_{ty} v' - (M_{tx1} + M_{tx2}) u/L - (M_{ty1} + M_{ty2}) v/L + P(y_0/2) \phi = 0$

Solve the modified equations of equilibrium simultaneously using a fourth order central difference approach and aforementioned central difference expressions. These terms are substituted into our modified lateral-torsion equations to obtain:

$B_x (-v_2 + 16v_1 - 30v_0 + 16 v_{-1} - v_{-2}) - \phi_0 M_{ty} = M_{tx}$

$B_y (-u_2 + 16u_1 - 30u_0 + 16 u_{-1} - u_{-2}) - \phi_0 M_{tx} = M_{ty}$

$C_w (- \Phi_3 + 8\phi_2 - 13\phi_1 + 13\phi_{-1} - 8\phi_{-2} + \phi_{-3})/8h^3 - (C_t + M_x\beta) (-\phi_2 + 8\phi_1 - 8\phi_{-1} + \phi_{-2})$

$- M_{tx} (-u_2 + 8u_1 - 8u_{-1} + u_{-2}) - M_{ty} (-v_2 + 8v_1 - 8v_{-1} + v_{-2})$

$- (M_{tx1} + M_{tx2}) u_0/L - (M_{ty1} + M_{ty2}) v_0/L + P(y_0/2) \phi_0 = 0$

Setting M_y to zero,

$a_{11}v_{-2} + a_{12}v_{-1} + a_{13}v_0 + a_{14}v_1 + a_{15}v_2 = M_{tx}$ [52a]

Where $a_{11} = -EI_x/12h^2$; $a_{12} = 4EI_x/3h^2$; $a_{13} = -5EI_x/2h^2$; $a_{14} = 4EI_x/3h^2$; $a_{15} = -EI_x/12h^2$;

$B_{21}u_{-2} + b_{22}u_{-1} + b_{23}u_0 + b_{24}u_1 + b_{25}u_2 + c_{21}\phi_0 = 0.0$ [52b]

where $b_{21} = -EI_x/12h^2$; $b_{22} = 4EI_x/3h^2$; $b_{23} = -5EI_x/2h^2$; $b_{24} = 4EI_x/3h^2$; $b_{25} = -EI_x/12h^2$;

$c_{21} = - M_{tx}$

$b_{31}u_{-2} + b_{32}u_{-1} + b_{33}u_0 + b_{34}u_1 + b_{35}u_2 + c_{31}\phi_{-3} + c_{32}\phi_{-2} + c_{33}\phi_{-1} + c_{34}\phi_0 + c_{35}\phi_1 + c_{36}\phi_2 + c_{37}\phi_1 = 0.0$

[52c]

where $b_{31} = -M_{tx}/12h$; $b_{32} = 2M_{tx}/3h$; $b_{33} = -(M_{tx1} + M_{tx2})/L$; $b_{34} = -2M_{tx}/3h$; $b_{35} = M_{tx}/12h$;

$c_{31} = C_w/8h^3$; $c_{32} = - C_w/h^3 - C_t/12h$; $c_{33} = 13C_w/8h^3 + 2C_t/3h$; $c_{34} = Py_0/2$;

$c_{35} = -13C_w/8h^3 - 2C_t/3h$; $c_{36} = C_w/h^3 + C_t/12h$; $c_{37} = - C_w/8h^3$.

For the vertical deflection values, use the same approach just demonstrated for the buckling limit except use the three governing equations and the load vector is not set to zero. $[K]u = F$. So solve for the deflections using the inverse K matrix, $u = [K]^{-1} F$. The vector u contains the unknowns v, u, and phi along the member. K matrix is demonstrated in Table 17.

Table 17. Central Difference K Matrix for Deflections. Investigation 4

Location 1			Location 2			Location 3			Location 4		
V	u	ϕ	v	u	ϕ	v	u	ϕ	v	u	ϕ
0.0	0.0	0.0	0.0	0.0	0.0	0.0	0.0	0.0	0.0	0.0	0.0
0.0	0.0	0.0	0.0	0.0	0.0	0.0	0.0	0.0	0.0	0.0	0.0
0.0	0.0	0.0	0.0	0.0	0.0	0.0	0.0	0.0	0.0	0.0	0.0
0.0	0.0	0.0	*a_{13}	0.0	0.0	a_{14}	0.0	0.0	a_{15}	0.0	0.0
0.0	0.0	0.0	0.0	b_{33}	c_{34}	0.0	b_{34}	c_{35}	0.0	b_{35}	c_{36}
0.0	0.0	0.0	0.0	b_{23}	c_{21}	0.0	b_{24}	0.0	0.0	b_{25}	0.0
0.0	0.0	0.0	a_{12}	0.0	0.0	a_{13}	0.0	0.0	a_{14}	0.0	0.0
0.0	0.0	0.0	0.0	b_{32}	c_{33}	0.0	b_{33}	c_{34}	0.0	b_{34}	c_{35}
0.0	0.0	0.0	0.0	b_{22}	0.0	0.0	b_{23}	c_{21}	0.0	b_{24}	0.0

Main diagonal

Zero out boundaries

For this problem, we used h=1.5 inches and 71 locations. Vertical deflections were tabulated based upon given info and applied P_2 loads from laboratory. See Table 18.

Table 18. Vertical Deflections. Investigation 4. Central Difference

	21.5" from support		19" from support		4" from support	
Load P, kips	$v_{1w/s}$(in.)	$v_{1w/o}$	$v_{2w/s}$	$v_{2w/o}$	$v_{3w/s}$	$v_{3w/o}$
0.00	0.00	0.00	0.00	0.00	0.00	0.00
.2770	.0770	.0664	.0625	.0540	.0097	.0083
.6562	.1824	.1572	.1481	.1280	.0231	.0197
.8359	.2324	.2003	.1887	.1630	.0294	.0251
1.006	.2796	.2410	.2270	.1961	.0354	.0302
1.154	.3208	.2765	.2605	.2251	.0406	.0347
1.385	.385	.3318	.3126	.2701	.0487	.0416
1.571	.4368	.3765	.3546	.3064	.0553	.0472
1.733	.4817	.4152	.3911	.3379	.0609	.0521
2.038	.5664	.4883	.4599	.3974	.0717	.0613
2.341	.6508	.5610	.5284	.4566	.0823	.0704
2.5	.695	.5991	.5643	.4876	.0879	.0751
2.65	.7366	.6350	.5981	.5168	.0932	.0797

2.4.2 Central Difference Solution Without Shear Deformation

For this approach, we use the three central difference governing equations previously developed to determine vertical, horizontal, and lateral deflection values along the beam. M_x= $M_{bending}$ and Ps=0. The ends of the conjugate beam are pinned-pinned. So, boundary conditions are set for pinned-pinned in the finite difference model.

Problem 2.4.2. Lab Investigation 4

Given: 3"x3" x ¼" fiberglass reinforced plastic beam in Figure 7. L=54". E=2997 ksi. Ix= 3.17in.^{4}. G = 450 ksi. I_y = 1.13 in.^{4}. k_t = .046. A = 2.13 in^2. I_w = 2.13 in.^{6}.

Find: Buckling limit and vertical deflections without shear.

For vertical deflections without shear, we simply do not apply the shear moment to the beam. In other words $P_s = 0.0$ and $M_{tx} = M_{bending}$. Procedure is exactly same as calculating critical load and vertical deflection outlined in previous problem which included shear. However, P loads from lab experiments are P_1 not P_2. Therefore, $M_{cr} = 10.9P$ for this problem. P_1 equals 2.63 kips at the buckling limit calculated using this approach. $M_{tx} = 28.67$ k-in. and vertical deflections are shown in Table 18.

2.4.3 ASCE LRFD Method

The ASCE buckling limit equation was developed using the classical approach solution for a simple beam solution introduced by Galambos. The LTB equations used in the classical approach were

$$EI_y u^{IV} + M_{tx} \phi'' + 2M'_{tx} \phi' = 0 \qquad [53]$$

And the 4th order solution of the third order equation of lateral deflection is

$$EI_w \phi^{IV} - (Gk_t + M_x \beta) \phi'' - M_x u'' - M'_x \beta_x \phi = 0 \qquad [54]$$

The LRFD approach and equations used here-in may be found in the ASCE LRFD Design Guide for Pultruded Members.

$$M_n = C_b (\pi^2 E_{L f} I_y D_j/L_b^2 + \pi^4 E_{Lf} I_y C_w/L_b^4)^{.5} \qquad [55]$$

where $D_j = Gk_t$; $C_w = I_w$; and $C_b = 12.5M_{max}/(2.5M_{max}+3M_A+4M_B+3M_C)$.

Problem 2.4.3. Lab Investigation 4

Given: 3”x3” x ¼” fiberglass reinforced plastic beam in Figure 7. L=54”. E=2997 ksi. I_x= 3.17in.^{4}. G = 450 ksi. I_y = 1.13 in.^{4}. k_t = .046. A = 2.13 in^2. I_w = 2.13 in.^{6}.

Find: Buckling limit.

The ASCE-LRFD equation for lateral-torsional buckling moment of an I-shaped cross section is

$$M_n = C_b (\pi^2 E_{L f} I_y D_j/L_b^2 + \pi^4 E_{Lf} I_y C_w/L_b^4)^{.5}$$

Where L_b is the braced length,

C_w is the warping constant,

E_{LF} is the Modulus Elasticity of the longitudinal flange,

$D_j = Gk_t$ and is the torsional rigidity, and

$C_b = 12.5M_{max}/(2.5M_{max}+3M_A+4M_B+3M_C)$

And is the moment modification factor.

M_A, M_B and M_C are moments at locations .25L, .5L, and .75L, respectively. See Figure 13

Location of M_{max} varies with location of point load and equilibrium conditions. For this problem, $M_{max} = M_B = 10.9P$ and $M_2 = 5.2P$. Plugging in moment values, $C_b = 1.42$. Plugging in given values and C_b, M_n= 32.89 kips.

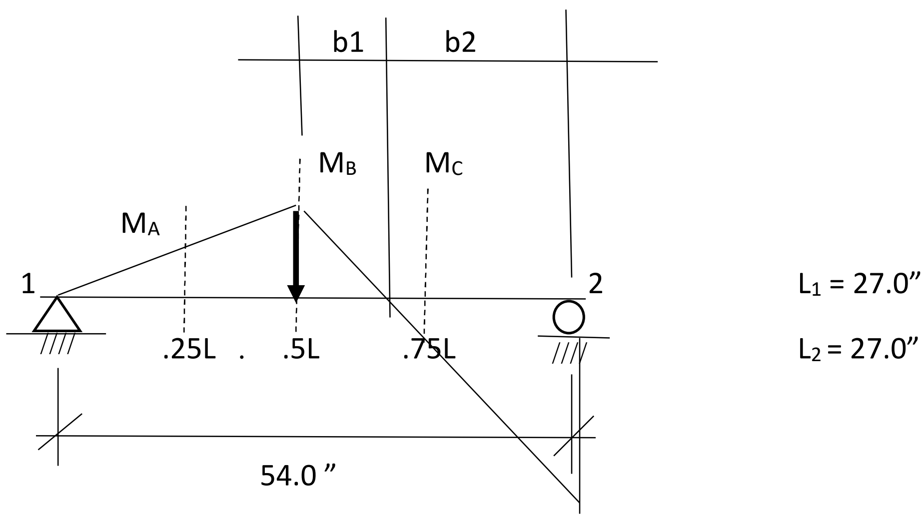

Figure 13. Moment Diagram for Investigation 4

Knowing the relationship between the critical moment and critical load, P_1, without shear moment; we can calculate the critical load, P_1.

$P_1 = M_n/10.9 = 3.02$ kips

Now. We must find the relationship of P_1, the critical load without shear moment, and P_2, the critical load with shear moment.

P_1 is associated with the moments on the conjugate beam when P_s is not present. P_2 is associated with the moments on the conjugate beam when M_s is present. The resultant of the moment on conjugate the beam when considering and not considering shear moment is of the same value or

$$.5(10.9P_1)L_1 + .5(10.9P_1)\, b_1 - .5(5.2P_1)\, b_2 = .5(10.9P_2)L_1 + .5(10.9P_2)\, b_1 - .5(5.2P_2)\, b_2 + P_s$$

Rearranged and solved, we get $P_2/P_1 = .873$. Therefore, $P_2 = 2.64$ kips.

2.4.4 Summary of Maximum Loads

Critical loads are summarized in Table 19 and will be compared to experimental load in Chapter. Deflections will be compared also. P_{cr}

Table 19. Summary of Critical Buckling Loads. Investigation 4

Section	Method	P_{cr}
2.4.1	Central Difference with Shear Deformation	2.3 kips
2.4.2	Central Difference without Shear Deformation	2.63 kips
2.4.3	ASCE-LRFD Method	2.64 kips

2.5 Stability Analysis for Two Span Beam with Point Load Off Center

Numerical formulations for the critical buckling load and translational and rotational deflections are presented for Investigation 5 in this section. Numerical methods formulated are sine approximation and fourth order central difference. Critical buckling load as determined from the ASCE-LRFD Prestandard is also presented. Beam loading with boundary conditions and moments on conjugate beam are defined in Figures 14.

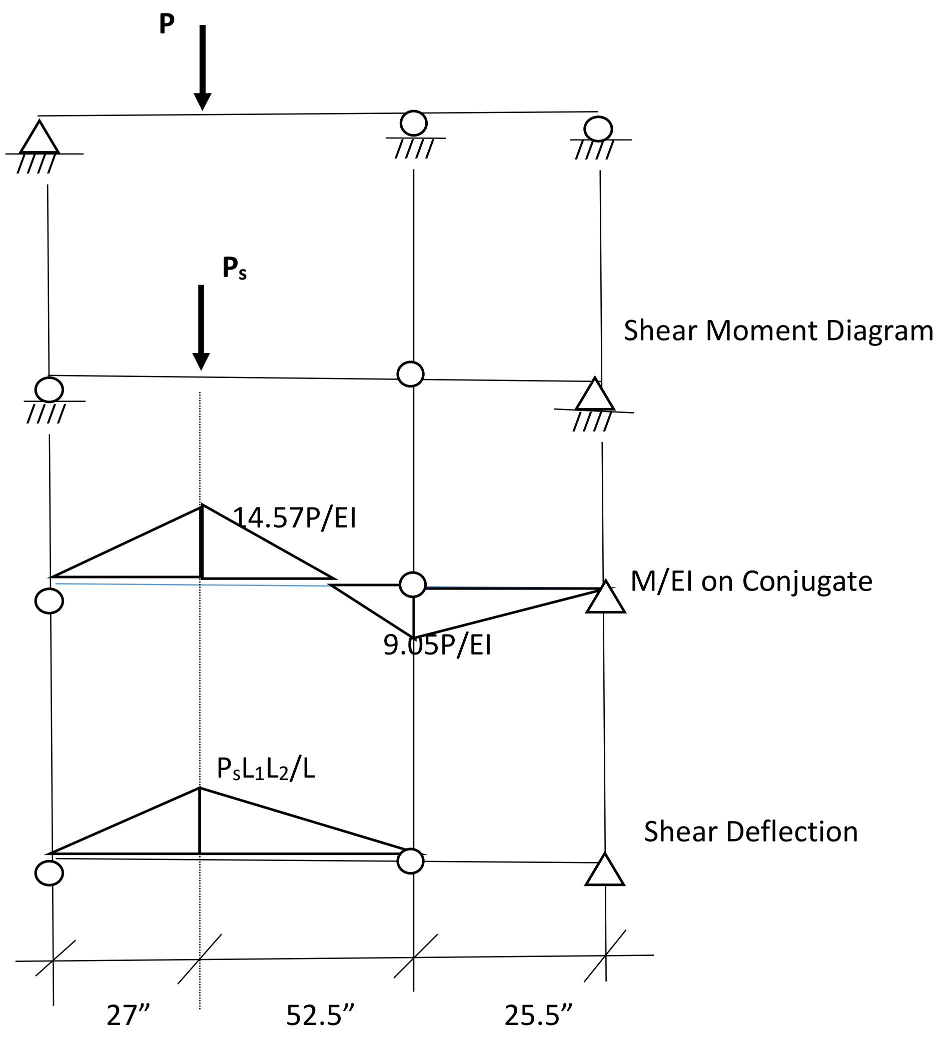

Figure 14. Investigation 5: Deflection Diagrams

Stability Analysis using Central Difference approach will be presented for beam shown in Figure 12, then ASCE LRFD guidelines buckling solution will be presented.

2.5.1 Central Difference Solution With Shear Deformation

For this approach, use the three central difference governing equations previously developed to determine vertical, horizontal and lateral deflection values along the beam. $M_x = M_{tx}$. For this approach, follow the instructions of Timoshenko to the letter. Simply place the Shear moment point load on the conjugate beam. The ends of the conjugate beam are pinned-pinned. So, boundary conditions are set for pinned-pinned in the finite difference model. Depending up on the length of an element of eccentricity, the shear moment P_s value varies from model to model. $P_s = P_2\ \alpha EI_x/(eAG)$ where e is the eccentricity or length of the element. With shear, $M_{tx} = M_{bending} + P_s$ on the conjugate beam.

Problem 2.5.1. Lab Investigation 5

Given: 3"x3" x ¼" fiberglass reinforced plastic beam in Figure 8. L= 79.5". E = 2997 ksi. I_x = 3.17 in.^{4}. G = 450 ksi. I_y = 1.13 in.^{4}. k = .046. A = 2.13 in.^{2}. I_w = 2.13 in.^{6}.

Find: Buckling limit and vertical deflections with shear.

As shown in Galambos, the 4th order solution of the second order bending equilibrium equation including the angle of twist is:

$$EI_y u^{IV} + M_{tx}\phi'' + 2M'_{tx}\phi' = 0 \qquad [46]$$

And the 4th order solution of the third order equation of lateral deflection is

$$EI_w \phi^{IV} + Gk_t\phi'' - M_{tx}u'' - M'_{tx}u' - (M'_{tx1} + M'_{tx2})\,u/L - (M_{tx1} + M_{tx2})\,u'/L = 0 \qquad [47]$$

Both equations take into consideration that M'_{tx} is not zero for a beam with a point load. Symmetrical properties of I beam have also been taken into consideration. Next, plug the 4th order central difference terms into the aforementioned lateral-torsion equations of equilibrium and obtain

$$a_{17}u_3 + a_{16}u_2 + a_{15}u_1 + a_{14}u_0 + a_{13}u_{-1} + a_{12}u_{-2} + a_{11}u_{-3} + b_{15}\phi_2 + b_{14}\phi_1 + b_{13}\phi_0 + b_{12}\phi_{-1} + b_{11}\phi_{-2} = 0 \qquad [48]$$

$a_{25}u_2 + a_{24}u_1 + a_{23}u_0 + a_{22}u_{-1} + a_{21}u_{-2} + b_{27}\phi_3 + b_{26}\phi_2 + b_{25}\phi_1 + b_{24}\phi_0 + b_{23}\phi_{-1} + b_{22}\phi_{-2} + b_{21}\phi_{-3} = 0$

[49]

where $a_{11} = -EI_y/6h^4$; $a_{12} = 2EI_y/h^4$; $a_{13} = -13EI_y/2h^4$; $a_{14} = 28EI_y/3h^4$; $a_{15} = -13EI_y/2h^4$;
$a_{16} = 2EI_y/h^4$; $a_{17} = -EI_y/6h^4$; $b_{11} = (-M_{tx}/12h^2 + M'_{tx}/6h)$; $b_{12} = (4M_{tx}/3h^2 - 4\ M'_{tx}/3h)$;
$b_{13} = -(5M_{tx}/2h^2$; $b_{14} = (4M_{tx}/3h^2 + 4\ M'_{tx}/3h)$; and $b_{15} = -(M_{tx}/12h^2 + M'_{tx}/6h)$, and
$a_{21} = (M_{tx}/12h^2 - M'_{tx}/12h) – ((M_{tx1} + M_{tx2})/\ 12hL)$;
$a_{22} = (-4M_{tx}/3h^2 + 2M'_{tx}/3h) + (2(M_{tx1} + M_{tx2})/\ 3hL)$; $a_{23} = (5M_{tx}/2h^2 - ((M'_{tx1} + M'_{tx2})/\ L)$;
$a_{24} = (-4M_{tx}/3h^2 - 2M'_{tx}/3h) - (2(M_{tx1} + M_{tx2})/\ 3hL)$;
$a_{25} = (M_{tx}/12h^2 + M'_{tx}/12h) + ((M_{tx1} + M_{tx2})/\ 12hL)$;
$b_{21} = -EI_y/6h^4$; $b_{22} = 2EI_y/h^4 + GK_t/12h^2$; $b_{23} = -13EI_y/2h^4 - 4GK_t/3h^2$; $b_{24} = 28EI_y/3h^4$;
$b_{25} = -13EI_y/2h^4 - 4GK_t/3h^2$; $b_{26} = 2EI_y/h^4 + GK_t/12h^2$; and $b_{27} = -EI_y/6h^4$.

Next. We define h to be a fraction of L. For this problem. L=79.5 in. and h=3.97 in. This gives us 21 locations. K matrix set up shown in Table 20. Boundary conditions are associated locations 1 and 21, and ghost boundary conditions are associated with locations 2,3,19 and 20. The term ghost is because columns extend out by two more imaginary locations beyond the boundary locations. This allows us to modify equations to identify whether supports are pinned or fixed. For example, the term a_{14} extended out two terms beyond the boundary gives us the two terms a_{12} and a_{11}. The modified term $*a_{14}$ goes in the location of term a_{14}, and $*a_{14} = a_{14} - a_{12}$; and $*a_{15} = a_{15} – a_{11}$, if support is pinned. For fixed support, $*a_{14} = a_{14} + a_{12}$; and $*a_{15} = a_{15} + a_{11}$. $*b_{13}$, $*a_{23}$, $*b_{24}$, and $*b_{25}$ also need to be determined.

Table 20. Central Difference K Matrix for Buckling. Investigation 5

1		2		3		Location →					
u	ϕ	u	ϕ	u	ϕ						
0.0	0.0	0.0	0.0	0.0							→ Supports at locations 1 and 21
0.0	0.0	0.0									→ Zero out boundary
0.0	0.0	*a_{14}	b_{13}	*a_{15}	b_{14}	a_{16}	b_{15}	a_{17}	0.0	0.0	
0.0	0.0	a_{23}	b_{24}	a_{24}	b_{25}	a_{25}	b_{26}	0.0	b_{27}	0.0	
0.0	0.0	a_{13}	b_{12}	a_{14}	b_{13}	a_{15}	b_{14}	a_{16}	b_{15}	a_{17}	
0.0	0.0	a_{22}	b_{23}	a_{23}	b_{24}	a_{24}	b_{25}	a_{25}	b_{26}	0.0	
0.0	0.0	a_{12}	b_{11}	a_{13}	b_{12}	a_{14}	b_{13}	a_{15}	b_{14}	a_{16}	
0.0	0.0	a_{21}	b_{22}	a_{22}	b_{23}	a_{23}	b_{24}	a_{24}	b_{25}	a_{25}	

Main diagonal

M_{tx} is the moment at the left end of an element because the element is being held there. M_{tx1} is also the moment at the left end while M_{tx2} is the moment at the right end of an element. Signs are opposite, typically. M'_{tx} is equal to the slope of the moment. $M' = R_1$ or R_2.

$$R_1L - M_{tx1} - PL_2 + M_{tx2} = 0 \quad [50]$$

$$R_2L - M_{tx2} - PL_1 + M_{tx1} = 0 \quad [51]$$

When dealing with a point load and discontinuity at its location, the slope is the same for each location to the left or right of the point load. Once values are assigned to all matrix locations including the shear moment location, solve the determinant of the matrix while increasing P_2 each time. When the matrix determinant value changes signs, the determinant has crossed zero and P_2 has reached the critical buckling limit. Value of P_{cr} with shear, P_2, for this problem is 1.08 kips.

The governing equations for deflections when considering lateral torsional buckling are:

$B_x v'' - \phi M_{ty} = M_{tx}$

$B_y u'' - \phi M_{tx} = M_{ty}$

$C_w \phi''' - (C_t + M_x\beta)\phi' - M_{tx} u' - M_{ty} v' - (M_{tx1} + M_{tx2})u/L - (M_{ty1} + M_{ty2})v/L + P(y_0/2)\phi = 0$

Solve the modified equations of equilibrium simultaneously using a fourth order central difference approach and aforementioned central difference expressions. These terms are substituted into our modified lateral-torsion equations to obtain:

$B_x(-v_2 + 16v_1 - 30v_0 + 16v_{-1} - v_{-2}) - \phi_0 M_{ty} = M_{tx}$

$B_y(-u_2 + 16u_1 - 30u_0 + 16u_{-1} - u_{-2}) - \phi_0 M_{tx} = M_{ty}$

$C_w(-\Phi_3 + 8\phi_2 - 13\phi_1 + 13\phi_{-1} - 8\phi_{-2} + \phi_{-3})/8h^3 - (C_t + M_x\beta)(-\phi_2 + 8\phi_1 - 8\phi_{-1} + \phi_{-2})$

$- M_{tx}(-u_2 + 8u_1 - 8u_{-1} + u_{-2}) - M_{ty}(-v_2 + 8v_1 - 8v_{-1} + v_{-2})$

$- (M_{tx1} + M_{tx2})u_0/L - (M_{ty1} + M_{ty2})v_0/L + P(y_0/2)\phi_0 = 0$

Setting M_y to zero,

$a_{11}v_{-2} + a_{12}v_{-1} + a_{13}v_0 + a_{14}v_1 + a_{15}v_2 = M_{tx}$ [52a]

where $a_{11} = -EI_x/12h^2$; $a_{12} = 4EI_x/3h^2$; $a_{13} = -5EI_x/2h^2$; $a_{14} = 4EI_x/3h^2$; $a_{15} = -EI_x/12h^2$;

$B_{21}u_{-2} + b_{22}u_{-1} + b_{23}u_0 + b_{24}u_1 + b_{25}u_2 + c_{21}\phi_0 = 0.0$ [52b]

where $b_{21} = -EI_x/12h^2$; $b_{22} = 4EI_x/3h^2$; $b_{23} = -5EI_x/2h^2$; $b_{24} = 4EI_x/3h^2$; $b_{25} = -EI_x/12h^2$;

$c_{21} = -M_{tx}$

$b_{31}u_{-2} + b_{32}u_{-1} + b_{33}u_0 + b_{34}u_1 + b_{35}u_2 + c_{31}\phi_{-3} + c_{32}\phi_{-2} + c_{33}\phi_{-1} + c_{34}\phi_0 + c_{35}\phi_1 + c_{36}\phi_2 + c_{37}\phi_1 = 0.0$

[52c]

where $b_{31} = -M_{tx}/12h$; $b_{32} = 2M_{tx}/3h$; $b_{33} = -(M_{tx1} + M_{tx2})/L$; $b_{34} = -2M_{tx}/3h$; $b_{35} = M_{tx}/12h$;

$c_{31} = C_w/8h^3$; $c_{32} = -C_w/h^3 - C_t/12h$; $c_{33} = 13C_w/8h^3 + 2C_t/3h$; $c_{34} = Py_0/2$;

$c_{35} = -13C_w/8h^3 - 2C_t/3h$; $c_{36} = C_w/h^3 + C_t/12h$; $c_{37} = -C_w/8h^3$.

For the vertical deflection values, use the same approach just demonstrated for the buckling limit except use the three governing equations and the load vector is not set to zero. [K]u = F. So, solve for the deflections using the inverse K matrix, $u = [K]^{-1} F$. The vector u contains the unknowns v, u, and phi along the member. K matrix is demonstrated in Table 21.

Table 21. Central Difference K Matrix for Deflections. Investigation 5

Location 1			Location 2			Location 3			Location 4		
V	u	ϕ	v	u	ϕ	v	u	ϕ	v	u	ϕ
0.0	0.0	0.0	0.0	0.0	0.0	0.0	0.0	0.0	0.0	0.0	0.0
0.0	0.0	0.0	0.0	0.0	0.0	0.0	0.0	0.0	0.0	0.0	0.0
0.0	0.0	0.0	0.0	0.0	0.0	0.0	0.0	0.0	0.0	0.0	0.0
0.0	0.0	0.0	*a_{13}	0.0	0.0	a_{14}	0.0	0.0	a_{15}	0.0	0.0
0.0	0.0	0.0	0.0	b_{33}	c_{34}	0.0	b_{34}	c_{35}	0.0	b_{35}	c_{36}
0.0	0.0	0.0	0.0	b_{23}	c_{21}	0.0	b_{24}	0.0	0.0	b_{25}	0.0
0.0	0.0	0.0	a_{12}	0.0	0.0	a_{13}	0.0	0.0	a_{14}	0.0	0.0
0.0	0.0	0.0	0.0	b_{32}	c_{33}	0.0	b_{33}	c_{34}	0.0	b_{34}	c_{35}
0.0	0.0	0.0	0.0	b_{22}	0.0	0.0	b_{23}	c_{21}	0.0	b_{24}	0.0

Main diagonal

Zero out boundaries

For this problem, we used h=1.5 inches and 71 locations. Vertical deflections were tabulated in Table 22 based upon given info and applied P_2 loads from laboratory.

Table 22. Vertical Deflections. Investigation 5. Central Difference

	5” from support		22” from support		35” from support	
Load P, kips	$v_{1w/s}$(in.)	$v_{1w/o}$	$v_{2w/s}$	$v_{2w/o}$	$v_{3w/s}$	$v_{3w/o}$
0.00	0.00	0.00	0.00	0.00	0.00	0.00
.2188	.00403	.0373	.1230	.1126	.1419	.13084
.4293	.079	.0732	.2413	.2209	.2785	.2567
.6399	.1178	.1091	.3597	.3292	.4151	.3827
.8488	.1562	.1447	.4772	.4367	.5507	.5076
1.056	.1944	.180	.5937	.5434	.6851	.6316
1.211	.2228	.2063	.6806	.6229	.7855	.7240
1.35	.2485	.2302	.7592	.6949	.8762	.8076
1.55	.2849	.2638	.8702	.7965	1.004	.9257

2.5.2 Central Difference Solution Without Shear Deformation

For this approach, we use the three central difference governing equations previously developed to determine vertical, horizontal, and lateral deflection values along the beam. Mx = $M_{bending}$ and $P_s = 0$. The ends of the conjugate beam are pinned-pinned. So, boundary conditions are set for pinned-pinned in the finite difference model.

Problem 2.5.5. Lab Investigation 5

Given: 3”x3” x ¼” fiberglass reinforced plastic beam in Figure 8. L= 79.5”. E = 2997 ksi. I_x = 3.17 in.^{4}. G = 450 ksi. I_y = 1.13 in.^{4}. k = .046. A = 2.13 in.^{2}. I_w = 2.13 in.^{6}.

Find: Buckling limit and vertical deflections without shear.

For vertical deflections without shear, we simply do not apply the shear moment to the beam. In other words P_s = 0.0 and $M_{tx} = M_{xbending}$. Procedure is exactly same as calculating critical load and vertical deflection outlined in previous problem which included shear. However, P loads from lab experiments are P_1 not P_2. Therefore, M_{cr} = 14.76P for this problem. See tabulated vertical deflection values for this problem in Table 22. P_1 equals 1.18 kips at the buckling limit calculated using this approach. M_{tx} = 17.40 k-

2.5.3 ASCE LRFD Method

The ASCE buckling limit equation was developed using the classical approach solution for a simple beam solution introduced by Galambos. The LTB equations used in the classical approach were

$EI_y u^{IV} + M_{tx} \phi'' + 2M'_{tx} \phi' = 0$ [53]

And the 4th order solution of the third order equation of lateral deflection is

$EI_w \phi^{IV} - (Gk_t + M_x \beta) \phi'' - M_x u'' - M'_x \beta_x \phi = 0$ [54]

The LRFD approach and equations used here-in may be found in the ASCE LRFD Design Guide for Pultruded Members.

$M_n = C_b (\pi^2 E_{Lf} I_y D_j/L_b^2 + \pi^4 E_{Lf} I_y C_w/L_b^4)^{.5}$ [55]

where $D_j = Gk_t$; $C_w = I_w$; and $C_b = 12.5M_{max}/(2.5M_{max}+3M_A+4M_B+3M_C)$.

Problem 2.5.3. Lab Investigation 5

Given: 3”x3” x ¼” fiberglass reinforced plastic beam in Figure 14. L= 79.5”. E = 2997 ksi.

$I_x = 3.17$ in. ^{4} . G = 450 ksi. $I_y = 1.13$ in.^{4}. k = .046. A = 2.13 in. ^{2} . $I_w = 2.13$ in. ^{6}.

Find: Buckling limit.

The ASCE-LRFD equation for lateral-torsional buckling moment of an I-shaped cross section is

$M_n = C_b (\pi^2 E_{Lf} I_y D_j/L_b^2 + \pi^4 E_{Lf} I_y C_w/L_b^4)^{.5}$

Where L_b is the braced length,

C_w is the warping constant,

E_{LF} is the Modulus Elasticity of the longitudinal flange,

$D_j = Gk_t$ and is the torsional rigidity, and

$C_b = 12.5M_{max}/(2.5M_{max}+3M_A+4M_B+3M_C)$.

And is the moment modification factor.

M_A, M_B and M_C are moments at locations .25L, .5L, and .75L, respectively. See Figure 15.

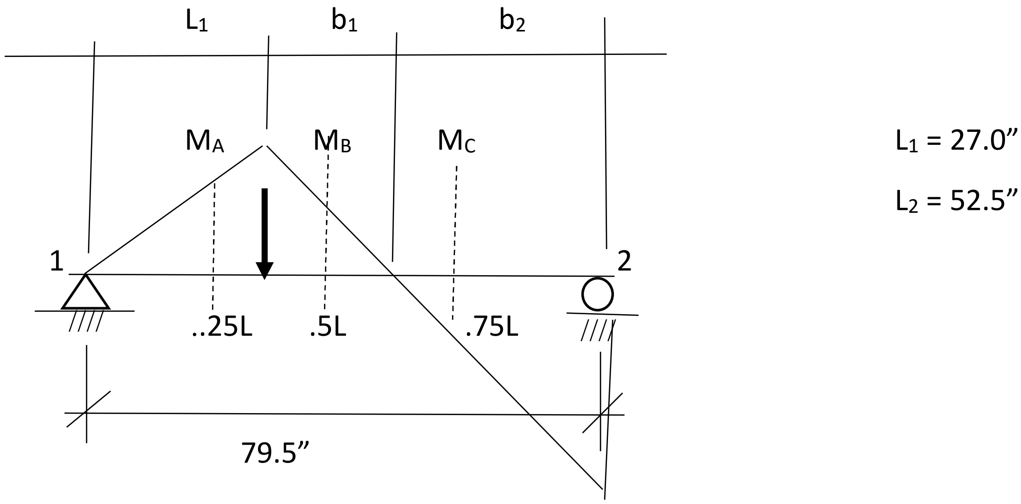

Figure 15. Moment Diagram for Investigation 5

Location of M_{max} varies with location of point load and equilibrium conditions. For this problem, M_{max} = 14.76P and M_2 = 9.05P. Plugging in moment values, we calculate C_b. Plugging in given values and C_b, M_n = 22.92 k=in. Knowing the relationship between the critical moment and critical load, P_1, without shear moment; we can calculate the critical load, P_1.

P_1 = 22.92/14.76 = 1.55 kips

Now. We must find the relationship of P_1, the critical load without shear moment, and P_2, the critical load with shear moment.

P_1 is associated with the moments on the conjugate beam when P_s is not present. P_2 is associate with the moments on the conjugate beam when M_x is present. The resultant of the moments on the conjugate beam when considering and not considering shear moment is of the same value or

$$.5(14.76P_1)L_1 + .5(14.76P_1)\,b_1 - .5(9.05P_1)\,b_2 = .5(14.76P_2)L_1 + .5(14.76P_2)\,b_1 - .5(9.05P_2)\,b_2 + P_s$$

Rearranged and solve, we get P_2/P_1 = .916. Therefore, P_2 = 1.42 kips

2.5.4 Summary of Maximum Loads

Critical loads are summarized in Table 23 and will be complared to experimental load in Chapter 4. Deflections will be compared also.

Table 23. Summary of Buckling Loads. Investigation 5

Section	Method	P_{cr}
2.5.1	Central Difference with Shear Deformation	1.08 kips
2.5.2	Central Difference without Shear Deformation	1.18 kips
2.5.3	ASCE-LRFD Method	1.42 kips

2.6 Stability Analysis for Three Span Beam with Point Load Midspan. Center Span

Numerical formulations for the critical buckling load and translational and rotational deflections are presented for Investigation 6 in this section. Numerical methods formulated are sine approximation and fourth order central difference. Critical buckling load as determined from the ASCE-LRFD prestandard is also presented. Beam loading with boundary conditions and moments on conjugate beam are defined in Figure 16.

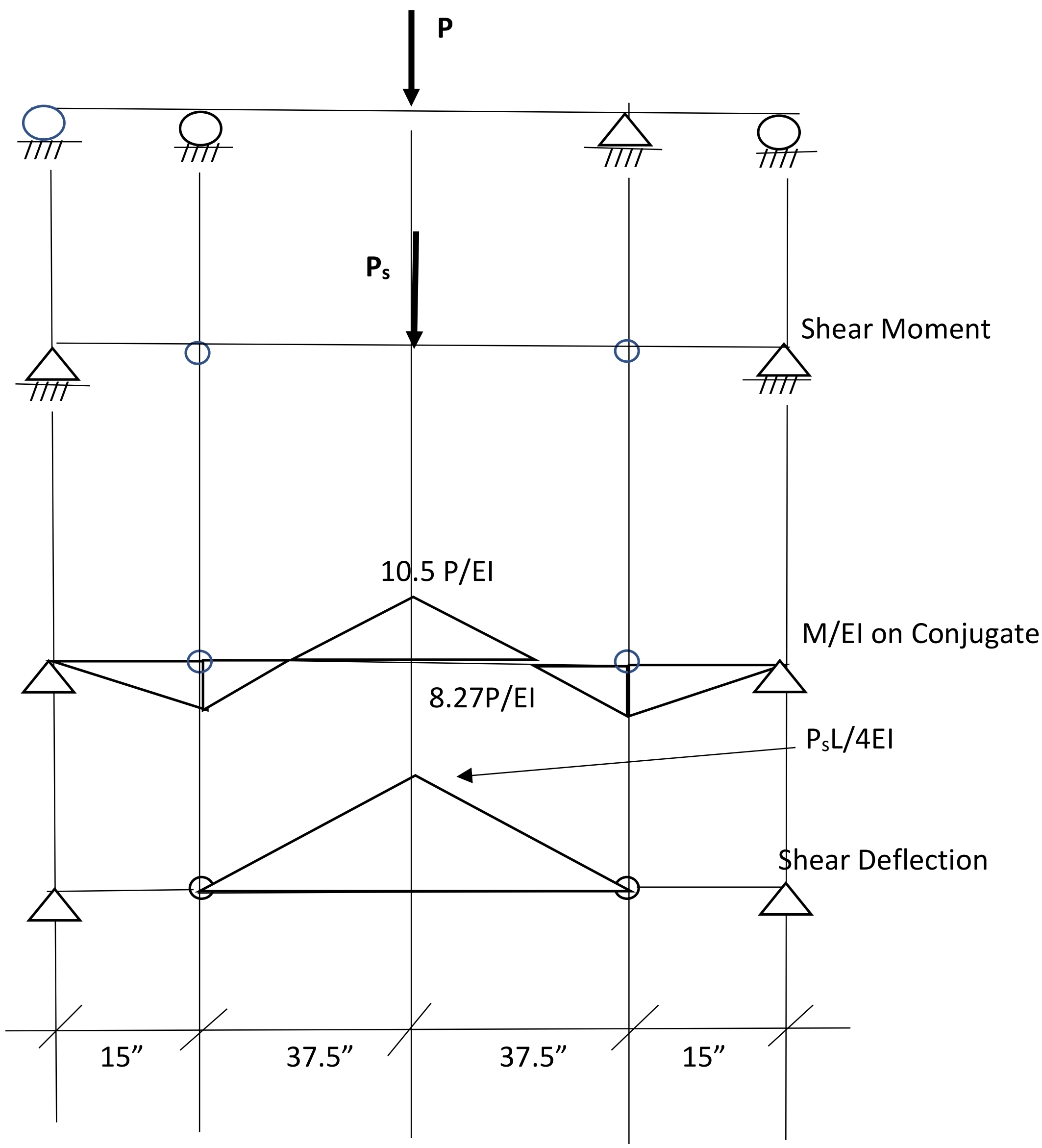

Figure 16. Investigation 6: Deflection Diagrams

2.6.1 Central Difference Solution with Shear Deformation

For this approach, use the three central difference governing equations previously developed to determine vertical, horizontal and lateral deflection values along the beam. $M_x = M_{tx}$. For this approach, follow the instructions of Timoshenko to the letter. Simply place the Shear moment point load on the conjugate beam. The ends of the conjugate beam are pinned-pinned. So, boundary conditions are set for pinned-pinned in the finite difference model. Depending up on the length of an element of eccentricity, the shear moment P_s value varies from model to model. $P_s = P_2\ \alpha EI_x/(eAG)$ where e is the eccentricity or length of the element. With shear, $M_{tx} = M_{bending} + P_s$ on the conjugate beam.

Problem 2.6.1. Lab Investigation 6

Given: 4"x4" x 1/4" fiberglass reinforced plastic beam in Figure 9. L=75". E=2997 ksi. I_x = 7.935 in.^{4}. G = 450 ksi. I_y = 2.67 in.^{4} . k_t = .0612. A = 2.85 in.^{2} . I_w = 9.375 in.^{4} .

Find: Buckling limit and vertical deflections with shear.

As shown in Galambos, the 4th order solution of the second order bending equilibrium equation including the angle of twist is:

$$EI_y u^{IV} + M_{tx}\phi'' + 2M'_{tx}\phi' = 0 \quad [46]$$

And the 4th order solution of the third order equation of lateral deflection is

$$EI_w \phi^{IV} + Gk_t\phi'' - M_{tx}u'' - M'_{tx}u' - (M'_{tx1} + M'_{tx2})\,u/L - (M_{tx1} + M_{tx2})\,u'/L = 0 \quad [47]$$

Both equations take into consideration that M'_{tx} is not zero for a beam with a point load. Symmetrical properties of I beam have also been taken into consideration. Next, plug the 4th order central difference terms into the aforementioned lateral-torsion equations of equilibrium and obtain

$$a_{17}u_3 + a_{16}u_2 + a_{15}u_1 + a_{14}u_0 + a_{13}u_{-1} + a_{12}u_{-2} + a_{11}u_{-3} + b_{15}\phi_2 + b_{14}\phi_1 + b_{13}\phi_0 + b_{12}\phi_{-1} + b_{11}\phi_{-2} = 0$$

[48]

$$a_{25}u_2 + a_{24}u_1 + a_{23}u_0 + a_{22}u_{-1} + a_{21}u_{-2} + b_{27}\phi_3 + b_{26}\phi_2 + b_{25}\phi_1 + b_{24}\phi_0 + b_{23}\phi_{-1} + b_{22}\phi_{-2} + b_{21}\phi_{-3} = 0$$

[49]

Where a_{11} = $-EI_y/6h^4$; a_{12} = $2EI_y/h^4$; a_{13} = $-13EI_y/2h^4$; a_{14} = $28EI_y/3h^4$; a_{15} = $-13EI_y/2h^4$;

a_{16} = $2EI_y/h^4$; a_{17} = $-EI_y/6h^4$; b_{11} = $(-M_{tx}/12h^2 + M'_{tx}/6h)$; b_{12} = $(4M_{tx}/3h^2 - 4 M'_{tx}/3h)$;

b_{13} = $-(5M_{tx}/2h^2$; b_{14} = $(4M_{tx}/3h^2 + 4 M'_{tx}/3h)$; and b_{15} = $-(M_{tx}/12h^2 + M'_{tx}/6h)$, and

a_{21} = $(M_{tx}/12h^2 - M'_{tx}/12h) – ((M_{tx1} + M_{tx2})/ 12hL)$;

a_{22} = $(-4M_{tx}/3h^2 + 2M'_{tx}/3h) + (2(M_{tx1} + M_{tx2})/ 3hL)$; a_{23} = $(5M_{tx}/2h^2 - ((M'_{tx1} + M'_{tx2})/ L)$;

a_{24} = $(-4M_{tx}/3h^2 - 2M'_{tx}/3h) - (2(M_{tx1} + M_{tx2})/ 3hL)$;

a_{25} = $(M_{tx}/12h^2 + M'_{tx}/12h) + ((M_{tx1} + M_{tx2})/ 12hL)$;

b_{21} = $-EI_y/6h^4$; b_{22} = $2EI_y/h^4 + GK_t/12h^2$; b_{23} = $-13EI_y/2h^4 - 4GK_t/3h^2$; b_{24} = $28EI_y/3h^4$;

b_{25} = $-13EI_y/2h^4 - 4GK_t/3h^2$; b_{26} = $2EI_y/h^4 + GK_t/12h^2$; and b_{27} = $-EI_y/6h^4$.

Next. We define h to be a fraction of L. For this problem, L=75.0 in. and h=3.75. This gives us 21 locations K matrix demonstrated in Table 24. Boundary conditions are associated locations 1 and 21, and ghost boundary conditions are associated with locations 2,3,19 and 20. The term ghost is because columns extend out by two more imaginary locations beyond the boundary locations. This allows us to modify equations to identify whether supports are pinned or fixed. For example, the term a_{14} extended out two terms beyond the boundary gives us the two terms a_{12} and a_{11}. The modified term $*a_{14}$ goes in the location of term a_{14}, and $*a_{14} = a_{14} - a_{12}$; and $*a_{15} = a_{15} – a_{11}$, if support is pinned. For fixed support, $*a_{14} = a_{14} + a_{12}$; and $*a_{15} = a_{15} + a_{11}$. $*b_{13}$, $*a_{23}$, $*b_{24}$, and $*b_{25}$ also need to be determined.

Table 24. Central Difference K Matrix for Buckling. Investigation 6

1		2		3		Location →					
u	ϕ	u	ϕ	u	ϕ						
0.0	0.0	0.0	0.0	0.0							→ Supports at locations 1 and 21
0.0	0.0	0.0									→ Zero out boundary
0.0	0.0	*a_{14}	b_{13}	*a_{15}	b_{14}	a_{16}	b_{15}	a_{17}	0.0	0.0	
0.0	0.0	a_{23}	b_{24}	a_{24}	b_{25}	a_{25}	b_{26}	0.0	b_{27}	0.0	
0.0	0.0	a_{13}	b_{12}	a_{14}	b_{13}	a_{15}	b_{14}	a_{16}	b_{15}	a_{17}	
0.0	0.0	a_{22}	b_{23}	a_{23}	b_{24}	a_{24}	b_{25}	a_{25}	b_{26}	0.0	
0.0	0.0	a_{12}	b_{11}	a_{13}	b_{12}	a_{14}	b_{13}	a_{15}	b_{14}	a_{16}	
0.0	0.0	a_{21}	b_{22}	a_{22}	b_{23}	a_{23}	b_{24}	a_{24}	b_{25}	a_{25}	

Main diagonal

M_{tx} is the moment at the left end of an element because the element is being held there. M_{tx1} is also the moment at the left end while M_{tx2} is the moment at the right end of an element. Signs are opposite, typically. M'_{tx} is equal to the slope of the moment. $M' = R_1$ or R_2.

$$R_1L - M_{tx1} - PL_2 + M_{tx2} = 0 \quad [50]$$

$$R_2L - M_{tx2} - PL_1 + M_{tx1} = 0 \quad [51]$$

When dealing with a point load and discontinuity at its location, the slope is the same for each location to the left or right of the point load. Once values are assigned to all matrix locations including the shear moment location, solve the determinant of the matrix while increasing P_2 each time. When the matrix determinant value changes signs, the determinant has crossed zero and P_2 has reached the critical buckling limit. Value of P_{cr} with shear, P_2, for this problem is 3.5 kips.

The governing equations for deflections when considering lateral torsional buckling are:

$B_x v'' - \phi M_{ty} = M_{tx}$

$B_y u'' - \phi M_{tx} = M_{ty}$

$C_w \phi''' - (C_t + M_x\beta)\phi' - M_{tx} u' - M_{ty} v' - (M_{tx1} + M_{tx2}) u/L - (M_{ty1} + M_{ty2}) v/L + P(y_0/2)\phi = 0$

Solve the modified equations of equilibrium simultaneously using a fourth order central difference approach and aforementioned central difference expressions. These terms are substituted into our modified lateral-torsion equations to obtain:

$B_x(-v_2 + 16v_1 - 30v_0 + 16v_{-1} - v_{-2}) - \phi_0 M_{ty} = M_{tx}$

$B_y(-u_2 + 16u_1 - 30u_0 + 16u_{-1} - u_{-2}) - \phi_0 M_{tx} = M_{ty}$

$C_w(-\Phi_3 + 8\phi_2 - 13\phi_1 + 13\phi_{-1} - 8\phi_{-2} + \phi_{-3})/8h^3 - (C_t + M_x\beta)(-\phi_2 + 8\phi_1 - 8\phi_{-1} + \phi_{-2})$

$- M_{tx}(-u_2 + 8u_1 - 8u_{-1} + u_{-2}) - M_{ty}(-v_2 + 8v_1 - 8v_{-1} + v_{-2})$

$- (M_{tx1} + M_{tx2}) u_0/L - (M_{ty1} + M_{ty2}) v_0/L + P(y_0/2)\phi_0 = 0$

Setting M_y to zero,

$a_{11}v_{-2} + a_{12}v_{-1} + a_{13}v_0 + a_{14}v_1 + a_{15}v_2 = M_{tx}$ [52a]

Where $a_{11} = -EI_x/12h^2$; $a_{12} = 4EI_x/3h^2$; $a_{13} = -5EI_x/2h^2$; $a_{14} = 4EI_x/3h^2$; $a_{15} = -EI_x/12h^2$;

$B_{21}u_{-2} + b_{22}u_{-1} + b_{23}u_0 + b_{24}u_1 + b_{25}u_2 + c_{21}\phi_0 = 0.0$ [52b]

where $b_{21} = -EI_x/12h^2$; $b_{22} = 4EI_x/3h^2$; $b_{23} = -5EI_x/2h^2$; $b_{24} = 4EI_x/3h^2$; $b_{25} = -EI_x/12h^2$;

$c_{21} = -M_{tx}$

$b_{31}u_{-2} + b_{32}u_{-1} + b_{33}u_0 + b_{34}u_1 + b_{35}u_2 + c_{31}\phi_{-3} + c_{32}\phi_{-2} + c_{33}\phi_{-1} + c_{34}\phi_0 + c_{35}\phi_1 + c_{36}\phi_2 + c_{37}\phi_1 = 0.0$

[52c]

where $b_{31} = -M_{tx}/12h$; $b_{32} = 2M_{tx}/3h$; $b_{33} = -(M_{tx1} + M_{tx2})/L$; $b_{34} = -2M_{tx}/3h$; $b_{35} = M_{tx}/12h$;

$c_{31} = C_w/8h^3$; $c_{32} = -C_w/h^3 - C_t/12h$; $c_{33} = 13C_w/8h^3 + 2C_t/3h$; $c_{34} = Py_0/2$;

$c_{35} = -13C_w/8h^3 - 2C_t/3h$; $c_{36} = C_w/h^3 + C_t/12h$; $c_{37} = -C_w/8h^3$.

For the vertical deflection values, use the same approach just demonstrated for the buckling limit except use the three governing equations and the load vector is not set to zero. $[K]u = F$. So solve for the deflections using the inverse K matrix, $u = [K]^{-1} F$. The vector u contains the unknowns v, u, and ϕ along the member. K matrix is demonstrated in Table 25.

Table 25. Central Difference K Matrix for Deflections. Investigation 6.

Location 1			**Location 2**			**Location 3**			**Location 4**		
V	**u**	**ϕ**	**v**	**u**	**ϕ**	**v**	**u**	**ϕ**	**v**	**u**	**ϕ**
0.0	0.0	0.0	0.0	0.0	0.0	0.0	0.0	0.0	0.0	0.0	0.0
0.0	0.0	0.0	0.0	0.0	0.0	0.0	0.0	0.0	0.0	0.0	0.0
0.0	0.0	0.0	0.0	0.0	0.0	0.0	0.0	0.0	0.0	0.0	0.0
0.0	0.0	0.0	*a_{13}	0.0	0.0	a_{14}	0.0	0.0	a_{15}	0.0	0.0
0.0	0.0	0.0	0.0	b_{33}	c_{34}	0.0	b_{34}	c_{35}	0.0	b_{35}	c_{36}
0.0	0.0	0.0	0.0	b_{23}	c_{21}	0.0	b_{24}	0.0	0.0	b_{25}	0.0
0.0	0.0	0.0	a_{12}	0.0	0.0	a_{13}	0.0	0.0	a_{14}	0.0	0.0
0.0	0.0	0.0	0.0	b_{32}	c_{33}	0.0	b_{33}	c_{34}	0.0	b_{34}	c_{35}
0.0	0.0	0.0	0.0	b_{22}	0.0	0.0	b_{23}	c_{21}	0.0	b_{24}	0.0

Main diagonal

Zero out boundaries

For this problem, we used h=1.5 inches and 71 locations. Vertical deflections were tabulated in Table 26 based upon given info and applied P_2 loads from laboratory.

Table 26. Vertical Deflections. Investigation 6. Central Difference

	7" from support		18.5" from support		32" from support	
Load P, kips	$v_{1w/s}$(in.)	$v_{1w/o}$	$v_{2w/s}$	$v_{2w/o}$	$v_{3w/s}$	$v_{3w/o}$
0.00	0.00	0.00	0.00	0.00	0.00	0.00
.2209	.0069	.0048	.0238	.0179	.0360	.0268
.6018	.0187	.013	.0648	.0488	.0982	.073
.9826	.0305	.0212	.1059	.0798	.1603	.1193
1.176	.0365	.0254	.1267	.0955	.1919	.1428
1.357	.0421	.0292	.1462	.1101	.2214	.1647
1.55	.0481	.0334	.1670	.1258	.2528	.1881
1.764	.0548	.0380	.1901	.1432	.2878	.2141
2.044	.0635	.0441	.2203	.1660	.3335	.2481
2.292	.0712	.0494	.247	.1860	.3739	.2781

2.6.2 Central Difference Solution Without Shear Deformation

For this approach, we use the three central difference governing equations previously developed to determine vertical, horizontal, and lateral deflection values along the beam.

$M_x = M_{bending}$ and $P_s = 0$.

The ends of the conjugate beam are pinned-pinned. So, boundary conditions are set for pinned-pinned in the finite difference model.

Problem 2.6.2. Lab Investigation 6

Given: 4”x4” x 1/4” fiberglass reinforced plastic beam in Figure 9. L=75”. E=2997 ksi. I_x = 7.935 in.^{4}. G = 450 ksi. I_y = 2.67 in.^{4} . k_t = .0612. A = 2.85 in.^{2} . I_w = 9.375 in.^{4} .

Find: Buckling limit and vertical deflections without shear.

For vertical deflections without shear, we simply do not apply the shear moment to the beam. In other words $P_s = 0.0$ and $M_{tx} = M_{xbending}$. Procedure is exactly same as calculating critical load and vertical deflection outlined in previous problem which included shear. However, P loads from lab experiments are P_1 not P_2. Therefore, M_{cr} = 10.48P for this problem. See tabulated vertical deflection values for this problem in Table 26. P_1 equals 6.05 kips at the buckling limit calculated using this approach. M_{tx} = 63.46 k-in.

2.6.3 ASCE LRFD Method

The ASCE buckling limit equation was developed using the classical approach solution for a simple beam solution introduced by Galambos. The LTB equations used in the classical approach were

$EI_y u^{IV} + M_{tx} \phi'' + 2M'_{tx} \phi' = 0$ [53]

And the 4th order solution of the third order equation of lateral deflection is

$EI_w \phi^{IV} – (Gk_t + M_x \beta) \phi'' - M_x u'' – M'_x \beta_x \phi = 0$ [54]

The LRFD approach and equations used here-in may be found in the ASCE LRFD Design Guide for Pultruded Members.

$M_n = C_b (\pi^2 E_{L f} I_y D_j/L_b^2 + \pi^4 E_{Lf} I_y C_w/L_b^4)^{.5}$ [55]

Where $D_j = Gk_t$; $C_w = I_w$; and $C_b = 12.5M_{max}/(2.5M_{max}+3M_A+4M_B+3M_C)$.

Problem 2.6.3. Lab Investigation 6

Given: 4"x4" x 1/4" fiberglass reinforced plastic beam in Figure 9. L=75". E=2997 ksi. I_x = 7.935 in.^{4}. G = 450 ksi. I_y = 2.67 in.^{4} . k_t = .0612. A = 2.85 in.^{2} . I_w = 9.375 in.^{4} .

Find: Buckling limit.

The ASCE-LRFD equation for lateral-torsional buckling moment of an I-shaped cross section is

$M_n = C_b (\pi^2 E_{L f} I_y D_j/L_b^2 + \pi^4 E_{Lf} I_y C_w/L_b^4)^{.5}$

Where L_b is the braced length,

C_w is the warping constant,

E_{LF} is the Modulus Elasticity of the longitudinal flange,

$D_j = Gk_t$, and is the torsional rigidity, and

$C_b = 12.5M_{max}/(2.5M_{max}+3M_A+4M_B+3M_C)$.

And is the moment modification factor.

M_A, M_B and M_C are moments at locations .25L, .5L, and .75L, respectively. See Figure 17.

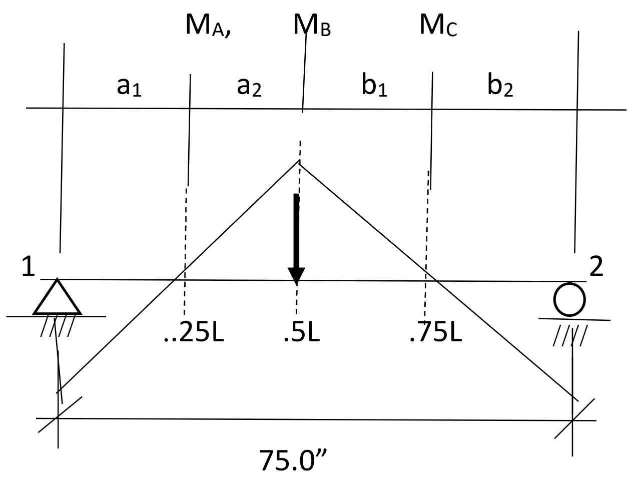

Figure 17. Moment Diagram for Investigation 6

Location of M_{max} varies with location of point load and equilibrium conditions. For this problem, $M_{max} = M_B = 10.48P$ and $M_2 = 8.27P$. Plugging in moment values, $C_b = 2.07$. Plugging in given values and C_b,

$M_n = 60.46$ k-in.

Knowing the relationship between the critical moment and critical load, P_1, without shear moment; we can calculate the critical load, P_1

$P_1 = 5.77$ k-in.

Now. We must find the relationship of P_1, the critical load without shear moment, and P_2, the critical load with shear moment. P_1 is associated with the moments on the conjugate beam when P_s is not present. P_2 is associated with the moments on the conjugate beam when P_s is present. The resultant of the moments on the conjugate beam when considering and not considering shear moment is of the same value or

$.5(10.48P_1)a2 + .5(10.48P_1)b_1 - .5(8.27P_1)b_2 - .5(8.27P_1)a1 = .5(10.48P_2)a2 + .5(10.48P_2)b_1 - .5(8.27P_2)b_2 - .5(8.27P_2)a1 + P_s$

Rearranged and solved, we get $P_2/P_1 = .578$. Therefore, $P_2 = 3.33$ kips.

2.6.4 Summary of Maximum Loads

Critical loads are summarized in Table 27 and will be compared to experimental load in Chapter. Deflections will be compared also.

Table 27. Summary of Buckling Loads. Investigation 6

Section	Method	P_{cr}
2.6.1	Central Difference with Shear Deformation	3.5 kips
2.6.2	Central Difference without Shear Deformation	6.05 kips
2.6.3	ASCE-LRFD Method	3.33 kips

2.7 Stability Analysis for Three Span Beam with Point Load Midspan. Outside Span.

Numerical formulations for the critical buckling load and translational and rotational deflections are presented for Investigation 7 in this section. Numerical methods formulated include fourth order central difference. Critical buckling load as determined from the ASCE-LRFD Prestandard is also presented. Beam loading with boundary conditions and moments on conjugate beam are defined in Figure 18.

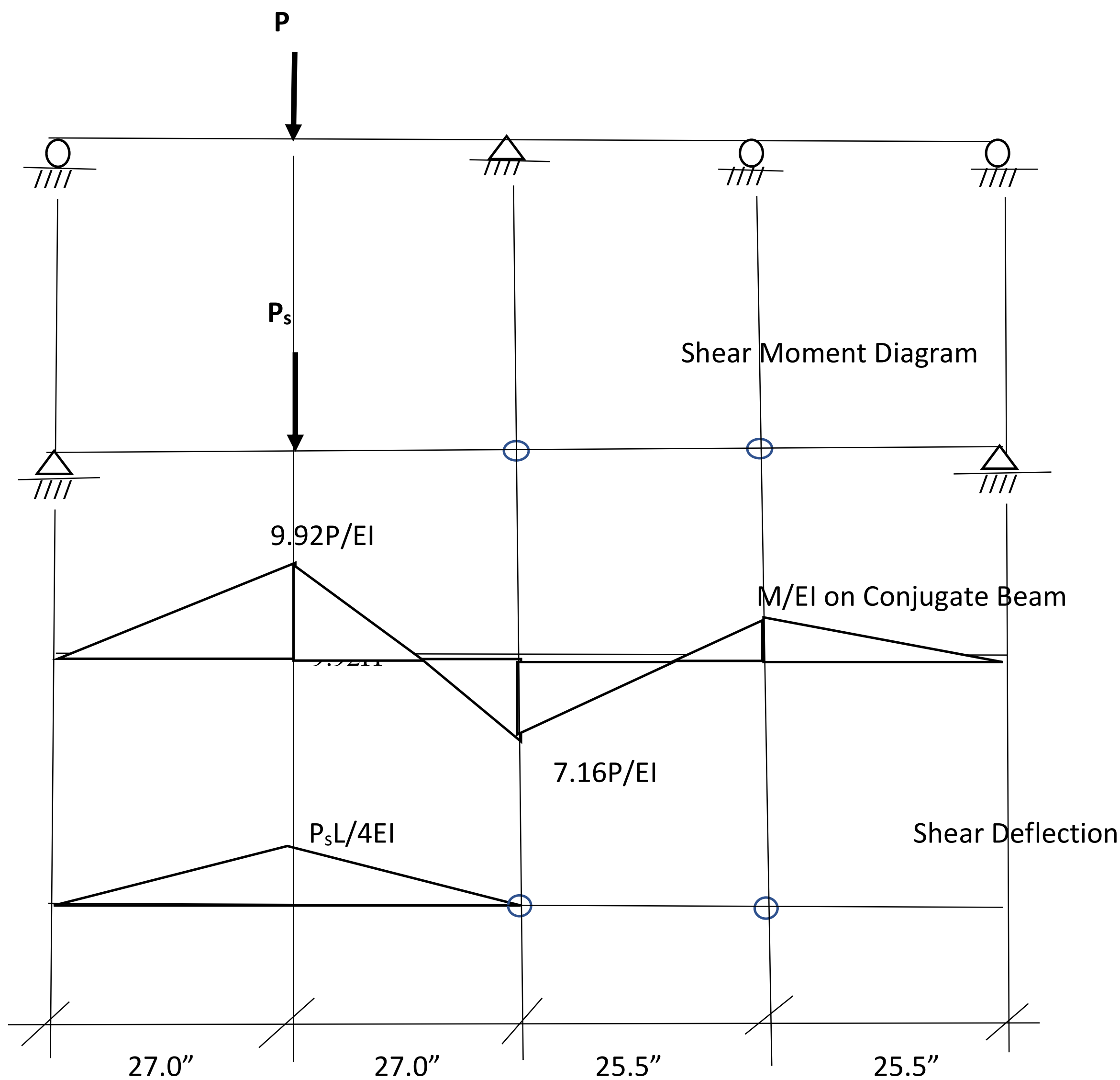

Figure 18. Investigation 7. Deflection Diagrams

2.7.1 Central Difference Solution With Shear Deformation

For this approach, use the three central difference governing equations previously developed to determine vertical, horizontal and lateral deflection values along the beam. $M_x = M_{tx}$. For this approach, follow the instructions of Timoshenko to the letter. Simply place the Shear moment point load on the conjugate beam. The ends of the conjugate beam are pinned-pinned. So, boundary conditions are set for pinned-pinned in the finite difference model. Depending up on the length of an element of eccentricity, the shear moment P_s value varies from model to model. $P_s = P_2\, \alpha EI_x/(eAG)$ where e is the eccentricity or length of the element. With shear, $M_{tx} = M_{bending} + P_s$ on the conjugate beam.

Problem 2.7.1. Lab Investigation 7

Given: 3”x3”x1/4” fiberglass reinforced plastic beam in Figure 18. L=54”. E=2997 ksi.

$I_x = 3.17$ in.^{4}. G = 450 ksi. $I_y = 1.13$ in.^{4}. k = .046. A = 2.13 in.^{2}. $I_w = 2.13$ in.^{6}.

Find: Buckling limit and vertical deflections with shear.

As shown in Galambos, the 4th order solution of the second order bending equilibrium equation including the angle of twist is:

$$EI_y u^{IV} + M_{tx} \phi'' + 2M'_{tx} \phi' = 0 \qquad [46]$$

And the 4th order solution of the third order equation of lateral deflection is

$$EI_w \phi^{IV} + Gk_t \phi'' - M_{tx} u'' - M'_{tx} u' - (M'_{tx1} + M'_{tx2}) u/L - (M_{tx1} + M_{tx2}) u'/L = 0 \qquad [47]$$

Both equations take into consideration that M'_{tx} is not zero for a beam with a point load. Symmetrical properties of I beam have also been taken into consideration. Next, plug the 4th order central difference terms into the aforementioned lateral-torsion equations of equilibrium and obtain

$$a_{17}u_3 + a_{16}u_2 + a_{15}u_1 + a_{14}u_0 + a_{13}u_{-1} + a_{12}u_{-2} + a_{11}u_{-3} + b_{15}\phi_2 + b_{14}\phi_1 + b_{13}\phi_0 + b_{12}\phi_{-1} + b_{11}\phi_{-2} = 0 \qquad [48]$$

$$a_{25}u_2 + a_{24}u_1 + a_{23}u_0 + a_{22}u_{-1} + a_{21}u_{-2} + b_{27}\phi_3 + b_{26}\phi_2 + b_{25}\phi_1 + b_{24}\phi_0 + b_{23}\phi_{-1} + b_{22}\phi_{-2} + b_{21}\phi_{-3} = 0 \qquad [49]$$

where $a_{11} = -EI_y/6h^4$; $a_{12} = 2EI_y/h^4$; $a_{13} = -13EI_y/2h^4$; $a_{14} = 28EI_y/3h^4$; $a_{15} = -13EI_y/2h^4$;

$a_{16} = 2EI_y/h^4$; $a_{17} = -EI_y/6h^4$; $b_{11} = (-M_{tx}/12h^2 + M'_{tx}/6h)$; $b_{12} = (4M_{tx}/3h^2 -4\ M'_{tx}/3h)$;

$b_{13} = -(5M_{tx}/2h^2$; $b_{14} = (4M_{tx}/3h^2 + 4\ M'_{tx}/3h)$; and $b_{15} = -(M_{tx}/12h^2 + M'_{tx}/6h)$, and

$a_{21} = (M_{tx}/12h^2 - M'_{tx}/12h) – ((M_{tx1} +M_{tx2})/ 12hL)$;

$a_{22} = (-4M_{tx}/3h^2 + 2M'_{tx}/3h) + (2(M_{tx1} +M_{tx2})/ 3hL)$; $a_{23} = (5M_{tx}/2h^2 - ((M'_{tx1} +M'_{tx2})/ L)$;

$a_{24} = (-4M_{tx}/3h^2 - 2M'_{tx}/3h) - (2(M_{tx1} +M_{tx2})/ 3hL)$;

$a_{25} = (M_{tx}/12h^2 + M'_{tx}/12h) + ((M_{tx1} +M_{tx2})/ 12hL)$;

$b_{21} = -EI_y/6h^4$; $b_{22} = 2EI_y/h^4 + GK_t/12h^2$; $b_{23} = -13EI_y/2h^4 - 4GK_t/3h^2$; $b_{24} = 28EI_y/3h^4$;

$b_{25} = -13EI_y/2h^4 - 4GK_t/3h^2$; $b_{26} = 2EI_y/h^4 + GK_t/12h^2$; and $b_{27} = -EI_y/6h^4$.

Next. We define h to be a fraction of L. For this problem, L=54.0 in. and h=2.7 in. This gives us 21 locations. K matrix set up is shown in Table 28. Boundary conditions are associated locations 1 and 21, and ghost boundary conditions are associated with locations 2,3,19 , and 20. The term ghost is because we extend the columns out by two more imaginary locations beyond the boundary location. This allows us to modify equations to identify whether supports are pinned or fixed. For example, the term a_{14} extended out two terms beyond the boundary gives us the two terms a_{12} and a_{11}. The modified term $*a_{14}$ goes in the location of term a_{14}, and $*a_{14} = a_{14} - a_{12}$; and $*a_{15} = a_{15} – a_{11}$, if support is pinned. For fixed support, $*a_{14} = a_{14} + a_{12}$; and $*a_{15} = a_{15} + a_{11}$. $*b_{13}$, $*a_{23}$, $*b_{24}$, and $*b_{25}$ also need to be determined.

Table 28. Central Difference K Matrix for Buckling. Investigation 7

1		2		3							Location →
u	ϕ	u	ϕ	u	ϕ						
0.0	0.0	0.0	0.0	0.0							→ Supports at locations 1 and 21
0.0	0.0	0.0									→ Zero out boundary
0.0	0.0	$*a_{14}$	b_{13}	$*a_{15}$	b_{14}	a_{16}	b_{15}	a_{17}	0.0	0.0	
0.0	0.0	a_{23}	b_{24}	a_{24}	b_{25}	a_{25}	b_{26}	0.0	b_{27}	0.0	
0.0	0.0	a_{13}	b_{12}	a_{14}	b_{13}	a_{15}	b_{14}	a_{16}	b_{15}	a_{17}	
0.0	0.0	a_{22}	b_{23}	a_{23}	b_{24}	a_{24}	b_{25}	a_{25}	b_{26}	0.0	
0.0	0.0	a_{12}	b_{11}	a_{13}	b_{12}	a_{14}	b_{13}	a_{15}	b_{14}	a_{16}	
0.0	0.0	a_{21}	b_{22}	a_{22}	b_{23}	a_{23}	b_{24}	a_{24}	b_{25}	a_{25}	

Main diagonal

M_{tx} is the moment at the left end of an element because the element is being held there. M_{tx1} is also the moment at the left end while M_{tx2} is the moment at the right end of an element. Signs are opposite, typically. M'_{tx} is equal to the slope of the moment. $M' = R_1$ or R_2.

$$R_1L - M_{tx1} - PL_2 + M_{tx2} = 0 \quad [50]$$

$$R_2L - M_{tx2} - PL_1 + M_{tx1} = 0 \quad [51]$$

When dealing with a point load and discontinuity at its location, the slope is the same for each location to the left or right of the point load. Once values are assigned to all matrix locations including the shear moment location, solve the determinant of the matrix while increasing P_2 each time. When the matrix determinant value changes signs, the determinant has crossed zero and P_2 has reached the critical buckling limit. Value of P_{cr} with shear, P_2, for this problem is 2.5 kips.

The governing equations for deflections when considering lateral torsional buckling are:

$B_x v'' - \phi M_{ty} = M_{tx}$

$B_y u'' - \phi M_{tx} = M_{ty}$

$C_w \phi''' - (C_t + M_x\beta)\phi' - M_{tx} u' - M_{ty} v' - (M_{tx1} + M_{tx2}) u/L - (M_{ty1} + M_{ty2}) v/L + P(y_0/2)\phi = 0$

Solve the modified equations of equilibrium simultaneously using a fourth order central difference approach and aforementioned central difference expressions. These terms are substituted into our modified lateral-torsion equations to obtain:

$B_x(-v_2 + 16v_1 - 30v_0 + 16v_{-1} - v_{-2}) - \phi_0 M_{ty} = M_{tx}$

$B_y(-u_2 + 16u_1 - 30u_0 + 16u_{-1} - u_{-2}) - \phi_0 M_{tx} = M_{ty}$

$C_w(-\Phi_3 + 8\phi_2 - 13\phi_1 + 13\phi_{-1} - 8\phi_{-2} + \phi_{-3})/8h^3 - (C_t + M_x\beta)(-\phi_2 + 8\phi_1 - 8\phi_{-1} + \phi_{-2})$

$- M_{tx}(-u_2 + 8u_1 - 8u_{-1} + u_{-2}) - M_{ty}(-v_2 + 8v_1 - 8v_{-1} + v_{-2})$

$- (M_{tx1} + M_{tx2}) u_0/L - (M_{ty1} + M_{ty2}) v_0/L + P(y_0/2)\phi_0 = 0$

Setting M_y to zero,

$a_{11}v_{-2} + a_{12}v_{-1} + a_{13}v_0 + a_{14}v_1 + a_{15}v_2 = M_{tx}$ [52a]

Where $a_{11} = -EI_x/12h^2$; $a_{12} = 4EI_x/3h^2$; $a_{13} = -5EI_x/2h^2$; $a_{14} = 4EI_x/3h^2$; $a_{15} = -EI_x/12h^2$;

$B_{21}u_{-2} + b_{22}u_{-1} + b_{23}u_0 + b_{24}u_1 + b_{25}u_2 + c_{21}\phi_0 = 0.0$ [52b]

Where $b_{21} = -EI_x/12h^2$; $b_{22} = 4EI_x/3h^2$; $b_{23} = -5EI_x/2h^2$; $b_{24} = 4EI_x/3h^2$; $b_{25} = -EI_x/12h^2$;

$c_{21} = -M_{tx}$

$b_{31}u_{-2} + b_{32}u_{-1} + b_{33}u_0 + b_{34}u_1 + b_{35}u_2 + c_{31}\phi_{-3} + c_{32}\phi_{-2} + c_{33}\phi_{-1} + c_{34}\phi_0 + c_{35}\phi_1 + c_{36}\phi_2 + c_{37}\phi_1 = 0.0$

[52c]

where $b_{31} = -M_{tx}/12h$; $b_{32} = 2M_{tx}/3h$; $b_{33} = -(M_{tx1} + M_{tx2})/L$; $b_{34} = -2M_{tx}/3h$; $b_{35} = M_{tx}/12h$;

$c_{31} = C_w/8h^3$; $c_{32} = -C_w/h^3 - C_t/12h$; $c_{33} = 13C_w/8h^3 + 2C_t/3h$; $c_{34} = Py_0/2$;

$c_{35} = -13C_w/8h^3 - 2C_t/3h$; $c_{36} = C_w/h^3 + C_t/12h$; $c_{37} = -C_w/8h^3$.

For the vertical deflection values, use the same approach just demonstrated for the buckling limit except use the three governing equations and the load vector is not set to zero. $[K]u = F$. So solve for the deflections using the inverse K matrix, $u = [K]^{-1} F$. The vector u contains the unknowns v, u, and phi along the member. K matrix is demonstrated in Table 29.

Table 29. Central Difference K Matrix for Deflection. Investigation 7

Location 1			**Location 2**			**Location 3**			**Location 4**		
V	**u**	**ϕ**	**v**	**u**	**ϕ**	**v**	**u**	**ϕ**	**v**	**u**	**ϕ**
0.0	**0.0**	**0.0**	**0.0**	**0.0**	**0.0**	**0.0**	**0.0**	**0.0**	**0.0**	**0.0**	**0.0**
0.0	**0.0**	**0.0**	**0.0**	**0.0**	**0.0**	**0.0**	**0.0**	**0.0**	**0.0**	**0.0**	**0.0**
0.0	**0.0**	**0.0**	**0.0**	**0.0**	**0.0**	**0.0**	**0.0**	**0.0**	**0.0**	**0.0**	**0.0**
0.0	**0.0**	**0.0**	*a_{13}	**0.0**	**0.0**	a_{14}	**0.0**	**0.0**	a_{15}	**0.0**	**0.0**
0.0	**0.0**	**0.0**	**0.0**	b_{33}	c_{34}	**0.0**	b_{34}	c_{35}	**0.0**	b_{35}	c_{36}
0.0	**0.0**	**0.0**	**0.0**	b_{23}	c_{21}	**0.0**	b_{24}	**0.0**	**0.0**	b_{25}	**0.0**
0.0	**0.0**	**0.0**	a_{12}	**0.0**	**0.0**	a_{13}	**0.0**	**0.0**	a_{14}	**0.0**	**0.0**
0.0	**0.0**	**0.0**	**0.0**	b_{32}	c_{33}	**0.0**	b_{33}	c_{34}	**0.0**	b_{34}	c_{35}
0.0	**0.0**	**0.0**	**0.0**	b_{22}	**0.0**	**0.0**	b_{23}	c_{21}	**0.0**	b_{24}	**0.0**

Main diagonal

Zero out boundaries

For this problem, we used h=1.5 inches and 71 locations. Vertical deflections were tabulated as shown in Table 30 based upon given info applied P_2 loads from laboratory.

Table 30. Vertical Deflections. Investigation 7. Central Difference

	21.0" from support		18" from support		4" from support	
Load P, kips	$v_{1w/s}$ (in.)	$v_{1w/o}$	$v_{2w/s}$	$v_{2w/o}$	$v_{3w/s}$	$v_{3w/o}$
0.00	0.00	0.00	0.00	0.00	0.00	0.00
.2285	.0544	.0463	.0437	.0367	.0059	.0047
.4446	.1059	.0900	.0850	.0713	.0114	.0091
.6250	.1489	.1265	.1194	.1003	.0161	.0128
.8108	.1932	.1641	.1550	.1301	.0208	.0167
1.001	.2384	.2026	.1913	.1606	.0257	.0206
1.122	.2673	.2271	.2144	.180	.0288	.0231
1.317	.3138	.2667	.2518	.2113	.0339	.0271
1.518	.3617	.3074	.2902	.2436	.039	.0312
1.714	.4083	.3469	.3276	.275	.0440	.0353
1.909	.4549	.3865	.3649	.3063	.0491	.0393
2.065	.4919	.418	.3946	.3313	.0531	.0425
2.227	.5306	.4509	.4257	.3573	.0572	.0458
2.354	.5608	.4765	.4499	.3777	.0605	.0485

2.7.2 Central Difference Solution Without Shear Deformation

For this approach, we use the three central difference governing equations previously developed to determine vertical, horizontal, and the lateral deflection values along the beam. $M_x = M_{bending}$ and $P_s = 0$. The ends of the conjugate beam are pinned-pinned. So, boundary conditions are set for pinned-pinned in the finite difference model.

Problem 2.7.2. Lab Investigation 7

Given: 3"x3" x ¼" fiberglass reinforced plastic beam in Figure 10. L=54". E=2997ksi.

$I_x = 3.17$ in.^{4} . G = 450 ksi. $I_y = 1.13$ in.^{4}. k = .046. A = 2.13 in.^{2} . $I_w = 2.13$ in.^{6}.

Find: Buckling limit and vertical deflections without shear.

For vertical deflections without shear, we simply do not apply the shear moment to the beam. In other words $P_s = 0.0$ and $M_{tx} = M_{xbending}$. Procedure is exactly same as calculating critical load and vertical deflection outlined in previous problem which included shear. However, P loads from lab experiments are P_1 not P_2. Therefore, $M_{cr} = 9.92P$ for this problem. See tabulated vertical deflection values for this problem in Table 30. P_1 equals 2.98 kips at the buckling limit calculated using this approach. $M_{tx} = 29.52$ k-in.

2.7.3 ASCE LRFD Method

The ASCE buckling limit equation was developed using the classical approach solution for a simple beam solution introduced by Galambos. The LTB equations used in the classical approach were

$$EI_y u^{IV} + M_{tx} \phi'' + 2M'_{tx} \phi' = 0 \qquad [53]$$

And the 4th order solution of the third order equation of lateral deflection is

$$EI_w \phi^{IV} - (Gk_t + M_x \beta) \phi'' - M_x u'' - M'_x \beta_x \phi = 0 \qquad [54]$$

The LRFD approach and equations used here-in may be found in the ASCE LRFD Design Guide for Pultruded Members.

$$M_n = C_b (\pi^2 E_{Lf} I_y D_j/L_b^2 + \pi^4 E_{Lf} I_y C_w/L_b^4)^{.5} \qquad [55]$$

Where $D_j = Gk_t$; $C_w = I_w$; and $C_b = 12.5M_{max}/(2.5M_{max}+3M_A+4M_B+3M_C)$.

Problem 2.7.3 Lab Investigation 7

Given: 3”x3” x ¼” fiberglass reinforced plastic beam in Figure 10. L=54”. ELF=3194 ksi.

$I_x = 3.17$ in.^{4}. G = 450 ksi. $I_y = 1.13$ in.^{4}. k = .046. A = 2.13 in.^{2}. $I_w = 2.13$ in.^{6}.

Find: Buckling limit.

The ASCE-LRFD equation for lateral-torsional buckling moment of an I-shaped cross section is

$$M_n = C_b (\pi^2 E_{Lf} I_y D_j/L_b^2 + \pi^4 E_{Lf} I_y C_w/L_b^4)^{.5}$$

Where Lb is the braced length,

C_w is the warping constant,

E_{LF} is the Modulus Elasticity of the longitudinal flange,

D_j – Gk_t and is the torsional rigidity, and

$C_b = 12.5M_{max}/(2.5M_{max}+3M_A+4M_B+3M_C)$

and is the moment modification factor.

M_A, M_B and M_C are moments at locations .25L, .5L, and .75L, respectively. See Figure 19

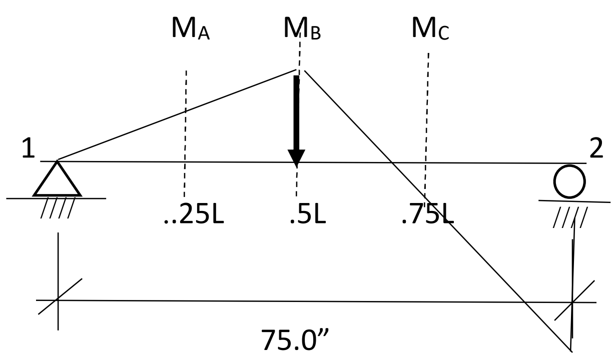

Figure 19. Moment Diagram for Investigation 7

Location of M_{max} varies with location of point load and equilibrium conditions. For this problem, $M_{max} = M_B = 9.92P$ and $M_2 = 7.16P$. Plugging in moment values, $C_b = 1.49$. Plugging in given values and C_b, $M_n = 34.1$ k-in.

Knowing the relationship between the critical moment and critical load, P_1, without shear moment; we can calculate the critical load, P_1.

$P_1 = 3.44$ kips

Now. We must find the relationship of P_1, the critical load without shear moment, and P_2, the critical load with shear moment. P_1 is associated with the moments on the conjugate beam when P_s is not present. P_2 is associated with the moments on the conjugate beam when P_s is present. The resultant of the moments on the conjugate beam when considering and not considering shear moment is of the same value or:

$$.5(9.92P_1)L_1 + .5(9.92P_1) b_1 - .5(7.16P_1) b_2 = .5(9.92P_2)L_1 + .5(9.92P_2) b_1 - .5(7.16P_2) b_2 + P_s$$

Rearranged and solved, we get $P_2/P_1 = .84$. Therefore, $P_2 = 2.89$ kips.

2.7.4 Summary of Maximum Loads

Critical loads are summarized in Table 31 and will be compared to experimental load in Chapter 4. Deflections will be compared also.

Table 31. Summary of Buckling Loads. Investigation 7

Section	Method	P_{cr}
2.7.1	Central Difference with Shear Deformation	2.5 kips
2.7.2	Central Difference without Shear Deformation	2.98 kips
2.7.3	ASCE-LRFD Method	2.89 kips

2.8 Stability Analysis for Three Span Beam with Point Load Off Center. Outside Span.

Numerical formulations for the critical buckling load and translational and rotational deflections are presented for Investigation 8 in this section. Numerical methods formulated include fourth order central difference. Critical buckling load as determined from the ASCE-LRFD Prestandard is also presented. Beam loading with boundary conditions and moments on conjugate beam are defined in Figure 20.

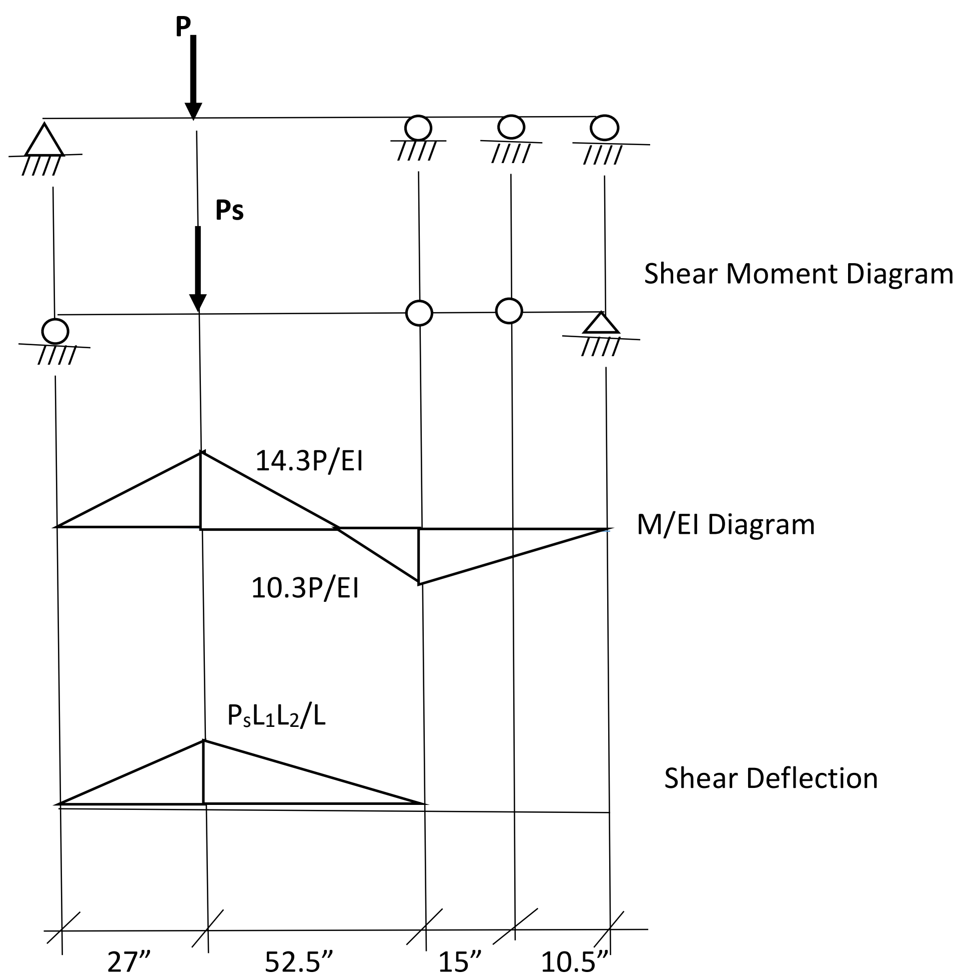

Figure 20. Investigation 8. Deflection Diagrams

2.8.1 Central Difference Solution With Shear Deformation

For this approach, use the three central difference governing equations previously developed to determine vertical, horizontal and lateral deflection values along the beam. $M_x = M_{tx}$. For this approach, follow the instructions of Timoshenko to the letter. Simply place the Shear moment point load on the conjugate beam. The ends of the conjugate beam are pinned-pinned. So, boundary conditions are set for pinned-pinned in the finite difference model. Depending up on the length of an element of eccentricity, the shear moment P_s value varies from model to model. $P_s = P_2\ \alpha EI_x/(eAG)$ where e is the eccentricity or length of the element. With shear, $M_{tx} = M_{bending} + P_s$ on the conjugate beam.

Problem 2.8.1 Lab Investigation 8

Given 3” x 3” x ¼” fiberglass reinforced plastic beam in Figure 11. L=79.5”. E=2997 ksi.

$I_x = 3.17$ in.^{4}. G = 450 ksi. $I_y = 1.13$ in.^{4}. k = .046. A = 2.13 in.^{2}. $I_w = 2.13$ in.^{6}.

Find: Buckling limit and vertical deflections with shear.

As shown in Galambos, the 4th order solution of the second order bending equilibrium equation including the angle of twist is:

$$EI_y u^{IV} + M_{tx}\phi'' + 2M'_{tx}\phi' = 0 \qquad [46]$$

And the 4th order solution of the third order equation of lateral deflection is

$$EI_w \phi^{IV} + Gk_t \phi'' - M_{tx} u'' - M'_{tx} u' - (M'_{tx1} + M'_{tx2})\, u/L - (M_{tx1} + M_{tx2})\, u'/L = 0 \qquad [47]$$

Both equations take into consideration that M'_{tx} is not zero for a beam with a point load. Symmetrical properties of I beam have also been taken into consideration. Next, plug the 4th order central difference terms into the aforementioned lateral-torsion equations of equilibrium and obtain

$$a_{17}u_3 + a_{16}u_2 + a_{15}u_1 + a_{14}u_0 + a_{13}u_{-1} + a_{12}u_{-2} + a_{11}u_{-3} + b_{15}\phi_2 + b_{14}\phi_1 + b_{13}\phi_0 + b_{12}\phi_{-1} + b_{11}\phi_{-2} = 0$$

[48]

$$a_{25}u_2 + a_{24}u_1 + a_{23}u_0 + a_{22}u_{-1} + a_{21}u_{-2} + b_{27}\phi_3 + b_{26}\phi_2 + b_{25}\phi_1 + b_{24}\phi_0 + b_{23}\phi_{-1} + b_{22}\phi_{-2} + b_{21}\phi_{-3} = 0$$

[49]

where $a_{11} = -EI_y/6h^4$; $a_{12} = 2EI_y/h^4$; $a_{13} = -13EI_y/2h^4$; $a_{14} = 28EI_y/3h^4$; $a_{15} = -13EI_y/2h^4$;

$a_{16} = 2EI_y/h^4$; $a_{17} = -EI_y/6h^4$; $b_{11} = (-M_{tx}/12h^2 + M'_{tx}/6h)$; $b_{12} = (4M_{tx}/3h^2 -4\ M'_{tx}/3h)$;

$b_{13} = -(5M_{tx}/2h^2$; $b_{14} = (4M_{tx}/3h^2 + 4\ M'_{tx}/3h)$; and $b_{15} = -(M_{tx}/12h^2 + M'_{tx}/6h)$, and

$a_{21} = (M_{tx}/12h^2 - M'_{tx}/12h) – ((M_{tx1} +M_{tx2})/ 12hL)$;

$a_{22} = (-4M_{tx}/3h^2 + 2M'_{tx}/3h) + (2(M_{tx1} +M_{tx2})/ 3hL)$; $a_{23} = (5M_{tx}/2h^2 - ((M'_{tx1} +M'_{tx2})/ L)$;

$a_{24} = (-4M_{tx}/3h^2 - 2M'_{tx}/3h) - (2(M_{tx1} +M_{tx2})/ 3hL)$;

$a_{25} = (M_{tx}/12h^2 + M'_{tx}/12h) + ((M_{tx1} +M_{tx2})/ 12hL)$;

$b_{21} = -EI_y/6h^4$; $b_{22} = 2EI_y/h^4 + GK_t/12h^2$; $b_{23} = -13EI_y/2h^4 - 4GK_t/3h^2$; $b_{24} = 28EI_y/3h^4$;

$b_{25} = -13EI_y/2h^4 - 4GK_t/3h^2$; $b_{26} = 2EI_y/h^4 + GK_t/12h^2$; and $b_{27} = -EI_y/6h^4$.

Next. We define h to be a fraction of lL. For this problem, L-79.5 in. and h=3.797 in. This gives us 21 locations K matrix is setu up in Table 32. Boundary conditions are associated locations 1 and 21, and ghost boundary conditions are associated with locations 2,3, 19, and 20. The term ghost is because we extend the columns out by two more imaginary locations beyond the boundary location. This allows us to modify equations to identify whether supports are pinned or fixed. For example, the term a_{14} extended out two terms beyond the boundary gives us the two terms a_{12} and a_{11}. The modified term $*a_{14}$ goes in the location of term a_{14}, and $*a_{14} = a_{14} - a_{12}$; and $*a_{15} = a_{15} – a_{11}$, if support is pinned. For fixed support, $*a_{14} = a_{14} + a_{12}$; and $*a_{15} = a_{15} + a_{11}$. $*b_{13}$, $*a_{23}$, $*b_{24}$, and $*b_{25}$ also need to be determined.

Table 32. Central Difference K Matrix for Buckling. Investigation 8

1		2		3		Location →					
u	ϕ	u	ϕ	u	ϕ						
0.0	0.0	0.0	0.0	0.0							→ Supports at locations 1 and 21
0.0	0.0	0.0									→ Zero out boundary
0.0	0.0	*a_{14}	b_{13}	*a_{15}	b_{14}	a_{16}	b_{15}	a_{17}	0.0	0.0	
0.0	0.0	a_{23}	b_{24}	a_{24}	b_{25}	a_{25}	b_{26}	0.0	b_{27}	0.0	
0.0	0.0	a_{13}	b_{12}	a_{14}	b_{13}	a_{15}	b_{14}	a_{16}	b_{15}	a_{17}	
0.0	0.0	a_{22}	b_{23}	a_{23}	b_{24}	a_{24}	b_{25}	a_{25}	b_{26}	0.0	
0.0	0.0	a_{12}	b_{11}	a_{13}	b_{12}	a_{14}	b_{13}	a_{15}	b_{14}	a_{16}	
0.0	0.0	a_{21}	b_{22}	a_{22}	b_{23}	a_{23}	b_{24}	a_{24}	b_{25}	a_{25}	

Main diagonal

M_{tx} is the moment at the left end of an element because the element is being held there. M_{tx1} is also the moment at the left end while M_{tx2} is the moment at the right end of an element. Signs are opposite, typically. M'_{tx} is equal to the slope of the moment. $M' = R_1$ or R_2.

$$R_1L - M_{tx1} - PL_2 + M_{tx2} = 0 \quad [50]$$

$$R_2L - M_{tx2} - PL_1 + M_{tx1} = 0 \quad [51]$$

When dealing with a point load and discontinuity at its location, the slope is the same for each location to the left or right of the point load. Once values are assigned to all matrix locations including the shear moment location, solve the determinant of the matrix while increasing P_2 each time. When the matrix determinant value changes signs, the determinant has crossed zero and P_2 has reached the critical buckling limit. Value of P_{cr} with shear, P_2, for this problem is 1.12 kips.

The governing equations for deflections when considering lateral torsional buckling are:

$B_x v'' - \phi M_{ty} = M_{tx}$

$B_y u'' - \phi M_{tx} = M_{ty}$

$C_w \phi''' - (C_t + M_x\beta)\phi' - M_{tx} u' - M_{ty} v' - (M_{tx1} + M_{tx2}) u/L - (M_{ty1} + M_{ty2}) v/L + P(y_0/2)\phi = 0$

Solve the modified equations of equilibrium simultaneously using a fourth order central difference approach and aforementioned central difference expressions. These terms are substituted into our modified lateral-torsion equations to obtain:

$B_x(-v_2 + 16v_1 - 30v_0 + 16v_{-1} - v_{-2}) - \phi_0 M_{ty} = M_{tx}$

$B_y(-u_2 + 16u_1 - 30u_0 + 16u_{-1} - u_{-2}) - \phi_0 M_{tx} = M_{ty}$

$C_w(-\Phi_3 + 8\phi_2 - 13\phi_1 + 13\phi_{-1} - 8\phi_{-2} + \phi_{-3})/8h^3 - (C_t + M_x\beta)(-\phi_2 + 8\phi_1 - 8\phi_{-1} + \phi_{-2})$

$- M_{tx}(-u_2 + 8u_1 - 8u_{-1} + u_{-2}) - M_{ty}(-v_2 + 8v_1 - 8v_{-1} + v_{-2})$

$- (M_{tx1} + M_{tx2}) u_0/L - (M_{ty1} + M_{ty2}) v_0/L + P(y_0/2)\phi_0 = 0$

Setting M_y to zero,

$a_{11}v_{-2} + a_{12}v_{-1} + a_{13}v_0 + a_{14}v_1 + a_{15}v_2 = M_{tx}$ [52a]

where $a_{11} = -EI_x/12h^2$; $a_{12} = 4EI_x/3h^2$; $a_{13} = -5EI_x/2h^2$; $a_{14} = 4EI_x/3h^2$; $a_{15} = -EI_x/12h^2$;

$B_{21}u_{-2} + b_{22}u_{-1} + b_{23}u_0 + b_{24}u_1 + b_{25}u_2 + c_{21}\phi_0 = 0.0$ [52b]

where $b_{21} = -EI_x/12h^2$; $b_{22} = 4EI_x/3h^2$; $b_{23} = -5EI_x/2h^2$; $b_{24} = 4EI_x/3h^2$; $b_{25} = -EI_x/12h^2$;

$c_{21} = -M_{tx}$

$b_{31}u_{-2} + b_{32}u_{-1} + b_{33}u_0 + b_{34}u_1 + b_{35}u_2 + c_{31}\phi_{-3} + c_{32}\phi_{-2} + c_{33}\phi_{-1} + c_{34}\phi_0 + c_{35}\phi_1 + c_{36}\phi_2 + c_{37}\phi_1 = 0.0$

[52c]

where $b_{31} = -M_{tx}/12h$; $b_{32} = 2M_{tx}/3h$; $b_{33} = -(M_{tx1} + M_{tx2})/L$; $b_{34} = -2M_{tx}/3h$; $b_{35} = M_{tx}/12h$;

$c_{31} = C_w/8h^3$; $c_{32} = -C_w/h^3 - C_t/12h$; $c_{33} = 13C_w/8h^3 + 2C_t/3h$; $c_{34} = Py_0/2$;

$c_{35} = -13C_w/8h^3 - 2C_t/3h$; $c_{36} = C_w/h^3 + C_t/12h$; $c_{37} = -C_w/8h^3$.

For the vertical deflection values, use the same approach just demonstrated for the buckling limit except use the three governing equations and the load vector is not set to zero. $[K]u = F$. So, solve for the deflections using the inverse K matrix, $u = [K]^{-1} F$. The vector u contains the unknowns v, u, and phi along the member. K matrix is demonstrated in Table 33.

Table 33. Central Difference K Matrix for Deflections. Investigation 8

Location 1			Location 2			Location 3			Location 4		
V	u	ϕ	v	u	ϕ	v	u	ϕ	v	u	ϕ
0.0	0.0	0.0	0.0	0.0	0.0	0.0	0.0	0.0	0.0	0.0	0.0
0.0	0.0	0.0	0.0	0.0	0.0	0.0	0.0	0.0	0.0	0.0	0.0
0.0	0.0	0.0	0.0	0.0	0.0	0.0	0.0	0.0	0.0	0.0	0.0
0.0	0.0	0.0	*a_{13}	0.0	0.0	a_{14}	0.0	0.0	a_{15}	0.0	0.0
0.0	0.0	0.0	0.0	b_{33}	c_{34}	0.0	b_{34}	c_{35}	0.0	b_{35}	c_{36}
0.0	0.0	0.0	0.0	b_{23}	c_{21}	0.0	b_{24}	0.0	0.0	b_{25}	0.0
0.0	0.0	0.0	a_{12}	0.0	0.0	a_{13}	0.0	0.0	a_{14}	0.0	0.0
0.0	0.0	0.0	0.0	b_{32}	c_{33}	0.0	b_{33}	c_{34}	0.0	b_{34}	c_{35}
0.0	0.0	0.0	0.0	b_{22}	0.0	0.0	b_{23}	c_{21}	0.0	b_{24}	0.0

Main diagonal

Zero out boundaries

For this problem, we used h=1.5 inches and 71 locations. Vertical deflections were tabulated in Table 34 based upon given info and applied P_2 loads from laboratory.

Table 34. Vertical Deflections. Investigation 8. Central Difference

	7" from support		19" from support		34" from support	
P Load, kips	$v_{1w/s}$ (in.)	$v_{1w/o}$	$v_{2w/s}$	$v_{2w/o}$	$v_{3w/s}$	$v_{3w/o}$
0.00	0.00	0.00	0.00	0.00	0.00	0.00
.2204	.0379	.035	.1032	.0944	.1338	.1221
.4409	.076	.070	.2067	.1887	.2682	.2443
.709	.1222	.1126	.3325	.3035	.4313	.3928
.8899	.1534	.1413	.4174	.3810	.5414	.4931
1.069	.1843	.1698	.5015	.4578	.6505	.5925
1.225	.2113	.1946	.5748	.5247	.7456	.6791
1.382	.2382	.2194	.6480	.5916	.8406	.7657
1.522	.2623	.2416	.7136	.6515	.9257	.8431

2.8.2 Central Difference Solution Without Shear Deformation

For this approach, we use the three central difference governing equations previously developed to determine vertical, horizontal, and lateral deflection values along the beam. $M_x = M_{bending}$ and $P_s = 0$. The ends of the conjugate beam are pinned-pinned. So, boundary conditions are set for pinned-pinned in the finite difference model.

Problem 2.8.2. Lab Investigation 8

Given: 3" x 3" x ¼" fiberglass reinforced plastic beam in Figure 11. L=79.5". E=2997 ksi.

$I_x = 3.17$ in.^{4}. G = 450 ksi. $I_y = 1.13$ in.^{4}. k = .046. A = 2.13 in.^{2}. $I_w = 2.13$ in.^{6}.

Find: Buckling limit and vertical deflections without shear.

For vertical deflections without shear, we simply do not apply the shear moment to the beam. In other words, $M_s = 0.0$ and $M_{tx} = M_{xbending}$. Procedure is exactly same as calculating critical load and vertical deflection outlined in previous problem which included shear. However, P loads from lab experiments are P_1 not P_2. Therefore, $M_{cr} = 14.34P$ for this problem. See tabulated vertical deflection values for this problem in Table 34. P_1 equals 1.22 kips at the buckling limit calculated using this approach. $M_{tx} = 17.53$ k-in.

2.8.3 ASCE LRFD Method

The ASCE buckling limit equation was developed using the classical approach solution for a simple beam solution introduced by Galambos. The LTB equations used in the classical approach were

$EI_y\, u^{IV} + M_{tx}\, \phi'' + 2M'_{tx}\, \phi' = 0$ [53]

And the 4th order solution of the third order equation of lateral deflection is

$EI_w\, \phi^{IV} – (Gk_t + M_x\, \beta)\, \phi'' - M_x\, u'' – M'_x\, \beta_x\, \phi = 0$ [54]

The LRFD approach and equations used here-in may be found in the ASCE LRFD Design Guide for Pultruded Members.

$M_n = C_b\, (\pi^2\, E_{L\,f}\, I_y\, D_j/L_b^2 + \pi^4\, E_{Lf}\, I_y\, C_w/L_b^4\,)^{.5}$ [55]

Where $D_j = Gk_t$; $C_w = I_w$; and $C_b = 12.5M_{max}/(2.5M_{max}+3M_A+4M_B+3M_C)$.

Problem 2.8.3 Lab Investigation 8

Given: 3” x 3” x ¼” fiberglass reinforced plastic beam in Figure 11. L=79.5”. ELF=3194 ksi.

I_x = 3.17 in. ^{4} . G = 450 ksi. I_y = 1.13 in.^{4}. k = .046. A = 2.13 in. ^{2} . I_w = 2.13 in. ^{6}.

Find: Buckling limit.

The ASCE-LRFD equation for lateral-torsional buckling moment of an I-shaped cross section is

$M_n = C_b\, (\pi^2\, E_{L\,f}\, I_y\, D_j/L_b^2 + \pi^4\, E_{Lf}\, I_y\, C_w/L_b^4\,)^{.5}$

Where Lb is the braced length,

C_w is the warping constant,

E_{LF} is the Modulus Elasticity of the longitudinal flange,

$D_j = Gk_t$ and is the torsional rigidity, and

$C_b = 12.5M_{max}/(2.5M_{max}+3M_A+4M_B+3M_C)$

and is the moment modification factor.

M_A, M_B and M_C are moments at locations .25L, .5L, and .75L, respectively. See Figure 21.

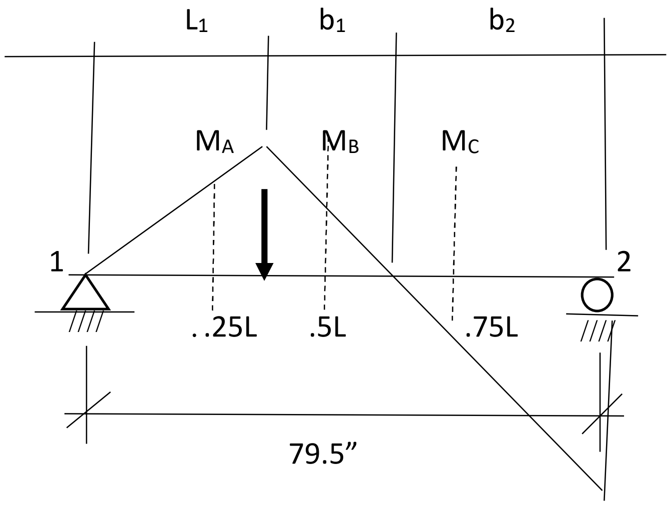

Figure 21. Moment Diagram for Investigation 8

Location of M_{max} varies with location of point load and equilibrium conditions. For this problem, $M_{max} = M_b = 14.34P$ and $M_2 = 10.29P$. Plugging in moment values, $C_b = 1.73$. Plugging in given values and C_b, M_n=22.90 k-in. Knowing the relationship between the critical moment and critical load, P_1, without shear moment; we can calculate the critical load, P_1. $P_1 = 1.60$ kips.

Now. We must find the relationship of P_1, the critical load without shear moment, and P_2, the critical load with shear moment. P_1 is associated with the moments on the conjugate beam when Ps is not present. P2 is associate with the moments on the conjugate beam when P_s is present. The resultant of the moments on the conjugate beam when considering and not considering shear moment is of the same value or

$$.5(14.34P_1)L_1 + .5(14.34P_1)b_1 - .5(10.29P_1)b_2 = .5(14.34P_2)L_1 + .5(14.34P_2)b_1 - .5(10.29P_2)b_2 + P_s$$

Rearranged and solved, we get $P_2/P_1 = .916$ Therefore, $P_2 = 1.47$ kips

2.8.4 Summary of Maximum Loads

Critical loads are summarized in Table 35 and will be compared to experimental load in Chapter 4. Deflections will be compared also.

Table 35. Summary of Buckling Loads. Investigation 8

Section	Method	P_{cr}
2.8.1	Central Difference with Shear Deformation	1.12 kips
2.8.2	Central Difference without Shear Deformation	1.22 kips
2.8.3	ASCE-LRFD Method	1.47 kips

2.9 Stability Analysis for Three Span Beam with Point Load Off Center. Biaxial

Numerical formulations for the critical buckling load and translational and rotational deflections are presented for Investigation 9 in this section. Numerical methods formulated include fourth order central difference. Critical buckling load as determined from the ASCE-LRFD prestandard is also presented. Beam loading with boundary conditions and moments on conjugate beam are defined in Figure 22.

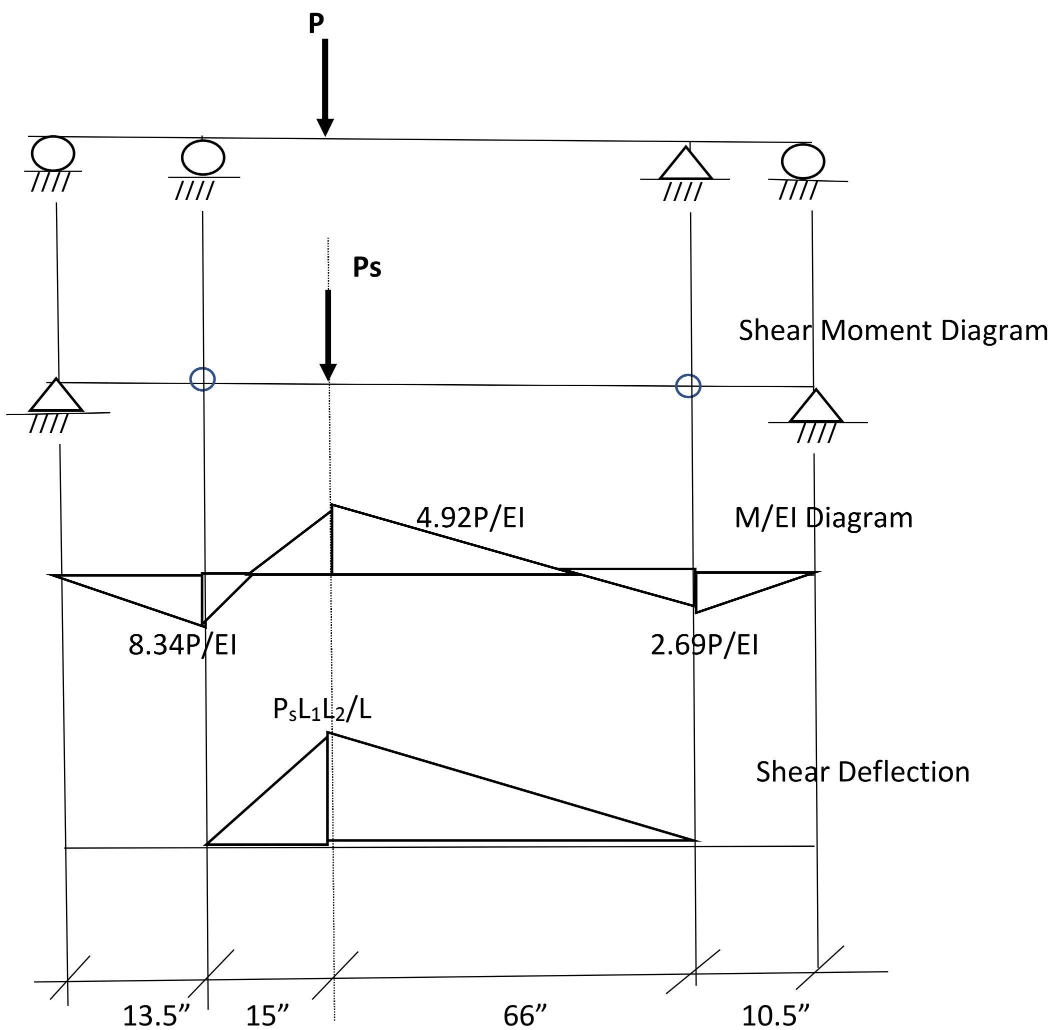

Figure 22. Investigation 9. Deflection Diagram

2.9.1 Central Difference Solution With Shear Deformation

For this approach, use the three central difference governing equations previously developed to determine vertical, horizontal and lateral deflection values along the beam. $M_x = M_{tx}$. Follow the instructions of Timoshenko to the letter. Simply place the shear moment point load on the conjugate beam. The ends of the conjugate beam are pinned-pinned. So, boundary conditions are set for pinned-pinned in the finite difference model. Depending up on the length of an element of eccentricity, the shear moment P_s value varies from model to model. $P_s = P_2\, \alpha EI_x /(AG)$.

Problem 2.9.1. Lab Investigation 9

Given : 4" x 4" x ¼" fiberglass reinforced plastic beam in Figure 12. L=75". E=3000 ksi.

I_x = 7.935 in. ^{4} . G = 450 ksi. I_y = 2.67 in.^{4}. k_t = .06. A = 2.85 in. ^{2} . I_w = 9.375 in. ^{6}.

Find: Buckling limit and vertical deflections with shear.

As shown in Galambos, the 4th order solution of the second order bending equilibrium equations including the angle of twist is:

$$EI_y u^{IV} + M_{tx} \phi'' + 2M'_{tx} \phi' = 0$$

$$EI_x v^{IV} + M_{ty} \phi'' + 2M'_{tx} \phi' = 0$$

And the 4th order solution of the third order equation of lateral deflection is

$$EI_w \phi^{IV} + Gk_t \phi'' - M_{tx} u'' - M'_{tx} u' - (M'_{tx1} + M'_{tx2}) u/L - (M_{tx1} + M_{tx2}) u'/L$$

$$- M_{ty} v'' - M'_{ty} v' - (M'_{ty1} + M'_{ty2}) v/L - (M_{ty1} + M_{ty2}) v'/L = 0$$

Equations take into consideration that My, $M'_{tx,}$ and M'_{ty} are not zero for a beam loaded biaxially. Symmetrical properties of I beam have also been taken into consideration. Next, plug the 4th order central difference terms into the aforementioned lateral-torsion equations of equilibrium and obtain

$$a_{17}v_3 + a_{16}v_2 + a_{15}v_1 + a_{14}v_0 + a_{13}v_{-1} + a_{12}v_{-2} + a_{11}v_{-3} + c_{15}\phi_2 + c_{14}\phi_1 + c_{13}\phi_0 + c_{12}\phi_{-1} + c_{11}\phi_{-2} = 0$$

$$b_{27}u_3 + b_{26}u_2 + b_{25}u_1 + b_{24}u_0 + b_{23}u_{-1} + b_{22}u_{-2} + b_{21}u_{-3} + c_{25}\phi_2 + c_{24}\phi_1 + c_{23}\phi_0 + c_{22}\phi_{-1} + c_{21}\phi_{-2} = 0$$

$b_{35}u_2 + b_{34}u_1 + b_{33}u_0 + b_{32}u_{-1} + b_{31}u_{-2} + c_{37}\phi_3 + c_{36}\phi_2 + c_{35}\phi_1 + c_{34}\phi_0 + c_{33}\phi_{-1} + c_{32}\phi_{-2} + c_{31}\phi_{-3} +$

$a_{35}v_2 + a_{34}v_1 + a_{33}v_0 + a_{32}v_{-1} + a_{31}v_{-2} = 0.$

where $a_{11} = -EI_y/6h^4$; $a_{12} = 2EI_y/h^4$; $a_{13} = -13EI_y/2h^4$; $a_{14} = 28EI_y/3h^4$; $a_{15} = -13EI_y/2h^4$;

$a_{16} = 2EI_y/h^4$; $a_{17} = -EI_y/6h^4$; $c_{11} = (-M_{tx}/12h^2 + M'_{tx}/6h)$; $c_{12} = (4M_{tx}/3h^2 - 4M'_{tx}/3h)$;

$c_{13} = -(5M_{tx}/2h^2$; $c_{14} = (4M_{tx}/3h^2 + 4M'_{tx}/3h)$; and $c_{15} = -(M_{tx}/12h^2 + M'_{tx}/6h)$, and

$b_{31} = (M_{tx}/12h^2 - M'_{tx}/12h) – ((M_{tx1} + M_{tx2})/ 12hL)$;

$b_{32} = (-4M_{tx}/3h^2 + 2M'_{tx}/3h) + (2(M_{tx1} + M_{tx2})/ 3hL)$; $b_{33} = (5M_{tx}/2h^2 - ((M'_{tx1} + M'_{tx2})/ L)$;

$b_{34} = (-4M_{tx}/3h^2 - 2M'_{tx}/3h) - (2(M_{tx1} + M_{tx2})/ 3hL)$;

$b_{35} = (M_{tx}/12h^2 + M'_{tx}/12h) + ((M_{tx1} + M_{tx2})/ 12hL)$;

$c_{31} = -EI_y/6h^4$; $c_{32} = 2EI_y/h^4 + GK_t/12h^2$; $c_{33} = -13EI_y/2h^4 - 4GK_t/3h^2$; $c_{34} = 28EI_y/3h^4$;

$c_{35} = -13EI_y/2h^4 - 4GK_t/3h^2$; $c_{36} = 2EI_y/h^4 + GK_t/12h^2$; and $c_{37} = -EI_y/6h^4$.

Next. We define h to be a fraction of L. For this problem, L=81.0 in. and h= 3.00 in. This gives us 28 locations K matrix set up shown in Table 36.

Table 36. Central Difference K Matrix for Buckling. Investigation 9

1		2		3		Location →
u	ϕ	u	ϕ	u	ϕ	
0.0	0.0	0.0	0.0	0.0		Supports at locations 1 and 21

Location 1			**Location 2**			**Location 3**			**Location 4**		
V	**u**	**ϕ**	**v**	**u**	**ϕ**	**v**	**u**	**ϕ**	**v**	**u**	**ϕ**
0.0	**0.0**	**0.0**	**0.0**	**0.0**	**0.0**	**0.0**	**0.0**	**0.0**	**0.0**	**0.0**	**0.0**
0.0	**0.0**	**0.0**	**0.0**	**0.0**	**0.0**	**0.0**	**0.0**	**0.0**	**0.0**	**0.0**	**0.0**
0.0	**0.0**	**0.0**	**0.0**	**0.0**	**0.0**	**0.0**	**0.0**	**0.0**	**0.0**	**0.0**	**0.0**
0.0	**0.0**	**0.0**	**$*a_{13}$**	**0.0**	**0.0**	**a_{14}**	**0.0**	**0.0**	**a_{15}**	**0.0**	**0.0**
0.0	**0.0**	**0.0**	**0.0**	**b_{33}**	**c_{34}**	**0.0**	**b_{34}**	**c_{35}**	**0.0**	**b_{35}**	**c_{36}**
0.0	**0.0**	**0.0**	**0.0**	**b_{23}**	**c_{21}**	**0.0**	**b_{24}**	**0.0**	**0.0**	**b_{25}**	**0.0**
0.0	**0.0**	**0.0**	**a_{12}**	**0.0**	**0.0**	**a_{13}**	**0.0**	**0.0**	**a_{14}**	**0.0**	**0.0**
0.0	**0.0**	**0.0**	**0.0**	**b_{32}**	**c_{33}**	**0.0**	**b_{33}**	**c_{34}**	**0.0**	**b_{34}**	**c_{35}**
0.0	**0.0**	**0.0**	**0.0**	**b_{22}**	**0.0**	**0.0**	**b_{23}**	**c_{21}**	**0.0**	**b_{24}**	**0.0**

Main diagonal

Zero out boundaries

Boundary conditions are associated locations 1 and 28, and ghost boundary conditions are associated with locations 2,3, 26, and 27. The term ghost is because we extend the columns out by two more imaginary locations beyond the boundary location. This allows us to modify equations to identify whether supports are pinned or fixed. For example, the term a_{14} extended out two terms beyond the boundary gives us the two terms a_{12} and a_{11}. The modified term $*a_{14}$ goes in the location of term a_{14}, and $*a_{14} = a_{14} - a_{12}$; if support is pinned. For fixed support, $*a_{14} = a_{14} + a_{12}$.

M_{tx} is the moment at the left end of an element because the element is being held there. M_{tx1} is also the moment at the left end while M_{tx2} is the moment at the right end of an element. Signs are opposite, typically. M'_{tx} is equal to the slope of the moment. $M' = R_1$ or R_2.

$$R_1L - M_{tx1} - PL_2 + M_{tx2} = 0 \quad [50]$$

$$R_2L - M_{tx2} - PL_1 + M_{tx1} = 0 \quad [51]$$

When dealing with a point load and discontinuity at its location, the slope is the same for each location to the left or right of the point load. Once values are assigned to all matrix locations including the shear moment location, solve the determinant of the matrix while increasing P_2 each time. When the matrix determinant value changes signs, the determinant has crossed zero and P_2 has reached the critical buckling limit. Value of P_{cr} with shear, P_2, for this problem is 2.9 kips.

The governing equations for deflections when considering lateral torsional buckling are:

$$B_x v'' - \phi M_{ty} = M_{tx}$$

$$B_y u'' - \phi M_{tx} = M_{ty}$$

$$C_w \phi''' - (C_t + M_x\beta)\phi' - M_{tx} u' - M_{ty} v' - (M_{tx1} + M_{tx2}) u/L - (M_{ty1} + M_{ty2}) v/L + P(y_0/2)\phi = 0$$

Solve the modified equations of equilibrium simultaneously using a fourth order central difference approach and aforementioned central difference expressions. These terms are substituted into our modified lateral-torsion equations to obtain:

$$B_x(-v_2 + 16v_1 - 30v_0 + 16v_{-1} - v_{-2}) - \phi_0 M_{ty} = M_{tx}$$

$$B_y(-u_2 + 16u_1 - 30u_0 + 16u_{-1} - u_{-2}) - \phi_0 M_{tx} = M_{ty}$$

$$C_w(-\Phi_3 + 8\phi_2 - 13\phi_1 + 13\phi_{-1} - 8\phi_{-2} + \phi_{-3})/8h^3 - (C_t + M_x\beta)(-\phi_2 + 8\phi_1 - 8\phi_{-1} + \phi_{-2})$$

$$- M_{tx}(-u_2 + 8u_1 - 8u_{-1} + u_{-2}) - M_{ty}(-v_2 + 8v_1 - 8v_{-1} + v_{-2})$$

$$- (M_{tx1} + M_{tx2}) u_0/L - (M_{ty1} + M_{ty2}) v_0/L + P(y_0/2)\phi_0 = 0$$

For the vertical deflection values, use the same approach just demonstrated for the buckling limit except use the three governing equations and the load vector is not set to zero. $[K]u = F$. So, solve for the deflections using the inverse K matrix, $u = [K]^{-1} F$. The vector u contains the unknowns v, u, and phi along the member. K matrix is demonstrated in Table 37.

Table 37. Central Difference K Matrix for Deflections. Biaxial. Investigation 9

Location 1			**Location 2**			**Location 3**			**Location 4**		
V	**u**	**ϕ**	**v**	**u**	**ϕ**	**v**	**u**	**ϕ**	**v**	**u**	**ϕ**
0.0	0.0	0.0	0.0	0.0	0.0	0.0	0.0	0.0	0.0	0.0	0.0
0.0	0.0	0.0	0.0	0.0	0.0	0.0	0.0	0.0	0.0	0.0	0.0
0.0	0.0	0.0	0.0	0.0	0.0	0.0	0.0	0.0	0.0	0.0	0.0
0.0	0.0	0.0	*a_{13}	0.0	c_{11}	a_{14}	0.0	0.0	a_{15}	0.0	0.0
0.0	0.0	0.0	a_{33}	b_{33}	c_{34}	a_{34}	b_{34}	c_{35}	a_{35}	b_{35}	c_{36}
0.0	0.0	0.0	0.0	b_{23}	c_{21}	0.0	b_{24}	0.0	0.0	b_{25}	0.0
0.0	0.0	0.0	a_{12}	0.0	0.0	a_{13}	0.0	0.0	a_{14}	0.0	0.0
0.0	0.0	0.0	a_{32}	b_{32}	c_{33}	a_{33}	b_{33}	c_{34}	a_{34}	b_{34}	c_{35}
0.0	0.0	0.0	0.0	b_{22}	0.0	0.0	b_{23}	c_{21}	0.0	b_{24}	0.0

Main diagonal

Zero out boundaries

For this problem, we used h=1.5 inches and 71 locations. Vertical deflections were tabulated in Table 38 based upon given info and applied P_2 loads from laboratory.

Table 38. Vertical Deflections. Investigation 9. Central Difference

	21.0" from support		18" from support		4" from support	
Load P, kips	$v_{1w/s}$ (in.)	$v_{1w/o}$	$v_{2w/s}$	$v_{2w/o}$	$v_{3w/s}$	$v_{3w/o}$
0.00	0.00	0.00	0.00	0.00	0.00	0.00
.5129	.0388	.0236	.0328	.024	.0068	.00427
.8089	.0612	.0373	.0516	.0378	.0107	.0067
1.11	.0841	.0512	.0708	.0520	.0147	.0092
1.29	.0977	.0595	.0822	.0605	.0171	.0107
1.398	.1057	.0644	.089	.0654	.0185	.0116
1.549	.1171	.0714	.0986	.0725	.0205	.0129
1.682	.1271	.0775	.1070	.0787	.0222	.0140
1.818	.1374	.0838	.1157	.0851	.024	.0151
1.935	.1462	.0892	.1231	.0905	.0256	.0161
2.114	.1598	.0974	.1345	.0989	.028	.0176
2.318	.1751	.1068	.1474	.1084	.0306	.0193

2.9.2 Central Difference Solution Without Shear Deformation

For this approach, we use the three central difference governing equations previously developed to determine vertical, horizontal, and lateral deflection values along the beam. $M_x=M_{bending}$ and $P_s = 0$. The ends of the conjugate beam are pinned-pinned. So, Boundary conditions are set for pinned-pinned in the finite difference model.

Problem 2.9.2. Lab Investigation 9

Given: 4" x 4" x ¼" fiberglass reinforced plastic beam in Figure 12. L=81". E=3000 ksi.

I_x = 3.17 in. ^{4} . G = 450 ksi. I_y = 1.13 in.^{4}. k = .046. A = 2.13 in. ^{2} . I_w = 2.13 in. ^{6}.

Find: Buckling limit and vertical deflections without shear.

For vertical deflections without shear, we simply do not apply the shear moment to the beam. In other words, $M_s = 0.0$ and $M_{tx} = M_{xbending}$. Procedure is exactly same as calculating critical load and vertical deflection outlined in previous problem which included shear. However, P loads from lab experiments are P_1 not P_2. Therefore, $M_{cr} = 8.34P$ for this problem. See tabulated vertical deflecioth values for this problem in Table 38. P_1 equals 7.25 kips at the buckling limit calculated using this approach. $M_{tx} = 60.46$ k-in.

2.9.3 ASCE LRFD Method

The ASCE buckling limit equation was developed using the classical approach solution for a simple beam solution introduced by Galambos. The LTB equations used in the classical approach were

$$EI_y u^{IV} + M_{tx} \phi'' + 2M'_{tx} \phi' = 0 \qquad [53]$$

And the 4th order solution of the third order equation of lateral deflection is

$$EI_w \phi^{IV} - (Gk_t + M_x \beta) \phi'' - M_x u'' - M'_x \beta_x \phi = 0 \qquad [54]$$

The LRFD approach and equations used here-in may be found in the ASCE LRFD Design Guide for Pultruded Members.

$$M_n = C_b (\pi^2 E_{L f} I_y D_j/L_b^2 + \pi^4 E_{Lf} I_y C_w/L_b^4)^{.5} \qquad [55]$$

where $D_j = Gk_t$; $C_w = I_w$; and $C_b = 12.5M_{max}/(2.5M_{max}+3M_A+4M_B+3M_C)$.

Problem 2.9.3 Lab Investigation 9

Given: 4" x 4" x ¼" fiberglass reinforced plastic beam in Figure 12. L=81". E=3000 ksi.

$I_x = 3.17$ in.^{4} . G = 450 ksi. $I_y = 1.13$ in.^{4}. k = .046. A = 2.13 in.^{2} . $I_w = 2.13$ in.^{6}.

Find: Buckling limit.

The ASCE-LRFD equation for lateral-torsional buckling moment of an I-shaped cross section is

$$M_n = C_b (\pi^2 E_{L f} I_y D_j/L_b^2 + \pi^4 E_{Lf} I_y C_w/L_b^4)^{.5}$$

where Lb is the braced length,

Cw is the warping constant,

E_{LF} is the Modulus Elasticity of the longitudinal flange,

$D_j = Gk_t$ and is the torsional rigidity, and

$C_b = 12.5M_{max}/(2.5M_{max}+3M_A+4M_B+3M_C)$.

and is the moment modification factor.

M_A, M_B and M_C are moments at locations .25L, .5L, and .75L, respectively. See Figure 23.

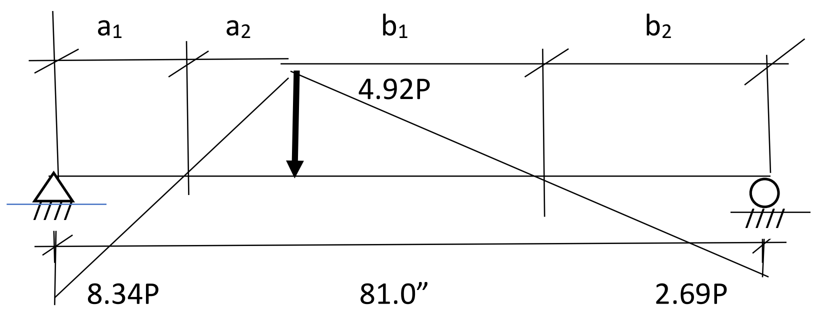

Figure 23. Moment Diagram for Investigation 9

Location of M_{max} varies with location of point load and equilibrium conditions. For this problem, M_{max} = 8.34P and M_2 = 2.69P. Plugging in moment values, C_b = 1.99. Plugging in given and C_b, M_n = 74.1 k-in.

Knowing the relationship between the critical moment and critical load, P_1, without shear moment; we can calculate the critical load, P_1. P_1 = 74.1/8.34 = 8.88 kips. Now. We must find the relationship of P_1, the critical load without shear moment, and P_2, the critical load with shear moment. P_1 is associated with the moment son the conjugate beam when P_s is not present. P_2 is associated with the moments on the conjugate beam when M_s is present. The resultant of the same value or:

$.5(4.92P_1)a2 + .5(4.92P_1) b_1 - .5(2.69P_1) b_2 - .5(8.34P_1) a1 = .5(4.92P_2)a2 + .5(4.92P_2) b_1 - .5(2.69P_2) b_2 - .5(8.34P_2) a1 + P_s$

Rearranged and solved, we get P_2/P_1 = .41. Therefore, P_2 = 3.64 kips. Because we are using Biaxial loads, we must use the interaction equation to determine the critical moment, M_x. Following procedure outlined, the critical moment M_{cry} = 84.4 k-in. The applied moment

M_y = 3.64 k-in. The interaction equation is

$M_x/M_{crx} + My/M_{cry} < 1.0$

Or $M_x < .96\ M_{crx} = 71.1$ k-in. So, $P_1 = 8.52$ kips and $P_2 = 3.41$ kips.

2.9.4 Summary of Maximum Loads

Critical loads are summarized in Table 39 and will be compared to experimental loads in Chapter 4. Deflections will be compared also.

Table 39. Summary of Buckling Limit. Investigation 9

Section	**Method**	**P_{cr}**
2.9.1	Central Difference with Shear Deformation	2.9 kips
2.9.2	Central Difference without Shear Deformation	7.25 kips
2.9.3	ASCE-LRFD Method	3.64 kips

CHAPTER 3

EXPERIMENTAL INVESTIGATION

Having determined critical buckling loads and translational and rotational deflections analytically in Chapter 2, empirical results are now determined from lab experiments for nine (9) investigations shown in Section 1.3.

Set up of lateral torsional testing apparatus is first discussed, then procedure for determining elastic modulus and shear modulus is demonstrated. These material properties vary among GFRP beam manufacturers.

Next, using ASCE-LRFD Prestandard, critical load limits for shear and local failure modes are determined then compare with lateral torsional buckling critical load limits. This was done to insure that the beams at the lengths and cross sections chosen fail lateral-torsionally.

Using a lateral torsional testing apparatus with dial gages mounted along its length, we gathered rotational and translational deflection data. Results are presented herein.

3.1 Experimental Equipment

Torsional testing to be performed is similar to rotational beam testing and is used to determine the angle of twist, the torsion failure load, and the maximum shear stress. The maximum angel of twist will be determined as the load at which the I beam fails to elastically return to its original state after unloading. Plastic limit will determined as the load at which the member is no longer able to support a load. In addition, information from torsional experiments will be used to develop an interaction equation and to review preliminary design guidelines for pultruded members as proposed by the ASCE.

To conduct the flexure torsional testing a flexural testing apparatus conceived by Dr. Sirjani and Dr. Razzaq is used. It is similar in design to a testing apparatus used by Lehigh University when conducting flexural experiments (See Figure 24). Consistency in testing procedure and testing equipment gives us a more accurate baseline with which to compare testing results from previous dissertations, textbooks, and experiments.

Figure 24. Lateral-Torsional Testing Apparatus at ODU

GFRP beams are held in place by metal supports fastened to the frame of the testing apparatus creating specified boundary conditions as shown in Figure 25. Each end of the beam is simply supported, one in a pinned-end and one in a roller condition, by a round bar assembly. The bar assemblies will be capable of being locked in position to allow different span lengths and creation of double and triple spans.

Figure 25. Supports

The test procedure involves providing testing loads through hydraulic pressure from hydraulic jacks as shown in Figure 26 and then recording deflections, strains, and the output from load cells so that we may evaluate twist, warping, stresses, deflections, and other strength parameters. The loads are to be applied in small increments and will be allowed to stabilize after two or three minutes after each increment before data is recorded.

The hydraulic jacks will be placed on fixed end steel beams located above the GFRP beam. This will allow application of loads so as not to inhibit rotation. Pistons pointing upward will be pushing upward against 6” x 24” x ½ “ steel plates which are supporting vertical steel rods. Vertical steel rods will be pulling up on steel plates which be placed in contact with the bottom of the test beam. The loads will be measured by calibrated load cells mounted upon each jack and plate assembly.

Figure 26. Hydraulic Jack and Pump

Jack and meter assemblies shown in Figure 27 will create loads through hydraulic pressure pumped manually and allow us to read load values. Tie rod assembly will allow the beam to develop lateral torsion and horizontal deflection as well as vertical deflection.

Figure 27. Jack and Meter for Hydraulic Pump

To measure translational and rotational deflections, dial gages will be positioned along the member as shown in Figure 28. Optionally, strain gages may be mounted along test beams to evaluate warping and twist.

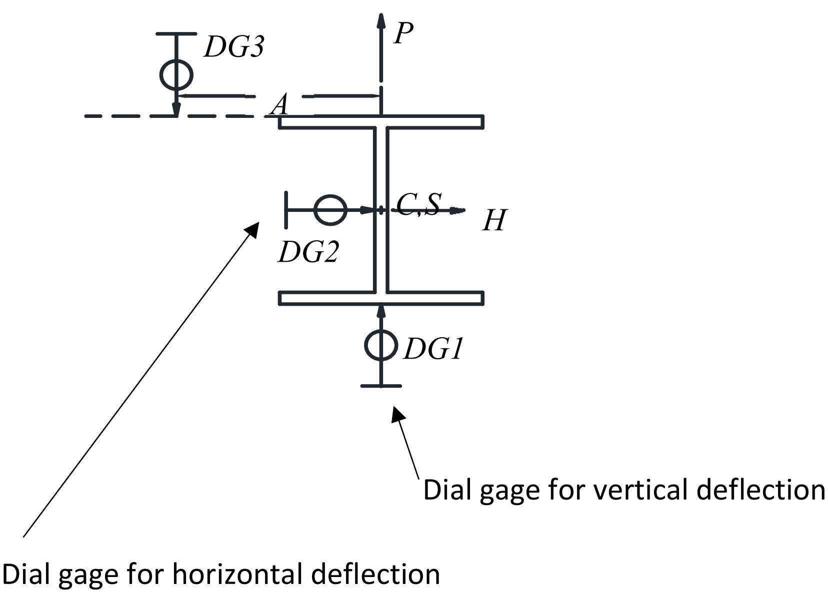

Figure 28. Dial Gages for Measuring Deflection

3.2 Material Properties and Specimens

One standard I beam of dimensions 4” x 4” x ¼” or 3” x 3” x ¼” and approximately 105 inches long is set up using single, double, or triple span boundary conditions and loaded for each investigation. The specimen is tested and results graphically compared. Vertical deflections, horizontal deflections, and torsional rotations obtained during experiment are compared with those predicted using our central difference approach. In addition, the failure modes of bending, lateral torsional buckling, shear, web or flange local buckling are observed and compared with those predicted using the ASCE guidelines. Because we are investigating lateral torsional buckling, these failure modes should not occur.

Elastic moduli, Young’s Modulus and Shear Modulus

Two of the most important elastic properties of the fiberglass reinforced plastic beams concerning shear deflection and torsion are associated with Young’s Modulus and the Shear Modulus, E and G, respectively. Thus, we will perform lab experiments to confirm their values for our 3” x 3” x ¼” and $’ x 4” x ¼” beams before we gin our analysis. Manufacturer’s data for the beams suggest that the range of the Elastic modules is between 2800 and 3200 x 10 ksi. E_x and E_y are shown to be the same.

During lab experiments to determine Modulus of Elasticity, cross sectional values of E_x and E_y were determined to be 2800 and 3194 ksi, respectively. These values were at the limits of the recommended manufacturer's range. For analysis purposes, E will be the average of these two values, 2997 ksi.

Shear modulus G from lab experiment was determined be 453 ksi. This is consistent with the recommended manufacturer's value. Analysis approaches to determine lab values of E and G are now presented herein.

Young's Modulus

Cantilevered beam is used as shown in Figure 29. This creates a uniform moment on the center span which we can consider free of shear deflection when we perform our deflection calculation. Once we determine the equations for deflection and run the experiment modeling it in the lab, we have one (1) unknown, E. Using the lab determined deflection value, we can solve for our unknown value of E.

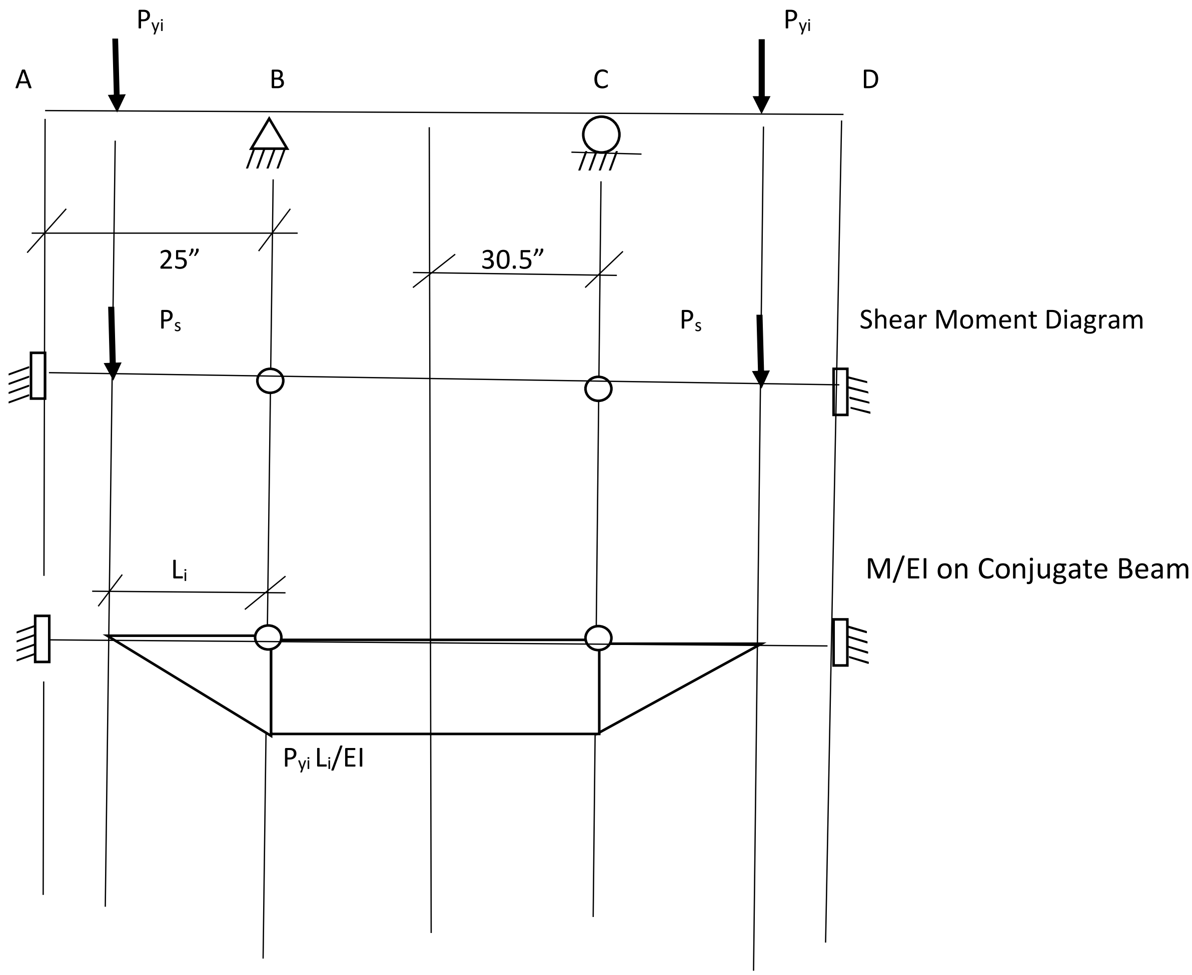

Figure 29. Shear and Moment Diagrams for Young’s Experiment

Using a superposition approach on the cantilever beam with hinge AC, we can determine what the reaction at the hinge is in the Y direction. Using this information and the moment load of the conjugate beam on BC, we can determine the deflection at the centerline BC.

On the major axis, the experimental deflection at centerline is .083”. With E_x =2800 ksi, we calculated a deflection of 1676.44/EI = .0755 without shear and .082 in. with shear. As such, E_x to be used in our analysis is 2800 ksi.

On the minor axis, the experimental deflection is .043”. With the understanding that the moment of inertia is about the bottom of the beam cross section and not the centroid. Our calculated value compares favorably to our experimental value and is .043” when using 3194 ksi for E_y. So, we have 2800 ksi for E_x, 3194 for E_y, and 2997 ksi for E when needing average. These values compare favorably with manufacturer's recommended value range of 2800 ksi to 3200 ksi.

Shear Modulus

In addition to the aforementioned experiment, the lateral deflection related to shear needs to be used to determine shear modulus which we need to use in our central difference calculations.

In our second material property experiment to determine the Shear Modulus, we load the beam as shown in Figure 30 to create a Torque T which is monitored along with the lateral deflection in the elastic range.

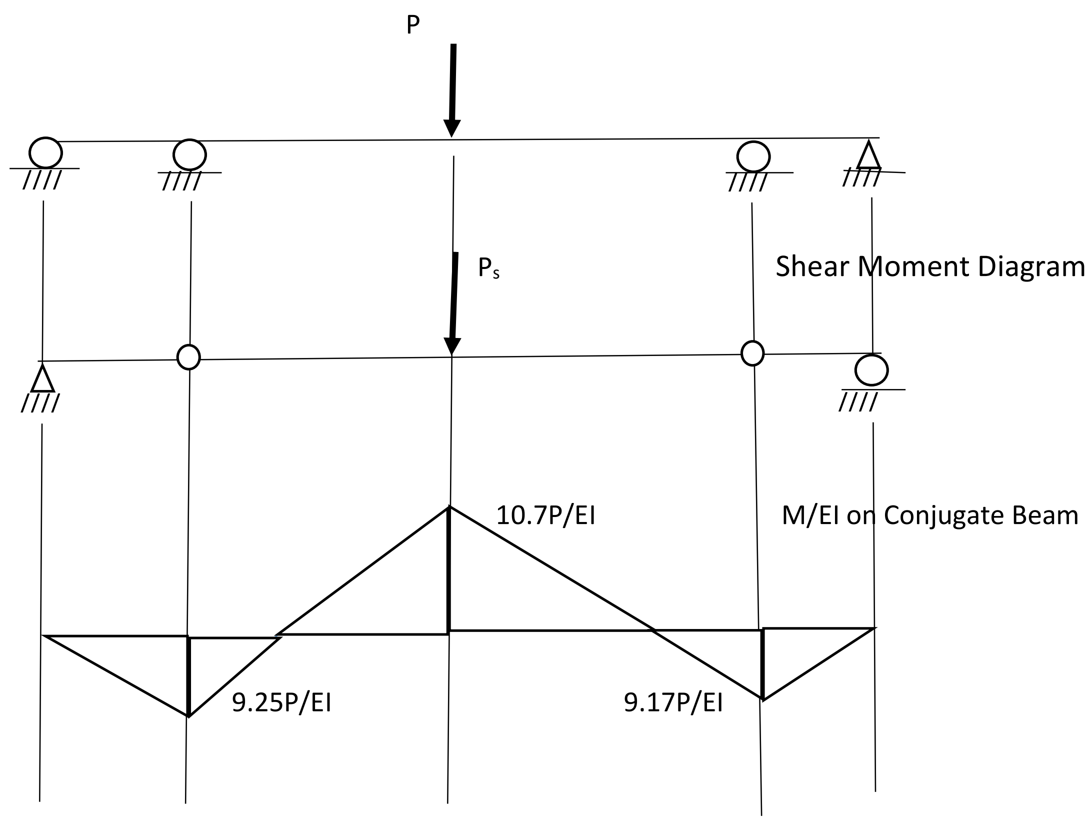

Figure 30. Shear and Moment Diagrams for Shear Modulus Experiment

Once we have experimental deflection values, we then model the experiment in central difference using the analytical approach we present herein. Using “G” as our unknown, we place known loads and other given info on the beam model then solve for G until we accomplish deflection observed in lab to obtain the same straightline deflection curve in the elastic range.

Solved. G was determined to be 453 ksi. Could not use typical classical finite difference approach because no relationships between in plane deflections and out of plane rotations are considered in typical torsion or bending moment equations. Consideration for end shears and differential warping between sections are included in the third equilibrium equation being used in our analysis approach presented herein. The equation is cited below:

$C_w\phi''' - (Ct + K)\phi' - M_x u' - M_y v' - v/L (M_{y1} + M_{y2}) - u/L (M_{x1} + M_{x2}) + (Py_o/2)\phi = 0$

The last five terms are not typically addressed in bending or torsion analysis.

3.3 Lab Investigations

Lab Investigation 1

Experimental results are now presented for investigation 1. Using ASCE-LRFD Prestandard, critical load limits for shear and local failure modes are determined then compared with lateral torsional buckling critical load limits. Beam established for investigation 1 predicted to fail in lateral torsion.

Experiment involves observance of vertical, horizontal, and lateral torsional deflections of a single span beam with point load at midspan. Dial gages are mounted along the beam with cross section, supports, and boundary conditions shown in Figure 31. Rotational and translational deflection data observed from lateral torsional testing for investigation 1 presented in this section.

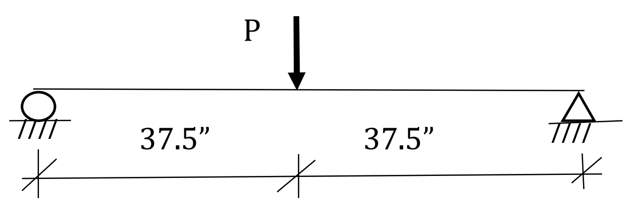

Figure 31. Investigation 1: Single Span Model

To determine what size beam to use in the beam testing apparatus, we evaluated the shear deflection and lateral torsional buckling characteristics of three fiber reinforced plastic I beams (See Figure 32). First, we eliminated the 6” x 6” x ¼” beam because the loading capacity of our testing apparatus may be exceeded.

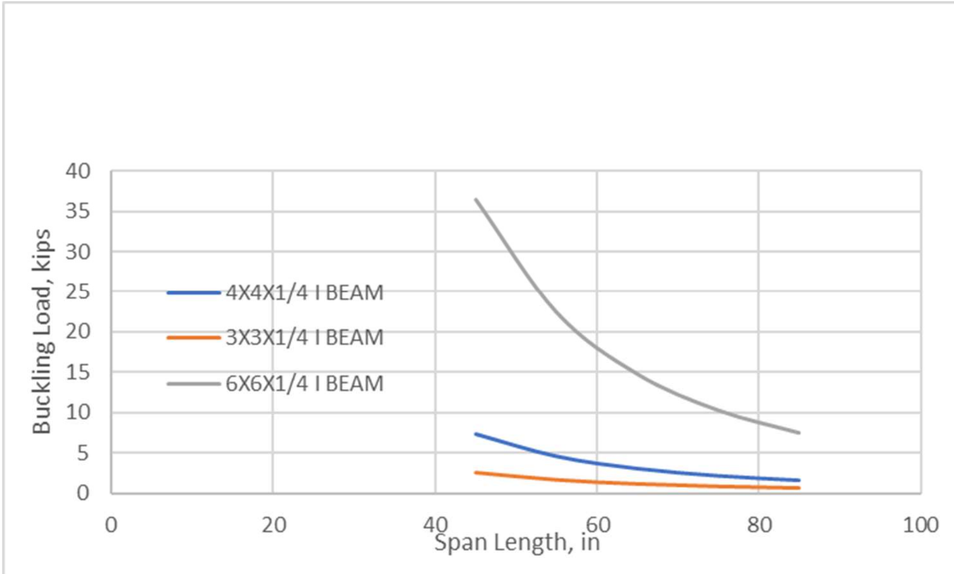

Figure 32. LTB Comparison of Cross Sections

Next, to establish a baseline for the investigation, we elected to perform single, double, and triple span experiments with the point load at midspan using the 4” x 4” x ¼” cross section. Alternatively, the 3” x 3” x ¼” cross section issued for single, double, and triple span experiments where the point loads are off-centered and moved toward the supports. The larger cross section is being used in the experiments associated with the location where the point load produces maximum deflection and max shear. Shorter span experiments were performed using the 3” x 3” x ¼” cross section. The objective was to keep buckling loads and deflections within range of testing apparatus and dial gages measuring deflections.

Lastly, beams were evaluated by their failure predictions as determined using the ASCE-LRFD Design Guide for Pultruded Members (See Appendix). These failures include material rupture, lateral torsional buckling, and shear. Since we are interested in lateral torsional buckling failure, we want to make sure beams fail lateral-torsionally before other failure modes are reached. Our own predictions for lateral-torsional buckling with shear were also considered. Graph showing lateral-torsional buckling failure is shown in Figure 33. It compares our central difference buckling solution with the ASCE-LRFD Design buckling solution.

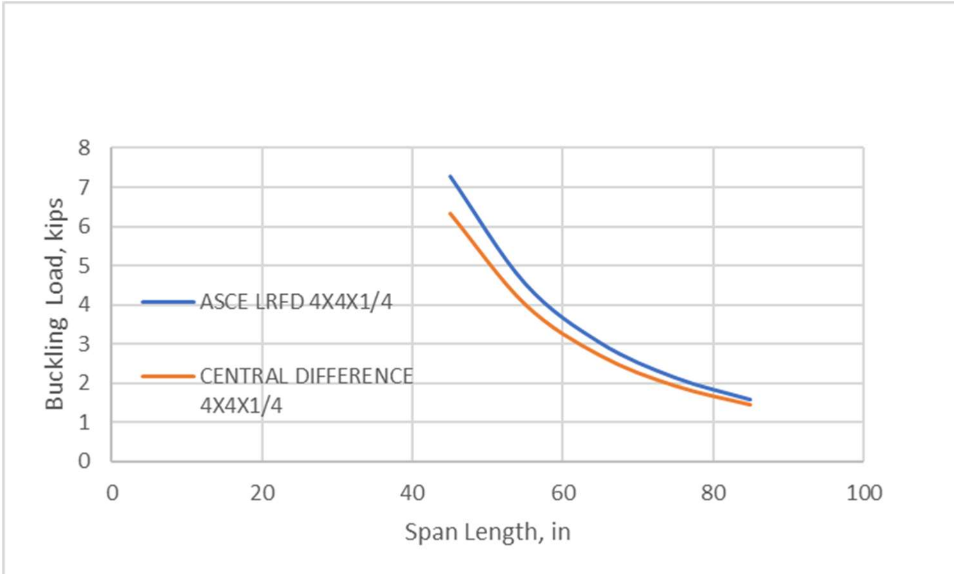

Figure 33. Central Diff vs ASCE Buckling Prediction Curves

A GFRP beam of dimensions 4” x 4” x ¼” x 75” is placed in our beam testing apparatus and in-plane loads will be placed upon the beam until it reaches lateral-torsional buckling failure. The objective is to identify in-plane deflection increases and out of plane deflections that are experienced as a result of shear. These typically unaddressed deflections often lead to premature buckling failure of the beam. We then compare buckling and deflection lab results to our predictions and ASCE Design values.

We are using an elastic modulus of 2997 ksi and a shear modulus of 453 ksi as determined during our material testing discussed earlier in Chapter 3. Looking at the manufacturer’s data for the fiberglass reinforced plastic beams, we see that the shear modulus is listed at .450 x 10 6 and the elastic modulus is typically between 2.8 and 3.2 x 10 6 psi. this information confirms our test results.

Beam Testing Apparatus shown previously includes a hydraulic pump and jack to place loads upon the specimen. Also, a meter for measuring the loads will be used. Dial gages are located along the beam as shown in Figure 34 for determination of vertical, horizontal, and lateral torsional deflections to be compared with deflection values obtained with our analytical models using the central difference approach for same locations.

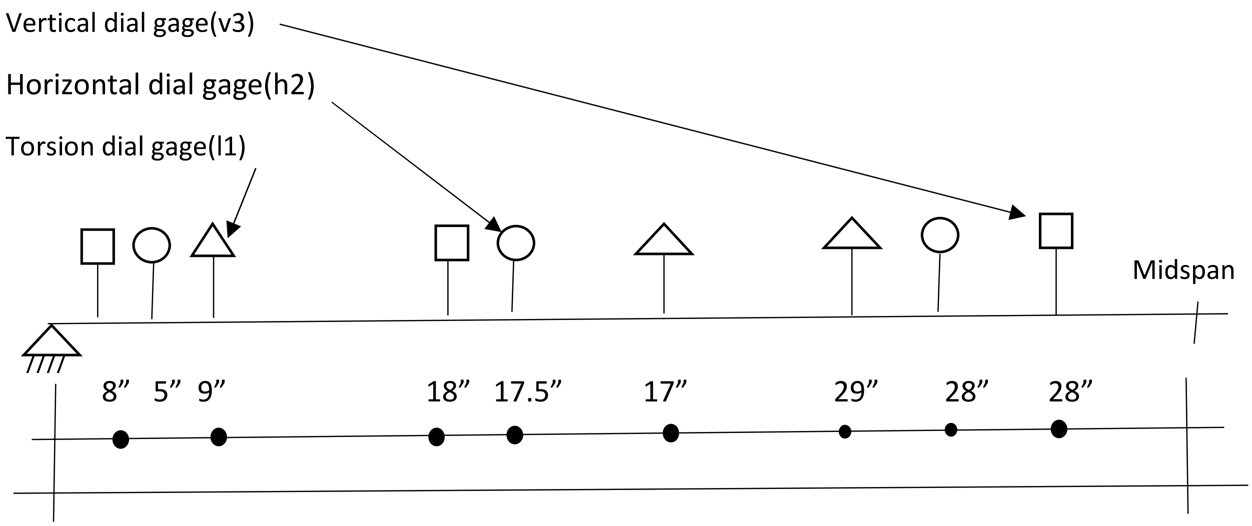

Figure 34. Dial Gage locations for Single Span Point Load Experiment

Mechanical properties and dimensions of the GFRP beam being used are as follows:

L = 75 inches; I beam is 4” x 4” x ¼”; Area A = 2.85 in.2; I = 7.93 in.4; F = 30 ksi; E = 2997 ksi; and G = 453 ksi.

Deflection values observed from lab experiment are shown in Table 40. They are compared with Central Difference deflection and buckling values and ASCE-LRFD buckling values in Chapter 4.

Table 40. Deflections from Lab. Investigation 1

	*8"	29"	18"	5"	17.5"	28"	9"	17"	28"
Load P	v1lab	v1lab	v1lab	h1	h1	h1	l1	l1	l1
0	0	0	0	0	0	0	0	0	0
.01408	.001	.004	.003	0	0	0	.0002	.00047	.00023
.12925	.019	.053	.042	.005	.006	.008	.0025	.00506	.00254
.31489	.043	.121	.093	.011	.017	.022	.0054	.01353	.006
.49130	.066	.178	.142	.016	.026	.034	.008	.0208	.00931
.6858	.091	.258	.189	.022	.036	.045	.011	.02871	.01377
.8787	.117	.329	.243	.029	.047	.056	.014	.03647	.01715
1.027	.137	.386	.284	.034	.055	.065	.016	.04282	.01977
1.362	.181	.509	.376	.045	.071	.082	.0208	.05588	.02554
1.612	.217	.607	.449	.052	.083	.094	.0246	.07153	.02969
1.832	.238	2.1	.489	.059	.09	.12	.0267	.09506	.03208
1.88	.248	2.7	.514	.062	.097	.15	.0279	.123	.03354

* Distance from support

Appendix 1. ASCE-LRFD Design Failure Modes. Investigation 1

For each investigation, we are examining several failure modes as defined by the ASCE to insure that each experiment fails in lateral-torsional buckling and not in another defined mode. Failure modes being evaluated include material rupture, compression flange local buckling, web local buckling, and shear.

For material rupture, the equation is:

$M_n = F_L(I/y)$ where $F_L = 30$ ksi and is the longitudinal strength of the member; $I = 7.935$ in.^{4};

And y = 2.0" and is the distance from the neutral axis to the extreme fiber of a member. Plugging in values, we have

$M_n = 30\ (7.935)/2.0\ ) = 119.025$ k-in.

The equation for compression flange local buckling is:

$M_n = f_{cr}(I/y)$ where

f_{cr} is the minimum critical buckling stress of the compression flange or the web. For compression flange local buckling,

$f_{cr} = (4t_f^2/b_f^2)\ ((7/12)(E_x\ E_y/(1 + 4.1\mathcal{E})).5 + G)$,

$\mathcal{E} = E_y t_f 3/(b_f k_t 6)$, and

$k_t = (E_x\ t_w^3/6h)\ (1 - ((48tr^2h^2E_y/(11.1\pi^2t_w^2b_r^2E_{LF}))(G/(1.25(E_y\ E_x)^{.5} + E_x v_{LT} + G)))$ where v_{LT} is Poisson's ratio , t_w is web thickness, and b_r is flange thickness. Plugging in values, we have

$f_{cr} = 19.59$ ksi.

For web local buckling,

$f_{cr} = (11.1\pi 2t_w^2/12h^2))(1.25(E_y\ E_x)^{.5} + E_x\ v_{LT} + G\ ) = 28.66$ ksi .

Critical stress of 19.59 ksi governs and

$M_n = 19.59\ (7.936/2.0) = 77.7$ k-in.

For shear, we will be examining shear and shear buckling failures. The equation for shear failure is:

$V_n = F_{LT}A_s$ where F_{LT} = 8 ksi and is the in-plane shear strength; and A_s = 4 in. x .25 = 1.0 in. ^{2}

And is the area of the web. Plugging these values in, we have

V_n = 8.0 x 1.0 = 8 kips.

The equation for web shear buckling is

$V_n = f_{cr}\ A_s$ where

$f_{c\,r} = (k_{LT}t_w^2/3h^2\ )(E_xE_y^3)^{.25}$ and $k_{LT} = 8.1 + 5.0(2G + E_y\, v_{LT}\ )/(E_x\ E_y\ )$ = 11.21. Plugging in values

f_{cr} =45.10 ksi and

V_n = 45.10(1.0) = 45.10 kips

For the 4" x 4" x ¼" beam, ASCE-LRFD failure mode values of shear and moment, V_n and M_n are as shown. The governing values of critical shear and critical moment for the ASCE-LRFD failure modes are shearing of the web and compression flange local buckling. For Investigation 1, the ASCE-LRFD P and M values for lateral-torsional buckling are 2.11 kips and 43.02 k-in. Because the critical values associated with the other failure modes are higher than the values determined using the lateral torsional buckling failure mode, the beam for this investigation is expected to fail in lateral torsional-buckling.

Lab Investigation 2

Experimental results are now presented for investigation 2. Using ASCE-LRFD Prestandard, critical load limits for shear and local failure modes are determined then compared with lateral-torsional buckling critical load limits. Beam established for investigation 2 predicted to fail in lateral-torsion.

Experiment involves observance of vertical, horizontal, and lateral- torsional deflections of a single span beam with a point load off center. Lateral- torsional buckling load is also being predicted and observed for the beam shown in Figure 35.

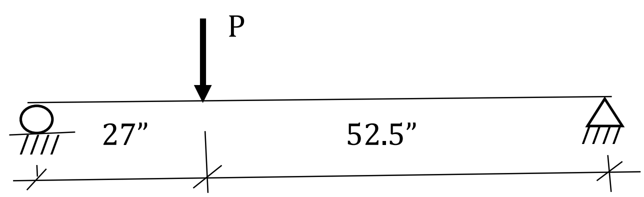

Figure 35. Investigation 2: Single Span Off Center

To determine what size beam to use in the beam testing apparatus, we evaluated the shear deflection and lateral- torsional buckling characteristics of three fiber reinforced plastic I beams (See Figure 36). First, we eliminated the 6” x 6” x ¼” beam because the loading capacity of our testing apparatus may be exceeded.

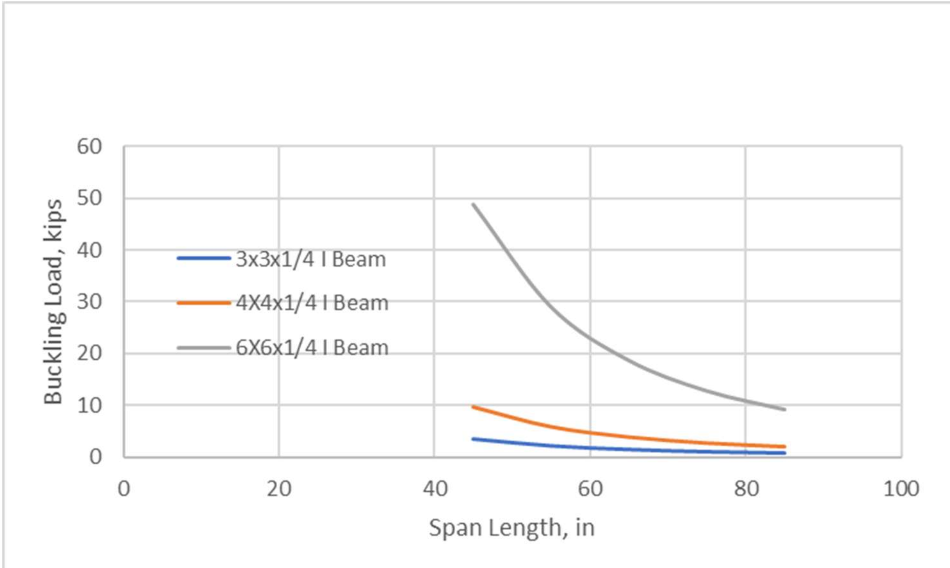

Figure 36. LTB Comparison of Cross Sections

Next, to establish a baseline for the investigation, we elected to perform single, double, and triple span experiments with the point load at midspan using the 4" x 4" x ¼" cross section. Alternatively, the 3" x 3" x ¼" cross section is used for single, double, and triple span experiments where the point loads are off-centered and on the outside span. The larger cross section is being used in the experiments associated with the location where the point load will produce maximum deflection and max shear. Shorter span experiments were performed using the 3" x 3" x ¼" cross section. The objective was to keep buckling loads and deflections within range of testing apparatus and dial gages measuring deflections.

Lastly, beams were evaluated by their failure predictions as determined using the ASCE-LRFD Design guide for Pultruded Members (See Appendix). These failures include material rupture, lateral- torsional buckling, and shear. Since we are interested in lateral- torsional buckling failure, we want to make sure beams fail lateral- torsionally before other failure modes are reached. Our own predictions for lateral- torsional buckling with shear were also considered. Graph showing lateral- torsional buckling failure is shown in Figure 37. It compares our central difference buckling solution with ASCE-LRFD Design buckling solution.

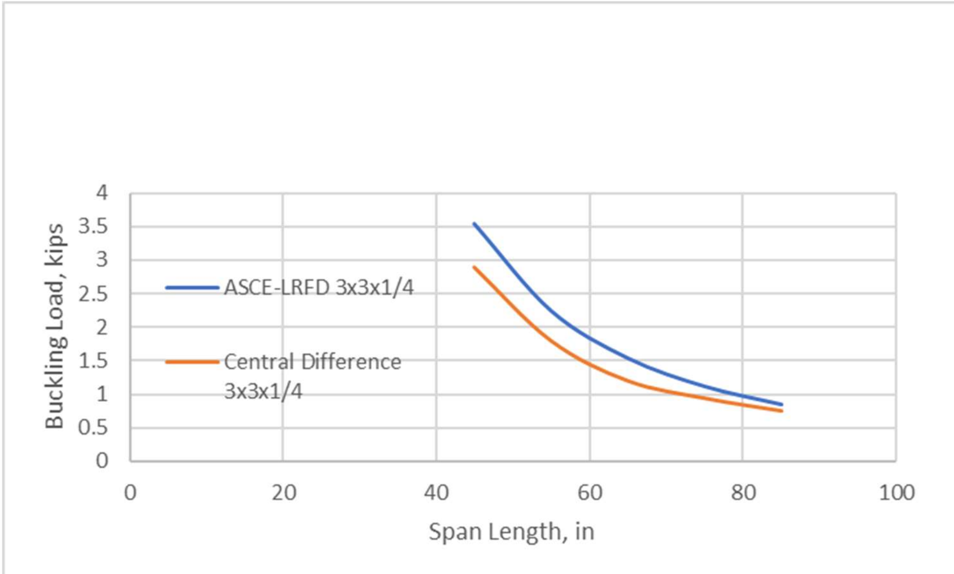

Figure 37. LTB and Failure Prediction Curves for 3 x 3 x ¼

A GFRP beam of dimensions 3" x 3" x ¼" x 79.5" will be placed in our beam testing apparatus and in-plane loads will be placed upon the beam as shown in Figure 35 until it reaches lateral- torsional buckling failure.

The objective is to identify in-plane deflection increases and out of plane deflections that are experienced as a result of shear. These typically unaddressed deflections often lead to premature buckling failure of the beam. We will then compare buckling results to our predictions and ASCE Design values.

We will be using an elastic modulus of 2997 ksi and a shear modulus of 453 psi as determined during our material testing discussed in Chapter 3. Looking at the manufacturer's data for the fiberglass reinforced plastic beams, we see that the shear modulus is listed at .450 x 10 6 and the elastic modulus is typically between 2.8 and 3.2 x 10 6 psi. This information confirms our test results.

Beam Testing Apparatus shown previously includes a hydraulic pump and jack to place loads up on the specimen. Also, a meter for measuring the loads will be used.

Dial gages were located along the beam as shown in Figure 38 for determination of vertical, horizontal, and lateral- torsional deflections to be compared with deflection values obtained with our analytical models using the central difference approach.

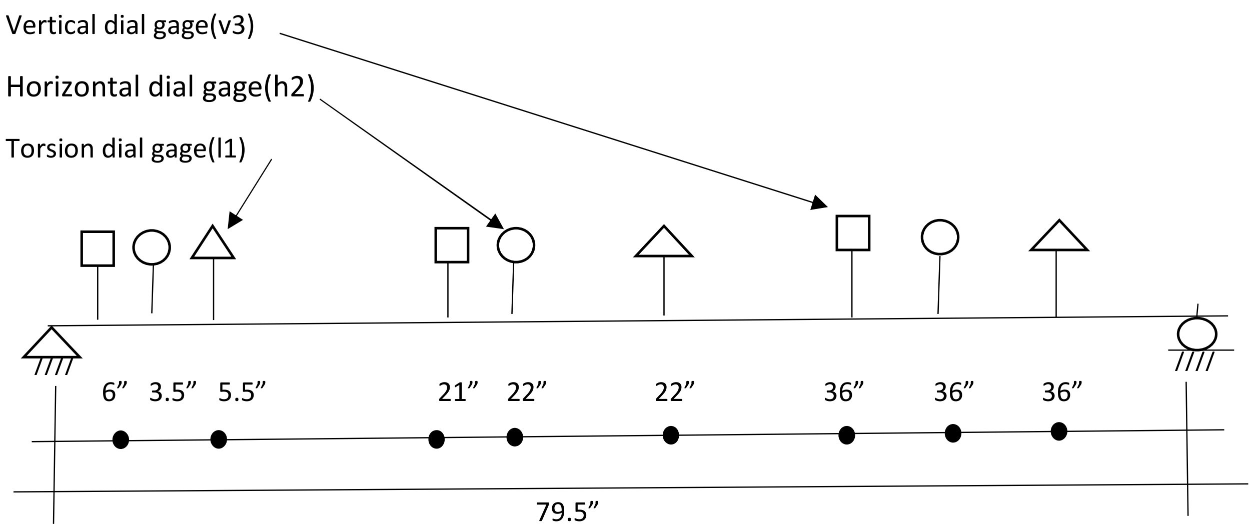

Figure 38. Dial Gage Locations for Single Span Point Load Off Center Experiment

Mechanical properties and dimensions of the GFRP beam being used are as follows: L = 79.5 inches; I beam is 3” x 3” x ¼”; Area A = 2.13 in. 2; I = 3.17 in. 4; F = 30 ksi; E = 2997 ksi; and G = 453 ksi.

Deflection values from lab experiment are shown in Table 41. They will be compared with Central Difference deflection and buckling values and ASCE-LRFD buckling values in Chapter 4.

Table 41. Deflections from Lab. Investigation 2

	*6"	21"	36"	3.5"	22"	36"	5.5"	22"	36"
Load P	v1 lab	v2 lab	v3 lab	h1	h2	h3	l1	l2	l3
0	0	0	0	0	0	0	0	0	0
.1826	.074	.23	.181	.002	0	.001	.077	.131	.0167
.4244	.132	.309	.399	.004	.003	.029	.14	.226	.0299
.6514	.206	.476	.593	.009	.005	.087	.199	.308	.0431
.8653	.338	.64	.792	.012	.008	.175	.263	.384	.0535
.91	.41	.794	.966	.023	.019	.33	.318	.449	.0763
.91			1.2			.8			.095
.91			1.4			.9			.105

*Distance from support

Appendix 2. ASCE-LRFD Design Failure Modes. Investigation 2

For each investigation, we are examining several failure modes as defined by the ASCE to insure that each experiment fails in lateral-torsional buckling and not in another defined mode. Failure modes being evaluated include material rupture, compression flange local buckling, web local buckling, and shear.

For material rupture, the equation is:

$M_n = F_L(I/y)$ where F_L = 30 ksi and is the longitudinal strength of the member; I = 3.17 in. ^{4};

And y = 1.5" and is the distance from the neutral axis to the extreme fiber of a member. Plugging in values, we have

M_n =30 (3.17)/1.5) = 63.4 k-in.

The equation for compression flange local buckling is:

$M_n = f_{cr}(I/y)$ where

f_{cr} is the minimum critical buckling stress of the compression flange or the web. For compression flange local buckling,

$f_{cr} = (4t_f^2/b_f^2)\ ((7/12)(E_x\ E_y/(1 + 4.1\mathcal{E})).5 + G)$,

$\mathcal{E} = E_y t_f 3/(b_f k_t 6)$, and

$k_t = (E_x\ t_w^3/6h)\ (1 - ((48tr^2h^2E_y/(11.1\pi^2t_w^2br^2E_{LF}))(G/(1.25(E_y\ E_x)^{.5} + E_x v_{LT} + G)))$ where v_{LT} is Poisson's ratio , t_w is web thickness, and br is flange thickness. Plugging in values, we have

f_{cr} = 34.82 ksi.

For web local buckling,

$f_{cr} = (11.1\pi 2t_w^2/12h^2))(1.25(E_y\ E_x)^{.5} + E_x\ v_{LT} + G) = 50.96$ ksi .

Critical stress of 34.82 ksi governs and

M_n =34.82 (3.17/1.5) = 73.6 k-in.

For shear, we will be examining shear and shear buckling failures. The equation for shear failure is:

$V_n = F_{LT}A_s$ where F_{LT} = 8 ksi and is the in-plane shear strength; and A_s = 3 in. x .25 = .75 in. ^{2}

And is the area of the web. Plugging these values in, we have

V_n = 8.0 x .75 = 6 kips.

The equation for web shear buckling is

$V_n = f_{cr} A_s$ where

$f_{cr} = (k_{LT}t_w^2/3h^2)(E_xE_y^3)^{.25}$ and $k_{LT} = 8.1 + 5.0(2G + E_y v_{LT})/(E_x E_y)$ = 11.21. Plugging in values

f_{cr} = 80.17 ksi and

V_n = 80.17(.75) = 60.13 kips

For the 3” x 3” x ¼” beam, ASCE-LRFD failure mode values of shear and moment, V_n and M_n are as shown. The governing values of critical shear and critical moment for the ASCE-LRFD failure modes are shearing of the web and compression flange local buckling. For Investigation 2, the ASCE-LRFD P_{cr} and M_{cr} values for lateral-torsional buckling are 1.0 kips and 18.68 k-in. Because the critical values associated with the other failure modes are higher than the values determined using the lateral torsional buckling failure mode, the beam for this investigation is expected to fail in lateral torsional-buckling.

Lab Investigation 3

Experimental results are now presented for investigation 3. Using ASCE-LRFD Prestandard, critical load limits for shear and local failure modes are determined then compared with lateral- torsional buckling critical load limits. Beam established for investigation 3 predicted to fail in lateral torsion.

Experiment involves observance of vertical, horizontal, and lateral torsional deflections of a two span beam with a point load at midspan of the longer span. Lateral-torsional buckling load is also being predicted and observed for the beam shown in Figure 39.

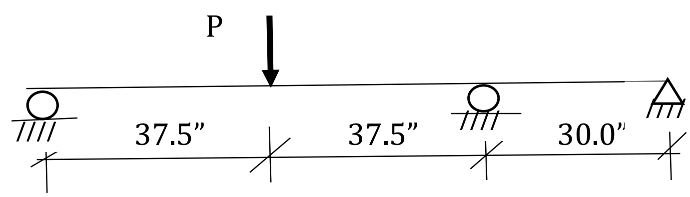

Figure 39. Investigation 3. Two Span Model

To determine what size beam to use in the beam testing apparatus, we evaluated the shear deflection and lateral-torsional buckling characteristics of three fiber reinforced plastic I beams (See Figure 40). First, we eliminated the 6” x 6” x ¼” beam because the loading capacity of our testing apparatus may be exceeded.

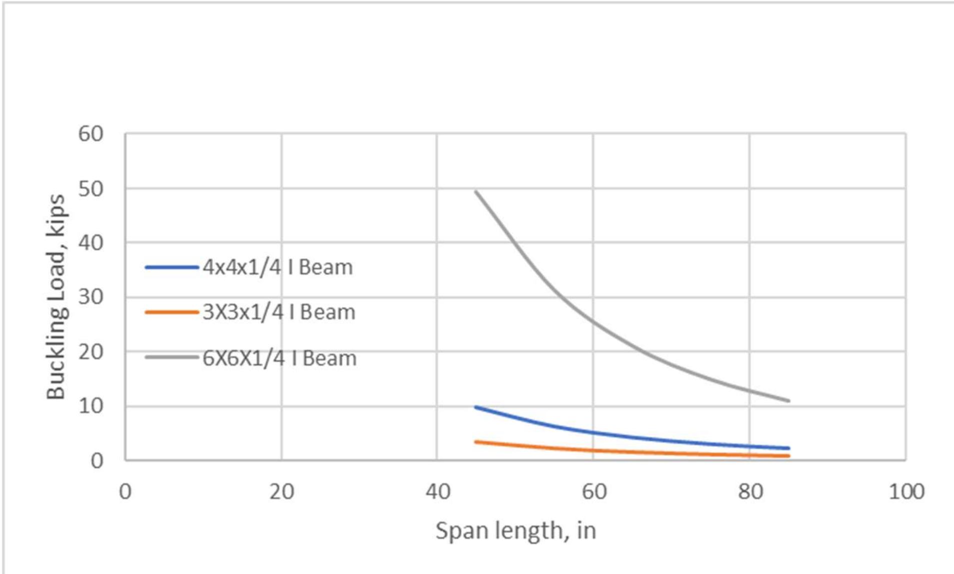

Figure 40. LTB Comparison of Cross Sections

Next, to establish a baseline for the investigation, we elected to perform single, double, and triple span experiments with the point load at midspan using the 4" x 4" x ¼" cross section. Alternatively, the 3" x 3" x ¼" cross section is used for single, double, and triple span experiments where the point loads are off-centered or on an outside span. The larger cross section is being used in the experiments associated with the location where the point load will produce maximum deflection and max shear. Shorter span experiments were performed using the 3" x 3" x ¼" cross section. The objective was to keep buckling loads and deflections within range of testing apparatus and dial gages measuring deflections.

Lastly, beams were evaluated by their failure predictions as determined using the ASCE-LRFD Design Guide for Pultruded Members (See Appendix). These failures include material rupture, lateral-torsional bucking, and shear. Since we are interested in lateral-torsional buckling failure, we want to make sure beams fail lateral- torsionally before other failure modes are reached. Our own predictions for lateral-torsional buckling with shear were also considered. Graph showing lateral-torsional buckling failure is shown in Figure 41. It compares our central difference buckling solution with the ASCE-LRFD Design buckling solution.

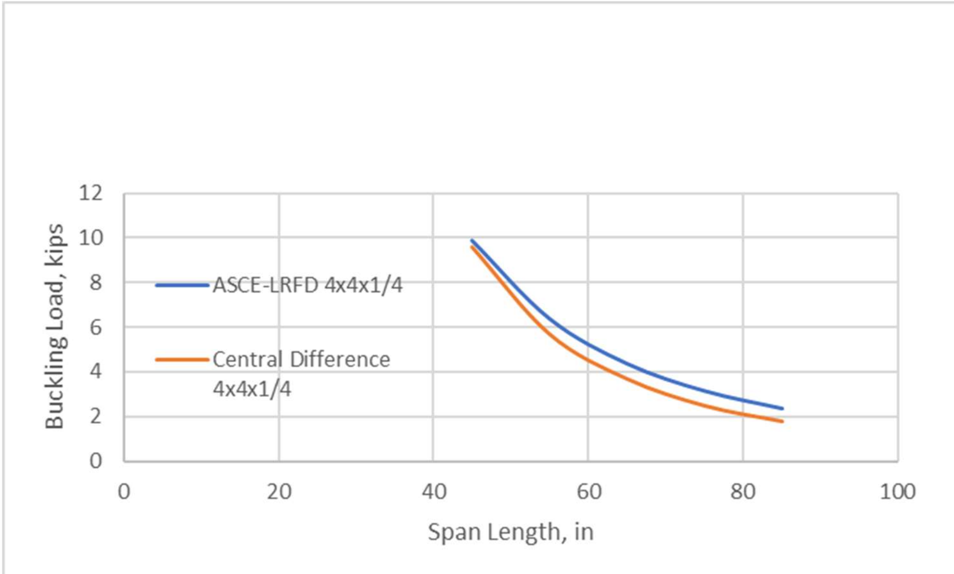

Figure 41. Central Diff vs ASCE Buckling Prediction Curves

A GFRP beam of dimensions 4” x 4” x ¼” x 105” will be placed in our beam testing apparatus and in-plane loads will be placed upon the beam as shown in Figure 39 until it reaches lateral torsional buckling failure.

The objective is to identify in-plane deflection increases and out of plane deflections that are experienced as a result of shear. These typically unaddressed deflections often lead to premature buckling failure of the beam. We will then compare buckling results to our predictions and ASCE Design values.

We will be using an elastic modulus of 2997 ksi and a shear modulus of 453 ksi as determined during our material testing discussed in Chapter 3. Looking at the manufacturer’s data for the fiberglass reinforced plastic beams, we see that the shear modulus is listed at .450 x 10 6 and the elastic modulus is typically between 2.8 and 3.2 x 10 6 psi. This information confirms our test results.

Beam Testing Apparatus shown previously includes a hydraulic pump and jack to place loads upon the specimen. Also, a meter for measuring the loads will be used.

Dial gages were located along the beam as shown in Figure 42 for determination of vertical, horizontal, and lateral torsional deflections to be compared with deflection values obtained with our analytical models using the central difference approach.

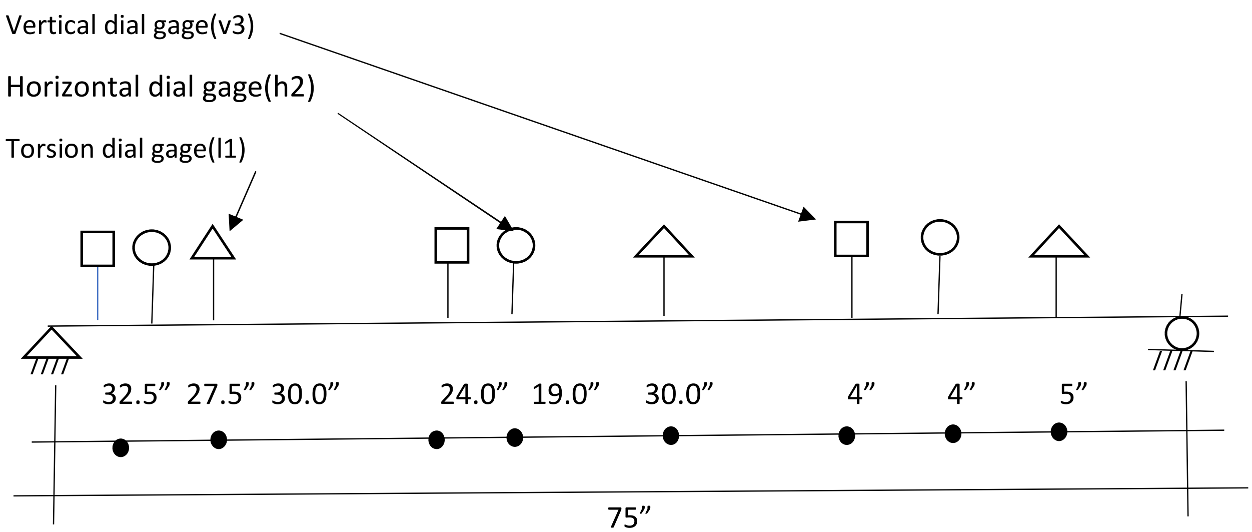

Figure 42. Dial Gages for Two Span Point Load Experiment

Mechanical properties and dimensions of the GFRP beam being used are as follows:

L_1 = 30 inches; L_2 = 75 inches; I beam is 4” x 4” x ¼”; Area A = 2.85 in.2; I = 7.93 in. 4; F = 30ksi; e = 2997 ksi; and G = 453 ksi.

Deflection values from lab experiment are shown in Table 42. They will be compared with Central Difference deflection and buckling values and AXCE-LRFD buckling values in Chapter 4.

Table 42. Deflections from Lab. Investigation 3

	*32.5"	29"	4"	27.5"	24"	4"	30"	30"	5"
Load P	**v1 lab**	**v2 lab**	**v3 lab**	**h1**	**h2**	**h3**	**l1**	**l2**	**l3**
0	0	0	0	0	0	0	0	0	0
.3464	.0897	.046	.022	0	0	0	.0081	.00554	0
.5803	.1503	.104	.037	.008	.002	.002	.0145	.01023	.00115
.8144	.2109	.146	.052	.009	.003	.003	.021	.01477	.00231
1.047	.2711	.202	.069	.016	.009	.004	.0272	.01931	.00354
1.245	.3223	.255	.083	.021	.014	.005	.0329	.02338	.00454
1.418	.3671	.3	.095	.027	.015	.006	.0374	.02662	.00546
1.617	.4188	.353	.109	.032	.02	.008	.043	.03046	.00646
1.794	.4645	.401	.122	.035	.022	.009	.0477	.03385	.00746
2.028	.5251	.464	.14	.05	.026	.011	.0544	.03862	.00877
2.326	.6023	.549	.163	.061	.038	.012	.0615	.04354	.00992
2.5	1.2			.07	.055		.12		
2.6	1.5			.16	.09		.15		

***Distance from support**

Appendix 3. ASCE-LRFD Design Failure Modes. Investigation 3

For each investigation, we are examining several failure modes as defined by the ASCE to insure that each experiment fails in lateral-torsional buckling and not in another defined mode. Failure modes being evaluated include material rupture, compression flange local buckling, web local buckling, and shear.

For material rupture, the equation is:

$M_n = F_L(I/y)$ where F_L = 30 ksi and is the longitudinal strength of the member; I = 7.935 in. ^{4};

And y = 2.0” and is the distance from the neutral axis to the extreme fiber of a member. Plugging in values, we have

M_n =30 (7.935)/2.0) = 119.025 k-in.

The equation for compression flange local buckling is:

$M_n = f_{cr}(I/y)$ where

f_{cr} is the minimum critical buckling stress of the compression flange or the web. For compression flange local buckling,

$f_{cr} = (4t_f^2/b_f^2)\ ((7/12)(E_x\ E_y/(1 + 4.1\mathcal{E})).5 + G)$,

$\mathcal{E} = E_y t_f 3/(b_f k_t 6)$, and

$k_t = (E_x\ t_w^3/6h)\ (1 - ((48tr^2h^2E_y/(11.1\pi^2t_w^2br^2E_{LF}))(G/(1.25(E_y\ E_x)^{.5} + E_x v_{LT} + G)))$ where v_{LT} is Poisson’s ratio , t_w is web thickness, and br is flange thickness. Plugging in values, we have

f_{cr} = 19.59 ksi.

For web local buckling,

$f_{cr} = (11.1\pi 2t_w^2/12h^2))(1.25(E_y\ E_x)^{.5} + E_x\ v_{LT} + G) = 28.66$ ksi .

Critical stress of 19.59 ksi governs and

M_n =19.59 (7.936/2.0) = 77.7 k-in.

For shear, we will be examining shear and shear buckling failures. The equation for shear failure is:

$V_n = F_{LT}A_s$ where F_{LT} = 8 ksi and is the in-plane shear strength; and A_s = 4 in. x .25 = 1.0 in. ^{2}

And is the area of the web. Plugging these values in, we have

V_n = 8.0 x 1.0 = 8 kips.

The equation for web shear buckling is

$V_n = f_{cr} A_s$ where

$f_{cr} = (k_{LT}t_w^2/3h^2)(E_xE_y^3)^{.25}$ and $k_{LT} = 8.1 + 5.0(2G + E_y v_{LT})/(E_x E_y)$ = 11.21. Plugging in values

f_{cr} =45.10 ksi and

V_n = 45.10(1.0) = 45.10 kips

For the 4" x 4" x ¼" beam, ASCE-LRFD failure mode values of shear and moment, V_n and M_n are as shown. The governing values of critical shear and critical moment for the ASCE-LRFD failure modes are shearing of the web and compression flange local buckling. For Investigation 3, the ASCE-LRFD P and M values for lateral-torsional buckling are 3.16 kips and 51.53 k-in. Because the critical values associated with the other failure modes are higher than the values determined using the lateral-torsional buckling failure mode, the beam for this investigation is expected to fail in lateral-torsional-buckling.

Lab Investigation 4

Experimental results are now presented for investigation 4. Using ASCE-LFRD Prestandard, critical load limits for shear and local failure modes are determined then compared with lateral torsional buckling critical load limits. Beam established for investigation 4 predicted to fail in lateral torsion.

Experiment involves observance of vertical, horizontal, and lateral torsional deflections of a two span I beam with point load at midspan and spans are near equal. Lateral torsional buckling load is also being predicted and observed on beam shown in Figure 43.

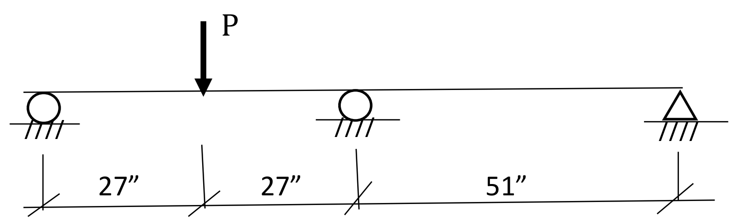

Figure 43. Investigation 4: Two Span Near Equal

To determine what size beam to use in the beam testing apparatus, we evaluated the shear deflection and lateral torsional buckling characteristics of three fiber reinforced plastic I beams (See Figure 44). First, we eliminated the 6” x 6” x ¼” beam because the loading capacity of our testing apparatus may be exceeded.

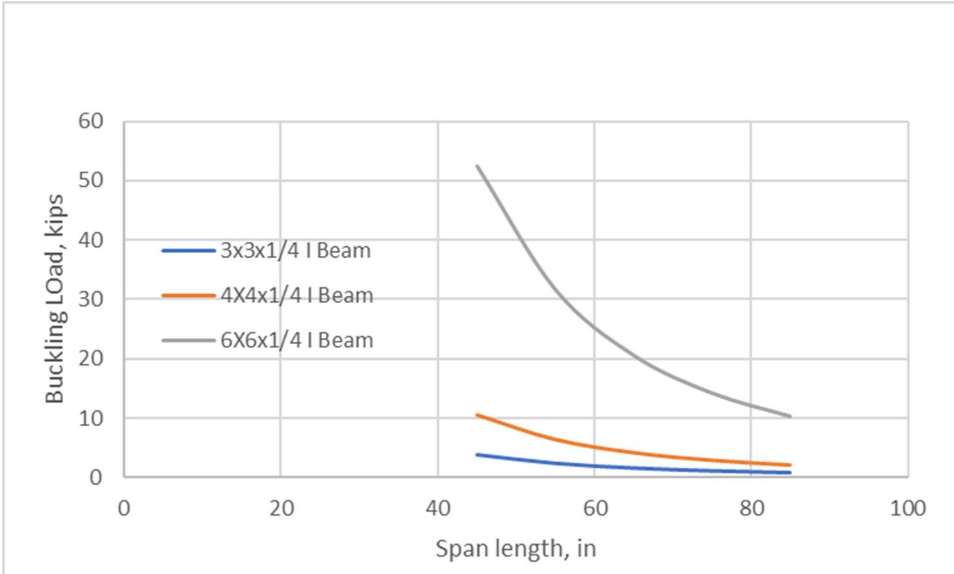

Figure 44. LTB Comparison of Cross Sections

Next, to establish a baseline for the investigation, we elected to perform single, double, and triple span experiments with the point load at midspan using the 4” x 4” x ¼” cross section. Alternatively, the 3” x 3” x ¼” cross section is used for single, double, and triple span experiments where the point loads are off-centered and moved toward the supports. The larger cross section is being used in the experiments associated with the location where the point load will produce maximum deflection and max shear. Shorter span experiments were also performed using the 3” x 3” x ¼” cross section. The objective was to keep buckling loads and deflections within range of testing apparatus and dial gages measuring deflections.

Lastly beams were evaluated by their failure predictions as determined suing the ASCE-LRFD Design Guide for Pultruded Members (See Appendix). These failures include material rupture, lateral torsional buckling, and shear. Since we are interested in lateral- torsional buckling failure, we want to make sure beams fail lateral- torsionally before other failure modes are reached. Our own predictions for lateral- torsional buckling with shear were also considered. Graph showing lateral- torsional buckling with shear were also considered. Graph showing lateral torsional buckling failure is shown in Figure 45. It compares our central difference buckling solutions with ASCE-LRFD Design buckling solutions.

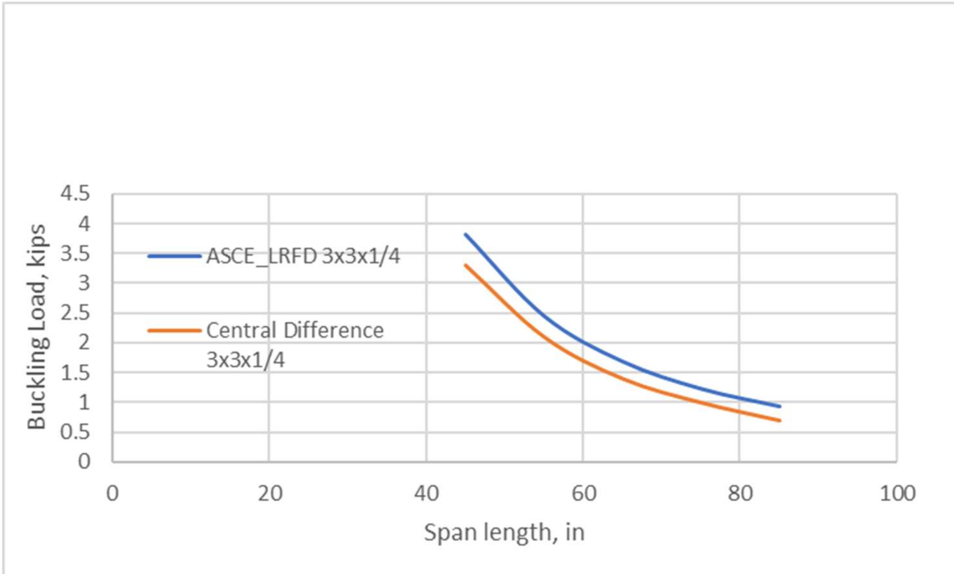

Figure 45. Central Diff vs ASCE Buckling Prediction Curves

A GFRP beam of dimensions 3” x 3” x ¼” x 105” will be placed in our beam testing apparatus and in-plane loads will be placed upon the beam as shown in Figure 43 until it reaches lateral-torsional buckling failure.

The objective is to identify in-plane deflection increases and out of plane deflections that are experienced as a result of shear. These typically unaddressed deflections often lead to premature buckling failure of the beam. We will then compare buckling results to our predictions and ASCE Design values.

We will be using an elastic modulus of 2997 ksi and a shear modulus of 453 ksi as determined during our material testing discussed in chapter 1. Looking at the manufacturer’s data for the fiberglass reinforced plastic beams, we see that the shear modulus is listed at .450 x 10 6 and the elastic modulus is typically between 2.8 and 3.2 x 10 6 psi. This information confirms our test results.

Beam Testing Apparatus shown previously includes a hydraulic pump and jack to place loads upon the specimen. Also, a meter for measuring the loads will be used.

Dial gages were located along the beam as shown in Figure 46 for determination of vertical, horizontal, and lateral torsional deflections to be compare with deflection values obtained with our analytical models using the central difference approach.

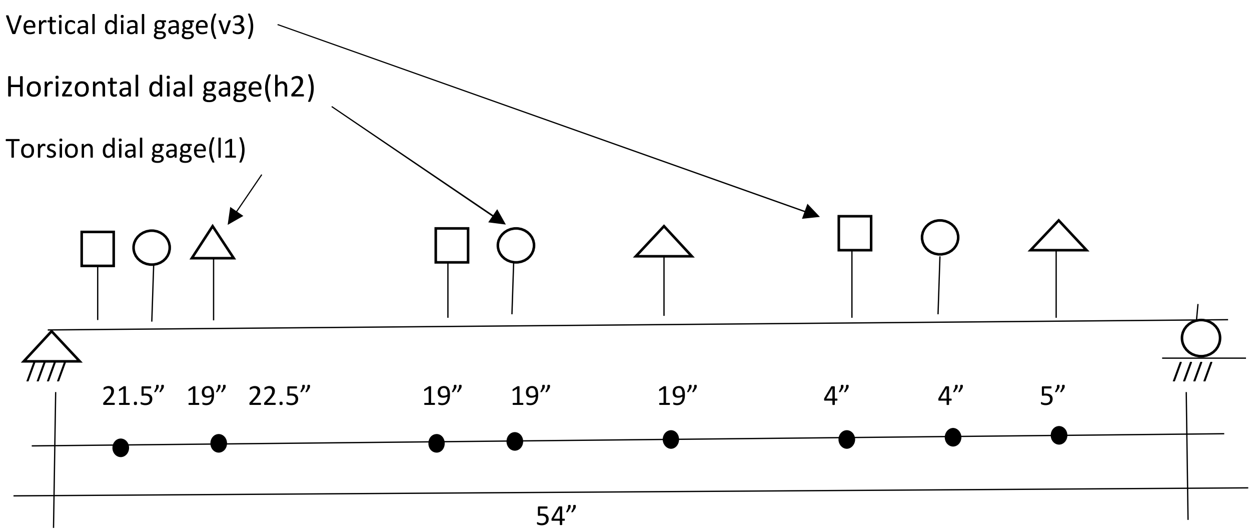

Figure 46. Dial Gage Locations for Two Span Near Equal Experiment

Mechanical properties and dimensions of the GFRP beam being used are as follows:

L_1 = 54.0 inches; I beam is 3” x 3” x ¼”; Area A = 2.13 in. 2; I = 3.17 in. 4; F = 30 ksi; E = 2997 ksi; and G = 453 ksi.

Deflection values from lab experiment are shown in Table 43. They will be compare with Central Difference deflection and buckling values and ASCE-LRFD buckling values in Chapter 4.

Table 43. Deflections from Lab. Investigation 4

	*21.5"	19"	4"	19"	19"	4"	22.5"	19"	5"
Load P	v1 lab	v2 lab	v3 lab	h1	h2	h3	l1	l2	l3
0	0	0	0	0	0	0	0	0	0
.2770	.1129	.0760	.02	.001	0	0	.0061	.0083	.00276
.6562	.2182	.1588	.046	.006	.004	0	.0165	.017	.00476
.8359	.2709	.2005	.06	.01	.007	.001	.0214	.0211	.00562
1.006	.3295	.2393	.076	.014	.01	.002	.0264	.025	.00548
1.154	.3762	.2766	.089	.016	.012	.003	.0309	.0287	.00724
1.385	.445	.3318	.109	.019	.015	.004	.0374	.0342	.00838
1.571	.5019	.3772	.126	.024	.019	.005	.043	.0387	.0092
1.733	.552	.419	.142	.028	.022	.006	.0477	.0425	.01
2.038	.6471	.495	.169	.039	.027	.007	.0559	.049	.01238
2.37	.8	.5696	.196	.058	.042	.008	.0666	.0582	.01828
2.37	1.43			.116					.0225

*Distance from support

Appendix 4. ASCE-LRFD Design Failure Modes. Investigation 4

For each investigation, we are examining several failure modes as defined by the ASCE to insure that each experiment fails in lateral-torsional buckling and not in another defined mode. Failure modes being evaluated include material rupture, compression flange local buckling, web local buckling, and shear.

For material rupture, the equation is:

$M_n = F_L(I/y)$ where F_L = 30 ksi and is the longitudinal strength of the member; I = 3.17 in. ^{4};

And y = 1.5" and is the distance from the neutral axis to the extreme fiber of a member. Plugging in values, we have

M_n =30 (3.17)/1.5) = 63.4 k-in.

The equation for compression flange local buckling is:

$M_n = f_{cr}(I/y)$ where

f_{cr} is the minimum critical buckling stress of the compression flange or the web. For compression flange local buckling,

$f_{cr} = (4t_f^2/b_f^2)\ ((7/12)(E_x\ E_y/(1 + 4.1\mathcal{E})).5 + G)$,

$\mathcal{E} = E_y t_f 3/(b_f k_t 6)$, and

$k_t = (E_x\ t_w^3/6h)\ (1 – ((48tr^2h^2E_y/(11.1\pi^2t_w^2br^2E_{LF}))(G/(1.25(E_y\ E_x)^{.5} + E_x v_{LT} + G)))$ where v_{LT} is Poisson's ratio , t_w is web thickness, and br is flange thickness. Plugging in values, we have

f_{cr} = 34.82 ksi.

For web local buckling,

$f_{cr} = (11.1\pi 2t_w^2/12h^2))(1.25(E_y\ E_x)^{.5} + E_x\ v_{LT} + G) = 50.96$ ksi .

Critical stress of 34.82 ksi governs and

M_n =34.82 (3.17/1.5) = 73.6 k-in.

For shear, we will be examining shear and shear buckling failures. The equation for shear failure is:

$V_n = F_{LT}A_s$ where F_{LT} = 8 ksi and is the in-plane shear strength; and A_s = 3 in. x .25 = .75 in. ^{2}

And is the area of the web. Plugging these values in, we have

V_n = 8.0 x .75 = 6 kips.

The equation for web shear buckling is

$V_n = f_{cr}\, A_s$ where

$f_{c\,r} = (k_{LT}t_w^2/3h^2\,)(E_xE_y^3)^{.25}$ and $k_{LT} = 8.1 + 5.0(2G + E_y\, v_{LT}\,)/(E_x\, E_y\,)$ = 11.21. Plugging in values

f_{cr} = 80.17 ksi and

V_n = 80.17(.75) = 60.13 kips

For the 3" x 3" x ¼" beam, ASCE-LRFD failure mode values of shear and moment, V_n and M_n are as shown. The governing values of critical shear and critical moment for the ASCE-LRFD failure modes are shearing of the web and compression flange local buckling. For Investigation 4, the ASCE-LRFD P_{cr} and M_{cr} values for lateral-torsional buckling are 2.64 kips and 32.89 k-in. Because the critical values associated with the other failure modes are higher than the values determined using the lateral-torsional buckling failure mode, the beam for this investigation is expected to fail in lateral-torsional buckling.

Lab Investigation 5

Experimental results are now presented for investigation 5. Using ASCE-LRFD Prestandard, critical load limits for shear and local failure modes are determined then compared with lateral-torsional buckling critical load limits. Beam established for investigation 5 predicted to fail in lateral-torsion.

Experiment involves observance of vertical, horizontal, and lateral- torsional deflections of a two span beam with point load off center. Lateral- torsional buckling load is also being predicted and observed for the beam shown in Figure 47.

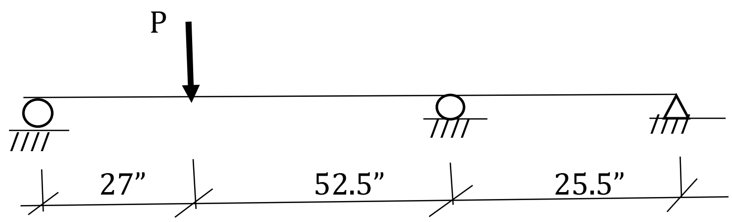

Figure 47. Investigation 5: Two Span Off Center Model

To determine what size beam to use in the beam testing apparatus, we evaluated the shear deflection and lateral torsional buckling characteristics of three fiber reinforced plastic I beams (See Figure 48). First, we eliminated the 6" x 6" x ¼" beam because the loading capacity of our testing apparatus may be exceeded.

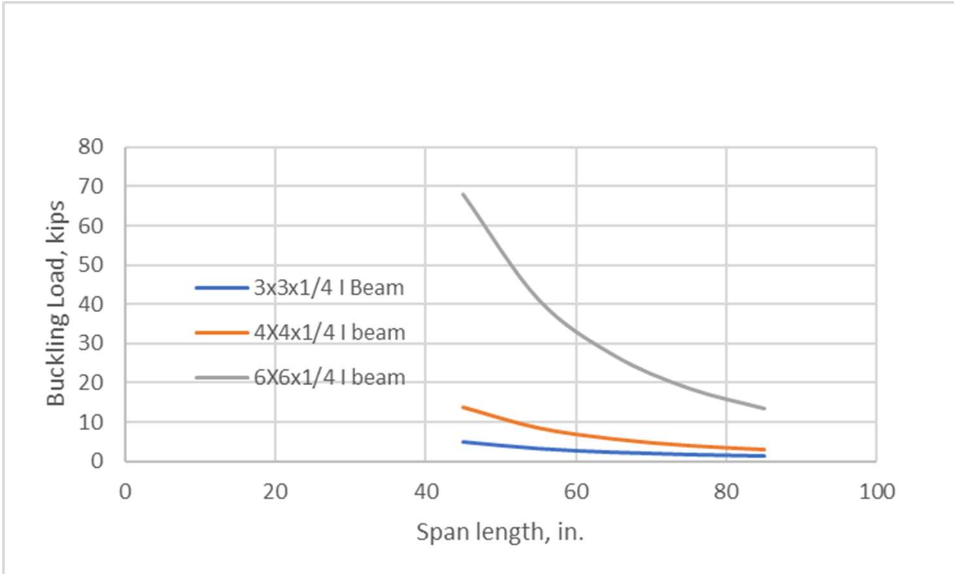

Figure 48. LTB Comparison of Cross Sections

Next, to establish a baseline for the investigation, we elected to perform single, double, and triple span experiments with the point load at midspan using the 4” x 4” x ¼” cross section. Alternatively, the 3” x 3” x ¼” cross section is used for single, double, and triple span experiments where the point loads are of-centered and moved toward the supports. The larger cross section is being used in the experiments associated with the location where the point load will produce maximum deflection and max shear. Shorter span experiments were performed using the 3 x 3 x ¼ cross section. The objective was to keep buckling loads and deflections within range of testing apparatus and dial gages measuring deflections.

Lastly, beams were evaluated by their failure predictions as determined using the ASCE-LRFD Design Guide for Pultruded Members (See Appendix). These failures include material rupture, lateral torsional buckling, and shear. Since we are interested in lateral torsional buckling failure, we want to make sure beams fail lateral- torsionally before other failure modes are reached. Our own predictions for lateral torsional buckling with shear were also considered. Graph showing lateral torsional buckling failure is shown in Figure 49. It compares the central difference buckling solutions with the ASXE-LRFD Design buckling solutions.

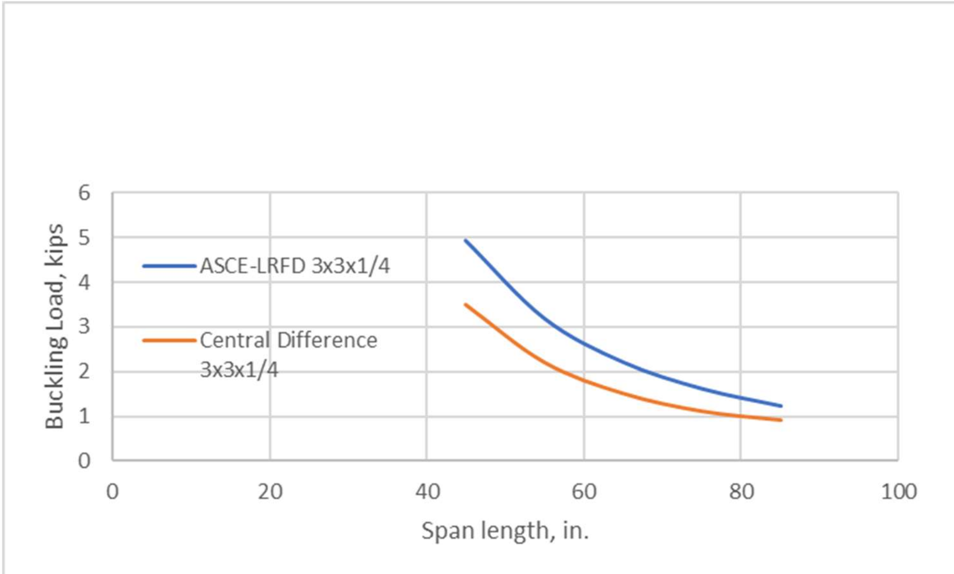

Figure 49. Central Diff vs ASCE Buckling Prediction Curves

A GFRP beam of dimensions 3” x 3” x ¼” x 105” will be placed in our beam testing apparatus and in-plane loads will be placed upon the beam as shown in Figure 47 until it reaches lateral torsional buckling failure.

The objective is to identify in-plane deflection increases and out of plane deflections that are experienced as a result of shear. These typically unaddressed deflections often lead to premature buckling failure of the beam. We will then compare buckling results to our predictions and ASCE Design values.

We will be using an elastic modulus of 2997 ksi and a shear modulus of 453 ksi as determined during our material testing discussed in Chapter 3. Looking at the manufacturer’s data for the fiberglass reinforced plastic beams, we see that the shear modulus is listed at .450 x 10 6 and the elastic modulus is typically between 2.8 and 3.2 x 10 6 psi. This information confirms our test results.

Dial gages were located along the beam as shown in Figure 50 for determination of vertical, horizontal, and lateral torsional deflections to be compare with deflection values obtained with our analytical modes using the central difference approach.

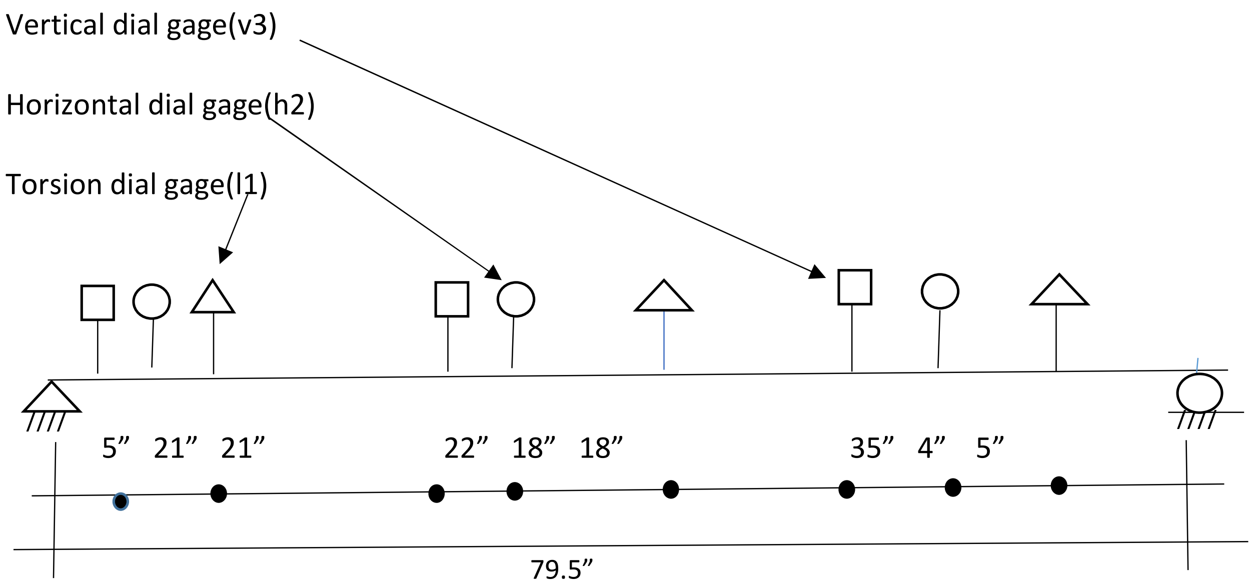

Figure 50. Dial Gage Locations for Two Span Point Load Off Ctr Experiment

Mechanical properties and dimensions of the GFRP beam being used are as follows:

L_1 = 79.5 inches; I beam is 3” x 3” x ¼”; Area A = 2.13 in. 2; I = 3.17 in. ^{4}; F = 30 ksi; E = 2997 ksi; and G = 453 ksi.

Deflection values from lab experiment are shown in Table 44. They will be compared with Central Difference deflection and buckling values and ASCE-LRFD buckling values in Chapter 4.

Table 44. Deflections from Lab. Investigation 5

	*5"	22"	35"	21"	18"	4"	21"	18"	5"
Load P	**v1 lab**	**v2 lab**	**v3 lab**	**h1**	**h2**	**h3**	**l1**	**l2**	**l3**
0	0	0	0	0	0	0	0	0	0
.2285	.069	.103	.129	0	0	0	.00191	.00482	.00158
.4446	.109	.222	.266	0	0	0	.00445	.01518	.01579
.625	.147	.339	.402	.002	.004	.004	.00709	.02591	.03042
.8108	.184	.456	.499	.004	.007	.007	.01018	.03664	.04484
1.001	.222	.575	.595	.011	.012	.011	.01355	.04755	.05947
1.12	.252	.664	.7	.023	.021	.017	.01664	.05609	.0707
1.2	.28	.747	.801	.036	.031	.022	.02009	.06427	.08158
1.2	.31	.866	.939	.05	.032	.031	.02445	.07582	.09642

***Distance from support**

Appendix 5. ASCE-LRFD Design Failure Modes. Investigation 5

For each investigation, we are examining several failure modes as defined by the ASCE to insure that each experiment fails in lateral-torsional buckling and not in another defined mode. Failure modes being evaluated include material rupture, compression flange local buckling, web local buckling, and shear.

For material rupture, the equation is:

$M_n = F_L(I/y)$ where F_L = 30 ksi and is the longitudinal strength of the member; I = 3.17 in. ^{4};

And y = 1.5" and is the distance from the neutral axis to the extreme fiber of a member. Plugging in values, we have

M_n =30 (3.17)/1.5) = 63.4 k-in.

The equation for compression flange local buckling is:

$M_n = f_{cr}(I/y)$ where

f_{cr} is the minimum critical buckling stress of the compression flange or the web. For compression flange local buckling,

$f_{cr} = (4t_f^2/b_f^2)\ ((7/12)(E_x\ E_y/(1 + 4.1Ɛ)).5 + G)$,

$Ɛ = E_y t_f 3/(b_f k_t 6)$, and

$k_t = (E_x\ t_w^3/6h)\ (1 – ((48tr^2h^2E_y/(11.1\pi^2t_w^2br^2E_{LF}))(G/(1.25(E_y\ E_x)^{.5} + E_x v_{LT} + G)))$ where v_{LT} is Poisson's ratio , t_w is web thickness, and br is flange thickness. Plugging in values, we have

f_{cr} = 34.82 ksi.

For web local buckling,

$f_{cr} = (11.1\pi 2t_w^2/12h^2))(1.25(E_y\ E_x)^{.5} + E_x\ v_{LT} + G\ )$ = 50.96 ksi .

Critical stress of 34.82 ksi governs and

M_n =34.82 (3.17/1.5) = 73.6 k-in.

For shear, we will be examining shear and shear buckling failures. The equation for shear failure is:

$V_n = F_{LT}A_s$ where F_{LT} = 8 ksi and is the in-plane shear strength; and A_s = 3 in. x .25 = .75 in. ^{2}

And is the area of the web. Plugging these values in, we have

V_n = 8.0 x .75 = 6 kips.

The equation for web shear buckling is

$V_n = f_{cr} A_s$ where

$f_{cr} = (k_{LT}t_w^2/3h^2)(E_xE_y^3)^{.25}$ and $k_{LT} = 8.1 + 5.0(2G + E_y v_{LT})/(E_x E_y)$ = 11.21. Plugging in values

f_{cr} = 80.17 ksi and

V_n = 80.17(.75) = 60.13 kips

For the 3" x 3" x ¼" beam, ASCE-LRFD failure mode values of shear and moment, V_n and M_n are as shown. The governing values of critical shear and critical moment for the ASCE-LRFD failure modes are shearing of the web and compression flange local buckling. For Investigation 4, the ASCE-LRFD P_{cr} and M_{cr} values for lateral-torsional buckling are 1.42 kips and 22.92 k-in. Because the critical values associated with the other failure modes are higher than the values determined using the lateral-torsional buckling failure mode, the beam for this investigation is expected to fail in lateral-torsional buckling.

Lab Investigation 6

Experimental results are now presented for investigation 6. Using ASCE-LRFD Prestandard, critical load limits for shear and local failure modes are determined then compared with lateral torsional buckling critical load limits. Beam established for investigation 6 predicted to fail in lateral- torsion.

Experiment involves observance of vertical, horizontal, and lateral torsional deflections of a three span I beam with point load at midspan of center span. Lateral torsional buckling load is also being predicted and observed for the beam shown in Figure 51.

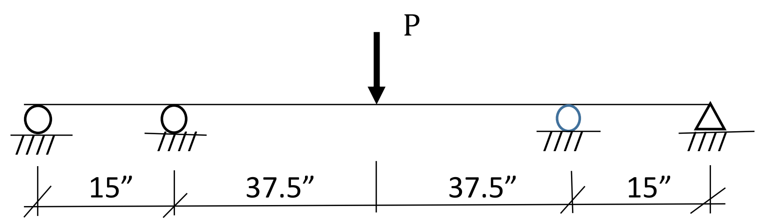

Figure 51. Investigation 6. Three Span Model

To determine what size beam to use in the beam testing apparatus, we evaluated the shear deflection and lateral torsional buckling characteristics of three fiber reinforced plastic I beams (See Figure 52). First, we eliminated the 6” x 6” x ¼” beam because the loading capacity of our testing apparatus may be exceeded.

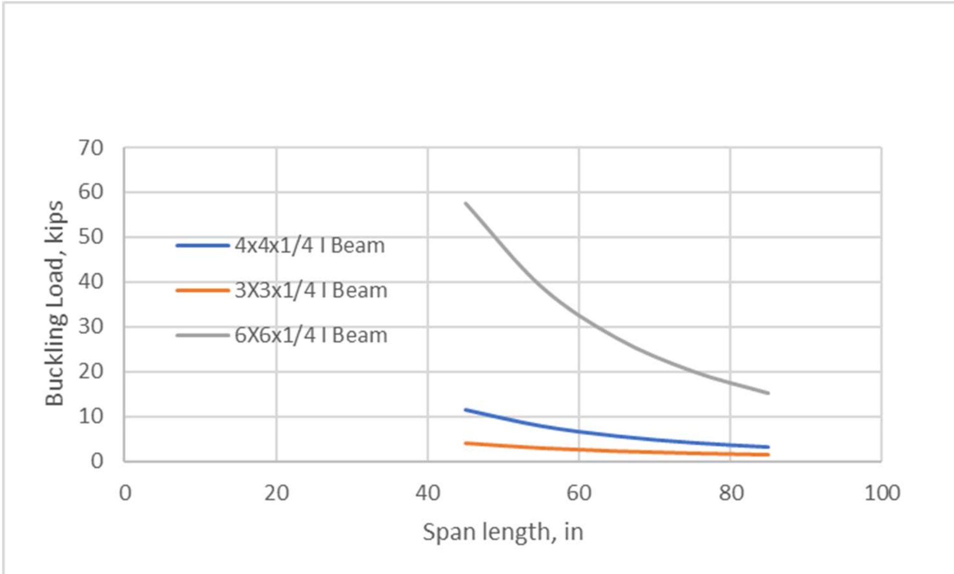

Figure 52. LTB Comparison of Cross Sections

Next, to establish a baseline for the investigation, we elected to perform single, double, and triple span experiments with the point load at midspan using the 4” x 4” x ¼” cross section. Alternatively, the 3” x 3” x ¼” cross section is used for single, double, and triple span experiments where the point loads are off-centered and moved toward the supports. The larger cross section is being used in the experiments associated with the location where the point load will produce maximum deflection and max shear. Shorter span experiments were performed using the 3” x 3” x ¼” cross section. The objective was to keep buckling loads and deflections within range of testing apparatus and dial gages measuring deflections.

Lastly, beams were evaluated by their failure predictions as determined suing the ASCE-LRFD Design Guide for Pultruded Members (See Appendix). These failures include material rupture, lateral- torsional buckling, and shear. Since we are interested in lateral torsional buckling failure, we want to make sure beams fail lateral- torsionally before other failure modes are reached. Our own predictions for lateral torsional buckling with shear were also considered. Graph showing lateral torsional buckling with shear were also considered. Graph showing lateral torsional buckling failure is shown in Figure 53. It compares our central difference buckling solutions with ASCE-LRFD Design buckling solutions.

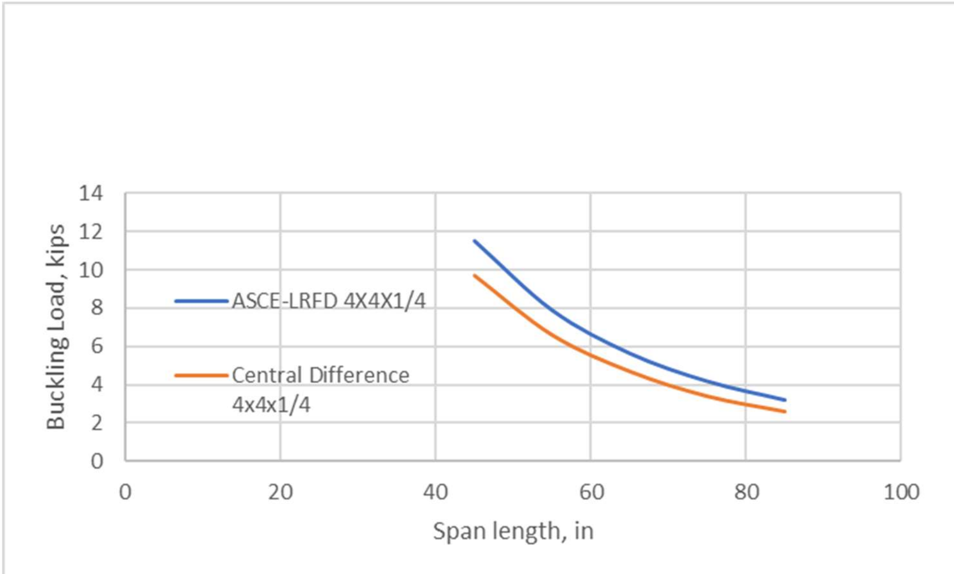

Figure 53. Central Diff vs ASCE Buckling Prediction Curves

A GFRP beam of dimensions 4” x 4” x ¼” x 105” will be placed in our beam testing apparatus and in-plane loads will be placed upon the beam as shown in Figure 51 until it reaches lateral torsional buckling failure.

The objective is to identify in-plane deflection increases and out of plane deflections that are experienced as a result of shear. These typically unaddressed deflections often lead to premature buckling failure of the beam. We will then compare buckling results to our predictions and ASCE Design values.

We will be using an elastic modulus of 2997 ksi and a shear modulus of 453 ksi as determined during our material testing discussed in Chapter 3. Looking at the manufacturer’s data for the fiberglass reinforced plastic beams, we see that the shear modulus is listed at .450 x 10 6 and the elastic modulus is typically between 2.8 and 3.2 x 10 6 psi. This information confirms our test results.

Beam Testing Apparatus shown previously includes a hydraulic pump and jack to place loads upon the specimen. Also, a meter for measuring the loads will be used.

Dial gages were located along the beam as shown in Figure 54 for determination of vertical, horizontal, and lateral torsional deflections to be compared with deflection values obtained with our analytical models using the central difference approach.

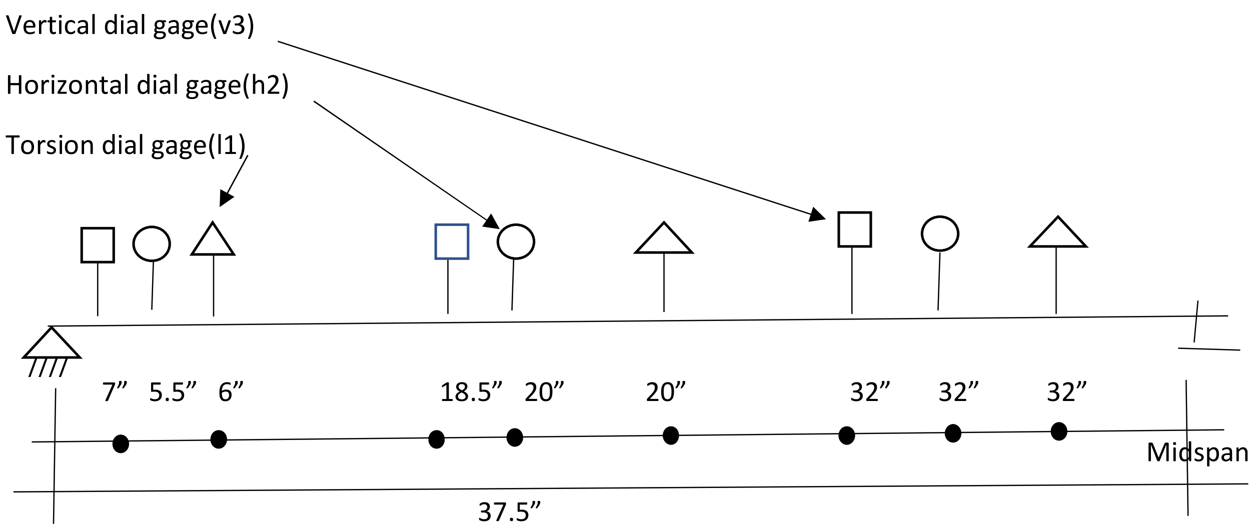

Figure 54. Dial Gage Locations Three Span Point Load at Midspan

Mechanical properties and dimensions of the GFRP beam being used are as follows:

L_1 = 30 inches; L_2 = 75 inches; I beam is 4” x 4” x ¼”; Area A = 2.85 in.2; I = 7.93 in. 4; F = 30ksi;

E = 2997 ksi; and G = 453 ksi.

Deflection values from lab experiment are shown in Table 45. They will be compared with Central Difference deflection and buckling values and ASCE-LRFD buckling values in Chapter 4.

Table 45. Deflections from Lab. Investigation 6

	*7”	18.5”	32”	5.5”	20”	32”	6”	20”	33”
Load P	v1	v2	v3	h1	h2	h3	l1	l2	l3
0	0	0	0	0	0	0	0	0	0
.2209	.008	.017	.0242	.003	.007	.007	.0013	.005	.0059
.6017	.023	.047	.0678	.013	.015	.02	.0041	.0128	.0152
.9826	.042	.088	.127	.029	.027	.038	.0081	.0234	.0284
1.176	.052	.11	.157	.035	.035	.045	.01	.0287	.0351
1.357	.059	.127	.1829	.041	.038	.051	.0119	.0332	.0407
1.55	.069	.148	.2134	.043	.043	.058	.0135	.0381	.0458
1.76	.08	.174	.2503	.053	.051	.071	.0163	.0442	.0534
2.04	.093	.205	.296	.057	.061	.085	.0243	.0514	.0601
2.29	.107	.2342	.338	.0667	.071	.101	.0319	.0577	.067

***Distance from support**

Appendix 6. ASCE-LRFD Design Failure Modes. Investigation 6

For each investigation, we are examining several failure modes as defined by the ASCE to insure that each experiment fails in lateral-torsional buckling and not in another defined mode. Failure modes being evaluated include material rupture, compression flange local buckling, web local buckling, and shear.

For material rupture, the equation is:

$M_n = F_L(I/y)$ where F_L = 30 ksi and is the longitudinal strength of the member; I = 7.935 in. ^{4};

And y = 2.0" and is the distance from the neutral axis to the extreme fiber of a member. Plugging in values, we have

M_n =30 (7.935)/2.0) = 119.025 k-in.

The equation for compression flange local buckling is:

$M_n = f_{cr}(I/y)$ where

f_{cr} is the minimum critical buckling stress of the compression flange or the web. For compression flange local buckling,

$f_{cr} = (4t_f^2/b_f^2)\ ((7/12)(E_x\ E_y/(1 + 4.1\varepsilon)).5 + G)$,

$\varepsilon = E_y t_f 3/(b_f k_t 6)$, and

$k_t = (E_x\ t_w^3/6h)\ (1 – ((48tr^2h^2E_y/(11.1\pi^2t_w^2br^2E_{LF}))(G/(1.25(E_y\ E_x)^{.5} + E_x v_{LT} + G)))$ where v_{LT} is Poisson's ratio , t_w is web thickness, and br is flange thickness. Plugging in values, we have

f_{cr} = 19.59 ksi.

For web local buckling,

$f_{cr} = (11.1\pi 2t_w^2/12h^2))(1.25(E_y\ E_x)^{.5} + E_x\ v_{LT} + G\ ) = 28.66$ ksi .

Critical stress of 19.59 ksi governs and

M_n =19.59 (7.936/2.0) = 77.7 k-in.

For shear, we will be examining shear and shear buckling failures. The equation for shear failure is:

$V_n = F_{LT}A_s$ where F_{LT} = 8 ksi and is the in-plane shear strength; and A_s = 4 in. x .25 = 1.0 in. ^{2}

And is the area of the web. Plugging these values in, we have

V_n = 8.0 x 1.0 = 8 kips.

The equation for web shear buckling is

$V_n = f_{cr} A_s$ where

$f_{cr} = (k_{LT}t_w^2/3h^2)(E_xE_y^3)^{.25}$ and $k_{LT} = 8.1 + 5.0(2G + E_y v_{LT})/(E_x E_y)$ = 11.21. Plugging in values

f_{cr} =45.10 ksi and

V_n = 45.10(1.0) = 45.10 kips

For the 4" x 4" x ¼" beam, ASCE-LRFD failure mode values of shear and moment, V_n and M_n are as shown. The governing values of critical shear and critical moment for the ASCE-LRFD failure modes are shearing of the web and compression flange local buckling. For Investigation 6, the ASCE-LRFD P and M values for lateral-torsional buckling are 3.33 kips and 60.46 k-in. Because the critical values associated with the other failure modes are higher than the values determined using the lateral-torsional buckling failure mode, the beam for this investigation is expected to fail in lateral- torsional buckling.

Lab Investigation 7

Experimental results are now presented for investigation 7. Using ASCE-LRFD Prestandard, critical load limits for shear and local failure modes are determined then compared with lateral- torsional buckling critical load limits. Beam established for investigation 7 predicted to fail in lateral- torsion.

Experiment involves observance of vertical, horizontal, and lateral torsional deflections of a three span I beam with point load at midspan of center span. Lateral torsional buckling load is also being predicted and observed for the beam shown in Figure 55.

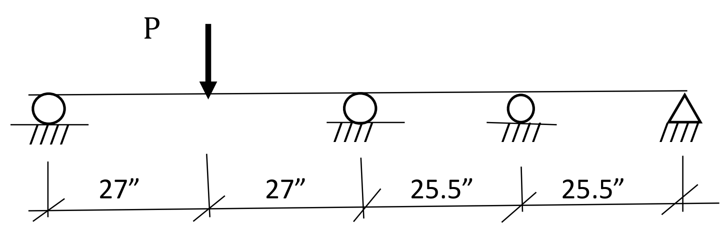

Figure 55. Investigation 7: Three Span. Outside Span

To determine what size beam to use in the beam testing apparatus, we evaluated the shear deflection and lateral torsional buckling characteristics of three fiber reinforced plastic I beams (See Figure 56). First, we eliminated the 6” x 6” x ¼” beam because the loading capacity of our testing apparatus may be exceeded.

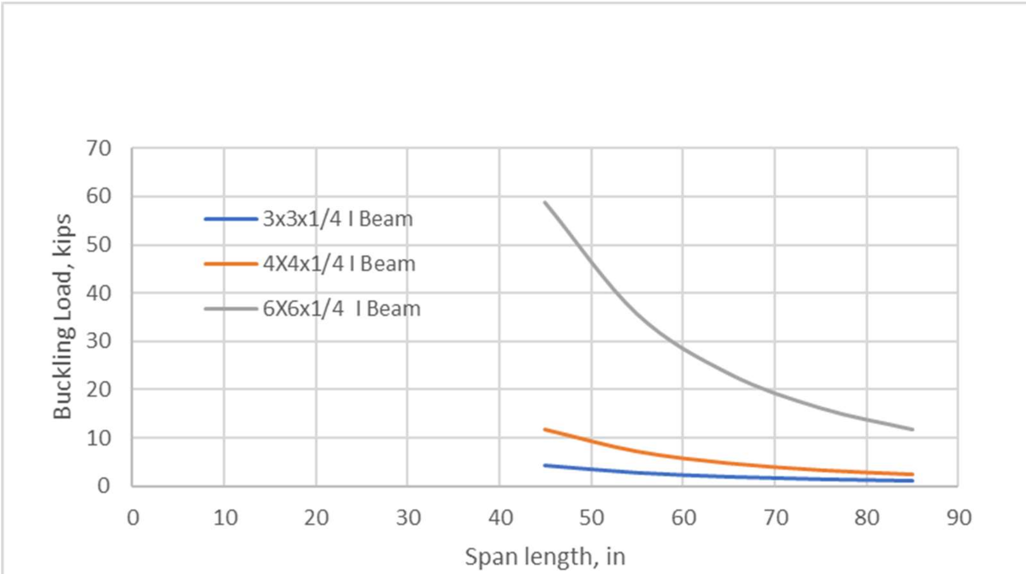

Figure 56. LTB Comparison of Cross Sections

Next, to establish a baseline for the investigation, we elected to perform single, double, and triple span experiments with the point load at midspan using the 4” x 4” x ¼” cross section. Alternatively, the 3” x 3” x ¼” cross section is used for single, double, and triple span experiments where the point loads are off-centered and moved toward the supports. The larger cross section is being used in the experiments associated with the location where the point load will produce maximum deflection and max shear. Shorter span experiments were performed using the 3” x 3” x ¼” cross section. The objective was to keep buckling loads and deflections within range of testing apparatus and dial gages measuring deflections.

Lastly, beams were evaluated by their failure predictions as determined suing the ASCE-LRFD Design Guide for Pultruded Members (See Appendix). These failures include material rupture, lateral torsional buckling, and shear. Since we are interested in lateral torsional buckling failure, we want to make sure beams fail lateral- torsionally before other failure modes are reached. Our own predictions for lateral torsional buckling with shear were also considered. Graph showing lateral- torsional buckling with shear were also considered. Graph showing lateral- torsional buckling failure is shown in Figure 57. It compares our central difference buckling solutions with ASCE-LRFD Design buckling solutions.

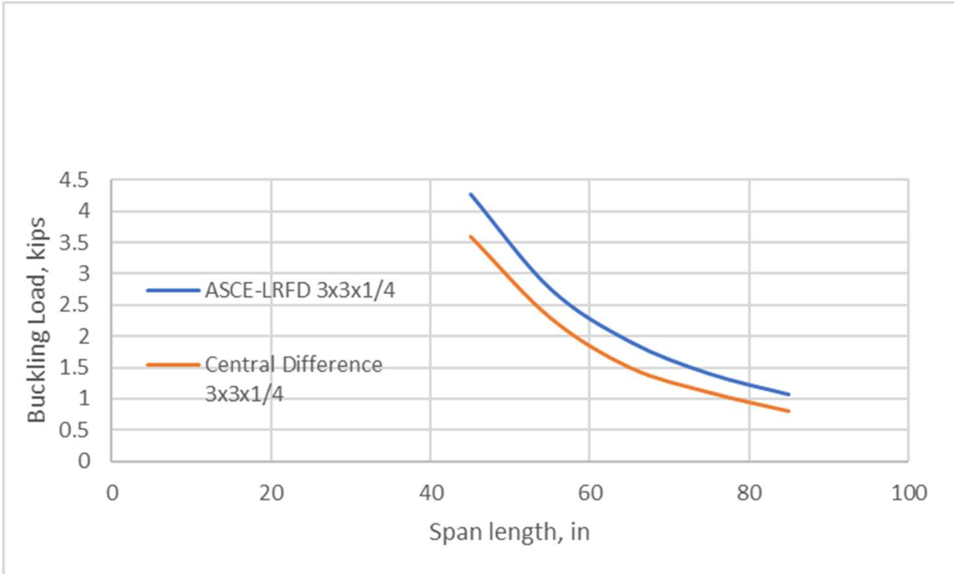

Figure 57. Central Diff vs ASCE Buckling Prediction Curves

A GFRP beam of dimensions 3” x 3” x ¼” x 105” will be placed in our beam testing apparatus and in-plane loads will be placed upon the beam as shown in Figure 55 until it reaches lateral torsional buckling failure.

The objective is to identify in-plane deflection increases and out of plane deflections that are experienced as a result of shear. These typically unaddressed deflections often lead to premature buckling failure of the beam. We will then compare buckling results to our predictions and ASCE Design values.

We will be using an elastic modulus of 2997 ksi and a shear modulus of 453 ksi as determined during our material testing discussed earlier in Chapter 3. Looking at the manufacturer’s data for the fiberglass reinforced plastic beams, we see that the shear modulus is listed at .450 x 10 6 and the elastic modulus is typically between 2.8 and 3.2 x 10 6 psi. This information confirms our test results.

Beam Testing Apparatus shown previously includes a hydraulic pump and jack to place loads upon the specimen. Also, a meter for measuring the loads will be used.

Dial gages were located along the beam as shown in Figure 58 for determination of vertical, horizontal, and lateral- torsional deflections to be compared with deflection values obtained with our analytical models using the central difference approach.

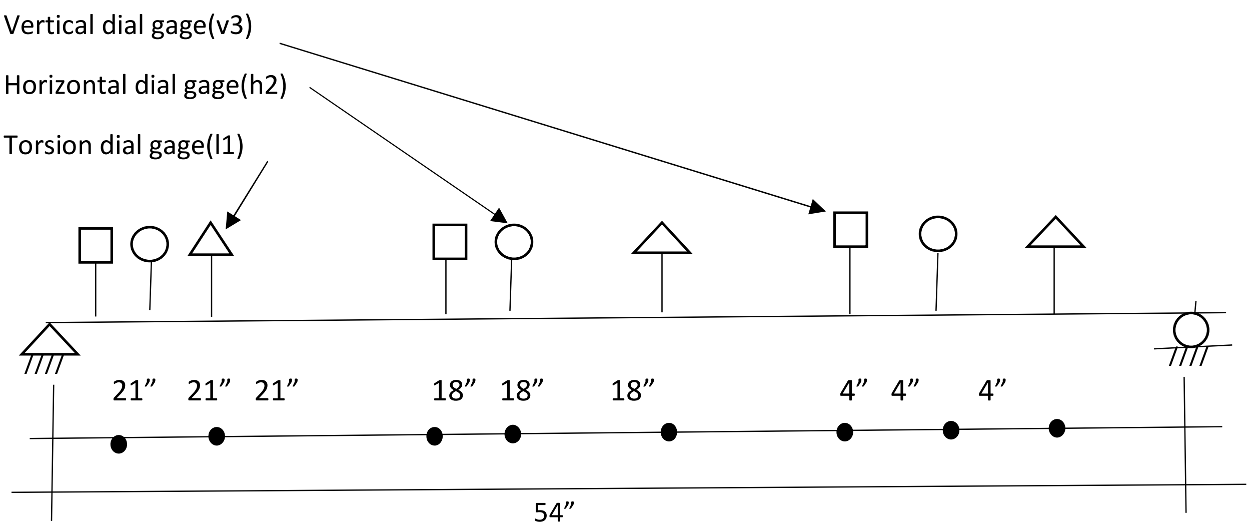

Figure 58. Dial Gage Locations for Three Span Point Load Midspan. Outside

Mechanical properties and dimensions of the GFRP beam being used are as follows:

L_1 = 54.0” ; I beam is 3” x 3” x ¼” ; A = 2.13 in. ^{2} ; I = 3.17 in. ^{4} ; E = 2997 ksi ; G = 453 ksi.

Deflection values from lab experiment are shown in Table 46. They will be compared with Central Difference deflection and buckling values and ASCE-LRFD buckling values in Chapter 4.

Table 46. Deflections from Lab. Investigation 7

	*4"	18"	21"	21"	18"	4"	21"	18"	5"
Load P	**v1**	**v2**	**v3**	**h1**	**h2**	**h3**	**l1**	**l2**	**l3**
0	0	0	0	0	0	0	0	0	0
.2285	.01136	.04872	.05674	.001	.001	0	.0054	.0035	.0012
.4446	.022	.0974	.1135	.003	.002	0	.0134	.0103	.0023
.625	.03266	.1403	.1633	.005	.003	0	.0203	.0171	.0039
.8108	.04331	.1848	.2158	.007	.006	0	.0263	.0231	.0053
1.001	.05396	.2285	.268	.011	.007	0	.0344	.029	.0066
1.112	.06106	.257	.30088	.012	.008	0	.0388	.0326	.0072
1.317	.07242	.302	.355	.015	.009	0	.0461	.039	.0088
1.518	.084	.351	.412	.02	.011	.005	.0538	.0454	.0108
1.714	.095	.3998	.469	.024	.017	.006	.0618	.0522	.0117
1.909	.107	.4477	.527	.028	.021	.007	.0699	.0593	.0133
2.065	.116	.49	.575	.033	.024	.008	.08	.0654	.0146
2.227	.127	.532	.75	.045	.027	.009	.09	.0719	.0161

- **Distance from support**

Appendix 7. ASCE-LRFD Design Failure Modes. Investigation 7

For each investigation, we are examining several failure modes as defined by the ASCE to insure that each experiment fails in lateral- torsional buckling and not in another defined mode. Failure modes being evaluated include material rupture, compression flange local buckling, web local buckling, and shear.

For material rupture, the equation is:

$M_n = F_L(I/y)$ where $F_L = 30$ ksi and is the longitudinal strength of the member; $I = 3.17$ in. ^{4};

And y = 1.5" and is the distance from the neutral axis to the extreme fiber of a member. Plugging in values, we have

$M_n = 30\ (3.17)/1.5\ ) = 63.4$ k-in.

The equation for compression flange local buckling is:

$M_n = f_{cr}(I/y)$ where

f_{cr} is the minimum critical buckling stress of the compression flange or the web. For compression flange local buckling,

$f_{cr} = (4t_f^2/b_f^2)\ ((7/12)(E_x\ E_y/(1 + 4.1\mathcal{E})).5 + G)$,

$\mathcal{E} = E_y t_f 3/(b_f k_t 6)$, and

$k_t = (E_x\ t_w^3/6h)\ (1 - ((48tr^2h^2E_y/(11.1\pi^2t_w^2br^2E_{LF}))(G/(1.25(E_y\ E_x)^{.5} + E_x v_{LT} + G)))$ where v_{LT} is Poisson's ratio , t_w is web thickness, and br is flange thickness. Plugging in values, we have

$f_{cr} = 34.82$ ksi.

For web local buckling,

$f_{cr} = (11.1\pi 2t_w^2/12h^2))(1.25(E_y\ E_x)^{.5} + E_x\ v_{LT} + G\ ) = 50.96$ ksi .

Critical stress of 34.82 ksi governs and

$M_n = 34.82\ (3.17/1.5) = 73.6$ k-in.

For shear, we will be examining shear and shear buckling failures. The equation for shear failure is:

$V_n = F_{LT}A_s$ where F_{LT} = 8 ksi and is the in-plane shear strength; and A_s = 3 in. x .25 = .75 in. ^{2}

And is the area of the web. Plugging these values in, we have

V_n = 8.0 x .75 = 6 kips.

The equation for web shear buckling is

$V_n = f_{cr} A_s$ where

$f_{cr} = (k_{LT}t_w^2/3h^2)(E_xE_y^3)^{.25}$ and $k_{LT} = 8.1 + 5.0(2G + E_y v_{LT})/(E_x E_y)$ = 11.21. Plugging in values

f_{cr} = 80.17 ksi and

V_n = 80.17(.75) = 60.13 kips

For the 3” x 3” x ¼” beam, ASCE-LRFD failure mode values of shear and moment, V_n and M_n are as shown. The governing values of critical shear and critical moment for the ASCE-LRFD failure modes are shearing of the web and compression flange local buckling. For Investigation 7, the ASCE-LRFD P_{cr} and M_{cr} values for lateral-torsional buckling are 2.89 kips and 34.12 k-in. Because the critical values associated with the other failure modes are higher than the values determined using the lateral-torsional buckling failure mode, the beam for this investigation is expected to fail in lateral-torsional buckling.

Lab Investigation 8

Experimental results are now presented for investigation 8. Using ASCE-LRFD Prestandard, critical load limits for shear and local failure modes are determined then compared with lateral torsional buckling critical load limits. Beam established for investigation 8 predicted to fail in lateral- torsion.

Experiment involves observance of vertical, horizontal, and lateral- torsional deflections of a three span I beam with point load at midspan of center span. Lateral- torsional buckling load is also being predicted and observed for the beam shown in Figure 59.

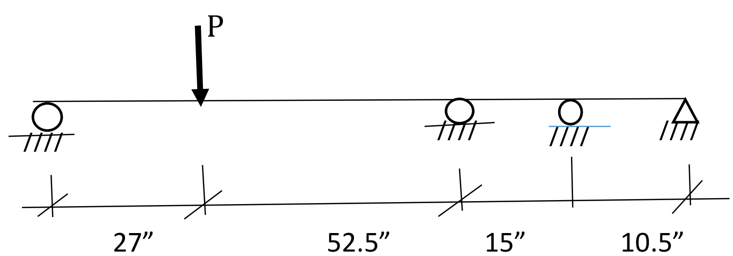

Figure 59. Investigation 8. Three Span Off Center

To determine what size beam to use in the beam testing apparatus, we evaluated the shear deflection and lateral torsional buckling characteristics of three fiber reinforced plastic I beams (See Figure 60). First, we eliminated the 6” x 6” x ¼” beam because the loading capacity of our testing apparatus may be exceeded.

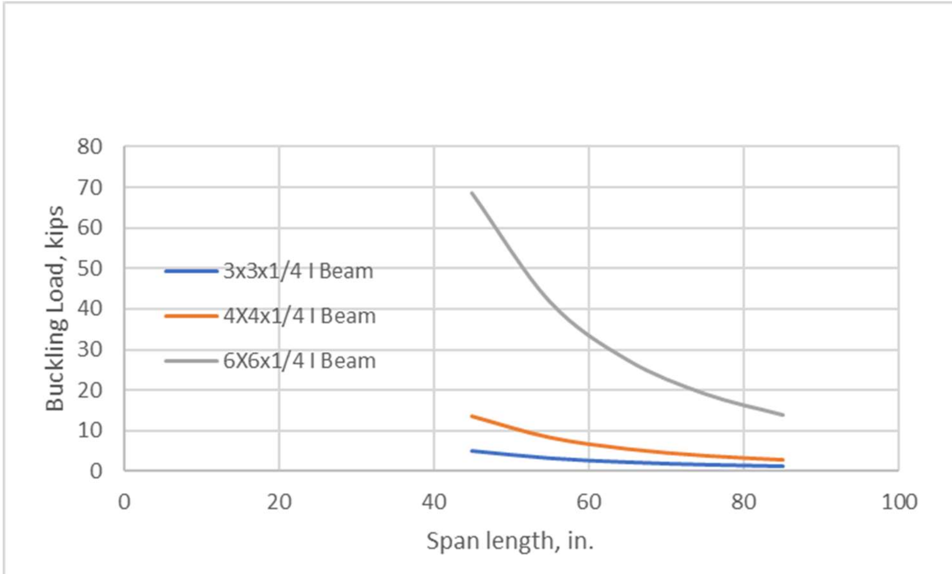

Figure 60. LTB Comparison of Cross Sections

Next, to establish a baseline for the investigation, we elected to perform single, double, and triple span experiments with the point load at midspan using the 4" x 4" x ¼" cross section. Alternatively, the 3" x 3" x ¼" cross section is used for single, double, and triple span experiments where the point loads are off-centered and moved toward the supports. The larger cross section is being used in the experiments associated with the location where the point load will produce maximum deflection and max shear. Shorter span experiments were performed using the 3" x 3" x ¼" cross section. The objective was to keep buckling loads and deflections within range of testing apparatus and dial gages measuring deflections.

Lastly, beams were evaluated by their failure predictions as determined using the ASCE-LRFD Design Guide for Pultruded Members (See Appendix). These failures include material rupture, lateral- torsional buckling, and shear. Since we are interested in lateral- torsional buckling failure, we want to make sure beams fail lateral- torsionally before other failure modes are reached. Our own predictions for lateral torsional buckling with shear were also considered. Graph showing lateral- torsional buckling with shear were also considered. Graph showing lateral- torsional buckling failure is shown in Figure 61. It compares our central difference buckling solutions with ASCE-LRFD Design buckling solutions.

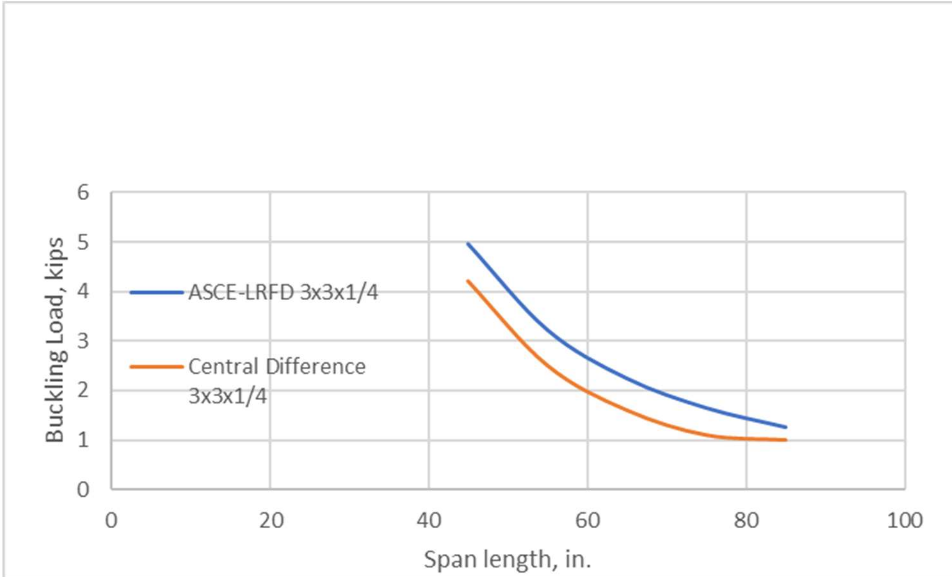

Figure 61. Central Diff vs ASCE Buckling Prediction Curve

A GFRP beam of dimensions 3” x 3” x ¼” x 105” will be placed in our beam testing apparatus and in-plane loads will be placed upon the beam as shown in Figure 59 until it reaches lateral torsional buckling failure.

The objective is to identify in-plane deflection increases and out of plane deflections that are experienced as a result of shear. These typically unaddressed deflections often lead to premature buckling failure of the beam. We will then compare buckling results to our predictions and ASCE Design values.

We will be using an elastic modulus of 2997 ksi and a shear modulus of 453 ksi as determined during our material testing discussed earlier in Chapter 3. Looking at the manufacturer’s data for the fiberglass reinforced plastic beams, we see that the shear modulus is listed at .450 x 10 6 and the elastic modulus is typically between 2.8 and 3.2 x 10 6 psi. This information confirms our test results.

Beam Testing Apparatus shown previously includes a hydraulic pump and jack to place loads upon the specimen. Also, a meter for measuring the loads will be used.

Dial gages were located along the beam as shown in Figure 58 for determination of vertical, horizontal, and lateral torsional deflections to be compared with deflection values obtained with our analytical models using the central difference approach.

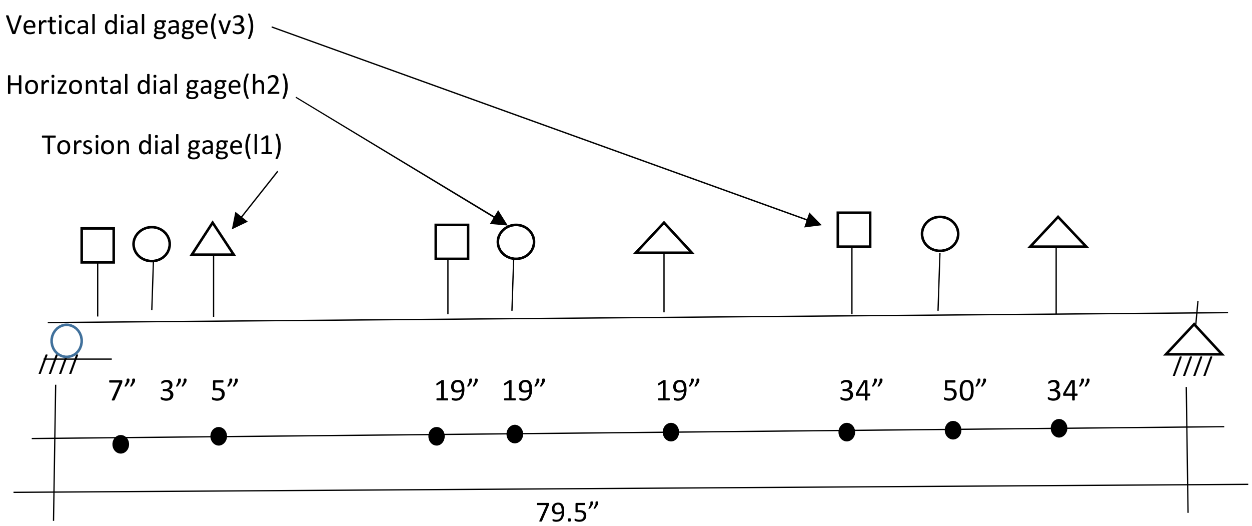

Figure 62. Dial Gage Locations for Three Span Point Load Off Center

Mechanical properties and dimensions of the GFRP beam being used are as follows:

L_1 = 79.5”; I beam is 3” x 3” x ¼” ; A= 2.13 in.^{2}; I_x = 7.935 in. ^{4} ; F = 30 ksi; E= 2997 ksi; G = 453 ksi.

Deflection values from lab experiment are shown in Table 47. They will be compared with Central Difference deflection and buckling values and ASCE-LRFD buckling values in Chapter 4.

Table 47. Deflections from Lab. Investigation 8

	***7”**	**19”**	**34”**	**3”**	**19”**	**50”**	**5”**	**19”**	**34”**
Load P	**v1**	**v2**	**v3**	**h1**	**h2**	**h3**	**l1**	**l2**	**l3**
0	0	0	0	0	0	0	0	0	0
.22	.021	.063	.122	0	0	0	.0008	.00524	.01
.44	.096	.136	.242	.018	.002	.004	.0033	.00924	.01886
.71	.175	.216	.364	.029	.008	.01	.0073	.01429	.028
.89	.227	.335	.513	.034	.014	.02	.0099	.02438	.04076
1.07	.279	.455	.627	.037	.034	.036	.0132	.02448	.05286
1.19	.325	.567	.763	.041	.084	.041	.0177	.03267	.0639
1.2	.371	.675	.879	.042	.122	.047	.0211	.03905	.07029
1.2	.371	.787	1.012	.042	.14	.047	.0211	.03905	.07476

***Distance from support**

Appendix 8. ASCE-LRFD Design Failure Modes. Investigation 8

For each investigation, we are examining several failure modes as defined by the ASCE to insure that each experiment fails in lateral-torsional buckling and not in another defined mode. Failure modes being evaluated include material rupture, compression flange local buckling, web local buckling, and shear.

For material rupture, the equation is:

$M_n = F_L(I/y)$ where F_L = 30 ksi and is the longitudinal strength of the member; I = 3.17 in. ^{4};

And y = 1.5" and is the distance from the neutral axis to the extreme fiber of a member. Plugging in values, we have

$M_n = 30\ (3.17)/1.5\ ) = 63.4$ k-in.

The equation for compression flange local buckling is:

$M_n = f_{cr}(I/y)$ where

f_{cr} is the minimum critical buckling stress of the compression flange or the web. For compression flange local buckling,

$f_{cr} = (4t_f^2/b_f^2)\ ((7/12)(E_x\ E_y/(1 + 4.1Ɛ)).5 + G)$,

$Ɛ = E_y t_f 3/(b_f k_t 6)$, and

$k_t = (E_x\ t_w^3/6h)\ (1 - ((48tr^2h^2E_y/(11.1\pi^2 t_w^2 br^2 E_{LF}))(G/(1.25(E_y\ E_x)^{.5} + E_x v_{LT} + G)))$ where v_{LT} is Poisson's ratio , t_w is web thickness, and br is flange thickness. Plugging in values, we have

f_{cr} = 34.82 ksi.

For web local buckling,

$f_{cr} = (11.1\pi 2 t_w^2/12h^2))(1.25(E_y\ E_x)^{.5} + E_x\ v_{LT} + G\ ) = 50.96$ ksi .

Critical stress of 34.82 ksi governs and

$M_n = 34.82\ (3.17/1.5) = 73.6$ k-in.

For shear, we will be examining shear and shear buckling failures. The equation for shear failure is:

$V_n = F_{LT}A_s$ where F_{LT} = 8 ksi and is the in-plane shear strength; and A_s = 3 in. x .25 = .75 in. ^{2}

And is the area of the web. Plugging these values in, we have

V_n = 8.0 x .75 = 6 kips.

The equation for web shear buckling is

$V_n = f_{cr} A_s$ where

$f_{c\,r} = (k_{LT}t_w^2/3h^2)(E_xE_y^3)^{.25}$ and $k_{LT} = 8.1 + 5.0(2G + E_y v_{LT})/(E_x E_y)$ = 11.21. Plugging in values

f_{cr} = 80.17 ksi and

V_n = 80.17(.75) = 60.13 kips

For the 3” x 3” x ¼” beam, ASCE-LRFD failure mode values of shear and moment, V_n and M_n are as shown. The governing values of critical shear and critical moment for the ASCE-LRFD failure modes are shearing of the web and compression flange local buckling. For Investigation 8, the ASCE-LRFD P_{cr} and M_{cr} values for lateral-torsional buckling are 1.47 kips and 22.9 k-in. Because the critical values associated with the other failure modes are higher than the values determined using the lateral-torsional buckling failure mode, the beam for this investigation is expected to fail in lateral- torsional buckling.

Lab Investigation 9

Experimental results are now presented for investigation 9. Using ASCE-LRFD Prestandard, critical load limits for shear and local failure modes are determined then compared with lateral torsional buckling critical load limits. Beam established for investigation 9 predicted to fail in lateral- torsion.

Experiment involves observance of vertical, horizontal, and lateral- torsional deflections of a three span I beam with point load at midspan of center span. Lateral- torsional buckling load is also being predicted and observed for the beam shown in Figure 63.

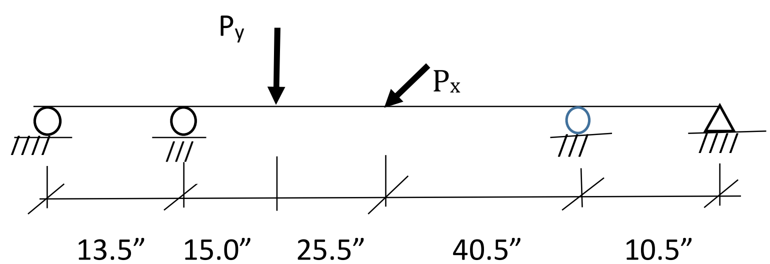

Figure 63. Investigation 9. Three Span Biaxial Model

To determine what size beam to use in the beam testing apparatus, we evaluated the shear deflection and lateral torsional buckling characteristics of three fiber reinforced plastic I beams. We then eliminated the 6” x 6” x ¼” beam because the loading capacity of our testing apparatus may be exceeded.

Next, to establish a baseline for the investigation, we elected to perform single, double, and triple span experiments with the point load at midspan using the 4” x 4” x ¼” cross section. Alternatively, the 3” x 3” x ¼” cross section is used for single, double, and triple span experiments where the point loads are off-centered and moved toward the supports. The larger cross section is being used in the experiments associated with the location where the point load will produce maximum deflection and max shear. Shorter span experiments were performed using the 3” x 3” x ¼” cross section. The objective was to keep buckling loads and deflections within range of testing apparatus and dial gages measuring deflections.

Lastly, beams were evaluated by their failure predictions as determined suing the ASCE-LRFD Design Guide for Pultruded Members. See Appendix at end of each lab investigation. These failures include material rupture, lateral torsional buckling, and shear. Since we are interested in lateral torsional buckling failure, we want to make sure beams fail lateral- torsionally before other failure modes are reached. Our own predictions for lateral torsional buckling with shear were also considered. Graph showing lateral torsional buckling with shear were also considered. Graph showing lateral torsional buckling failure is shown in Figure 64. It compares our central difference buckling solutions with ASCE-LRFD Design buckling solutions.

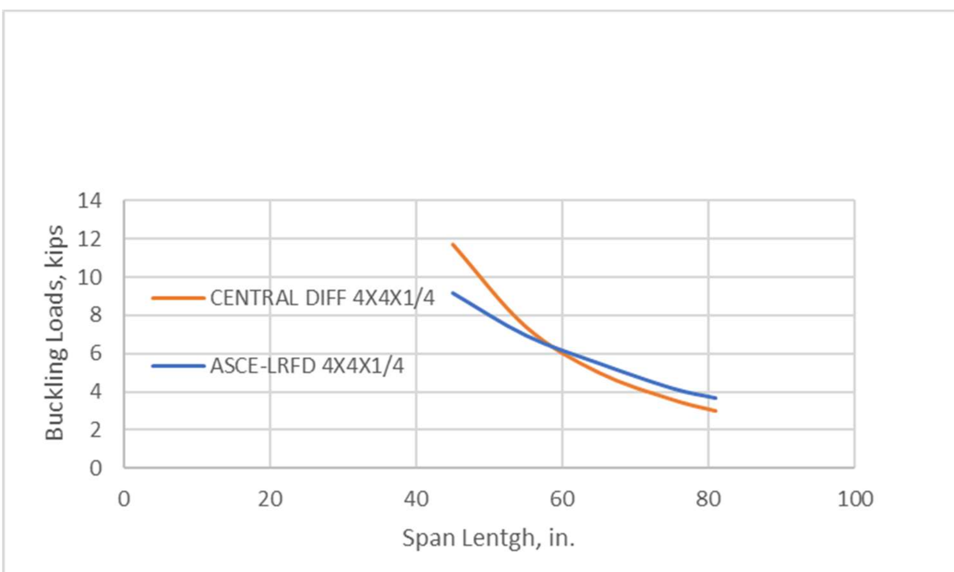

Figure 64. Central Diff vs ASCE Buckling Prediction Curves

A GFRP beam of dimensions 4” x 4” x ¼” x 105” will be placed in our beam testing apparatus and in-plane loads will be placed upon the beam as shown in Figure 63 until it reaches lateral- torsional buckling failure.

The objective is to identify in-plane deflection increases and out of plane deflections that are experienced as a result of shear. These typically unaddressed deflections often lead to premature buckling failure of the beam. We will then compare buckling results to our predictions and ASCE Design values.

We will be using an elastic modulus of 2997 ksi and a shear modulus of 453 ksi as determined during our material testing discussed earlier in Chapter 3. Looking at the manufacturer’s data for the fiberglass reinforced plastic beams, we see that the shear modulus is listed at .450 x 10 6 and the elastic modulus is typically between 2.8 and 3.2 x 10 6 psi. This information confirms our test results.

Beam Testing Apparatus shown previously includes a hydraulic pump and jack to place loads upon the specimen. Also, a meter for measuring the loads will be used.

Dial gages were located along the beam as shown in Figure 65 for determination of vertical, horizontal, and lateral torsional deflections to be compared with deflection values obtained with our analytical models using the central difference approach.

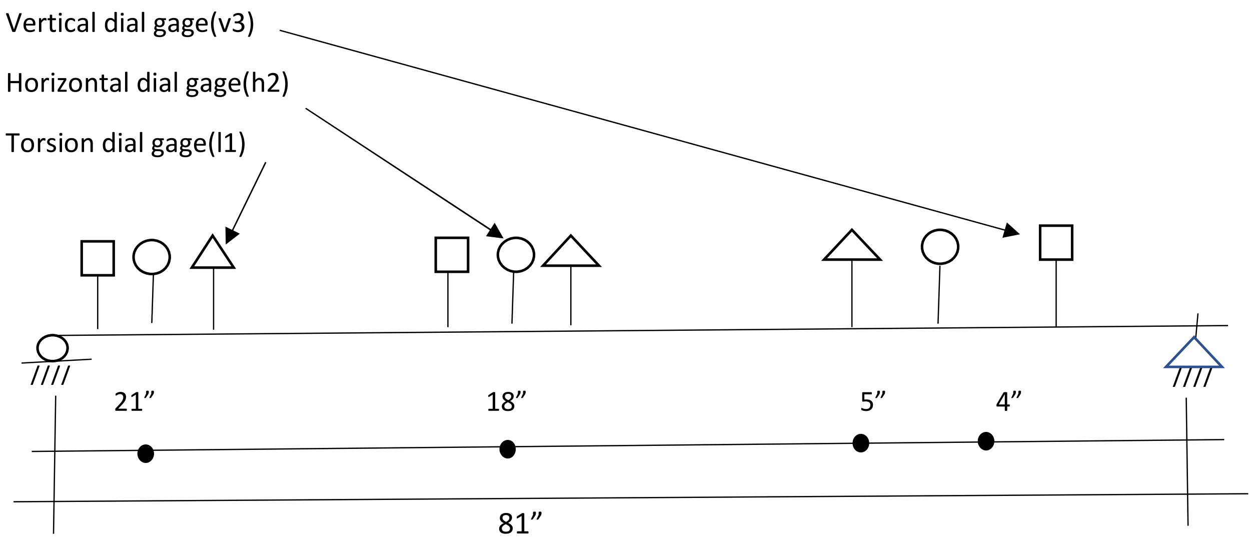

Figure 65. Dial Gage Locations for Three Span Biaxial Point Load

Mechanical properties and dimensions of the GFRP beam being used are as follows:

L_2 = 81.0 inches; I beam is 4” x 4” x ¼”; A=2.85 in. ^{2}; I^x = 7.935 in. ^{4} ;F = 30 ksi; E= 2997 ksi; and G= 453 ksi.

Deflection values from lab experiment are shown in Table 48. They will be compared with Central Difference deflection and buckling values and ASCE-LRFD buckling values in Chapter 4.

Table 48. Deflections from Lab. Investigation 9

	*21”	18”	4”	21”	18”	4”	21”	18”	5”
Load P	**v1 lab**	**v2 lab**	**v3 lab**	**h1**	**h2**	**h3**	**l1**	**l2**	**l3**
0	0	0	0	0	0	0	0	0	0
.513	.0247	.0193	.018	.007	.004	.003	.118	.0036	.009
.809	.0483	.0423	.026	.007	.007	.004	.183	.00728	.009
1.11	.0723	.065	.0337	.009	.008	.005	.261	.012	.012
1.29	.088	.0807	.04	.009	.008	.006	.309	.016	.014
1.4	.0973	.0893	.043	.009	.008	.007	.338	.01824	.017
1.55	.1097	.1017	.0473	.009	.008	.008	.38	.02152	.021
1.68	.121	.1123	.0513	.009	.009	.008	.417	.02456	.023
1.82	.134	.1247	.0553	.009	.01	.008	.454	.02744	.026
1.93	.146	.1373	.0597	.012	.011	.008	.493	.0304	.04
2.11	.162	.153	.0653	.013	.012	.008	.533	.03392	.043
2.32	.183	.173	.0723	.013	.015	.008	.595	.03896	.047

***Distance from support**

Appendix 9. ASCE-LRFD Design Failure Modes. Investigation 9

For each investigation, we are examining several failure modes as defined by the ASCE to insure that each experiment fails in lateral-torsional buckling and not in another defined mode. Failure modes being evaluated include material rupture, compression flange local buckling, web local buckling, and shear.

For material rupture, the equation is:

$M_n = F_L(I/y)$ where F_L = 30 ksi and is the longitudinal strength of the member; I = 7.935 in. ^{4};

And y = 2.0" and is the distance from the neutral axis to the extreme fiber of a member. Plugging in values, we have

M_n =30 (7.935)/2.0) = 119.025 k-in.

The equation for compression flange local buckling is:

$M_n = f_{cr}(I/y)$ where

f_{cr} is the minimum critical buckling stress of the compression flange or the web. For compression flange local buckling,

$f_{cr} = (4t_f^2/b_f^2)\ ((7/12)(E_x\ E_y/(1 + 4.1\mathcal{E})).5 + G)$,

$\mathcal{E} = E_y t_f 3/(b_f k_t 6)$, and

$k_t = (E_x\ t_w^3/6h)\ (1 - ((48tr^2h^2E_y/(11.1\pi^2t_w^2br^2E_{LF}))(G/(1.25(E_y\ E_x)^{.5} + E_x v_{LT} + G)))$ where v_{LT} is Poisson's ratio , t_w is web thickness, and br is flange thickness. Plugging in values, we have

f_{cr} = 19.59 ksi.

For web local buckling,

$f_{cr} = (11.1\pi 2t_w^2/12h^2))(1.25(E_y\ E_x)^{.5} + E_x\ v_{LT} + G) = 28.66$ ksi .

Critical stress of 19.59 ksi governs and

M_n =19.59 (7.936/2.0) = 77.7 k-in.

For shear, we will be examining shear and shear buckling failures. The equation for shear failure is:

$V_n = F_{LT}A_s$ where F_{LT} = 8 ksi and is the in-plane shear strength; and A_s = 4 in. x .25 = 1.0 in. ^{2}

And is the area of the web. Plugging these values in, we have

V_n = 8.0 x 1.0 = 8 kips.

The equation for web shear buckling is

$V_n = f_{cr} A_s$ where

$f_{cr} = (k_{LT}t_w^2/3h^2)(E_xE_y^3)^{.25}$ and $k_{LT} = 8.1 + 5.0(2G + E_y v_{LT})/(E_x E_y)$ = 11.21. Plugging in values

f_{cr} =45.10 ksi and

V_n = 45.10(1.0) = 45.10 kips

For the 4" x 4" x ¼" beam, ASCE-LRFD failure mode values of shear and moment, V_n and M_n are as shown. The governing values of critical shear and critical moment for the ASCE-LRFD failure modes are shearing of the web and compression flange local buckling. For Investigation 9, the ASCE-LRFD P and M values for lateral-torsional buckling are 3.64 kips and 74.1 k-in. Because the critical values associated with the other failure modes are higher than the values determined using the lateral-torsional buckling failure mode, the beam for this investigation is expected to fail in lateral-torsional-buckling.

CHAPTER 4

COMPARISON OF THEORY AND EXPERIMENT

This chapter presents a comparison of theoretical formulations of the problems presented in Section 1.3 with the experimental lab results of the same problems. Translational and rotational deflections from theoretical formulations which include shear deformation and laboratory experiments are tabulated for each investigation. Critical load values from theoretical formulations which include shear deformations, ASCE-LRFD Prestandard provisions, and laboratory experiments concerning lateral- torsional buckling are plotted versus translational and rotational deflection for each investigation. Theoretical critical buckling values are noted to compare favorably or unfavorably with empirical results and percentage differences noted for each investigation.

4.1 Investigation 1

This section presents a comparison of analytical and experimental translational and rotational deflections for investigation 1. Translational and rotational deflections from theoretical formulations which includes shear deformation and laboratory experiments are shown for investigation 1 in Table 49. Critical load values from theoretical formulations which include shear deformations, ASCE-LRFD Prestandard provisions and laboratory experiments concerning lateral torsional buckling are plotted versus translational and rotational deflection for investigation 1 in Figures 66, 67, and 68. Favorable or unfavorable differences are noted.

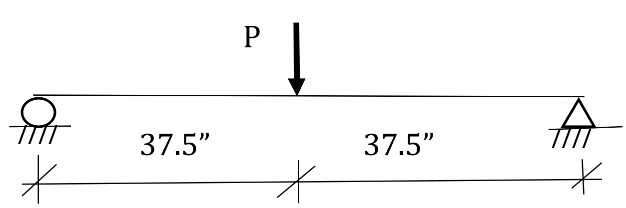

Table 49. Deflections. Investigation 1

VERTICAL	8"	8" from support		29"	29" from support		18"	18" from support	
LOAD P	v1 lab	v1calcw/s	v1calcw/o	v2 lab	v2calcw/s	v2calcw/o	v3lab	v3calcw/s	v3calcw/o
1E-07	0	0	0	0	0	0	0	0	0
0.014078	-0.001	0.001974	0.001814	0.004	0.003735	0.003414	0.003	0.005384	0.004849
0.12925	-0.019	0.017997	0.016534	0.053	0.034052	0.031127	0.042	0.049084	0.044208
0.31489	-0.043	0.043845	0.040281	0.121	0.082959	0.075832	0.093	0.11958	0.1077
0.491298	-0.066	0.068407	0.062846	0.178	0.129434	0.118313	0.142	0.186569	0.168035
0.685838	-0.091	0.095494	0.087732	0.258	0.180687	0.165162	0.189	0.260446	0.234572
0.87873	-0.117	0.122352	0.112407	0.329	0.231505	0.211614	0.243	0.333696	0.300545
1.0271	-0.137	0.143012	0.131387	0.386	0.270595	0.247346	0.284	0.390043	0.351294
1.3618	-0.181	0.189611	0.174199	0.509	0.358767	0.327942	0.376	0.517135	0.465761
1.6124	-0.217	0.224503	0.206254	0.607	0.424787	0.38829	0.449	0.612298	0.551469
1.8316	-0.238	0.243786	0.22397	2.1	0.461272	0.42164	0.489	0.664888	0.598835
1.88	-0.248	0.255034	0.234303	2.7	0.482555	0.441094	0.514	0.695566	0.626465
	5"	17.5"	28"	9"	17"	28"			
LOAD P	h1	h2	h3	l1	l2	l3			
1E-07	0	0	0	0	0	0			
0.014078	0	0	0	0.0002	0.000471	0.000231			
0.12925	0.005	0.006	0.008	0.0025	0.005059	0.002538			
0.31489	0.011	0.017	0.022	0.0054	0.013529	0.006			
0.491298	0.016	0.026	0.034	0.008	0.020824	0.009308			
0.685838	0.022	0.036	0.045	0.0111	0.028706	0.013769			
0.87873	0.029	0.047	0.056	0.0141	0.036471	0.017154			
1.0271	0.034	0.055	0.065	0.0162	0.042824	0.019769			
1.3618	0.045	0.071	0.082	0.0208	0.055882	0.025538			
1.6124	0.052	0.083	0.094	0.0246	0.071529	0.029692			
1.8316	0.059	0.09	0.12	0.0267	0.095059	0.032077			
1.88	0.062	0.097	0.15	0.0279	0.123	0.033538			

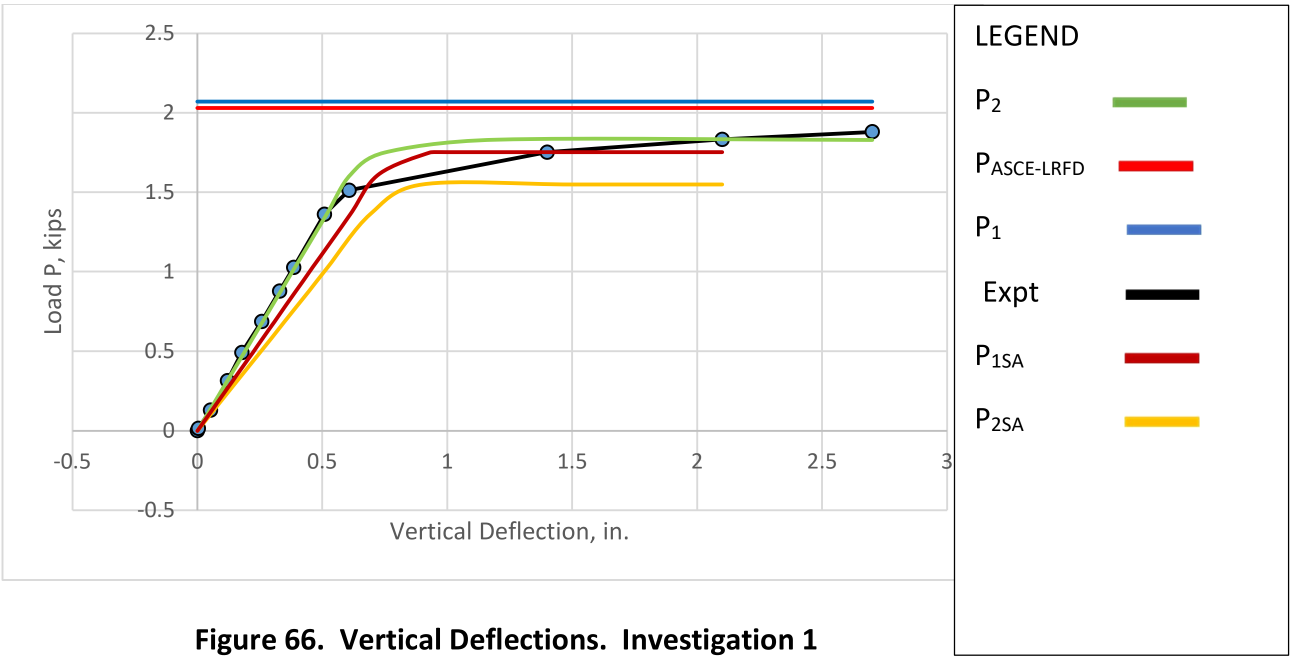

Figure 66. Vertical Deflections. Investigation 1

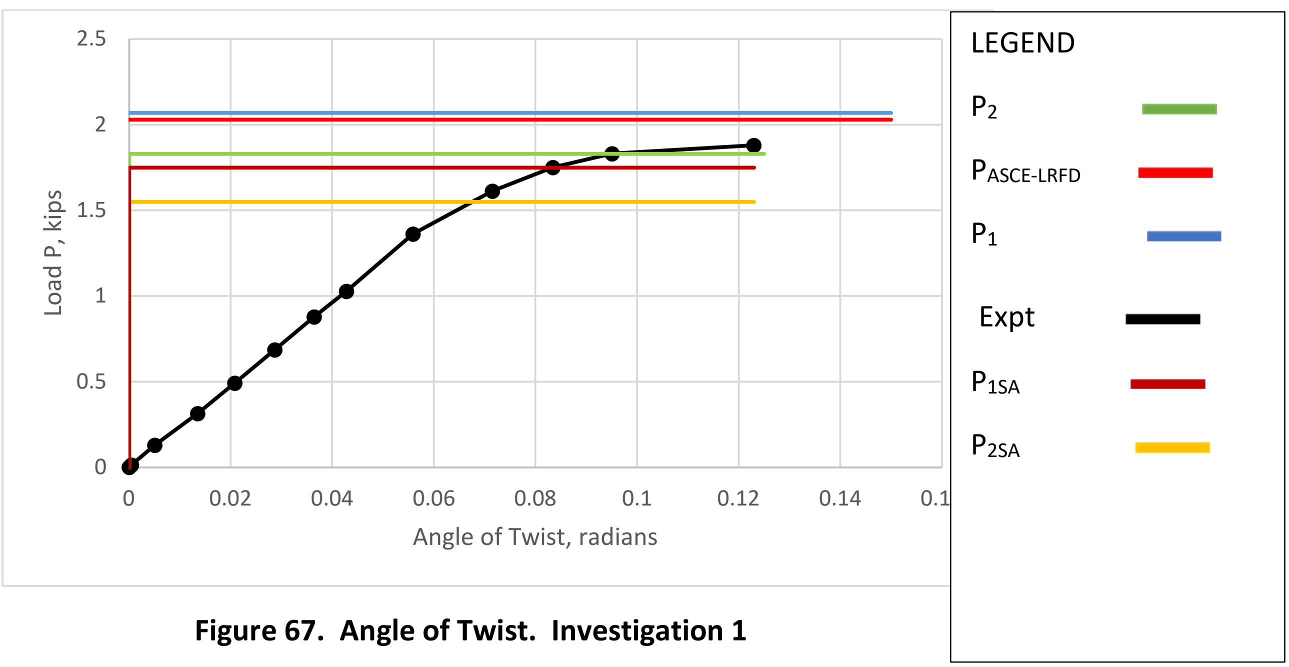

Figure 67. Angle of Twist. Investigation 1

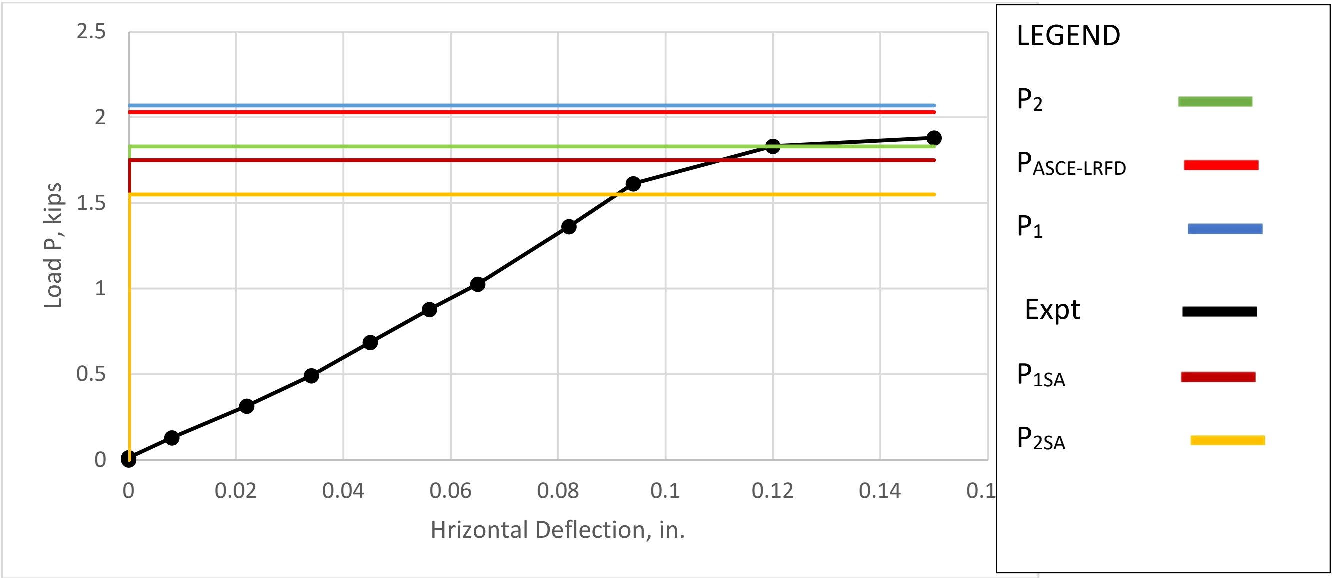

Figure 68. Horizontal Deflections. Investigation 1

Experimental deflections for investigation 1 are shown in Table 49. The experimental critical buckling value was determined to be 1.88 kips from Figures 67 and 68. The Central Difference critical moment value is 37.29 kip-in. The lab moment value is 38.31 kip-in; and the ASCE guideline calculated value is 43.0 kip-in. Knowing the relationship and solving for P, P = 1.83 kips.

This value compared favorably with the lab experiment value of 1.88 kips and the ASCE calculated value of 2.11 kips is considered a little high. Our experimental value was within 95% of the lab value while the ASCE value was within 88%.

Because there is no load in the x direction and M is zero, the horizontal deflections and the angle of twist within the elastic range will be zero for Central difference calcs. Central Difference vertical deflection values were taken at same locations along the beam as the locations of the vertical deflection dial gages observed during experiments. As shown in Figure 66, they compare favorably. As the length of the beam decreases, the percentage of the vertical deflection due to shear moment increases. Fixed supports increase the value of the moment contribution due to shear moment.

4.2 Investigation 2

This section presents a comparison of analytical and experimental translational and rotational deflections for investigation 2. Translational and rotational deflections from theoretical formulations which include shear deformation and laboratory experiments are shown for investigation 2 in Table 50. Critical load values from theoretical formulations which include shear deformations, ASCE-LRFD Prestandard provisions, and laboratory experiments concerning lateral- torsional buckling are plotted versus translational and rotational deflection for investigation 2 in Figures 69, 70, and 71. Favorable or unfavorable differences are noted.

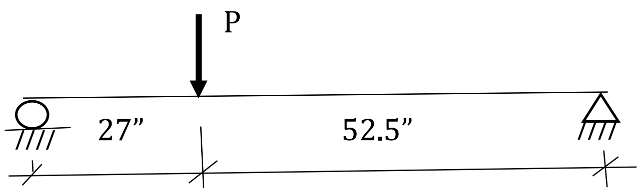

Table 50. Deflections. Investigation 2

VERTICAL	6" from Support			21" from Support			36" from Support		
LOAD P	v1 lab	v1calcw/s	v1calcw/o	v2 lab	v2calcw/s	v2calcw/o	V3LAB	v3calcw/s	v3calcw/o
0	0	0	0	0	0	0	0	0	0
0.1826	0.074	-0.04672	-0.04426	0.23	-0.14554	-0.13692	0.181	-0.18109	-0.17191
0.4244	0.132	-0.1086	-0.10287	0.309	-0.33829	-0.31824	0.399	-0.42092	-0.39957
0.6514	0.206	-0.16669	-0.1579	0.476	-0.51924	-0.48846	0.593	-0.64607	-0.61329
0.8653	0.338	-0.22141	-0.20973	0.64	-0.6897	-0.64881	0.792	-0.85816	-0.81462
0.91	0.41	-0.27445	-0.25997	0.794	-0.85491	-0.80423	0.966	-1.06372	-1.00976
0.91							1.2		
0.91							1.4		
	3.5"	22"	36"	5.5"	22"	36"			
LOAD P	h1	h2	h3	l1	l2	l3			
0	0	0	0	0	0	0			
0.1826	0.002	0	0.001	0.077	0.131	0.0167			
0.4244	0.004	0.003	0.029	0.14	0.226	0.0299			
0.6514	0.009	0.005	0.087	0.199	0.308	0.0431			
0.8653	0.012	0.008	0.175	0.263	0.384	0.0535			
0.91	0.023	0.019	0.33	0.318	0.449	0.0763			
0.91			0.8			0.095			
0.91			0.9			0.105			
	X. DEFLECTIONS OF A SINGLE SPAN W/ PT. LOAD. OFF CENTER.								
	ANALYTICAL AND EXPERIMENTAL VERTICAL DEFLECTIONS.								
	EXPERIMENTAL HORIZONTAL AND LATERAL TORSIONAL DEFLECTIONS								

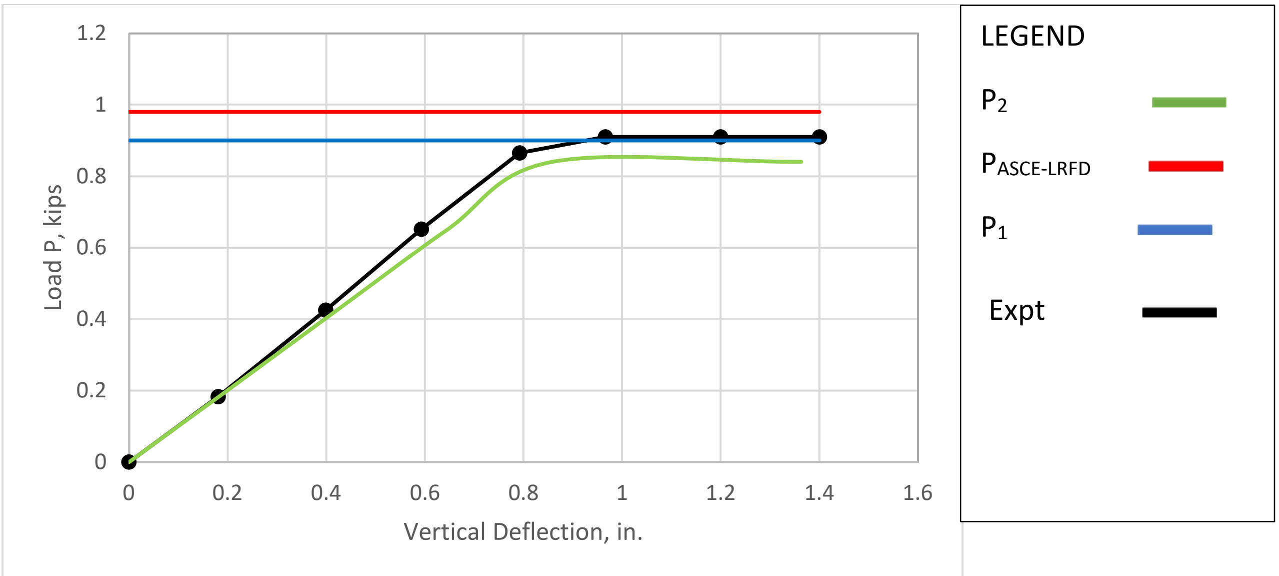

Figure 69. Vertical Deflections. Investigation 2

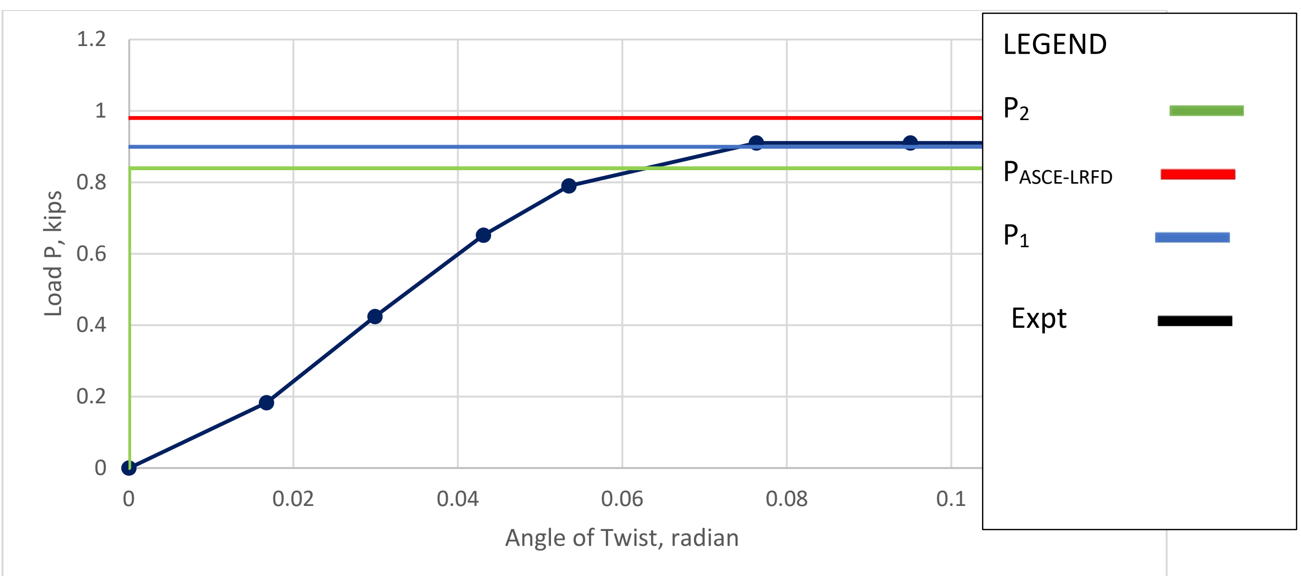

Figure 70. Angle of Twist. Investigation 2

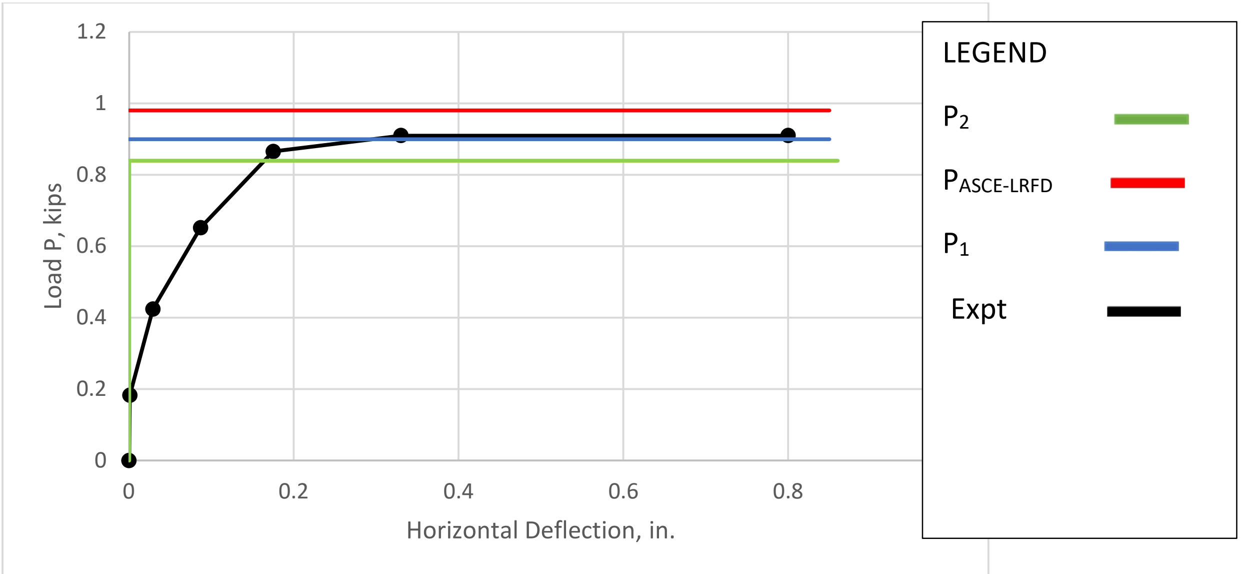

Figure 71. Horizontal Deflections. Investigation 2

Experimental deflections for investigation 2 are shown in Table 50. The experimental critical buckling value was determined to be .91 kips from Figures 70 and 71. The Central Difference critical moment value Mcr is 15.69 k-in. The lab moment value is 16.97 kip-in; and the ASCE guideline calculated value is 18.68 kip-in. Knowing the relationship and solving for P, P = .84 kips.

This value compared favorably with the lab experiment value of .91 kips and the ASCE calculated value of 1.0 kips compares favorably. Our experimental value was within 92% of the lab value while the ASCE value was within 90%.

Because there is no load in the x direction and M is zero, the horizontal deflections and the angle of twist within the elastic range will be zero for Central difference calcs. Central Difference vertical deflection values were taken at same locations along the beam as the locations of the vertical deflection dial gages observed during experiments. As shown in Figure 69, they compare favorably. As the length of the beam decreases, the percentage of the vertical deflection due to shear moment increases. Fixed supports increase the value of the moment contribution due to shear moment.

4.3 Investigation 3

This section presents a comparison of analytical and experimental translational and rotational deflections for investigation 3. Translational and rotational deflections from theoretical formulations which include shear deformation and laboratory experiments are shown for investigation 3 in Table 51. Critical load values from theoretical formulations which include shear deformations, ASCE-LRFD Prestandard provisions, and laboratory experiments concerning lateral- torsional buckling are plotted versus translational and rotational deflection for investigation 3 in Figures 72, 73, and 74. Favorable or unfavorable differences are noted.

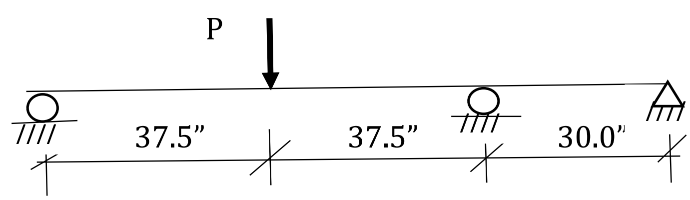

Table 51. Deflections. Investigation 3

VERTICAL	32.5"			29"			4"		
LOAD P	v1 lab	v1calcw/s	v1calcw/o	v2 lab	v2calcw/s	v2calcw/o	v3lab	v3calcw/s	v3calcw/o
0	0	0	0	0	0	0	0	0	0
0.346381	0.08969	-0.08967	-0.07595	0.046	-0.07794	-0.06553	0.022	-0.00634	-0.00503
0.580324	0.150266	-0.15024	-0.12725	0.104	-0.13058	-0.10979	0.037	-0.01062	-0.00843
0.814432	0.210884	-0.21085	-0.17859	0.146	-0.18326	-0.15407	0.052	-0.01491	-0.01184
1.046892	0.271076	-0.27103	-0.22956	0.202	-0.23557	-0.19805	0.069	-0.01916	-0.01521
1.24473	0.322303	-0.32225	-0.27294	0.255	-0.28009	-0.23548	0.083	-0.02278	-0.01809
1.417838	0.367126	-0.36706	-0.3109	0.3	-0.31904	-0.26823	0.095	-0.02595	-0.0206
1.617324	0.41878	-0.41871	-0.35464	0.353	-0.36393	-0.30597	0.109	-0.02961	-0.0235
1.79373	0.464457	-0.46438	-0.39332	0.401	-0.40362	-0.33934	0.122	-0.03283	-0.02607
2.027838	0.525076	-0.52498	-0.44466	0.464	-0.4563	-0.38363	0.14	-0.03712	-0.02947
2.326243	0.602343	-0.60224	-0.51009	0.549	-0.52345	-0.44008	0.163	-0.04258	-0.03381
2.5	1.2	-0.6876	-0.58239		-0.59765	-0.50246		-0.04862	-0.0386
2.6	1.5								
	27.5"	24"	4"	30"	30"	5"			
LOAD P	h1	h2	h3	l1	l2	l3			
0	0	0	0	0	0	0			
0.346381	0	0	0	0.0081	0.005538	0			
0.580324	0.008	0.002	0.002	0.0145	0.010231	0.001154			
0.814432	0.009	0.003	0.003	0.021	0.014769	0.002308			
1.046892	0.016	0.009	0.004	0.0272	0.019308	0.003538			
1.24473	0.021	0.014	0.005	0.0329	0.023385	0.004538			
1.417838	0.027	0.015	0.006	0.0374	0.026615	0.005462			
1.617324	0.032	0.02	0.008	0.043	0.030462	0.006462			
1.79373	0.035	0.022	0.009	0.0477	0.033846	0.007462			
2.027838	0.05	0.026	0.011	0.0544	0.038615	0.008769			
2.326243	0.061	0.038	0.012	0.0615	0.043538	0.009923			
2.5	0.07	0.055		0.12					
2.6	0.16	0.09		0.15					

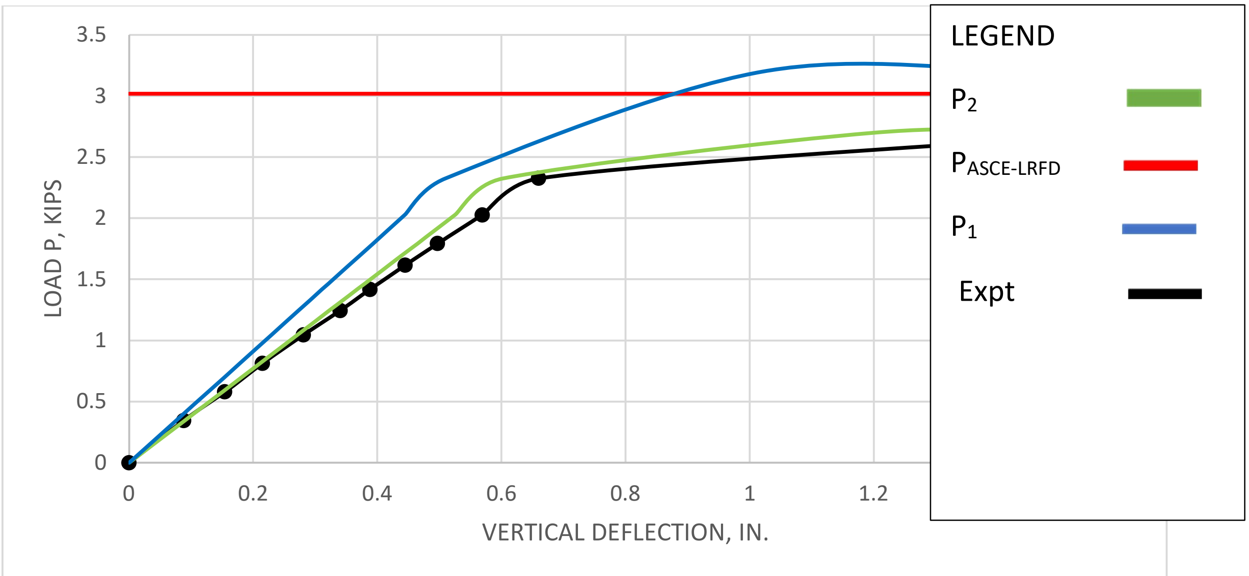

Figure 72. Vertical Deflections. Investigation 3

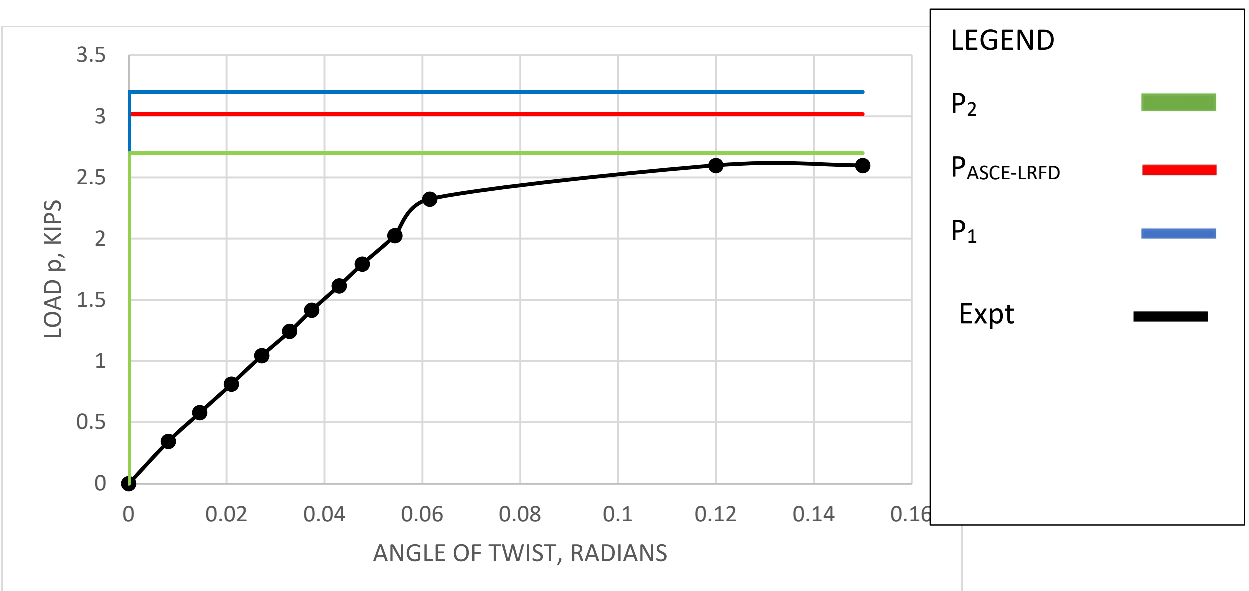

Figure 73. Angle of Twist. Investigation 3

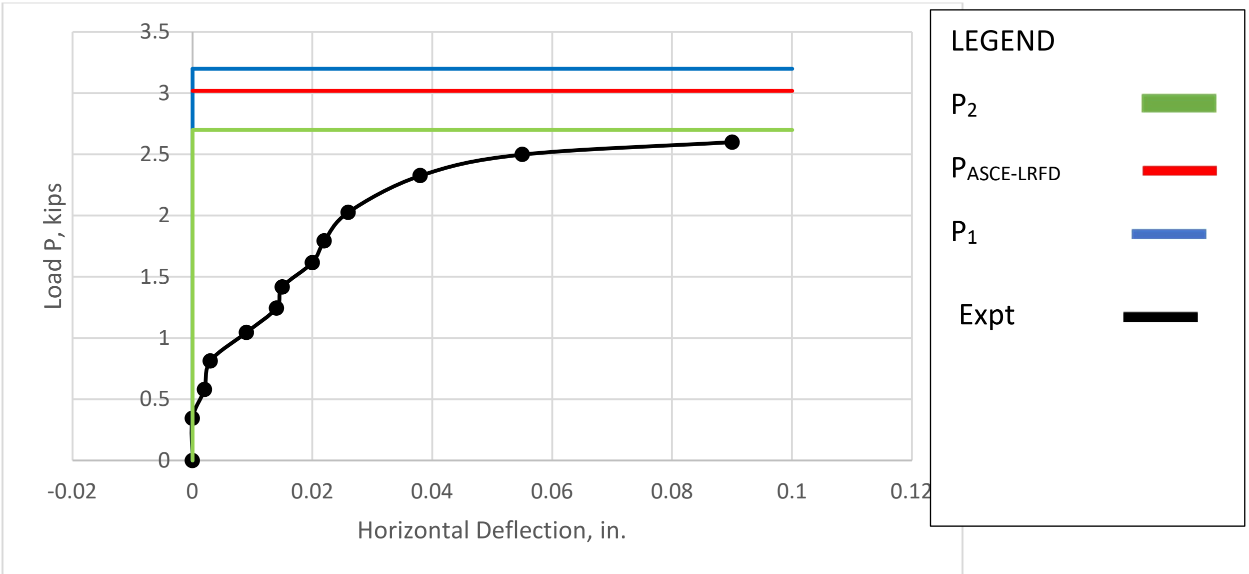

Figure 74. Horizontal Deflections. Investigation 3

Experimental deflections for investigation 3 are shown in Table 51. The rise in the curve after the elastic range represents strain hardening and lateral- torsion. The experimental critical buckling value was determined to be 2.6 kips from Figures 73 and 74. The Central Difference critical moment value M_{cr} is 43.97 k-in. The lab moment value is 42.28 kip-in; and the ASCE guideline calculated value is 51.52 kip-in. Knowing the relationship of P and solving for P, P = 2.7 kips.

This value compared favorably with the lab experiment value of 2.6 kips and the ASCE calculated value of 3.16 kips compares favorably. Our experimental value was within 95% of the lab value while the ASCE value was within 78%; however, the ASCE buckling load value is not conservative.

Because there is no load in the x direction and M is zero, the horizontal deflections and the angle of twist within the elastic range will be zero for Central difference calcs. Central Difference vertical deflection values were taken at same locations along the beam as the locations of the vertical deflection dial gages observed during experiments. As shown in Figure 72, they compare favorably. As the length of the beam decreases, the percentage of the vertical deflection due to shear moment increases. Fixed supports increase the value of the moment contribution due to shear moment.

4.4 Investigation 4

This section presents a comparison of analytical and experimental translational and rotational deflections for investigation 4. Translational and rotational deflections from theoretical formulations which include shear deformation and laboratory experiments are shown for investigation 4 in Table 52. Critical load values from theoretical formulations which include shear deformations, ASCE-LRFD Prestandard provisions, and laboratory experiments concerning lateral-torsional buckling are plotted versus translational and rotational deflection for investigation 4 in Figures 75, 76, and 77. Favorable or unfavorable differences are noted.

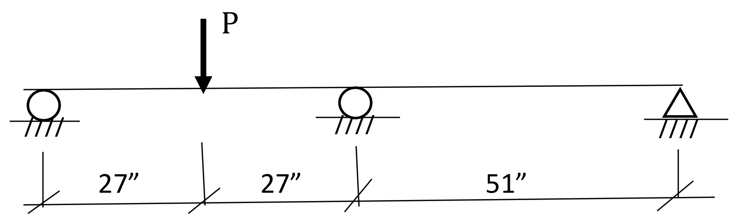

Table 52. Deflections. Investigation 4

VERTICAL	21.5" from support			19" from support			4"		
LOAD P	v1 lab	v1calcw/s	v1calcw/o	v2 lab	v2calcw/s	v2calcw/o	v3 lab	v3calcw/s	v3calcw/o
0	0	0	0	0	0	0	0	0	0
0.276973	0.112948	-0.077	-0.0663	0.076046	0.062518	0.054018	0.02	-0.00974	-0.00832
0.656163	0.218252	-0.18241	-0.15707	0.158803	0.148107	0.127971	0.046	-0.02308	-0.01971
0.835866	0.270905	-0.23237	-0.20009	0.200553	0.188669	0.163019	0.06	-0.02941	-0.0251
1.005677	0.329502	-0.27958	-0.24074	0.239322	0.226999	0.196137	0.076	-0.03538	-0.0302
1.154055	0.376209	-0.32083	-0.27626	0.2766	0.26049	0.225075	0.089	-0.0406	-0.03466
1.384866	0.444997	-0.38499	-0.33151	0.331771	0.312588	0.27009	0.109	-0.04872	-0.04159
1.571163	0.501896	-0.43678	-0.37611	0.377249	0.354639	0.306424	0.126	-0.05527	-0.04718
1.732731	0.552	-0.4817	-0.41479	0.419	0.391107	0.337934	0.142	-0.06096	-0.05204
2.037731	0.647114	-0.56649	-0.4878	0.495047	0.459951	0.397418	0.169	-0.07169	-0.0612
2.37	0.8	-0.65082	-0.56042	0.569602	0.528423	0.456581	0.196	-0.08236	-0.07031
2.37	1.43								
	19"	19"	4"	22.5"	19"	5"			
LOAD P	h1	h2	h3	l1	l2	l3			
0	0	0	0	0	0	0			
0.276973	0.001	0	0	0.006087	0.008333	0.002762			
0.656163	0.006	0.004	0	0.016522	0.017	0.004762			
0.835866	0.01	0.007	0.001	0.021391	0.021083	0.005619			
1.005677	0.014	0.01	0.002	0.026435	0.025	0.006476			
1.154055	0.016	0.012	0.003	0.03087	0.028667	0.007238			
1.384866	0.019	0.015	0.004	0.037391	0.034167	0.008381			
1.571163	0.024	0.019	0.005	0.042957	0.03875	0.0092			
1.732731	0.028	0.022	0.006	0.047739	0.0425	0.01			
2.037731	0.039	0.027	0.007	0.055913	0.049	0.012381			
2.37	0.058	0.042	0.008	0.066609	0.05825	0.018275			
2.37	0.116					0.0225			

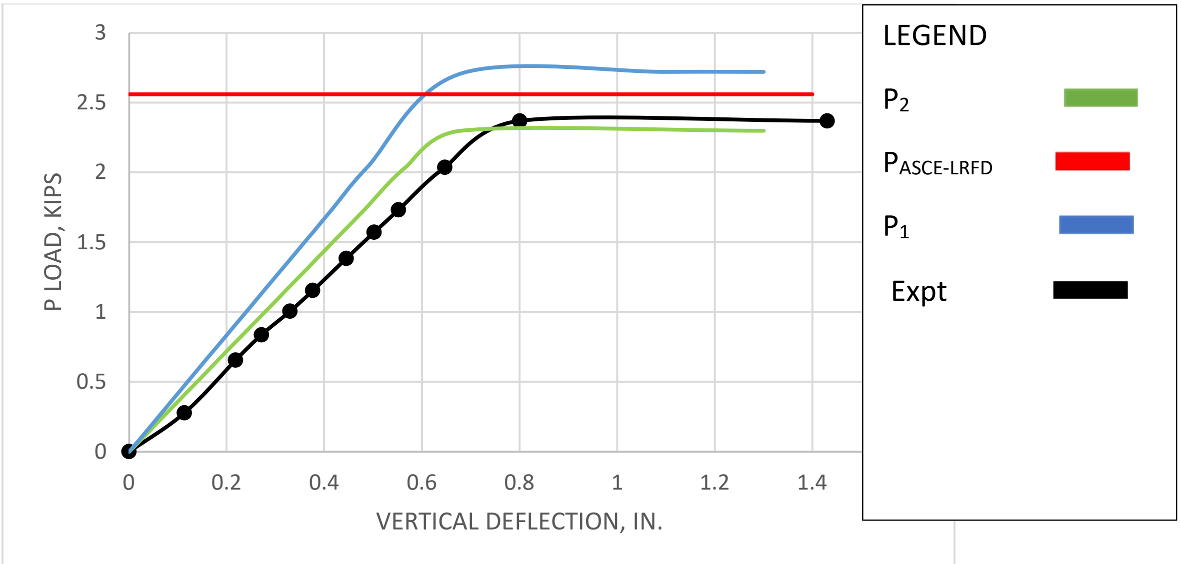

Figure 75. Vertical Deflections. Investigation 4

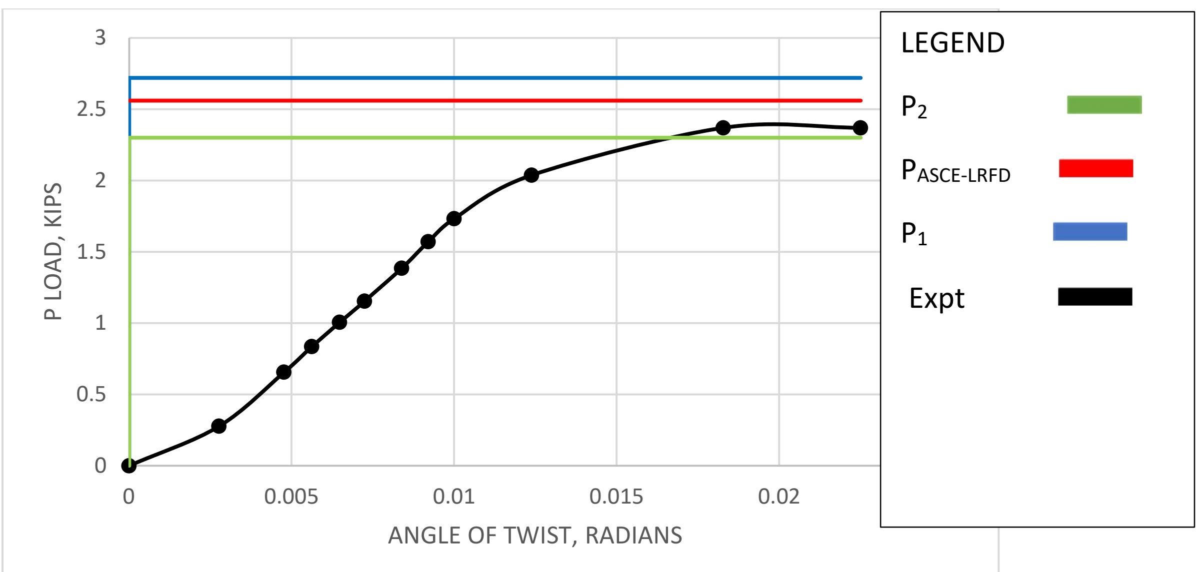

Figure 76. Angle of Twist. Investigation 4

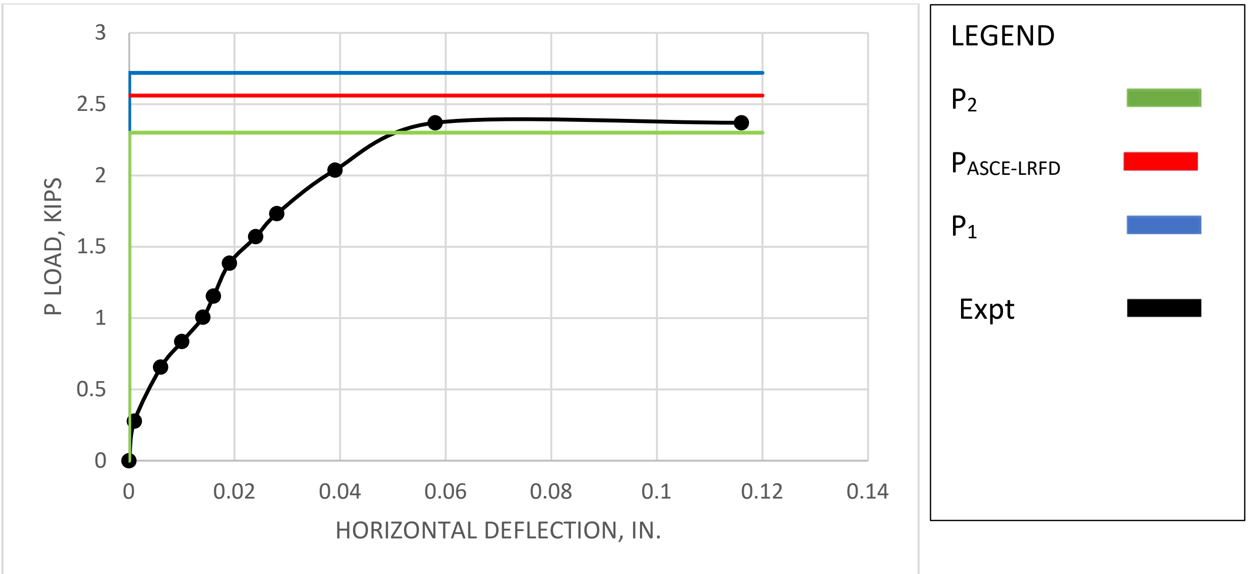

Figure 77. Horizontal Deflections. Investigation 4

Experimental deflections for investigation 4 are shown in Table 52. The experimental critical buckling value was determined to be 2.37 kips from Figures 76 and 77. The Central Difference critical moment value M_{cr} is 28.67 k-in. The lab moment value is 29.59 kip-in; and the ASCE guideline calculated value is 32.89 kip-in. Knowing the relationship of P and solving for P, P = 2.3 kips.

This value compared favorably with the lab experiment value of 2.37 kips and the ASCE calculated value of 2.64 kips is not conservative. Our experimental value was within 95% of the lab value while the ASCE value was within 88%.

Because there is no load in the x direction and M is zero, the horizontal deflections and the angle of twist within the elastic range will be zero for Central difference calcs. Central Difference vertical deflection values were taken at same locations along the beam as the locations of the vertical deflection dial gages observed during experiments. As shown in Figure 75, they compare favorably. As the length of the beam decreases, the percentage of the vertical deflection due to shear moment increases. Fixed supports increase the value of the moment contribution due to shear moment.

4.5 Investigation 5

This section presents a comparison of analytical and experimental translational and rotational deflections for investigation 5. Translational and rotational deflections from theoretical formulations which include shear deformation and laboratory experiments are shown for investigation 5 in Table 53. Critical load values from theoretical formulations which include shear deformations, ASCE-LRFD Prestandard provisions, and laboratory experiments concerning lateral-torsional buckling are plotted versus translational and rotational deflection for investigation 5 in Figures 78, 79, and 80. Favorable or unfavorable differences are noted.

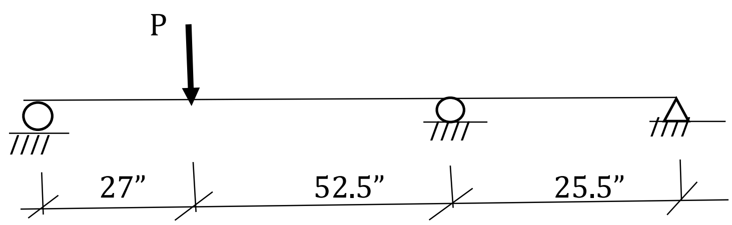

Table 53. Deflections. Investigation 5

VERTICAL	5" from support			22" from support			35" from support		
LOAD P	v1LAB	v1calcw/s	v3calcw/o	V22LAB	V2calcw/s	v3calcw/o	v33LAB	v3calcw/s	v3calcw/o
0	0	0	0	0	0	0	0	0	0
0.2285189	0.069	-0.0402638	-0.03729	0.103	-0.12299	-0.1125705	0.129	-0.14193	-0.13084
0.4446483	0.109	-0.07901504	-0.07317	0.222	-0.24135	-0.2209091	0.266	-0.27854	-0.25676
0.6249855	0.147	-0.11776692	-0.10906	0.339	-0.35972	-0.3292476	0.402	-0.41514	-0.38267
0.8108292	0.184	-0.15621623	-0.14466	0.456	-0.47717	-0.4367398	0.499	-0.55068	-0.50761
1.0008027	0.222	-0.19436265	-0.17999	0.575	-0.59369	-0.5433856	0.595	-0.68515	-0.63156
1.1219453	0.252	-0.22282089	-0.20634	0.664	-0.68062	-0.6229467	0.7	-0.78547	-0.72403
1.2	0.28	-0.24855422	-0.23017	0.747	-0.75922	-0.6948903	0.801	-0.87618	-0.80765
1.2	0.31	-0.28488335	-0.26382	0.866	-0.87019	-0.7964577	0.939	-1.00424	-0.9257
	21"	18"	4"	21"	18"	5"			
LOAD P	h11LAB	h22LAB	h33LAB	l11LAB	l22LAB	l33LAB			
0	0	0	0	0	0	0			
0.2285189	0	0	0	0.001909	0.004818	0.00157895			
0.4446483	0	0	0	0.004455	0.015182	0.01578947			
0.6249855	0.002	0.004	0.004	0.007091	0.025909	0.03042105			
0.8108292	0.004	0.007	0.007	0.010182	0.036636	0.04484211			
1.0008027	0.011	0.012	0.011	0.013545	0.047545	0.05947368			
1.1219453	0.023	0.021	0.017	0.016636	0.056091	0.07073684			
1.2	0.036	0.031	0.022	0.020091	0.064273	0.08157895			
1.2	0.05	0.032	0.031	0.024455	0.075818	0.09642105			

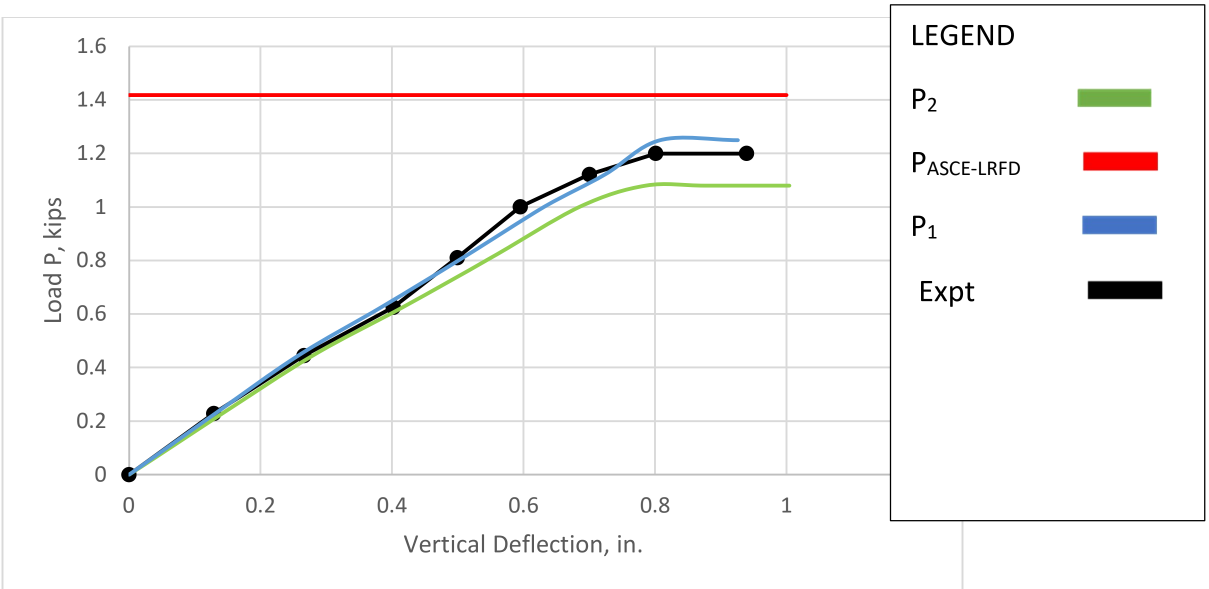

Figure 78. Vertical Deflections. Investigation 5

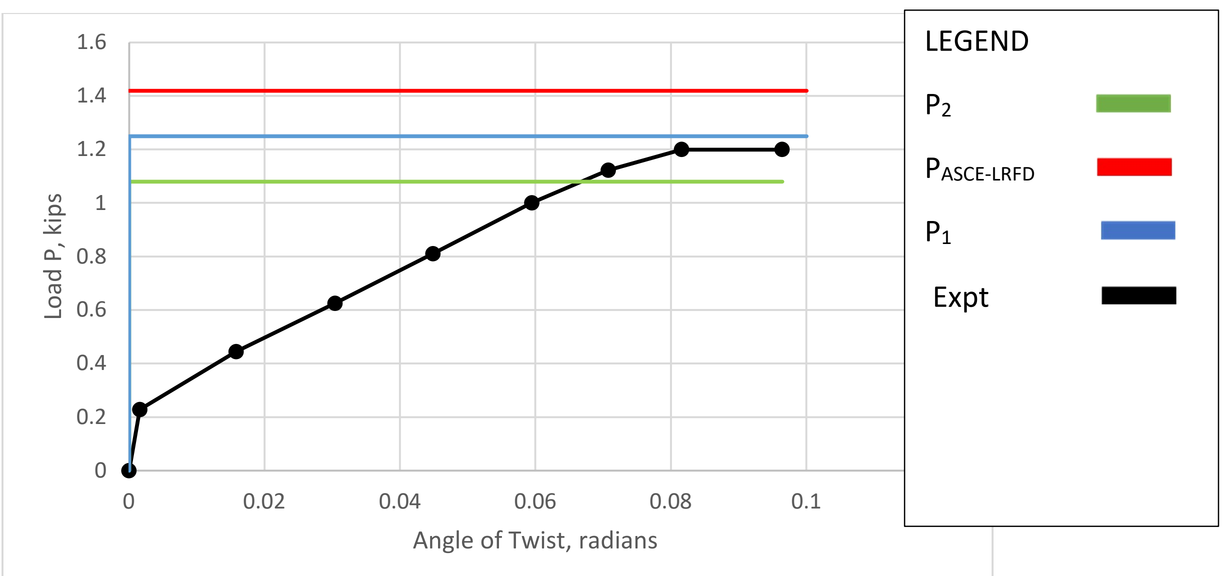

Figure 79. Angle of Twist. Investigation 5

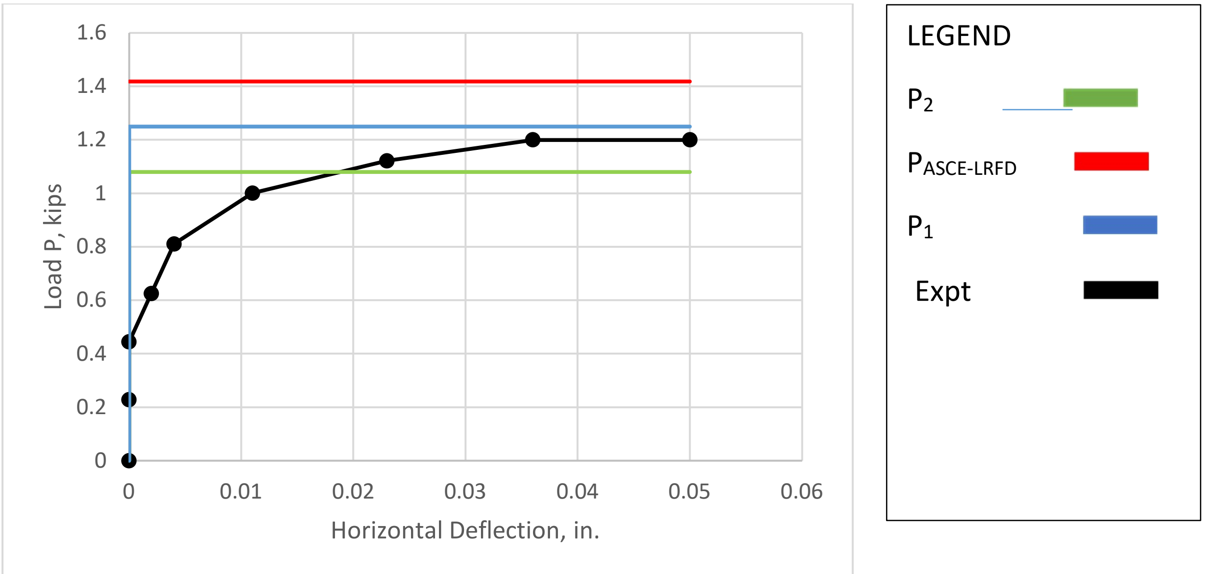

Figure 80. Horizontal Deflections. Investigation 5

Experimental deflections for investigation 5 are shown in Table 53. The experimental critical buckling value was determined to be 1.2 kips from Figures 79 and 80. The Central Difference critical moment value M_{cr} is 17.40 k-in. The lab moment value is 19.34 kip-in; and the ASCE guideline calculated value is 22.92 kip-in. Knowing the relationship of P and solving, P = 1.08 kips.

This value compared favorably with the lab experiment value of 1.2 kips and the ASCE calculated value of 1.419 kips is not conservative. Our experimental value was within 90% of the lab value while the ASCE value was within 80%.

Because there is no load in the x direction and M is zero, the horizontal deflections and the angle of twist within the elastic range will be zero for Central difference calcs. Central Difference vertical deflection values were taken at same locations along the beam as the locations of the vertical deflection dial gages observed during experiments. As shown in Figure 78, they compare favorably. As the length of the beam decreases, the percentage of the vertical deflection due to shear moment increases. Fixed supports increase the value of the moment contribution due to shear moment.

4.6 Investigation 6

This section presents a comparison of analytical and experimental translational and rotational deflections for investigation 6. Translational and rotational deflections from theoretical formulations which include shear deformation and laboratory experiments are shown for investigation 6 in Table 54. Critical load values from theoretical formulations which include shear deformations, ASCE-LRFD prestandard provisions, and laboratory experiments concerning lateral torsional buckling are plotted versus translational and rotational deflection for investigation 6 in Figures 81, 82, and 83. Favorable or unfavorable differences are noted.

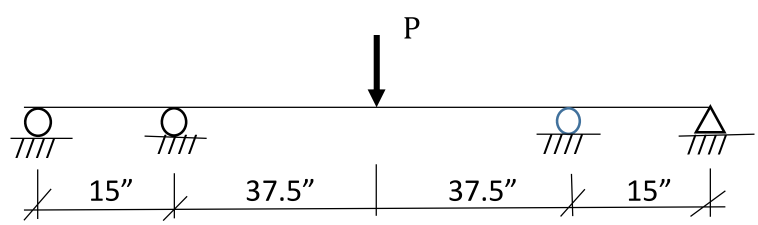

Table 54. Deflections. Investigation 6

VERTICAL	7" from support			18.5" from support			32" from support		
LOAD P	v1	v1calcw/s	v1calcw/o	v2	v2calcw/s	v2calcw/o	v3	v3calcw/s	v3calcw/o
0	0	0	0	0	0	0	0	0	0
0.2209191	0.00836	-0.0068606	-0.0047631	0.017004944	-0.0238077	-0.0179347	0.0241996	-0.0360449	-0.0268159
0.60175725	0.0228	-0.0186875	-0.0129742	0.047150072	-0.0648494	-0.0488521	0.0678381	-0.098182	-0.07304331
0.9825954	0.0418	-0.0305145	-0.0211853	0.088116528	-0.1058912	-0.0797694	0.1273452	-0.1603191	-0.11927073
1.17614691	0.05168	-0.0365252	-0.0253583	0.109759184	-0.1267496	-0.0954824	0.1570987	-0.1918987	-0.14276466
1.35683895	0.0589	-0.0421366	-0.0292542	0.127150604	-0.1462222	-0.1101514	0.1828852	-0.2213803	-0.16469766
1.549731	0.06878	-0.0481269	-0.033413	0.148020308	-0.1670096	-0.1258108	0.2134321	-0.2528524	-0.18811155
1.7640555	0.08056	-0.0547827	-0.038034	0.1739142	-0.1901067	-0.1432102	0.2503265	-0.2878213	-0.21412698
2.044326	0.09348	-0.0634865	-0.0440767	0.20483228	-0.2203106	-0.1659632	0.2963454	-0.3335501	-0.24814715
2.2916235	0.10716	-0.0711664	-0.0494086	0.234204456	-0.2469612	-0.1860394	0.338	-0.3738989	-0.27816495
3							0.58		
3.2							0.8		
3.3							1		
3.5							1.5		
	5.5"	20"	32"	6"	20"	33"			
LOAD P	h1	h2	h3	l1	l2	l3			
0	0	0	0	0	0	0			
0.2209191	0.003	0.007	0.007	0.0013	0.005	0.0059			
0.60175725	0.013	0.015	0.02	0.0041	0.0128	0.0152			
0.9825954	0.029	0.027	0.038	0.0081	0.0234	0.0284			
1.17614691	0.035	0.035	0.045	0.01	0.0287	0.0351			
1.35683895	0.041	0.038	0.051	0.0119	0.0332	0.0407			
1.549731	0.043	0.043	0.058	0.0135	0.0381	0.0458			
1.7640555	0.053	0.051	0.071	0.0163	0.0442	0.0534			
2.044326	0.057	0.061	0.085	0.0243	0.0514	0.0601			
2.2916235	0.066	0.071	0.101	0.0319	0.0577	0.067			
3	0.09					0.09069869			
3.2	0.12					0.1			
3.3	0.15					0.125			
3.5	0.165					0.14			

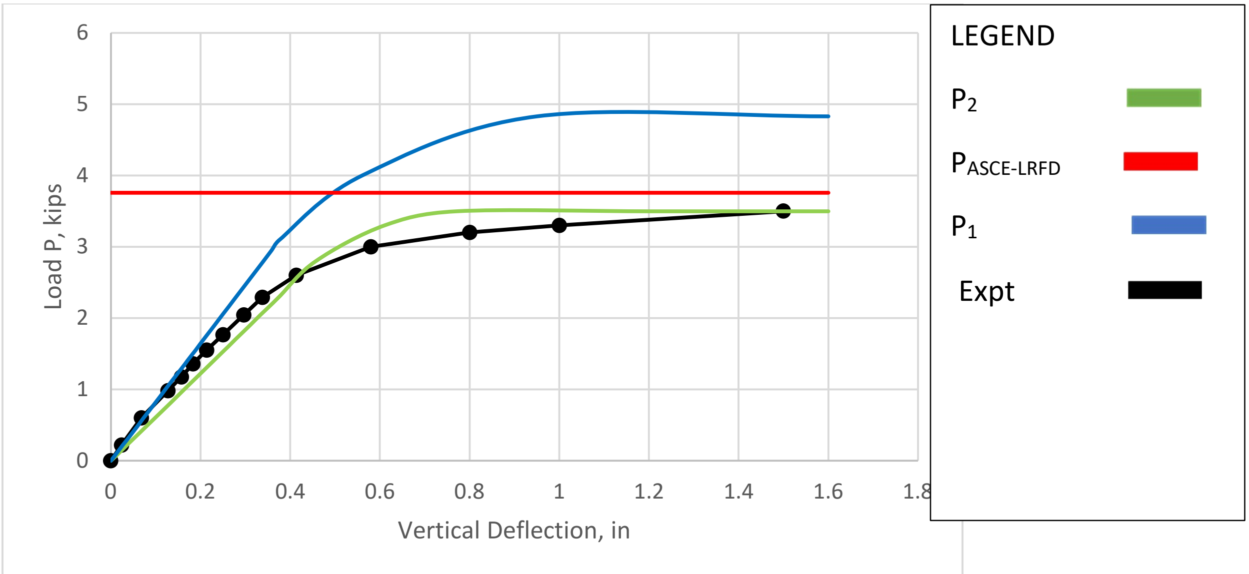

Figure 81. Vertical Deflections. Investigation 6

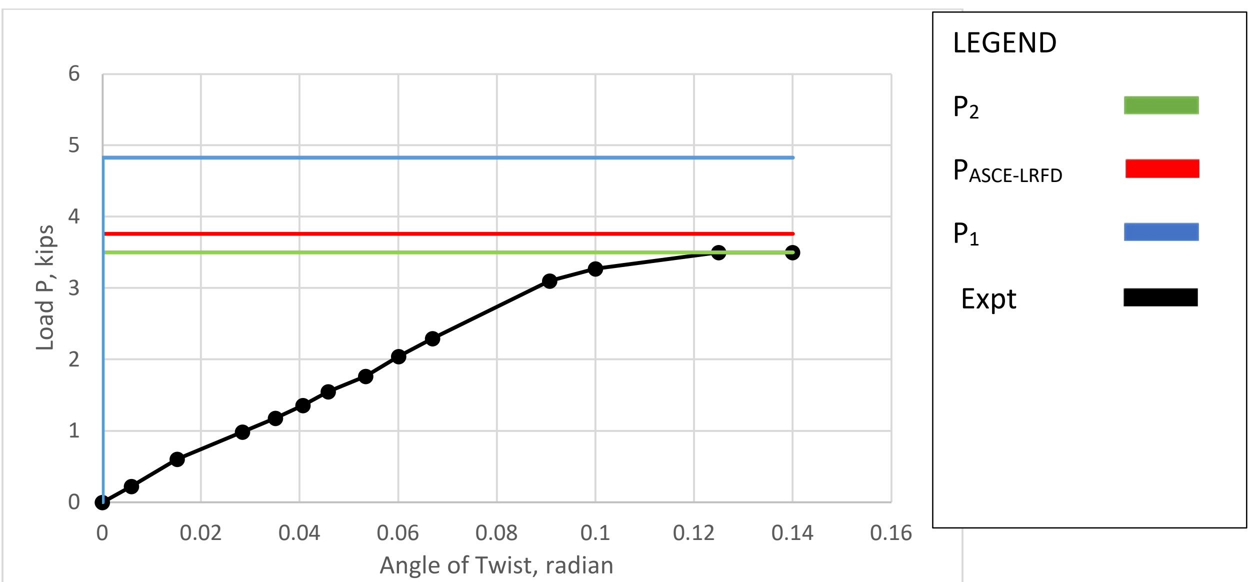

Figure 82. Angle of Twist. Investigation 6

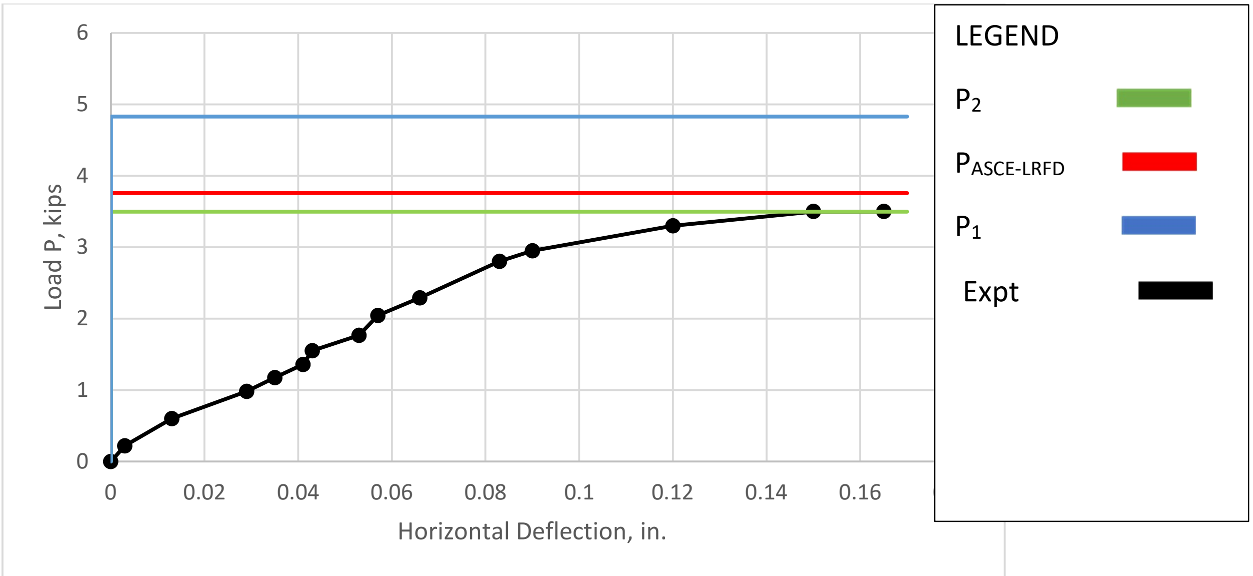

Figure 83. Horizontal Deflections. Investigation 6

Experimental deflections for investigation 6 are shown in Table 54. The experimental critical buckling value was determined to be 3.5 kips from Figures 82 and 83. The Central Difference critical moment value M_{cr} is 63.46 k-in. The lab moment value is 63.46 kip-in; and the ASCE guideline calculated value is 60.46 kip-in. Knowing the relationship of P and solving, P = 3.5 kips.

This value compared favorably with the lab experiment value of 3.5 kips. The ASCE calculated value of 3.33 kips is conservative. Our experimental value was within 99% of the lab value while the ASCE value was within 95%.

Because there is no load in the x direction and M is zero, the horizontal deflections and the angle of twist within the elastic range will be zero for Central difference calcs. Central Difference vertical deflection values were taken at same locations along the beam as the locations of the vertical deflection dial gages observed during experiments. As shown in Figure 81, they compare favorably. As the length of the beam decreases, the percentage of the vertical deflection due to shear moment increases. Fixed supports increase the value of the moment contribution due to shear moment.

4.7 Investigation 7

This section presents a comparison of analytical and experimental translational and rotational deflections for investigation 7. Translational and rotational deflections from theoretical formulations which include shear deformation and laboratory experiments are shown for investigation 7 in Table 55. Critical load values from theoretical formulations which include shear deformations, ASCE-LRFD Prestandard provisions, and laboratory experiments concerning lateral-torsional buckling are plotted versus translational and rotational deflection for investigation 7 in Figures 84, 85, and 86. Favorable or unfavorable differences are noted.

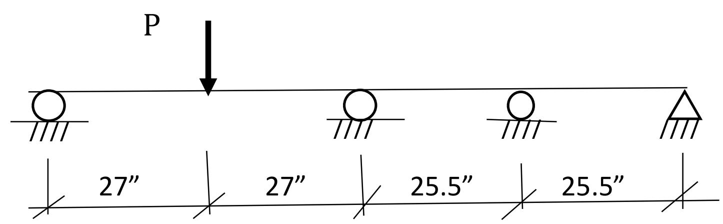

Table 55. Deflections. Investigation 7

	4" from support			18" From Support			21" from support		
P	v3lab	v3calcw/s	v3calcw/o	v2lab	v2calcw/s	v2calcw/o	v1lab	v1calcw/s	v1calcw/o
0	0	0	0	0	0	0	0	0	0
0.22851892	0.01136	-0.00587	-0.0047	0.04872	-0.0436748	-0.03666	0.056737	-0.05444	-0.04626
0.44464826	0.02201	-0.01143	-0.00915	0.09744	-0.0849817	-0.07134	0.113474	-0.10593	-0.09001
0.62498548	0.03266	-0.01606	-0.01287	0.14028	-0.1194479	-0.10027	0.163334	-0.14889	-0.12652
0.81082918	0.04331	-0.02084	-0.01669	0.1848	-0.1549666	-0.13008	0.215772	-0.19316	-0.16414
1.00080274	0.05396	-0.02572	-0.0206	0.22848	-0.1912746	-0.16056	0.268211	-0.23842	-0.20259
1.1219453	0.06106	-0.02883	-0.02309	0.25704	-0.2144275	-0.18	0.300878	-0.26728	-0.22711
1.31742534	0.07242	-0.03386	-0.02712	0.3024	-0.2517878	-0.21136	0.355035	-0.31385	-0.26669
1.51841186	0.08449	-0.03902	-0.03126	0.35112	-0.2902006	-0.2436	0.411772	-0.36173	-0.30737
1.7138919	0.09514	-0.04405	-0.03528	0.39984	-0.327561	-0.27497	0.469369	-0.4083	-0.34694
1.90937194	0.10721	-0.04907	-0.0393	0.44772	-0.3649213	-0.30633	0.526965	-0.45487	-0.38651
2.06493	0.11644	-0.05307	-0.04251	0.48972	-0.3946518	-0.33128	0.575106	-0.49193	-0.418
2.22737116	0.12709	-0.05724	-0.04585	0.53172	-0.4256977	-0.35735	0.75	-0.53063	-0.45089
2.51							1.6		
2.51									
	21"	18"	4"	21"	18"	5"			
LOAD P	h1	h2	h3	l1	l2	l3			
0	0	0	0	0	0	0			
0.22851892	0.001	0.001	0	0.0054	0.0035	0.0012			
0.44464826	0.003	0.002	0	0.0134	0.0103	0.0023			
0.62498548	0.005	0.003	0	0.0203	0.0171	0.0039			
0.81082918	0.007	0.006	0	0.0263	0.0231	0.0053			
1.00080274	0.011	0.007	0	0.0344	0.029	0.0066			
1.1219453	0.012	0.008	0	0.0388	0.0326	0.0072			
1.31742534	0.015	0.009	0	0.0461	0.039	0.0088			
1.51841186	0.02	0.011	0.005	0.0538	0.0454	0.0108			
1.7138919	0.024	0.017	0.006	0.0618	0.0522	0.0117			
1.90937194	0.028	0.021	0.007	0.0699	0.0593	0.0133			
2.06493	0.033	0.024	0.008	0.08	0.0654	0.0146			
2.22737116	0.045	0.027	0.009	0.09	0.0719	0.0161			
2.51	0.06			0.12					
2.51	0.0725			0.15					

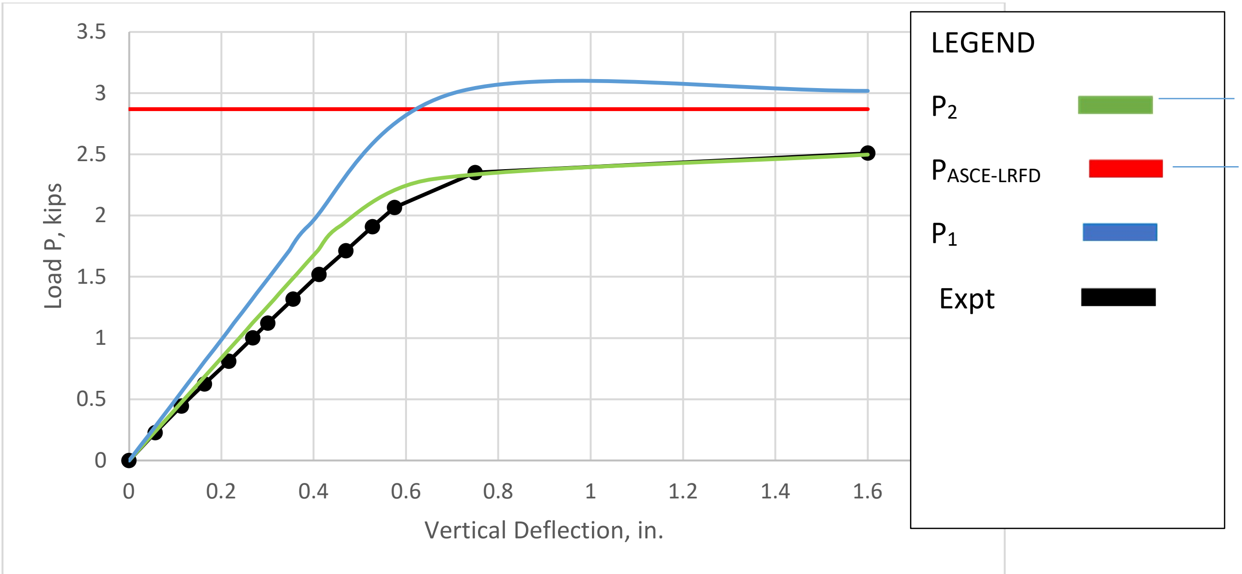

Figure 84. Vertical Deflections. Investigation 7

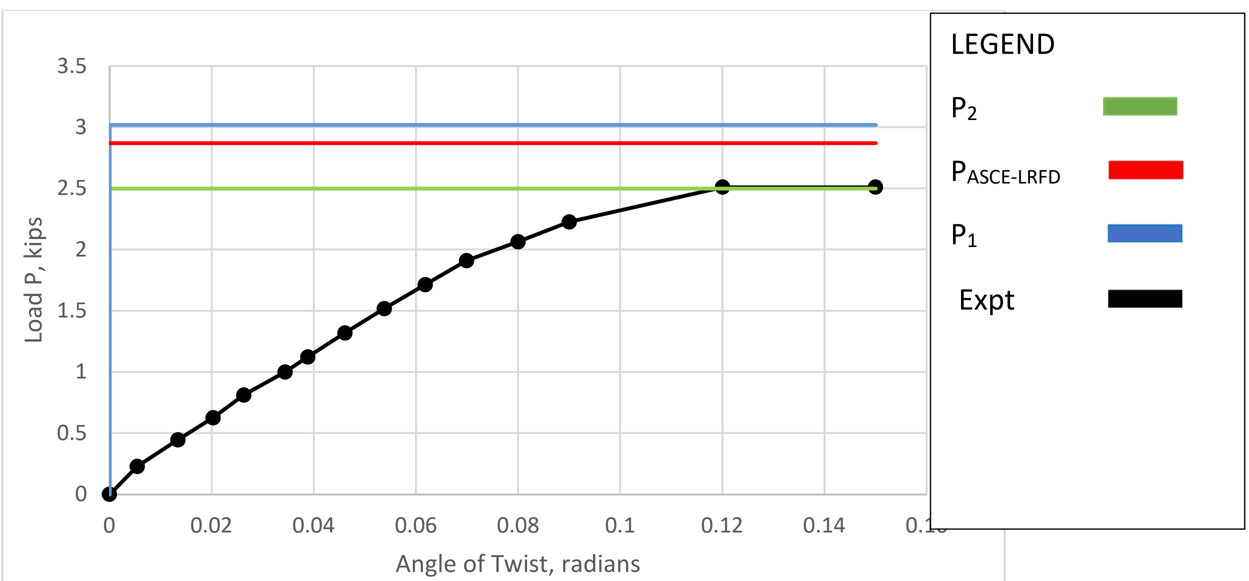

Figure 85. Angle of Twist. Investigation 7

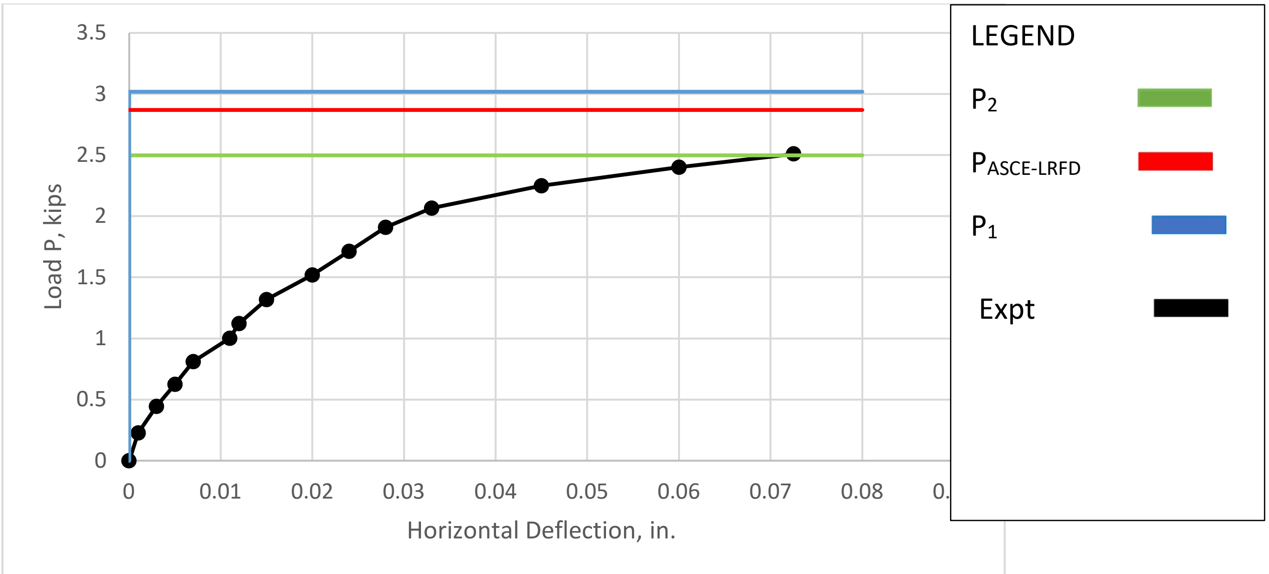

Figure 86. Horizontal Deflections. Investigation 7

Experimental deflections for investigation 7 are shown in Table 55. The experimental critical buckling value was determined to be 2.53 kips from Figures 85 and 86. The Central Difference critical moment value M_{cr} is 29.52 k-in. The lab moment value is 29.88 kip-in; and the ASCE guideline calculated value is 34.12 kip-in. Knowing the relationship of P and solving, P = 2.5 kips.

This value compared favorably with the lab experiment value of 2.53 kips. The ASCE calculated value of 2.89 kips is not conservative. Our experimental value was within 99% of the lab value while the ASCE value was within 85%.

Because there is no load in the x direction and M is zero, the horizontal deflections and the angle of twist within the elastic range will be zero for Central difference calcs. Central Difference vertical deflection values were taken at same locations along the beam as the locations of the vertical deflection dial gages observed during experiments. As shown in Figure 84, they compare favorably. As the length of the beam decreases, the percentage of the vertical deflection due to shear moment increases. Fixed supports increase the value of the moment contribution due to shear moment.

4.8 Investigation 8

This section presents a comparison of analytical and experimental translational and rotational deflections for investigation 8. Translational and rotational deflections from theoretical formulations which include shear deformation and laboratory experiments are shown for investigation 8 in Table 56. Critical load values from theoretical formulations which include shear deformations, ASCE-LRFD Prestandard provisions, and laboratory experiments concerning lateral-torsional buckling are plotted versus translational and rotational deflection for investigation 8 in Figures 87, 88, and 89. Favorable or unfavorable differences are noted.

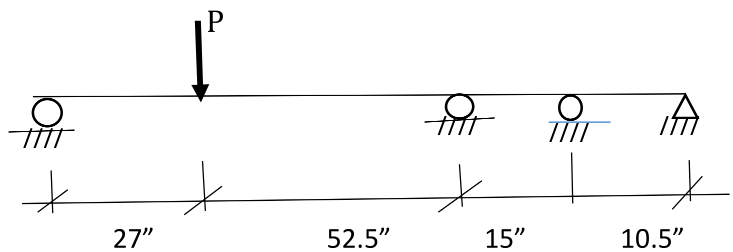

Table 56. Deflections. Investigation 8

VERTICAL	7" from support			19" from support			34" from support		
LOAD P	V1LAB	v1calcw/s	v1calcw/o	V22LAB	v2calcw/s	v2calcw/o	V33LAB	v3calcw/s	v3calcw/o
0	0	0	0	0	0	0	0	0	0
0.22043	0.021	-0.037921	-0.03499646	0.063	-0.1031695	-0.0943754	0.122	-0.13383028	-0.12214
0.44086	0.096	-0.0759916	-0.06999291	0.136	-0.2067462	-0.1887507	0.242	-0.26818903	-0.24428
0.708995	0.175	-0.1222129	-0.11256323	0.216	-0.3324985	-0.3035506	0.364	-0.43131376	-0.39285
0.889945	0.227	-0.1534062	-0.14129166	0.335	-0.4173647	-0.3810229	0.513	-0.54140147	-0.49312
1.06925	0.279	-0.1843166	-0.16975893	0.455	-0.5014612	-0.4577909	0.627	-0.65049074	-0.59247
1.19	0.325	-0.2112573	-0.19456985	0.567	-0.5747577	-0.5246988	0.763	-0.74557015	-0.67906
1.2	0.371	-0.2381984	-0.21938077	0.675	-0.6480552	-0.5916067	0.879	-0.84065077	-0.76566
1.2	0.371	-0.2623039	-0.24158002	0.787	-0.7136378	-0.6514716	1.012	-0.92572369	-0.84313
1.2							1.23		

	3"	19"	50"	5"	19"	34"
LOAD P	H11LAB	H22LAB	H33LAB	L11LAB	L22LAB	L33LAB
0	0	0	0	0	0	0
0.22043	0	0	0	0.0008	0.0052381	0.01
0.44086	0.018	0.002	0.004	0.0033	0.0092381	0.0188571
0.708995	0.029	0.008	0.01	0.0073	0.01428571	0.028
0.889945	0.034	0.014	0.02	0.0099	0.02438095	0.0407619
1.06925	0.037	0.034	0.036	0.0132	0.02447619	0.0528571
1.19	0.041	0.084	0.041	0.0177	0.03266667	0.0639048
1.2	0.042	0.122	0.047	0.0211	0.03904762	0.0702857
1.2	0.042	0.14	0.047	0.0211	0.03904762	0.0747619
1.2						0.09

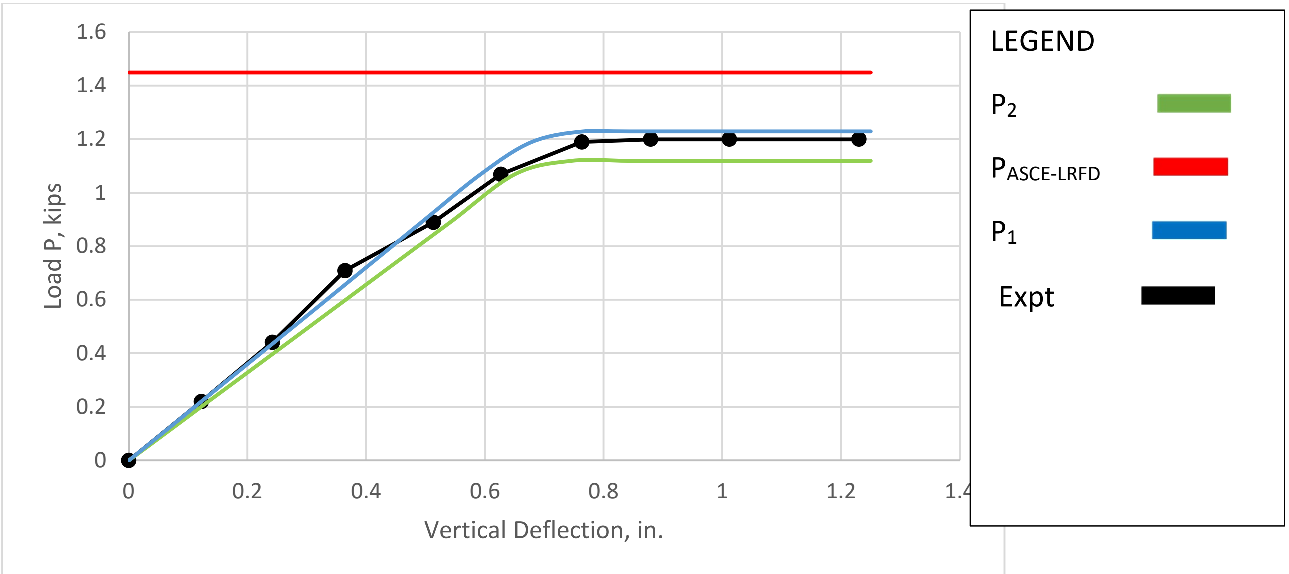

Figure 87. Vertical Deflections. Investigation 8

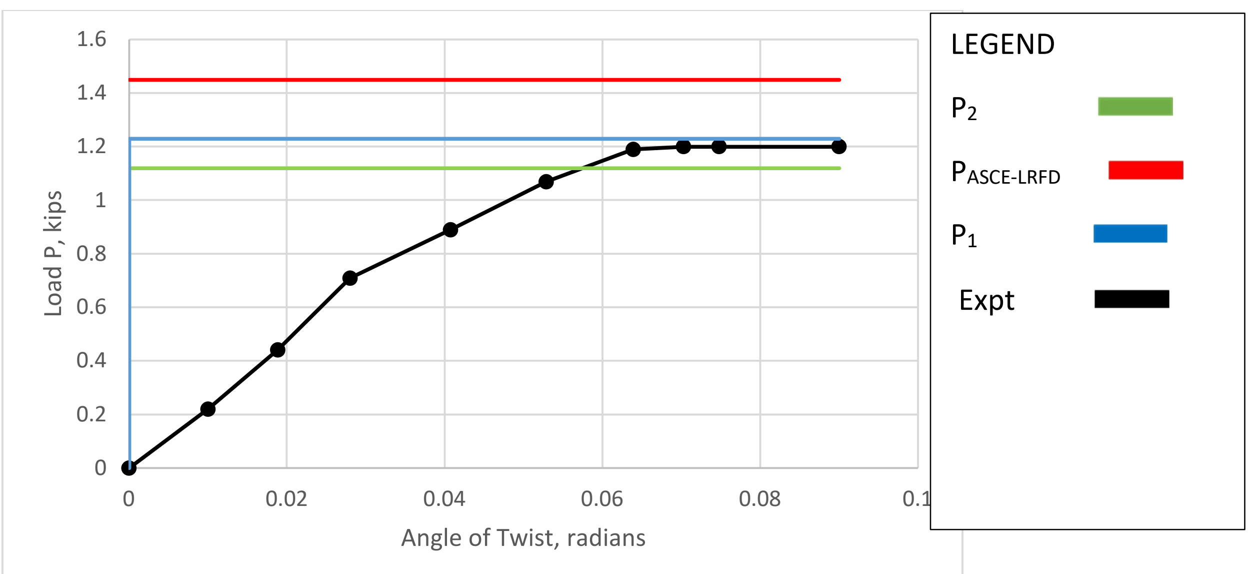

Figure 88. Angle of Twist. Investigation 8

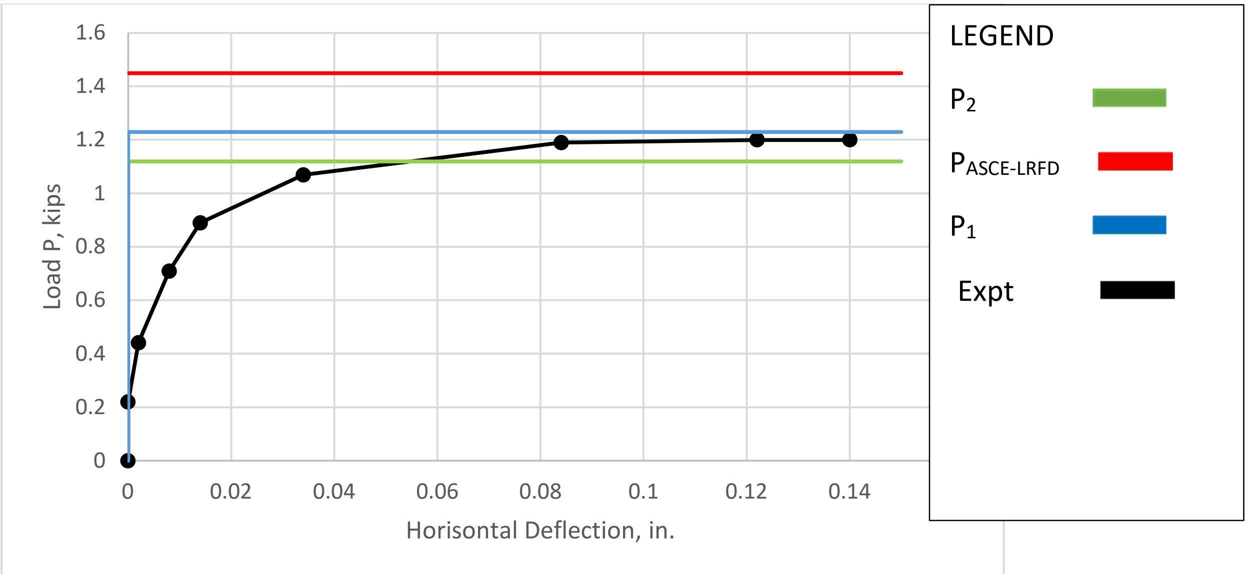

Figure 89. Horizontal Deflections. Investigation 8

Experimental deflections for investigation 8 are shown in Table 56. The experimental critical buckling value was determined to be 1.2 kips from Figures 88 and 89. The Central Difference critical moment value M_{cr} is 17.53 k-in. The lab moment value is 18.78 kip-in; and the ASCE guideline calculated value is 22.9 kip-in. Knowing the relationship of P and solving, P = 1.12 kips.

This value compared favorably with the lab experiment value of 1.2 kips. The ASCE calculated value of 1.47 kips is not conservative. Our experimental value was within 90% of the lab value while the ASCE value was within 78%.

Because there is no load in the x direction and M is zero, the horizontal deflections and the angle of twist within the elastic range will be zero for Central difference calcs. Central Difference vertical deflection values were taken at same locations along the beam as the locations of the vertical deflection dial gages observed during experiments. As shown in Figure 87, they compare favorably. As the length of the beam decreases, the percentage of the vertical deflection due to shear moment increases. Fixed supports increase the value of the moment contribution due to shear moment.

4.9 Investigation 9

This section presents a comparison of analytical and experimental translational and rotational deflections for investigation 9. Translational and rotational deflections from theoretical formulations which include shear deformation and laboratory experiments are shown for investigation 9 in Table 57. Critical load values from theoretical formulations which include shear deformations, ASCE-LRFD Prestandard provisions, and laboratory experiments concerning lateral-torsional buckling are plotted versus translational and rotational deflection for investigation 9 in Figures 90, 91, and 92. Favorable or unfavorable differences are noted.

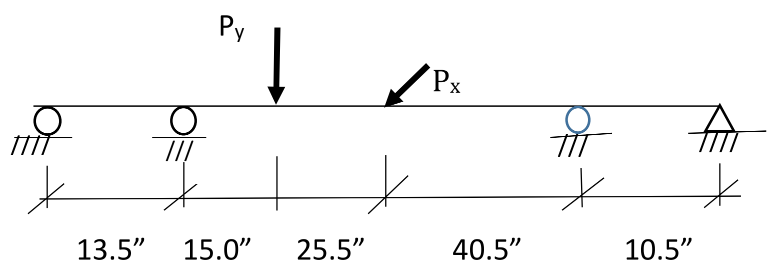

Table 57. Deflections. Investigation 9

	21"			18"			4"		
P load	V1LAB	V1w/s	V1w/o	V22LAB	V2w/s	V2w/o	V33LAB	V3w/s	V3w/o
0	0	0	0	0	0	0	0	0	0
0.512929	-0.02467	-0.03884	-0.02364	-0.01933	-0.03276	-0.024	-0.018	-0.00682	-0.00427
0.808902	-0.04833	-0.06119	-0.03728	-0.04233	-0.05156	-0.03785	-0.026	-0.01073	-0.00673
1.111758	-0.07233	-0.08407	-0.05123	-0.065	-0.0708	-0.05202	-0.03367	-0.01473	-0.00925
1.292096	-0.088	-0.09769	-0.05954	-0.08067	-0.08226	-0.06046	-0.04	-0.01711	-0.01075
1.398095	-0.09733	-0.10569	-0.06443	-0.08933	-0.08899	-0.06542	-0.043	-0.01851	-0.01163
1.549523	-0.10967	-0.11713	-0.0714	-0.10167	-0.09861	-0.0725	-0.04733	-0.0205	-0.01289
1.681679	-0.12133	-0.12711	-0.07749	-0.11233	-0.107	-0.07869	-0.05133	-0.02225	-0.01399
1.817964	-0.13367	-0.13741	-0.08377	-0.12467	-0.11566	-0.08506	-0.05533	-0.02405	-0.01513
1.934977	-0.14567	-0.14625	-0.08917	-0.13733	-0.12309	-0.09054	-0.05967	-0.02559	-0.0161
2.113938	-0.162	-0.15976	-0.09741	-0.153	-0.13446	-0.09891	-0.06533	-0.02796	-0.01759
2.317677	-0.18267	-0.17515	-0.1068	-0.173	-0.14741	-0.10845	-0.07233	-0.03065	-0.01929
2.61				0.21					
2.8				0.25					
3				0.31					
3.05				0.36					
	21"	18"	4"	21"	18"	3"			
	H11LAB	H22LAB	H33LAB	L11LAB	L22LAB	L33LAB			
0	0	0	0	0	0	0			
0.512929	0.007	0.004	0.003	0.118	0.0036	0.009			
0.808902	0.007	0.007	0.004	0.183	0.00728	0.009			
1.111758	0.009	0.008	0.005	0.261	0.012	0.012			
1.292096	0.009	0.008	0.006	0.309	0.016	0.014			
1.398095	0.009	0.008	0.007	0.338	0.01824	0.017			
1.549523	0.009	0.008	0.008	0.38	0.02152	0.021			
1.681679	0.009	0.009	0.008	0.417	0.02456	0.023			
1.817964	0.009	0.01	0.008	0.454	0.02744	0.026			
1.934977	0.012	0.011	0.008	0.493	0.0304	0.04			
2.113938	0.013	0.012	0.008	0.533	0.03392	0.043			
2.317677	0.013	0.015	0.008	0.595	0.03896	0.047			
2.61		0.021			0.048				
2.8		0.027			0.05496				
3		0.035			0.068				
3.05		0.043			0.0776				

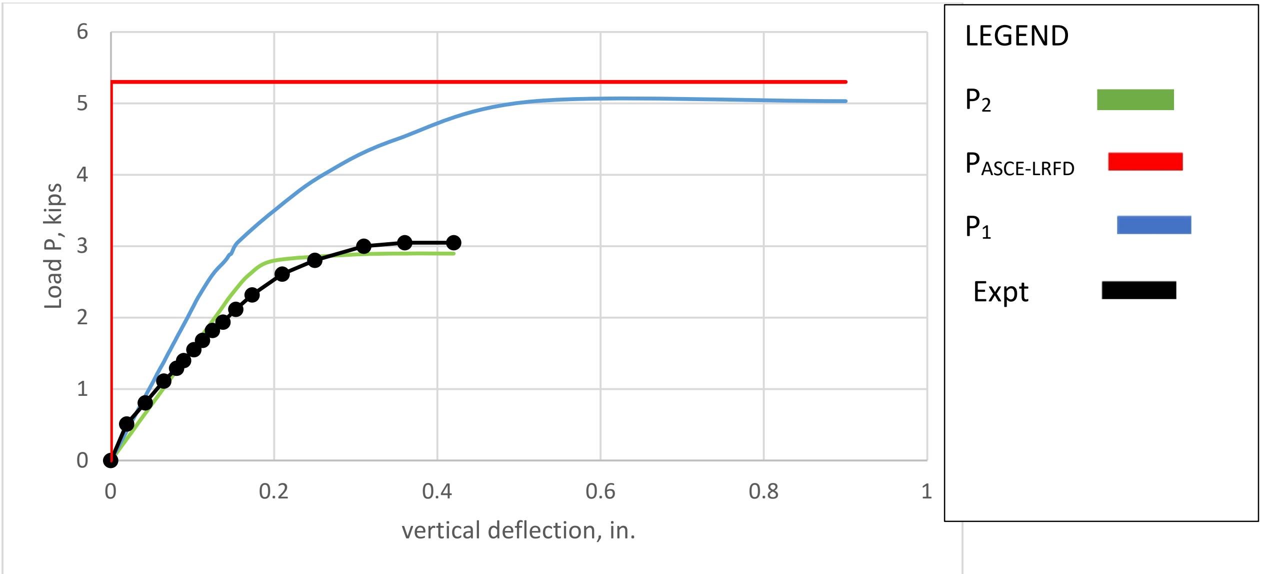

Figure 90. Vertical Deflections. Investigation 9

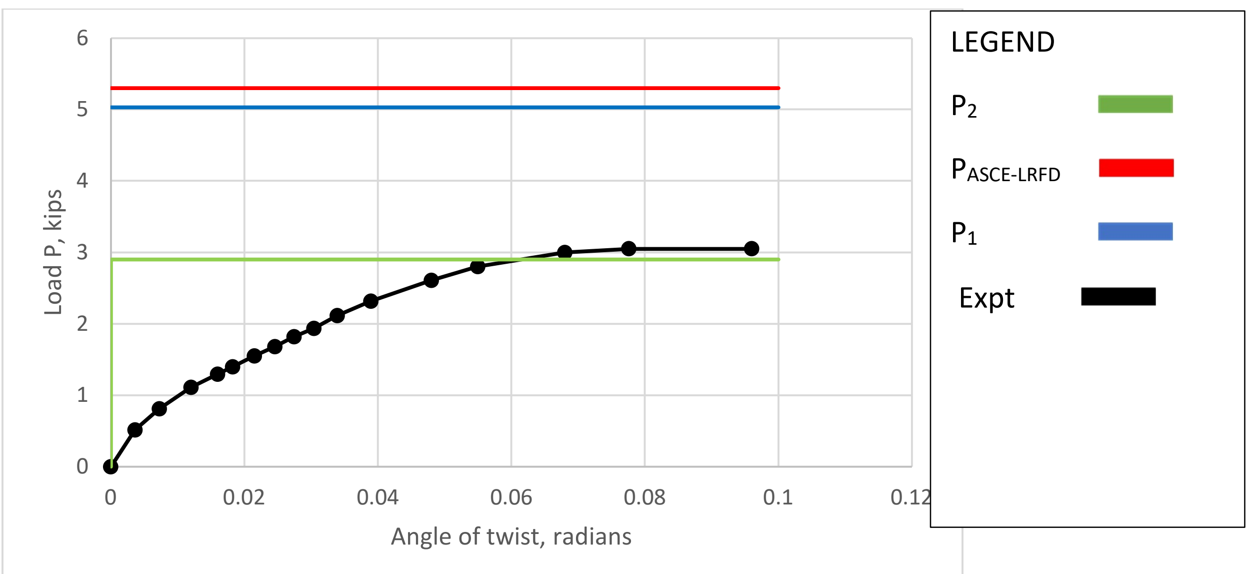

Figure 91. Angle of Twist. Investigation 9

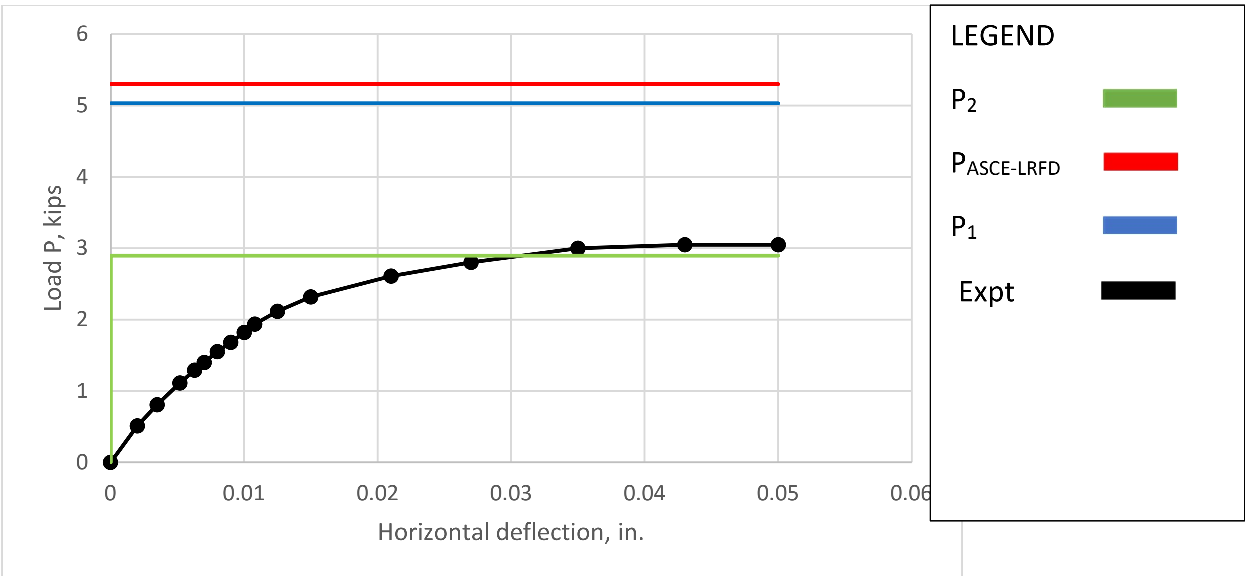

Figure 92. Horizontal Deflections. Investigation 9

Experimental deflections for investigation 9 are shown in Table 57. The experimental critical buckling value was determined to be 3.03 kips from evaluating Figures 91 and 92. The Central Difference critical moment value M_{cr} is 60.46 k-in. The lab moment value is 63.17 kip-in; and the ASCE guideline calculated value is 74.1 kip-in. Knowing the relationship of P and solving, P = 2.9 kips.

This value compared favorably with the lab experiment value of 3.03 kips. The ASCE calculated value of 3.64 kips is not conservative. Our experimental value was within 95% of the lab value while the ASCE value was within 80%.

The load in the x direction was approximately 6% of the load in the y direction. It changed the critical load P_2 by approximately only 3% and, as such, it does not explain the large difference in critical load we encountered while comparing the ASCE-LRFD Design buckling value to our Central Difference value including shear.

When the load P which is perpendicular to the weak axis is zero, the critical point load P_{cr} in the y-direction and perpendicular to the strong axis is 3.0 kips. When the load P_x which is perpendicular to the weak axis is 1 kip, the critical point load P_{cr} in the y-direction and perpendicular to the strong axis is 0.0 kips (See Figure 93). This graph is based upon the Central

Difference Biaxial solution for P_2. Moreover, it confirms the fact that the critical buckling value for lateral torsional buckling is proportionate to moment of inertia, I_x and I_y. The ratio of I_x to I_y is 2.97 for our 4" x 4" x ¼" beam section.

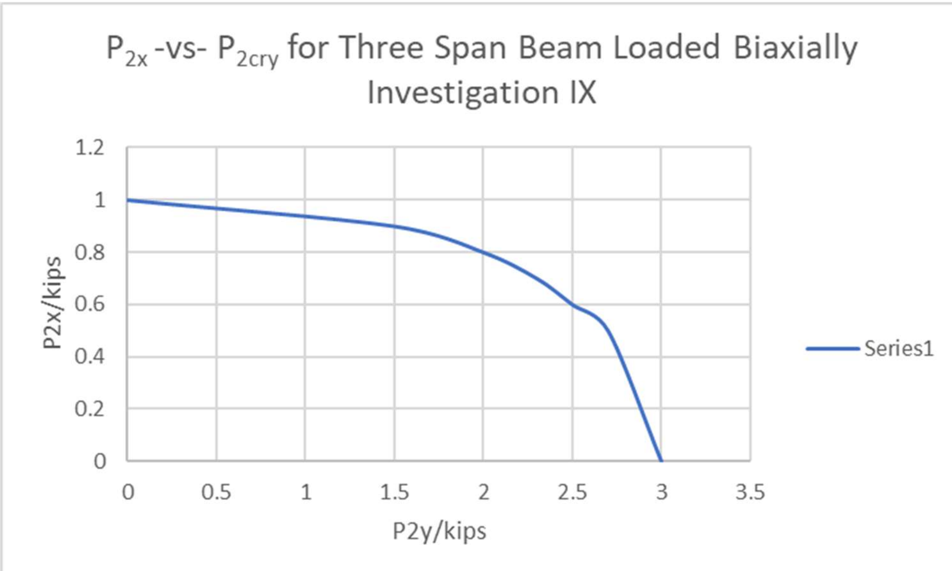

Figure 93. P_{2x} vs P_{2cry}

Central Difference vertical deflection values were taken at same locations along the beam as the locations of the vertical deflection dial gages observed during experiments. As shown in Figure 90, they compare favorably. As the length of the beam decreases, the percentage of the vertical deflection due to shear moment increases. Fixed supports increase the value of the moment contribution due to shear moment.

Using the 3 equilibrium equations typically used for out of plane rotations, we can solve the determinant to obtain buckling values. Galambos solves this problem with end moments and no loading in the weak axis direction. Thus, we are solving for point loads, end moments, and the biaxial solution.

Following procedure is outlined in Galambos and small deflection theory. The first two equations reduce to

$u'' = - M_x \phi / EI_y$ [69]

and

$v'' = - M_y \phi / EI_x$ [70]

After plugging the first two equations into the third equation, it becomes:

$EI_w \phi^{IV} - (GK_t) \phi'' + (M^2_{tx}/EI_y) \phi + (M^2_{ty}/EI_x) \phi = 0$ [71]

For doubly symmetric sections such as I beams, β_x reduces to 0, so it was deleted. For constant end moments, $M'_t = 0.0$

Now, the ordinary differential equation is of the form

$\Phi^{IV} - \lambda_1 \Phi'' - \lambda_2 \Phi = 0.0$ [72]

For pinned-pinned and loading of the beam biaxially, it can be shown that the solution of this equation yields the same 4th order solution form established by Galambos and being used by the ASCE today.

$\lambda_2 = (M^2_{tx}/EI_wEI_y) + (M^2_{ty}/EI_wEI_x)$ for biaxial loading and not (M^2_{tx}/EI_wEI_y) .

4.10 COMPARATIVE SUMMARY AND PROPOSAL

As shown in Table 58, Central Difference critical load values fall within an average of more than 95% of laboratory experiment values. ASCE-LRFD critical load values fall within an average of only 86% of laboratory experiment values. As such, propose a new ASCE design approach which considers shear deflection.

Table 58. Comparative Summary of Labs with Analysis

1. Single Span with Point Load Ctr	M_{cr} (k-in.)	P_1 (kips)	P_2 (kips)	CD/Lab	ASCE/Lab
(4 in. x 4 in. x 1/4 in.)				.97	1.12
a. Lab	38.31	2.04	1.88		
b. Central Diff	37.29	1.99	1.83		
c. ASCE	43.02	2.29	2.11		
2. Single Span w/ Pt Load Off Ctr					
(3 iin. X 3 in. x ¼ in.)				.93	1.10
a. Lab	16.97	.95	.91		
b. Central Diff	15.69	.88	.84		
c. ASCE	18.58	1.05	1.00		
3. Two Span w/ Pt Load Ctr					
(4 in. x 4 in. x 1/4 in.)				1.04	1.22
a. Lab	43.28	3.1	2.6		
b. Central Diff	43.97	3.2	2.7		
c. ASCE	51.53	3.75	3.16		
4. Two Span w/ Pt Ld Near Equal					
(3 iin. X 3 in. x ¼ in.)				.97	1.11
a. Lab	29.59	2.71	2.37		
b. Central Diff	28.67	2.63	2.3		
c. ASCE	32.89	3.02	2.64		

Table 58 (Continued)

5. Two Span w/ Pt Load Off Ctr	M_{cr} (k-in.)	P_1 (kips)	P_2 (kips)	CD/Lab	ASCE/Lab
(3 iin. X 3 in. x ¼ in.)				.90	1.19
a. Lab	19.34	1.31	1.2		
b. Central Diff	17.40	1.18	1.08		
c. ASCE	22.92	1.55	1.42		
6. Three Span w/ Pt Ld Ctr. Mid					
(4 in. x 4 in. x 1/4 in.)				1.0	.95
a. Lab	63.46	6.05	3.5		
b. Central Diff	63.46	6.05	3.5		
c. ASCE	60.46	5.77	3.33		
7. Three Span w/ Pt Load Ctr. Out					
(3 iin. X 3 in. x ¼ in.)				.99	1.14
a. Lab	29.88	3.01	2.53		
b. Central Diff	29.52	2.98	2.5		
c. ASCE	34.12	3.44	2.89		
8. Three Span w/ Pt Ld Off Ctr					
(3 iin. X 3 in. x ¼ in.)				.93	1.22
a. Lab	18.78	1.31	1.2		
b. Central Diff	17.53	1.22	1.12		
c. ASCE	22.90	1.60	1.47		
9. Three Span w/ Pt Lds. Biaxial					
(4 in. x 4 in. x 1/4 in.)				.96	1.13
a. Lab	29.59	2.71	2.37		
b. Central Diff	28.67	2.63	2.3		
c. ASCE	32.89	3.02	2.64		

Proposed Solutions

Proposed values represent Critical moments for lateral torsional buckling when considering shear deflection. These values are based upon an equation developed based upon observation of second order and fourth order classical and semi-analytical solutions. The proposed equation being used is:

$M_x^2 – (M_x (*M'_{x1} + *M'_{x2})/L)/ (\pi/L)^2 = C_w B_y (\pi/L)^4 + C_t B_y (\pi /L)^2$ [73]

M_x is the bending moment contribution, when shear moment is being considered; ;
$*M'_{x1} = s(M_x - M_{x1}) /L_1$ and $*M'_{x1} = t(M_x - M_{x2}) /L_2$; and s and t are defined by end conditions and the location of the point load. Once we determine M_x and determine the relationship of the moment with shear and without shear, we can find M_{tx} , the total moment.

Rearranging and solving for M_x, we get:

$M_x = ((C_w B_y (\pi/L)^4 + C_t B_y (\pi /L)^2) / (1-f))^{.5}$

and $M_{xs} = M_x/SF$

where $SF = P_2/P_1$

and $f = ((s/L_1)(1- M_{x1}) + (t/L_2)(1- M_{x2})(L/\pi^2)$

Note: M_{x1} and M_{x2} are a function of M_x.

Steps for Defining Factors s and t

Define a and b from end conditions. For a simple beam, ends are labeled as shown. If ends a and b are pinned-pinned than a and b are equal to .5. If ends a and b are fixed-fixed, then a and b are equal to .5 also. However, if ends a and b are pinned-fixed, then a and b are .7 and .3, respectively.

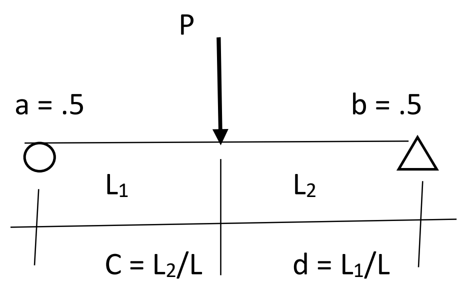

Define c and d from location of point on the beam.

$c = L_2/L$

$d = L_1/L$

Calculate p and q.

p = ac

q = bd

Now, calculate s and t.

s = p/(p + q)

t = q/ (q + p)

Proposed Biaxial Stress Approach

Our proposed biaxial equation is not of similar form. While we have considered buckling, we have not considered biaxial stresses. They must also be evaluated. The longitudinal stress relationship for biaxial loading is:

$\sigma = M_x c_y/I_x - M_y c_x/I_y$ [74]

Including the warping stress term,

$\sigma = M_x c_y/I_x - M_y c_x/I_y + EI_w \phi''$ [75]

For longitudinal stress of a fiberglass reinforced pultruded member, the limit is 30 ksi.

Thus, setting the limit, our modified equation for stress becomes:

$\sigma = M_x c_y/I_x - M_y c_x/I_y + EI_w \phi'' = 30$ ksi.

Our solution of this equation includes applying the Timoshenko shear moment as previously demonstrated in our central difference approach.

Applying equation [73] for Investigations 1 through 8 and biaxial equation [75] for Investigation 9, we get the Proposed critical moments shown in Table 59. They include shear deflection. All values are within 10% of central difference calculated values of critical loads.

Table 59. Modified Comparative Summary of Investigation

1. Single Span with Point Load Ctr	M_{cr} (k-in.)	P_2/P_1	100(CD-Proposed)/CD(%)
(4 in. x 4 in. x 1/4 in.)		.92	
a. Lab	38.31		
b. Central Diff	37.29		
c. Proposed	39.76		6.6
2. Single Span w/ Pt Load Off Ctr			
(3 iin. X 3 in. x ¼ in.)		.956	
a. Lab	16.97		
b. Central Diff	15.69		
c. Proposed	15.62		.3
3. Two Span w/ Pt Load Ctr			
(4 in. x 4 in. x 1/4 in.)		.843	
a. Lab	43.28		
b. Central Diff	43.97		
c. Proposed	43.39		1.3
4. Two Span w/ Pt Ld Near Equal			
(3 iin. X 3 in. x ¼ in.)		.873	
a. Lab	29.59		
b. Central Diff	28.67		
c. Proposed	28.2		1.8

Table 59 (Continued)

5. Two Span w/ Pt Load Off Ctr	M_{cr} (k-in.)	P_2/P_1	100(CD-Proposed)/CD(%)
(3 iin. X 3 in. x ¼ in.)		.916	
a. Lab	19.34		
b. Central Diff	17.40		
c. Proposed	16.38		5.9
6. Three Span w/ Pt Ld Ctr. Mid			
(4 in. x 4 in. x 1/4 in.)		.578	
a. Lab	63.46		
b. Central Diff	63.46		
c. Proposed	57.86		8.8
7. Three Span w/ Pt Load Ctr. Out			
(3 iin. X 3 in. x ¼ in.)		.84	
a. Lab	29.88		
b. Central Diff	29.52		
c. Proposed	29.1		1.4
8. Three Span w/ Pt Ld Off Ctr			
(3 iin. X 3 in. x ¼ in.)		.9	
a. Lab	18.78		
b. Central Diff	17.53		
c. Proposed	16.76		4.2
9. Three Span w/ Pt Lds. Biaxial			
(4 in. x 4 in. x 1/4 in.)			
a. Lab	29.59	.4	
b. Central Diff	28.67		
c. Proposed	54.21		10.0

Problem 4.1 For the 4" x 4" x ¼" fiberglass I beam with moments shown in Figure 94, determine its lateral-torsional buckling moment. Include shear deflection moment. Beam was used in Investigation 1. E = 2997 ksi; I_x = 7.935 in.^{4}; I_y = 2.67 in. ^{4}; k_t = .06; G = 453 ksi; A = 2.85 in. ^{2}; α = 3.23; and I_w = 9.375 in. ^{6} .

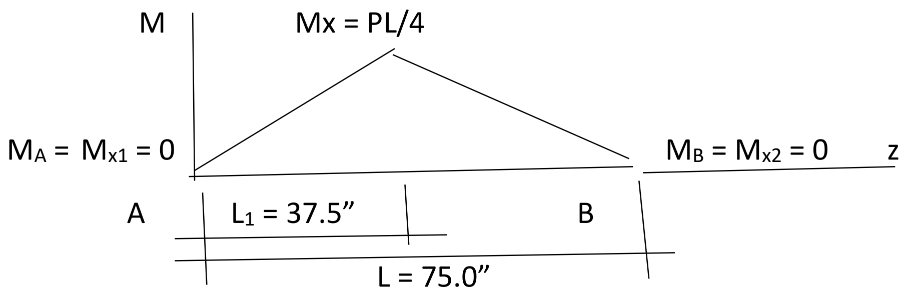

Figure 94. Moments on Targeted Beam. Investigation 1

1. Proposed equation for lateral-torsional buckling including shear is

$M_x = ((C_w B_y (\pi/L)^4 + C_t B_y (\pi /L)^2) / (1-f))^{.5}$

And $M_{xs} = M_x /SF$

Where SF = P_2/P_1

And f = (($s/L_1)(1- M_{x1}) + (t/L_2)(1- M_{x2})(L/\pi^2)$.

Note: M_{x1} and M_{x2} are relative to M_x.

M_x = PL/4 and M_{x1} and M_{x2} = 0.

2. Define Factors s and t

a. Define a and b from end conditions. Ends A and B are pinned-pinned, so a and b are equal to .5.

b. Define c and d from location of point on the beam.

c= L_2/L = .5

d= L_1/L = .5

c. Calculate p and q.

$p = ac = .5 * .5 = .25$

$q = bd = .5 * .5 = .25$

d. Now, calculate s and t.

$s = p/(p + q) = .5$

$t = q/ (q + p) = .5$

3. Plug in all the knowns

a. $C_w B_y (\pi/L)^4 + C_t B_y (\pi /L)^2 = 1070.34$

b. Plug in M_{x1} and M_{x2} relative to M_x. Solve 1- f.

4. Solve for Mx.

$Mx^2 = 1070.34/.80 = 1337.92$

or Mx = 36.58 k-in.

M_x represents the bending contribution to the total moment.

$M_{tx} = M_{x\ bending} + M_{x\ shear}$

5. Find the shear factor, SF.

a. Place moment diagram on conjugate beam without and with shear moment. Set resultants equal to each other.

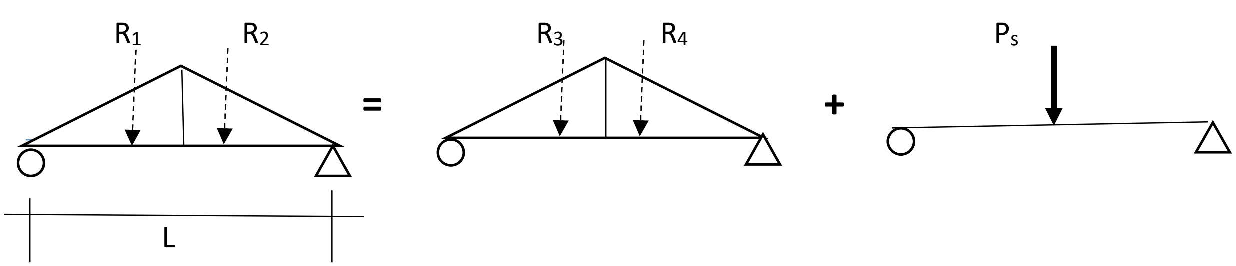

Figure 95. Moments on Targeted Conjugate Beam

b. Write Resultant equation

$R_1 + R_2 = R_3 + R_4 + P_s$

$(1/2)(L/2)\, P_1L/4 + (1/2)(L/2)\, P_1L/4 = 1/2)\, (L/2)P_2L/4 + 1/2)\, (L/2)P_2L/4 + \alpha P_2EI_x/AG$

Rearrange,

$P_2/P_1 = (L2/8) /[\, (L2/8) + \alpha EIx/AG\,]$

Solving SF = .92. Therefore,

$M_{tx} = M_x/.92 = 39.76$ k-in.

This value is within 6.6% of the value obtained using Central Difference.

where

$R_1 = R_2 = (1/2)(L/2)\, P_1L/4$; $R_3 = R_4 = (1/2)\, (L/2)P_2L/4$; and $P_s = \alpha P_2EI_x/AG$.

Problem 4.2 For the 3" x 3" x ¼" fiberglass I beam with moments shown in Figure 96, determine its lateral-torsional buckling moment. Include shear deflection moment. Beam was used in Investigation 2. E = 2997 ksi; I_x = 3.17 in.^{4}; I_y = 1.13 in. ^{4}; k_t = .046; G = 453 ksi; A = 2.13 in. ^{2}; α = 3.26; and I_w = 2.13 in. ^{6} .

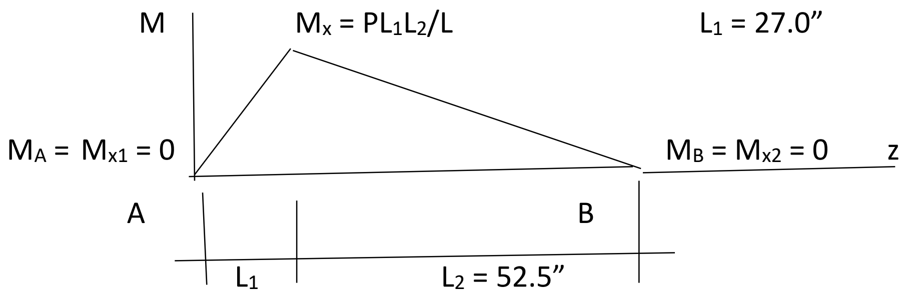

Figure 96. Moments on Targeted Beam. Investigation 2

1. Proposed equation for lateral-torsional buckling including shear is

$M_x = ((C_w B_y (\pi/L)^4 + C_t B_y (\pi /L)^2) / (1-f))^{.5}$

And $M_{xs} = M_x /SF$

where $SF = P_2/P_1$

And $f = ((s/L_1)(1- M_{x1}) + (t/L_2)(1- M_{x2})(L/\pi^2)$.

Note: M_{x1} and M_{x2} are relative to M_x.

$M_x = PL_1L_2/L$ and M_{x1} and M_{x2} = 0.

2. Define Factors s and t

a. Define a and b from end conditions. Ends A and B are pinned-pinned, so a and b are equal to .5.

b. Define c and d from location of point on the beam.

$c= L_2/L = .66$

$d= L_1/L = .34$

c. Calculate p and q.

p = ac = .5* .66 = .33

q = bd= .5* .34 = .17

d. Now, calculate s and t.

s = p/(p + q) = .66

t = q/ (q + p) = .34

3. Plug in all the knowns

a. $C_w B_y (\pi/L)^4 + C_t B_y (\pi/L)^2 = 167.5$

b. Plug in M_{x1} and M_{x2} relative to M_x. Solve 1- f.

4. Solve for Mx.

$M_x^2 = 167.5/.7516$

And $M_x = 14.93$ k-in.

M_x represents the bending contribution to the total moment.

$M_{tx} = M_{x\ bending} + M_{x\ shear}$

5. Find the shear factor, SF.

a. Place moment diagram on conjugate beam without and with shear moment. Set resultants equal to each other.

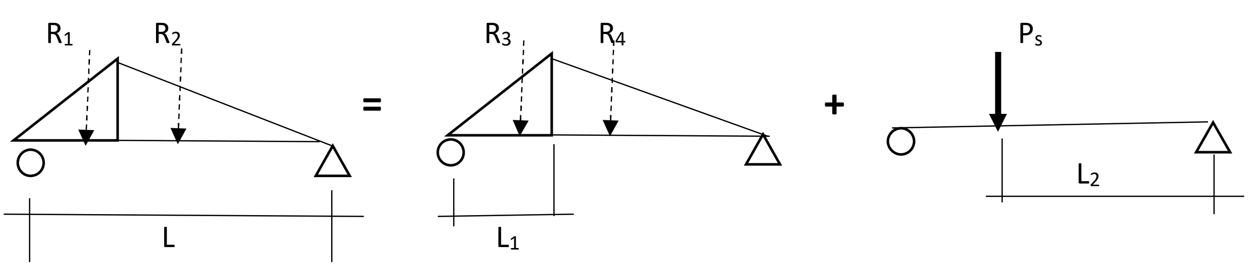

Figure 97. Moments on Targeted Conjugate Beam

b. Write Resultant equation

$R_1 + R_2 = R_3 + R_4 + P_s$

$(1/2)(L_1)\, P_1L_1L_2/L + (1/2)(L_2)\, P_1L_1L_2/L = (1/2)\,(L_1)P_2L_1L_2/L + (1/2)\,(L_2)P_2L_1L_2/L + \alpha P_2EI_x/AG$

Rearrange,

$P_2/P_1 = [(.5)(L_1)L_1L_2/L + (.5)(L_2)\, L_1L_2/L\,] \,/\, [\,(.5)\,(L_1)L_1L_2/L + (.5)(L_2)L_1L_2/L + \alpha EI_x/AG\,]$

Solving SF = .956. Therefore,

$M_{tx} = M_x/.956 = 15.62$ k-in.

This value is within .3% of the value obtained using Central Difference.

Problem 4.3 For the 4" x 4" x ¼" fiberglass I beam with moments shown in Figure 98, determine its lateral-torsional buckling moment. Include shear deflection moment. Beam was used in Investigation 3. E = 2997 ksi; I_x = 7.935 in.^{4}; I_y = 2.67 in. ^{4}; k_t = .06; G = 453 ksi; A = 2.85 in. ^{2}; α = 3.23; and I_w = 9.375 in. ^{6} .

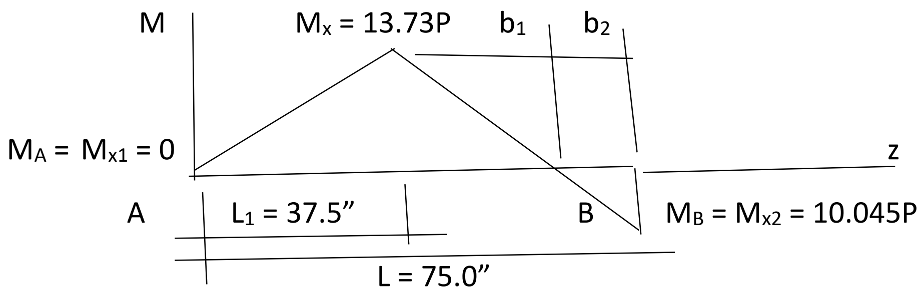

Figure 98. Moments on Targeted Beam. Investigation 3

1. Proposed equation for lateral-torsional buckling including shear is

$M_x = ((C_w B_y (\pi/L)^4 + C_t B_y (\pi/L)^2) / (1-f))^{.5}$

And $M_{xs} = M_x / SF$

where $SF = P_2/P_1$

and $f = ((s/L_1)(1- M_{x1}) + (t/L_2)(1- M_{x2})(L/\pi^2)$.

Note: M_{x1} and M_{x2} are relative to M_x.

M_x = 13.73P and M_{x1} = 0 and M_{x2} = 10.045P.

2. Define Factors s and t

a. Define a and b from end conditions. Ends A and B are pinned-fixed, so a and b are .7 and .3, respectively.

b. Define c and d from location of point on the beam.

$c = L_2/L = .5$

$d = L_1/L = .5$

c. Calculate p and q.

p = ac = .7* .5 = .35

q = bd= .3* .5 = .15

d. Now, calculate s and t.

s = p/(p + q) = .7

t = q/ (q + p) = .3

3. Plug in all the knowns

a. $C_w B_y (\pi/L)^4 + C_t B_y (\pi/L)^2 = 1070.34$

b. Plug in M_{x1} and M_{x2} relative to M_x. Solve 1- f.

4. Solve for Mx.

$Mx^2 = 1070.34/.80 = 1337.92$

or Mx = 36.58 k-in.

M_x represents the bending contribution to the total moment.

$M_{tx} = M_{x\ bending} + M_{x\ shear}$

5. Find the shear factor, SF.

a. Place moment diagram on conjugate beam without and with shear moment. Set resultants equal to each other.

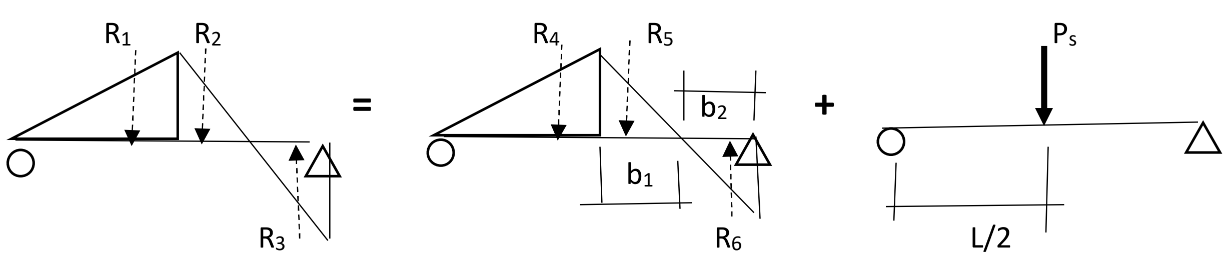

Figure 99. Moment Diagrams on Targeted Conjugate Beam

b. Write Resultant equation

$R_1 + R_2 + R_3 = R_4 + R_5 + R_6 + P_s$

$(.5)13.73P_1L_1 + (.5)13.73P_1b_1 - (.5)10.045P_1b_2 = (.5)13.73P_2L_1 + (.5)13.73P_2b_1 - (.5)10.045P_2b_2 + \alpha P_2EI_x/AG$

Rearrange,

$P_2/P_1 =$

$[(.5)13.73L_1 + (.5)13.73b_1 - (.5)10.045b_2] / [(.5)13.73L_1 + (.5)13.73b_1 - (.5)10.045b_2 + \alpha EI_x/AG]$

Solving SF = .843. Therefore,

$M_{tx} = M_x /.843 = 43.39$ k-in.

This value is within 1.3% of the value obtained using Central Difference.

Problem 4.4 For the 3" x 3" x ¼" fiberglass I beam with moments shown in Figure 100, determine its lateral-torsional buckling moment. Include shear deflection moment. Beam was used in Investigation 4. E = 2997 ksi; I_x = 3.17 in.^{4}; I_y = 1.13 in. ^{4}; k_t = .046; G = 453 ksi; A = 2.13 in. ^{2}; α = 3.26; and I_w = 2.13 in. ^{6} .

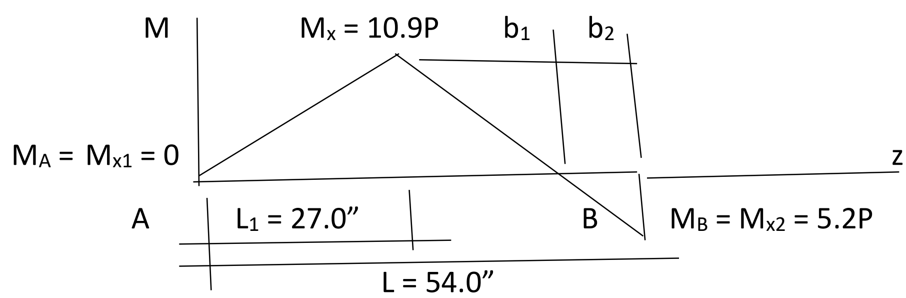

Figure 100. Moments on Targeted Beam. Investigation 4

1. Proposed equation for lateral-torsional buckling including shear is

$M_x = ((C_w B_y (\pi/L)^4 + C_t B_y (\pi /L)^2) / (1-f))^{.5}$

and $M_{xs} = M_x /SF$

where $SF = P_2/P_1$

and $f = ((s/L_1)(1- M_{x1}) + (t/L_2)(1- M_{x2})(L/\pi^2)$.

Note: M_{x1} and M_{x2} are relative to M_x.

M_x = 10.9P and M_{x1} = 0 and M_{x2} = 5.2P.

2. Define Factors s and t

a. Define a and b from end conditions. Ends A and B are pinned-fixed, so a and b are .7 and .3, respectively.

b. Define c and d from location of point on the beam.

$c = L_2/L = .5$

$d = L_1/L = .5$

c. Calculate p and q.

p = ac = .7* .5 = .35

q = bd= .3* .5 = .15

d. Now, calculate s and t.

s = p/(p + q) = .7

t = q/ (q + p) = .3

3. Plug in all the knowns

a. $C_w B_y (\pi/L)^4 + C_t B_y (\pi/L)^2 = 502.22$

b. Plug in M_{x1} and M_{x2} relative to M_x. Solve 1- f.

4. Solve for Mx.

$M_x^2 = 502.22/.8265$

And $M_x = 24.65$ k-in.

M_x represents the bending contribution to the total moment.

$M_{tx} = M_{x\ bending} + M_{x\ shear}$

5. Find the shear factor, SF.

a. Place moment diagram on conjugate beam without and with shear moment. Set resultants equal to each other.

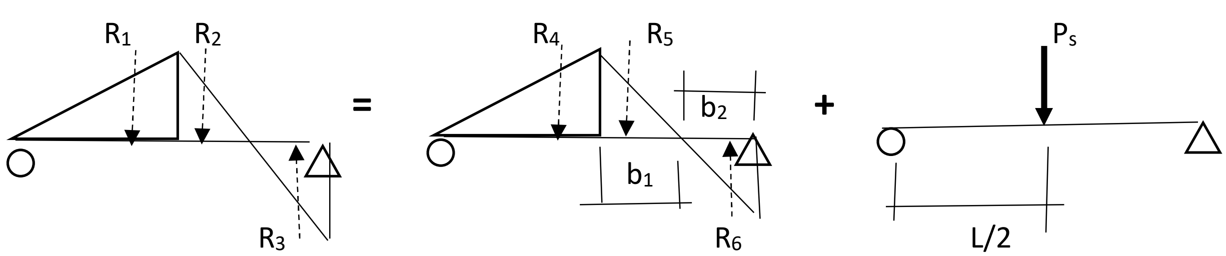

Figure 101. Moment Diagrams on Targeted Conjugate Beam

b. Write Resultant equation

$R_1 + R_2 + R_3 = R_4 + R_5 + R_6 + P_s$

$(.5)10.9P_1L_1 + (.5)10.9P_1b_1 - (.5)5.2P_1b_2 = (.5)10.9P_2L_1 + (.5)10.9P_2b_1 - (.5)5.2P_2b_2 + \alpha P_2EI_x/AG$

Rearrange,

$P_2/P_1 =$

$[(.5)10.9L_1 + (.5)10.9b_1 - (.5)5.2b_2] / [(.5)10.9L_1 + (.5)10.9b_1 - (.5)5.2b_2 + \alpha EI_x/AG]$

Solving SF = .873. Therefore,

$M_{tx} = M_x/.873 = 28.2$ k-in.

This value is within 1.6% of the value obtained using Central Difference.

Problem 4.5 For the 3" x 3" x ¼" fiberglass I beam with moments shown in Figure 102, determine its lateral-torsional buckling moment. Include shear deflection moment. Beam was used in Investigation 5. E = 2997 ksi; I_x = 3.17 in.^{4}; I_y = 1.13 in. ^{4}; k_t = .046; G = 453 ksi; A = 2.13 in. ^{2}; α = 3.26; and I_w = 2.13 in. ^{6} .

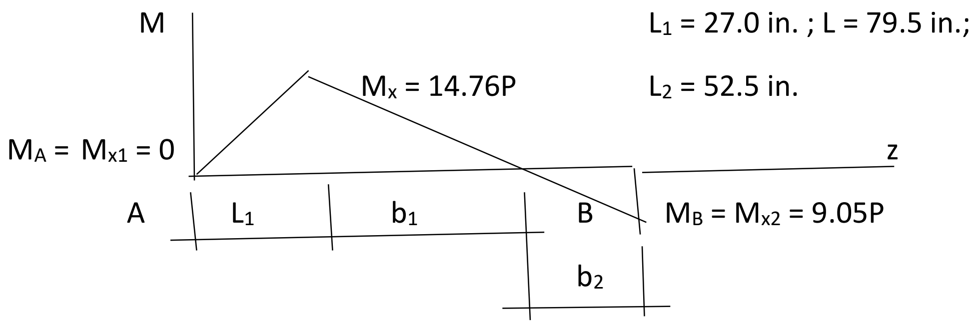

Figure 102. Moments on Targeted Beam. Investigation 5

1. Prposed equation for lateral-torsional buckling including shear is

$M_x = ((C_w B_y (\pi/L)^4 + C_t B_y (\pi /L)^2) / (1-f))^{.5}$

and $M_{xs} = M_x /SF$

where $SF = P_2/P_1$

and $f = ((s/L_1)(1- M_{x1}) + (t/L_2)(1- M_{x2})(L/\pi^2)$.

Note: M_{x1} and M_{x2} are relative to M_x.

M_x = 14.76P and M_{x1} = 0 and M_{x2} = 9.05P.

2. Define Factors s and t

a. Define a and b from end conditions. Ends A and B are pinned-fixed, so a and b are .7 and .3, respectively.

b. Define c and d from location of point on the beam.

c= L_2/L = .66

d= L_1/L = .34

c. Calculate p and q.

p = ac = .7* .66 = .462

q = bd= .3* .34 = .102

d. Now, calculate s and t.

s = p/(p + q) = .82

t = q/ (q + p) = .18

3. Plug in all the knowns

a. $C_w B_y (\pi/L)^4 + C_t B_y (\pi/L)^2 = 167.5$

b. Plug in M_{x1} and M_{x2} relative to M_x. Solve 1- f.

4. Solve for Mx.

$M_x^2 = 167.5/.7444$

And $M_x = 15.0$ k-in.

M_x represents the bending contribution to the total moment.

$M_{tx} = M_{x\ bending} + M_{x\ shear}$

5. Find the shear factor, SF.

a. Place moment diagram on conjugate beam without and with shear moment. Set resultants equal to each other.

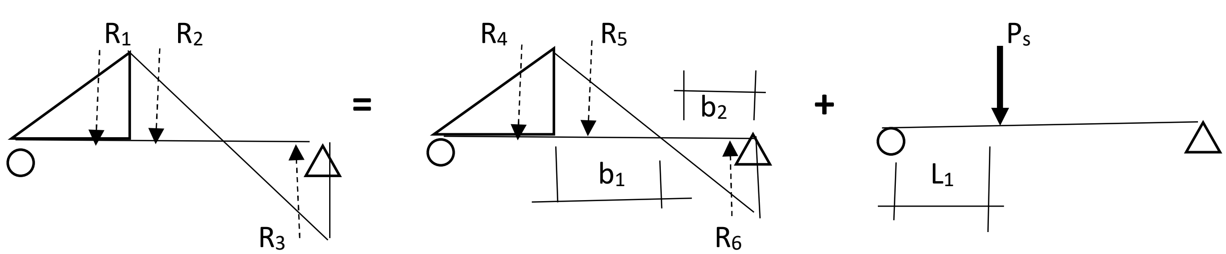

Figure 103. Moment Diagrams on Targeted Conjugate Beam

b. Write Resultant equation

$R_1 + R_2 + R_3 = R_4 + R_5 + R_6 + P_s$

$(.5)14.76P_1L_1 + (.5)14.76P_1b_1 - (.5)9.05P_1b_2 = (.5)14.76P_2L_1 + (.5)14.76P_2b_1 - (.5)9.05P_2b_2 + \alpha P_2EI_x/AG$

Rearrange,

$P_2/P_1 =$

$[(.5)14.76L_1 + (.5)14.76b_1 - (.5)9.05b_2] / [(.5)14.76L_1 + (.5)14.76b_1 - (.5)9.05b_2 + \alpha EI_x/AG]$

Solving SF = .916. Therefore,

$M_{tx} = M_x /.916 = 16.38$ k-in.

This value is within 6% of the value obtained using Central Difference.

Problem 4.6 For the 4" x 4" x ¼" fiberglass I beam with moments shown in Figure 104, determine its lateral-torsional buckling moment. Include shear deflection moment. Beam was used in Investigation 6. E = 2997 ksi; I_x = 7.935 in.^{4}; I_y = 2.67 in. ^{4}; k_t = .06; G = 453 ksi; A = 2.85 in. ^{2}; α = 3.23; and I_w = 9.375 in. ^{6} .

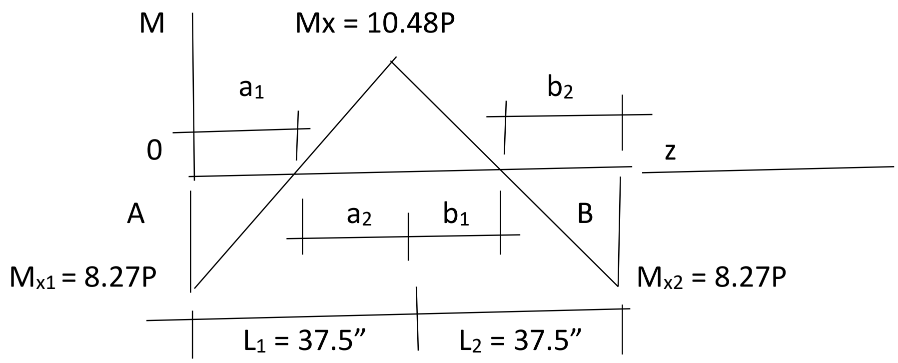

Figure 104. Moments on Targeted Beam. Investigation 6

1. Proposed equation for lateral-torsional buckling including shear is

$M_x = ((C_w B_y (\pi/L)^4 + C_t B_y (\pi /L)^2) / (1-f))^{.5}$

and $M_{xs} = M_x /SF$

where SF = P_2/P_1

and f = $((s/L_1)(1- M_{x1}) + (t/L_2)(1- M_{x2})(L/\pi^2)$.

Note: M_{x1} and M_{x2} are relative to M_x.

M_x = 10.48P and M_{x1} and M_{x2} = 8.27P.

2. Define Factors s and t

a. Define a and b from end conditions. Ends A and B are fixed-fixed, so a and b are equal to .5.

b. Define c and d from location of point on the beam.

c= L_2/L = .5

d= L_1/L = .5

c. Calculate p and q.

p = ac = .5* .5 = .25

q = bd= .5* .5 = .25

d. Now, calculate s and t.

s = p/(p + q) = .5

t = q/ (q + p) = .5

3. Plug in all the knowns

a. $C_w B_y (\pi/L)^4 + C_t B_y (\pi/L)^2 = 1070.34$

b. Plug in M_{x1} and M_{x2} relative to M_x. Solve 1- f.

4. Solve for M_x.

$Mx^2 = 1070.34/.9573$

and Mx = 33.44 k-in.

M_x represents the bending contribution to the total moment.

$M_{tx} = M_{x\ bending} + M_{x\ shear}$

5. Find the shear factor, SF.

a. Place moment diagram on conjugate beam without and with shear moment. Set resultants equal to each other.

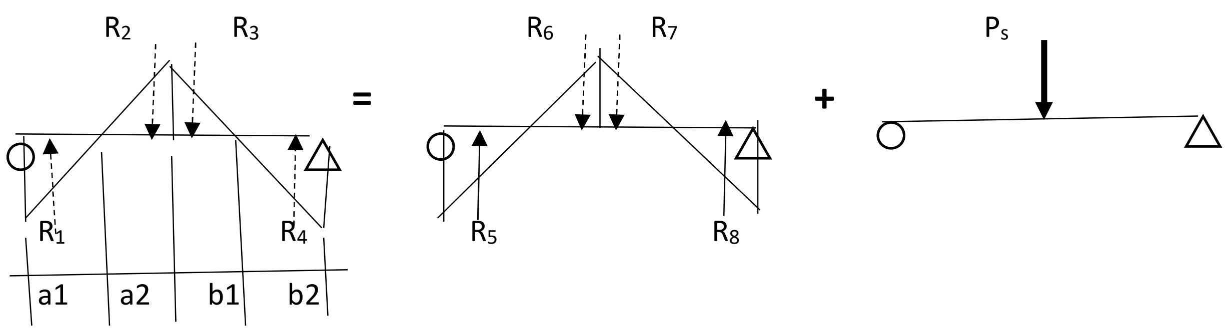

Figure 105. Moments on Targeted Conjugate Beam

b. Write Resultant equation

$R_1 + R_2 + R_3 + R_4 = R_5 + R_6 + R_7 + R_8 + P_s$

$-(.5)8.27P_1(a_1) + (.5)10.48P_1(a_2) + (.5)10.48P_1(b_1) - (.5)8.27P_1(b_2) =$

$-(.5)8.27P_2(a_1) + (.5)10.48P_2(a_2) + (.5)10.48P_2(b_1) - (.5)8.27P_2(b_2) + \alpha P_2EI_x/AG$

Rearrange,

$$P_2/P_1 = \frac{[-(.5)8.27(a_1) + (.5)10.48(a_2) + (.5)10.48(b_1) - (.5)8.27(b_2)]}{[-(.5)8.27(a_1) + (.5)10.48(a_2) + (.5)10.48(b_1) - (.5)8.27(b_2) + \alpha EI_x/AG]}$$

Solving SF = .578. Therefore,

$M_{tx} = M_x/.578 = 57.86$ k-in.

This value is within 9% of the value obtained using Central Difference.

Problem 4.7 For the 3" x 3" x ¼" fiberglass I beam with moments shown in Figure 106, determine its lateral-torsional buckling moment. Include shear deflection moment. Beam was used in Investigation 7. E = 2997 ksi; I_x = 3.17 in.^{4}; I_y = 1.13 in. ^{4}; k_t = .046; G = 453 ksi; A = 2.13 in. ^{2}; α = 3.26; and I_w = 2.13 in. ^{6} .

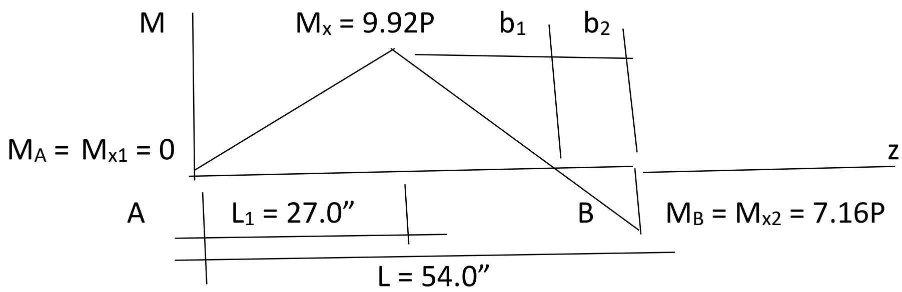

Figure 106. Moments on Targeted Beam. Investigation 7

1. Proposed equation for lateral-torsional buckling including shear is

$M_x = ((C_w B_y (\pi/L)^4 + C_t B_y (\pi/L)^2) / (1-f))^{.5}$

and $M_{xs} = M_x / SF$

where $SF = P_2/P_1$

and $f = ((s/L_1)(1- M_{x1}) + (t/L_2)(1- M_{x2})(L/\pi^2)$.

Note: M_{x1} and M_{x2} are relative to M_x.

M_x = 9.92P and M_{x1} = 0 and M_{x2} = 7.16P.

2. Define Factors s and t

a. Define a and b from end conditions. Ends A and B are pinned-fixed, so a and b are .7 and .3, respectively.

b. Define c and d from location of point on the beam.

$c= L_2/L = .5$

$d= L_1/L = .5$

c. Calculate p and q.

p = ac = .7* .5 = .35

q = bd= .3* .5 = .15

d. Now, calculate s and t.

s = p/(p + q) = .7

t = q/ (q + p) = .3

3. Plug in all the knowns

a. $C_w B_y (\pi/L)^4 + C_t B_y (\pi/L)^2 = 502.22$

b. Plug in M_{x1} and M_{x2} relative to M_x. Solve 1- f.

4. Solve for M_x.

$M_x^2 = 502.22/.84$

And $M_x = 24.45$ k-in.

M_x represents the bending contribution to the total moment.

$M_{tx} = M_{x\,bending} + M_{x\,shear}$

5. Find the shear factor, SF.

a. Place moment diagram on conjugate beam without and with shear moment. Set resultants equal to each other.

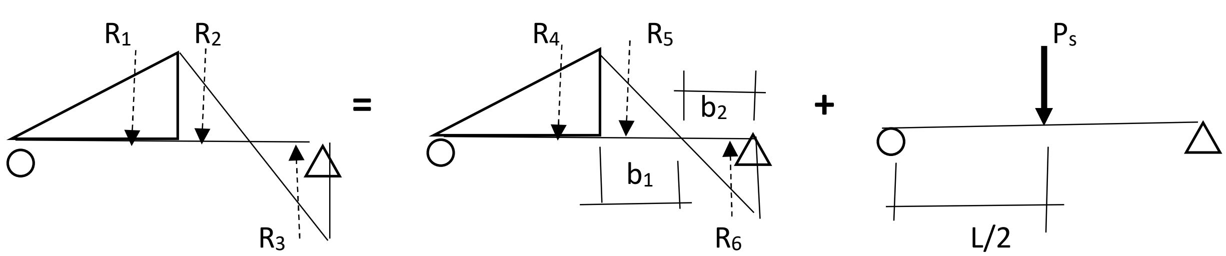

Figure 107. Moment Diagrams on Targeted Conjugate Beam

b. Write Resultant equation

$R_1 + R_2 + R_3 = R_4 + R_5 + R_6 + P_s$

$(.5)9.92P_1L_1 + (.5)9.92P_1b_1 - (.5)7.16P_1b_2 = (.5)9.92P_2L_1 + (.5)9.92P_2b_1 - (.5)7.16P_2b_2 + \alpha P_2EI_x/AG$

Rearrange,

$P_2/P_1 =$

$[(.5)9.92L_1 + (.5)9.92b_1 - (.5)7.16b_2] / [(.5)9.92L_1 + (.5)9.92b_1 - (.5)7.16b_2 + \alpha EI_x/AG]$

Solving SF = .84. Therefore,

$M_{tx} = M_x /.84 = 29.11$ k-in.

This value is within 1.4% of the value obtained using Central Difference.

Problem 4.8 For the 3” x 3” x ¼” fiberglass I beam with moments shown in Figure 108, determine its lateral-torsional buckling moment. Include shear deflection moment. Beam was used in Investigation 8. E = 2997 ksi; I_x = 3.17 in.^{4}; I_y = 1.13 in. ^{4}; k_t = .046; G = 453 ksi; A = 2.13 in. ^{2}; α = 3.26; and I_w = 2.13 in. ^{6} .

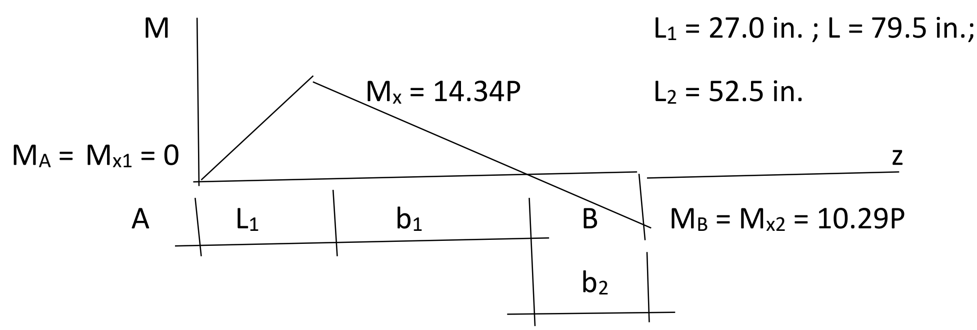

Figure 108. Moments on Targeted Beam. Investigation 8

1. Proposed equation for lateral-torsional buckling including shear is

$M_x = ((C_w B_y (\pi/L)^4 + C_t B_y (\pi /L)^2) / (1-f))^{.5}$

and $M_{xs} = M_x /SF$

where SF = P_2/P_1

and $f = ((s/L_1)(1- M_{x1}) + (t/L_2)(1- M_{x2})(L/\pi^2)$.

Note: M_{x1} and M_{x2} are relative to M_x.

M_x = 14.34P and M_{x1} = 0 and M_{x2} = 10.29P.

2. Define Factors s and t

a. Define a and b from end conditions. Ends A and B are pinned-fixed, so a and b are .7 and .3, respectively.

b. Define c and d from location of point on the beam.

c= L_2/L = .66

d= L_1/L = .34

c. Calculate p and q.

p = ac = .7* .66 = .462

q = bd= .3* .34 = .102

d. Now, calculate s and t.

s = p/(p + q) = .82

t = q/ (q + p) = .18

3. Plug in all the knowns

a. $C_w B_y (\pi/L)^4 + C_t B_y (\pi/L)^2 = 167.5$

b. Plug in M_{x1} and M_{x2} relative to M_x. Solve 1- f.

4. Solve for M_x.

$M_x^2 = 167.5/.736$

And M_x = 15.086 k-in.

M_x represents the bending contribution to the total moment.

$M_{tx} = M_{x\ bending} + M_{x\ shear}$

5. Find the shear factor, SF.

a. Place moment diagram on conjugate beam without and with shear moment. Set resultants equal to each other.

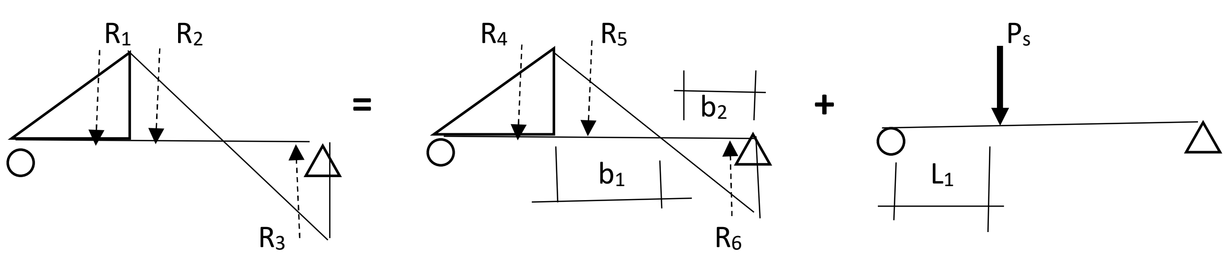

Figure 109. Moment Diagrams on Targeted Conjugate Beam

b. Write Resultant equation

$R_1 + R_2 + R_3 = R_4 + R_5 + R_6 + P_s$

$(.5)14.34P_1L_1 + (.5)14.34P_1b_1 - (.5)10.29P_1b_2 = (.5)14.34P_2L_1 + (.5)14.34P_2b_1 - (.5)10.29P_2b_2 + \alpha P_2EI_x/AG$

Rearrange,

$P_2/P_1 =$

$[(.5)14.34L_1 + (.5)14.34b_1 - (.5)10.29b_2] / [(.5)14.34L_1 + (.5)14.34b_1 - (.5)10.29b_2 + \alpha EI_x/AG]$

Solving SF = .9. Therefore,

$M_{tx} = M_x /.9 = 16.76$ k-in.

This value is within 5% of the value obtained using Central Difference.

Problem 4.9 For the 4" x 4" x ¼" fiberglass I beam with moments shown in Figure 110, determine the critical stress when the max normal stress is 30 ksi. Include shear deflection moment. Beam was used in Investigation 9. $E = 2997$ ksi; $I_x = 7.935$ in.^{4}; $I_y = 2.67$ in.^{4}; $k_t = .06$; $G = 453$ ksi; $A = 2.85$ in.^{2}; $\alpha = 3.23$; and $I_w = 9.375$ in.^{6}.

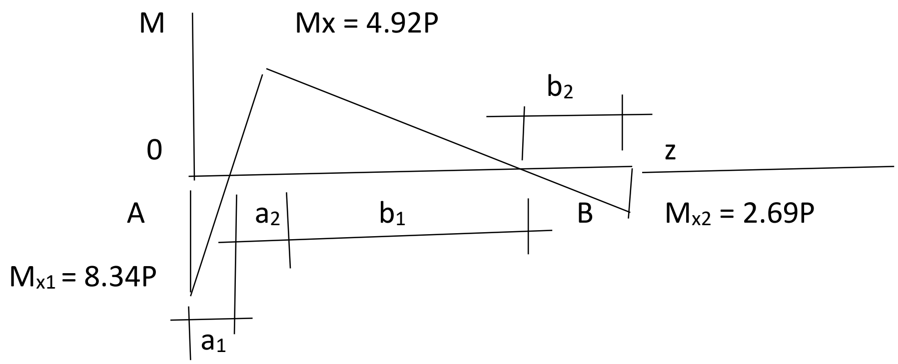

Figure 110. Moments on Targeted Beam. Investigation 6

Using the central difference procedure presented in Chapter 2 for calculation of unknown deflections u, v, and ϕ; increase the applied point load P_2 until the max normal stress is reached. The governing biaxial stress equation will include a warping stress and is

$$\sigma_{max} = M_x c_y / I_x - M_y c_x / I_y + E I_w \phi'' = 30 \text{ ksi} \qquad [75]$$

At $P_2 = 2.6$ kips, $v'' = 4.87 \times 10^{-3}$, $u'' = 1.25 \times 10^{-4}$, and $\phi'' = 1.04 \times 10^{-5}$, and the max stress at the point of load is 30.0 ksi. Primary stresses and warping stress are found using the unknowns and the following relationships: $M_x = EI_x v''$; $M_y = EI_y u''$; and $M_w = EI_w \phi''$. Knowing the applied load P_2, determine P_1 and the moment using the shear factor, SF.

Find the shear factor, SF.

a. Place moment diagram on conjugate beam without and with shear moment. Set resultants equal to each other.

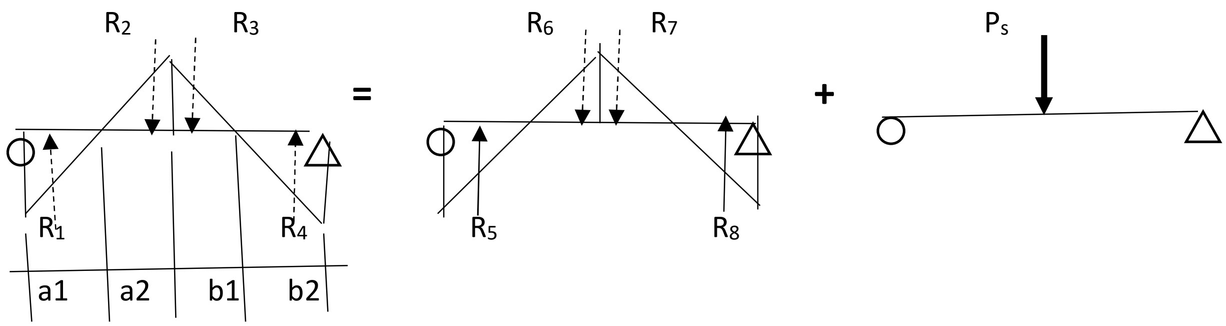

Figure 111. Moments on Targeted Conjugate Beam

b. Write Resultant equation

$R_1 + R_2 + R_3 + R_4 = R_5 + R_6 + R_7 + R_8 + P_s$

$-(.5)8.34P_1(a_1) + (.5)4.92P_1(a_2) + (.5)4.92P_1(b_1) - (.5)2.69P_1(b_2) =$

$-(.5)8.34P_2(a_1) + (.5)4.92P_2(a_2) + (.5)4.92P_2(b_1) - (.5)2.69P_2(b_2) + \alpha P_2EI_x/AG$

Rearrange,

$$P_2/P_1 = \frac{[-(.5)8.34(a_1) + (.5)4.92(a_2) + (.5)4.92(b_1) - (.5)2.69(b_2)]}{[-(.5)8.34(a_1) + (.5)4.92(a_2) + (.5)4.92(b_1) - (.5)2.69(b_2) + \alpha EI_x/AG]}$$

Solving SF = .40. Therefore,

$P_1 = P_2/.40 = 6.5$ kips

M_{tx} = 6.5 x 8.34 = 54.21 k-in.

This value is within 10% of the value obtained using Central Difference.

Proposed equations introduced here and our design approach will be discussed further in next chapter.

CHAPTER 5

DESIGN

Using design equations and material properties of the I beams used in the investigations, calculated the lateral- torsional buckling moments for the I beams varying span lengths. Curves are shown in Figure 112. Shorter beams fail in material rupture before lateral torsional buckling. The flat part of each curve is the rupture limit for an I beam of that cross section. The equation used for rupture is

$M_n = F_L I/y$ where the rupture limiting stress is 30000 psi.

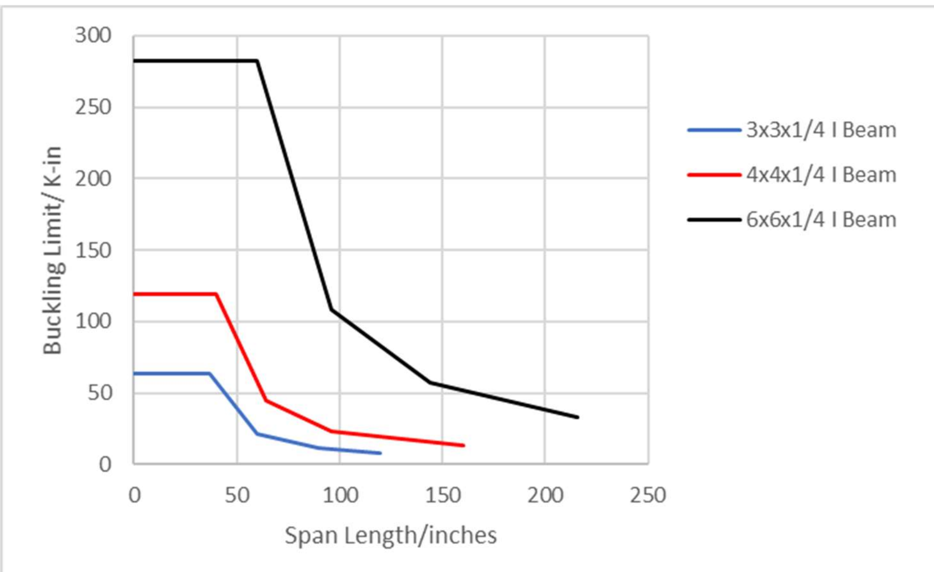

Figure 112. Lateral-Torsional Buckling Moment for Single Span I Beam. Pinned-Pinned

Example 6.1: a. Calculate the material rupture for a 6 in. x 6 in. x 3/8 in. I beam.

b. Would a 6 x 6 x 3/8 I beam 35 inches long fail lateral-torsionally?

c. What about a 6 x 6 x 3/8 with a span of 70 inches?

d. What is its buckling limit?

Solution:

a. $M_n = F_L I/y$ = 30 (28.28)/3 = 282.8 k-in..

b. No. According to the curve for a 6x6x1/4, it will fail in material rupture at 35 inches.

c. at 70 inches, the 6x6x1/4 will fail lateral-torsionally versus material rupture.

d. From the curve, its critical moment is approximately 210 k-in.

5.1 Buckling Design Curves

While for many of the cases defined by our equations of equilibrium, the present lateral torsional buckling equation without shear and our proposed buckling equation fall within 0 to 20% of each other, there are instances where they disagree drastically from each other within the lateral-torsional buckling design range. Single span, two span, and three span beam buckling limits were graphed for 4 in. x 4 in. x ¼ in. , 6 in. x 6 in. x 3/8 in., 8 in. x 8 in. x 3/8 in. , and 12 in. x 12 in. x 1/2 in. fiberglass beams. See Figures 113 thru 124 below. Approximately 25% of ASCE-LRFD Prestandard critical buckling values fall within 20% of Proposed critical values and 50% of ASCE-LRFD Prestandard critical buckling values fall within 20 to 100% of Proposed critical values, However, 25% of ASCE-LRFD Prestandard critical buckling limits are over 100% higher than critical buckling limits. Buckling limits using the present lateral-torsional buckling equations without shear are not conservative and need to be addressed to reduce design liabilities.

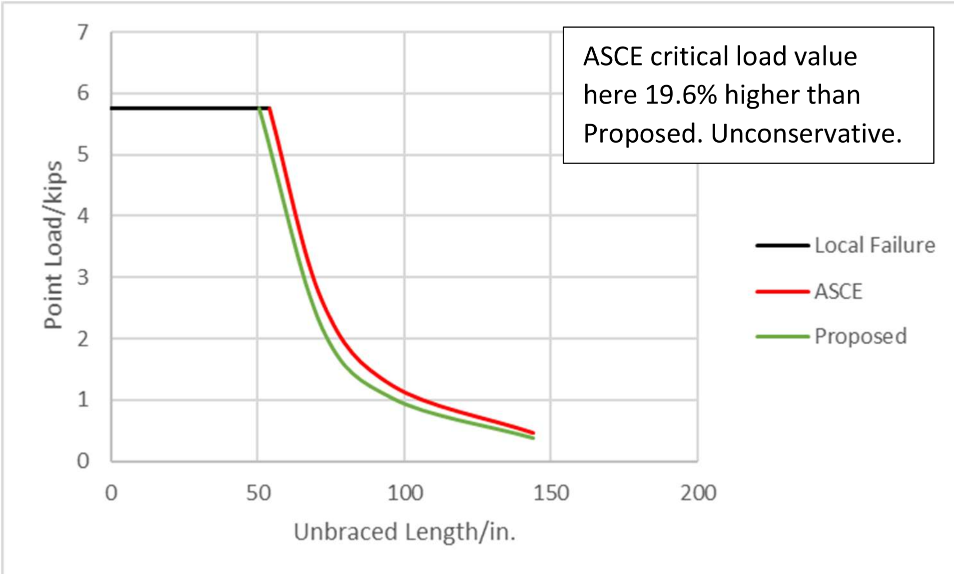

Figure 113. 4 in. x 4 in. x 1/4 in. Single Span I beam. Point Load Center Span

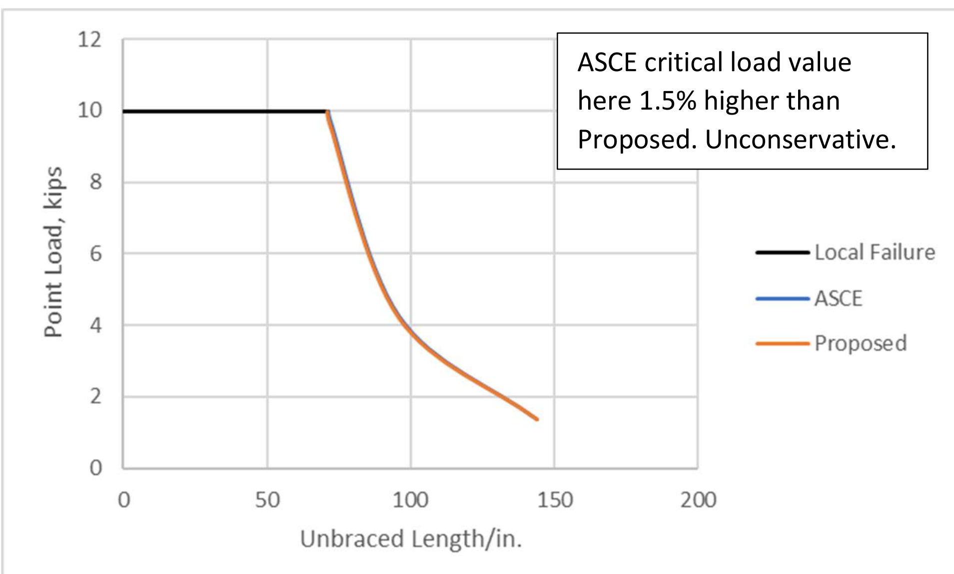

Figure 114. 6 in. x 6 in. x 3/8 in. Single Span I beam. Point Load Center Span

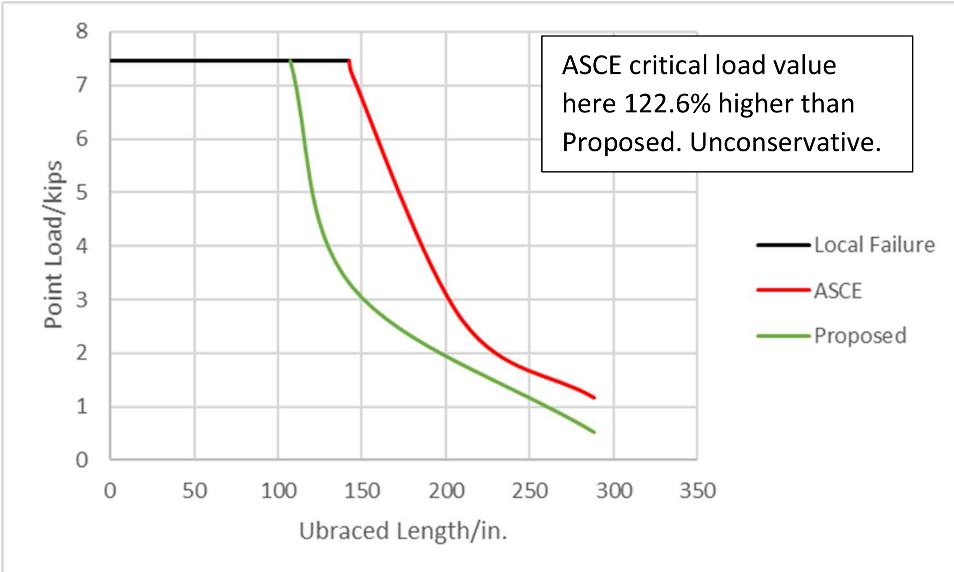

Figure 115. 8 in. x 8 in. x 3/8 in. Single Span I beam. Point Load Center Span

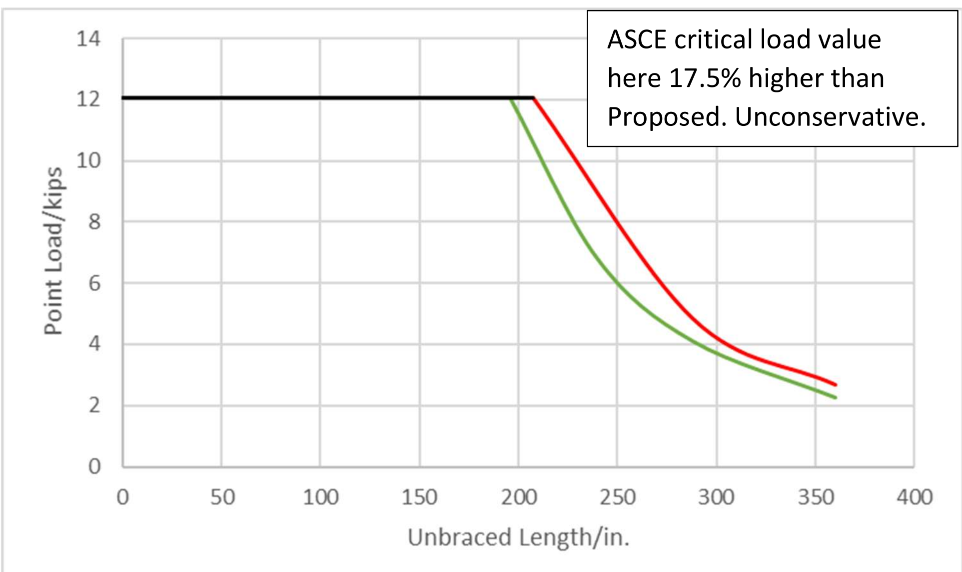

Figure 116. 12 in. x 12 in. x 1/2 in. Single Span I beam. Point Load Center Span

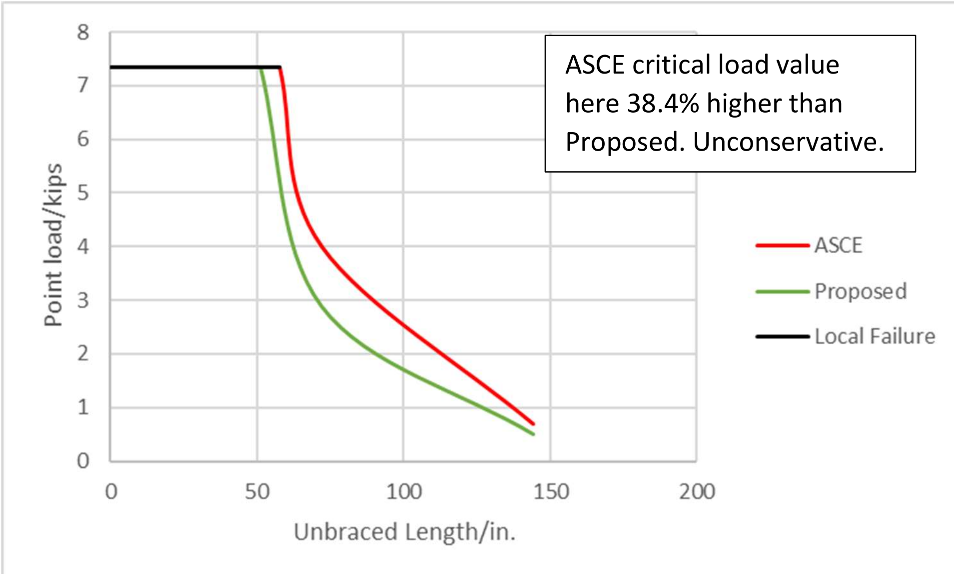

Figure 117. 4 in. x 4 in. x 1/4 in. Two Span I beam. Point Load Center Span

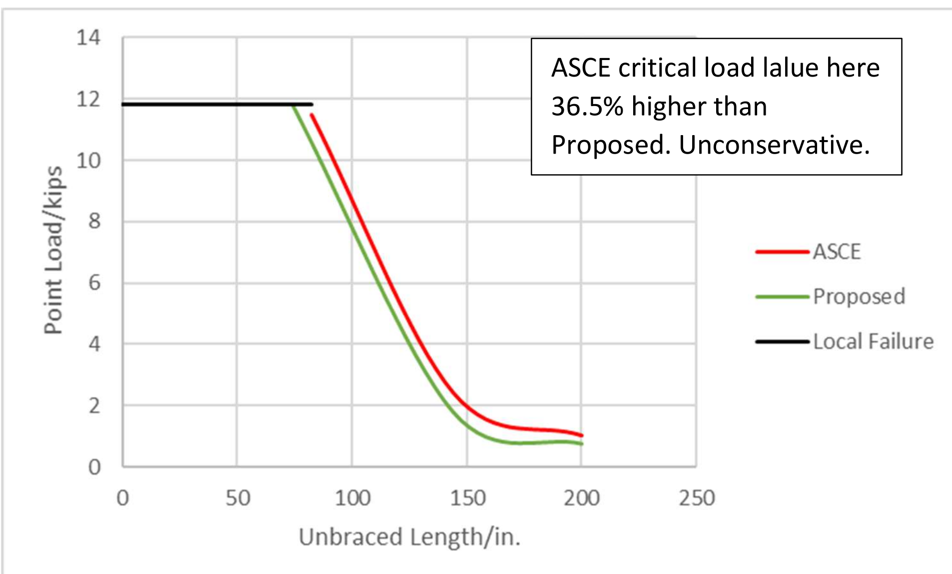

Figure 118. 6 in. x 6 in. x 3/8 in. Two Span I beam. Point Load Center Span

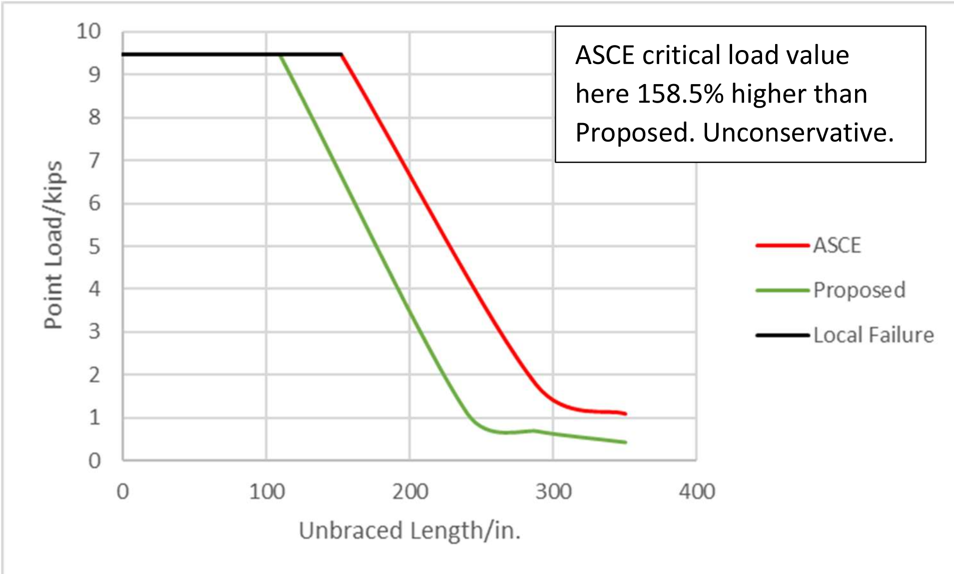

Figure 119. 8 in. x 8 in. x 3/8 in. Two Span I beam. Point Load Center Span

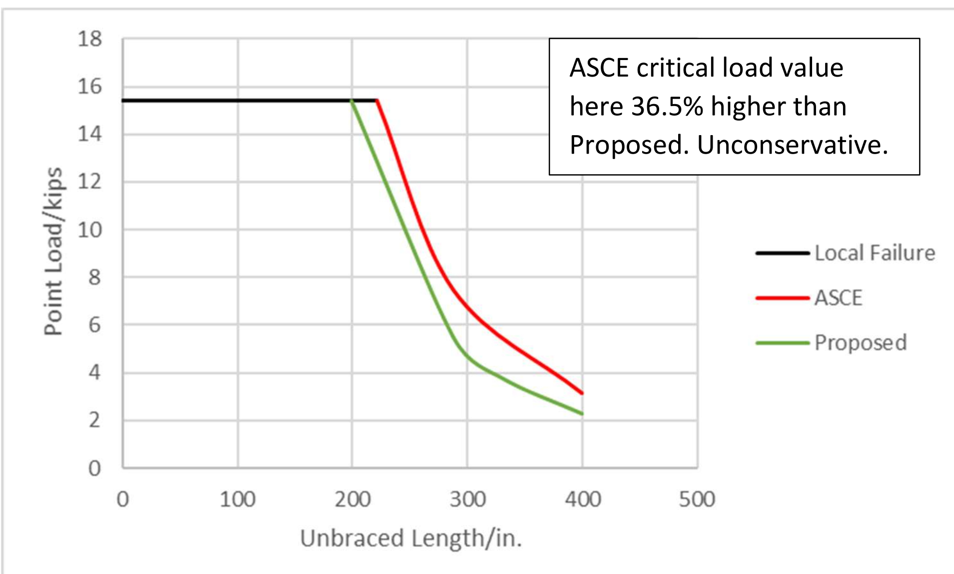

Figure 120. 12 in. x 12 in. x 1/2 in. Two Span I beam. Point Load Center Span

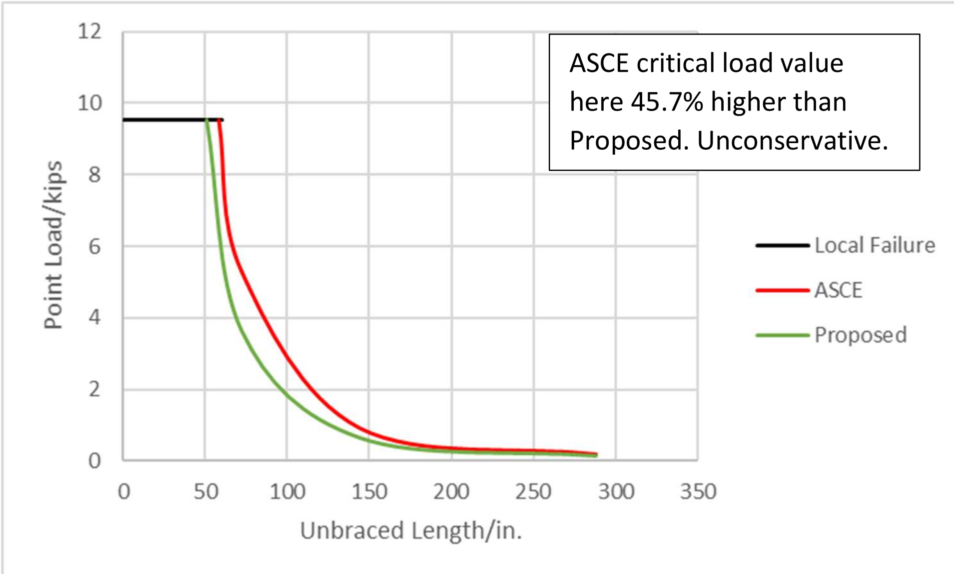

Figure 121. 4 in. x 4 in. x 1/4 in. Three Span I beam. Point Load Center Span

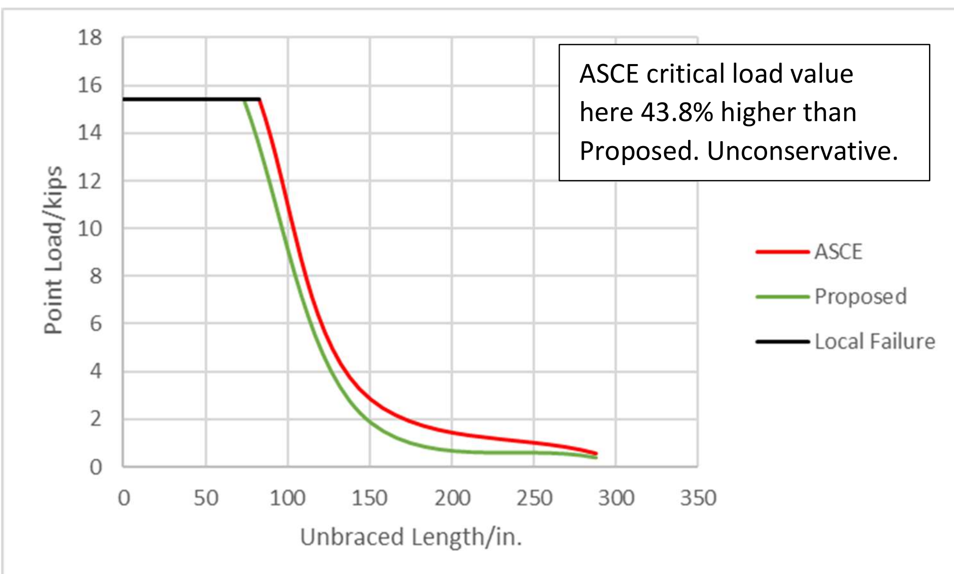

Figure 122. 6 in. x 6 in. x 3/8 in. Three Span I beam. Point Load Center Span

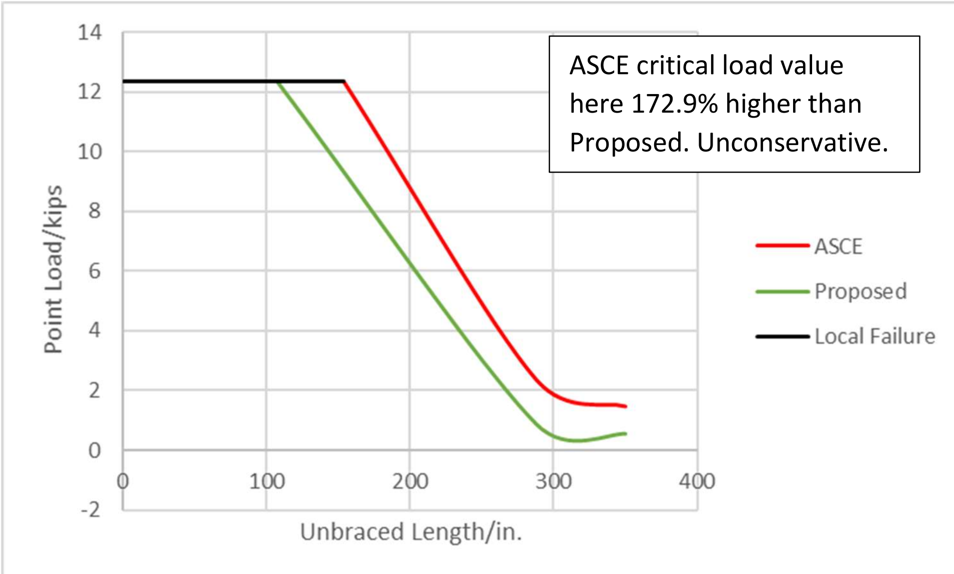

Figure 123. 8 in. x 8 in. x 3/8 in. Three Span I beam. Point Load Center Span

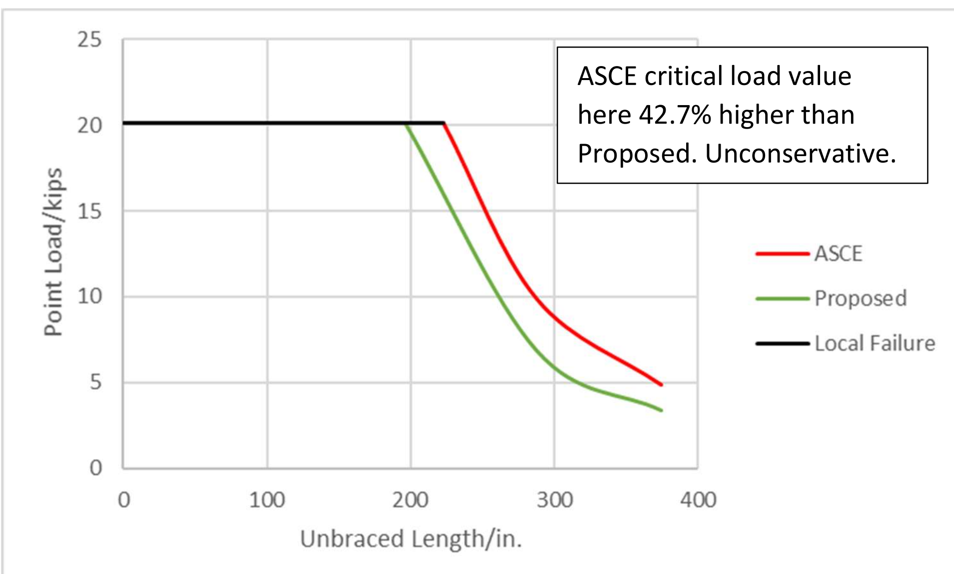

Figure 124. 12 in. x 12 in. x 1/2 in. Three Span I beam. Point Load Center Span

5.2 Biaxial Bending Design

Example 5.2: Using the modified stress equation which includes induced torsion , plot M_x versus ϕ at a stress of 30 ksi for single span 4" x 4" x ¼"; two span 6" x 6" x 3/8"; three span 8" x 8" x 3/8" ; and single 12" x 12" x ½" loaded biaxially as shown in Figures 125a thru 125d. Plot with and without Timoshenko shear moment. Beam properties shown in Table 60.

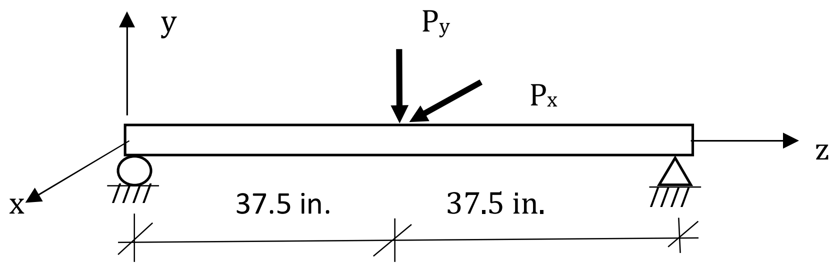

a. 4 in. x 4 in. x 1/4 in. I Beam. Midspan Biaxial loads.

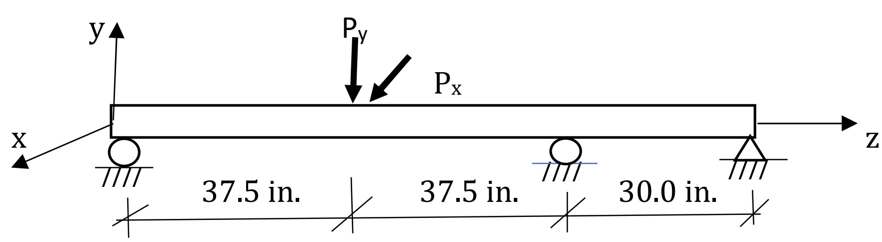

b. 6 in. x 6 in. x 3/8 in. I Beam. Midspan Biaxial loads

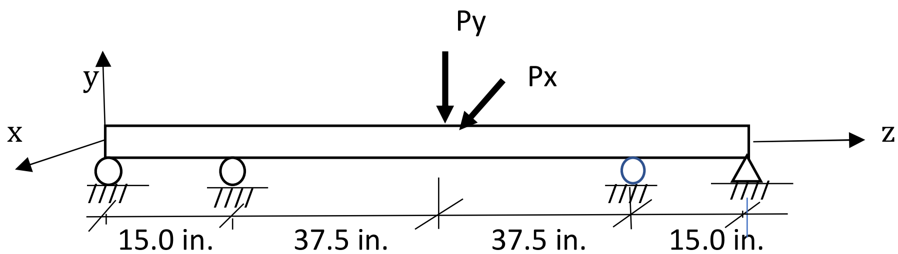

c. 8 in. x 8 in. x 3/8 in. I Beam. Midspan Biaxial loads.

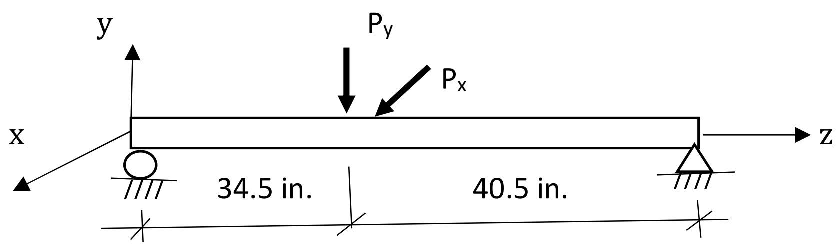

d. 12 in. x 12 in. x ½ in. I Beam. Off Center Biaxial loads

Figure 125. GFRP I Beams with Point Loads

Table 60. Fiberglass I Beam Properties

Dimensions (in.)	Area (in. ^{2})	I_w (in. ^{4})	K_t	I_x (in. ^{4})	I_y (in. ^{4})	G(ksi)	E(ksi)
4x4x1/4	2.85	9.735	.06	7.935	2.67	450	3000
6x6x3/8	4.375	74.39	.091	28.27	9	450	3000
8x8x3/8	8.72	465.1	.41	99.19	32.03	450	3000
12x12x1/2	24.50	4761	1.46	256.21	83.43	450	3000

With Central Difference procedure demonstrated in problems found in Chapter 2, solve for unknown deflections u, v, and ϕ. For deflection values, [K]u = F. So, solve for the deflections using the inverse K matrix , u = [K]-1 F. The vector u contains the unknowns u, v, and ϕ along the member . The modified stress equation to be used is

$$\sigma_{max} = M_x c_y / I_x - M_y c_x / I_y + E I_w \phi'' = 30 \text{ ksi} \quad [75]$$

Knowing $M_x = EI_x v''$; $M_y = EI_y u''$; and $M_w = EI_w \phi''$; and plugging in our unknowns while varying the applied load with shear, P_x, we find values of the applied load with or without considering shear. The max stress is 30 ksi. Figures 127, 129, 131, 133 show how the magnitude of the applied loads vary when considering versus not considering shear moment. Graph showing the moment M_x versus the angle of twist are also shown for each example. See figures 128, 130, 132, and 134.

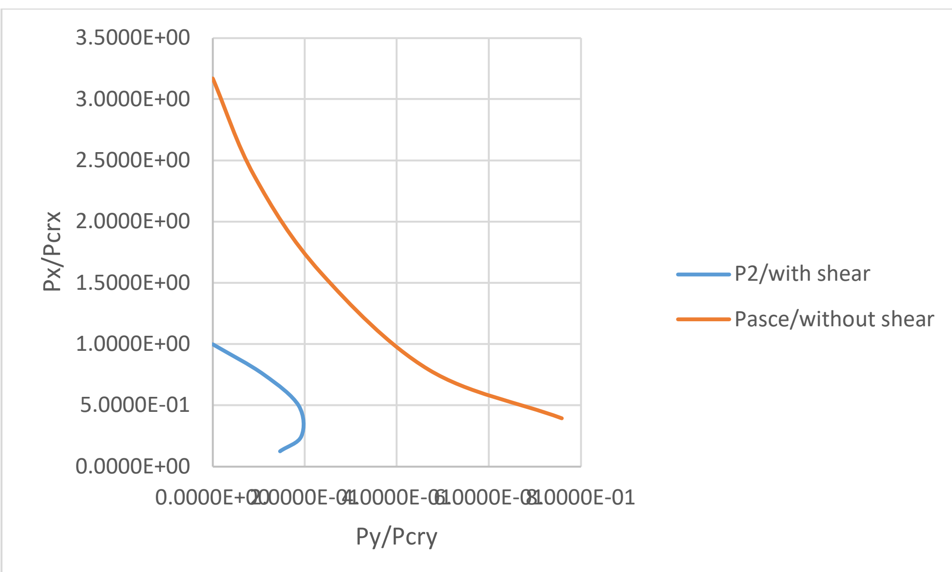

Figure 126. P_y vs P_x . Biaxial Bending , 4 in. x 4 in. x 1/4 in. Single Span.

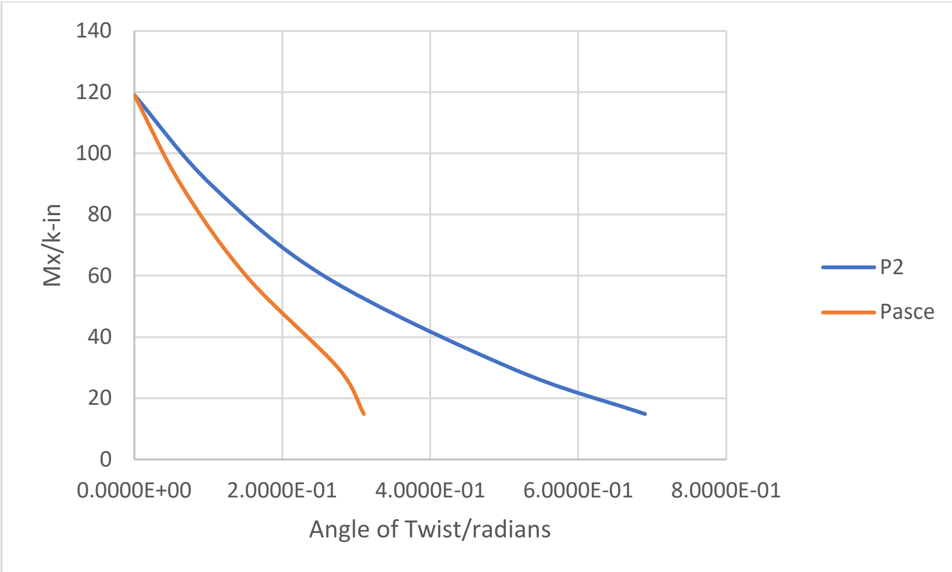

Figure 127. Moment vs Angle of Twist. Biaxial Bending. 4 in. x 4 in. x ½ in. Single Span

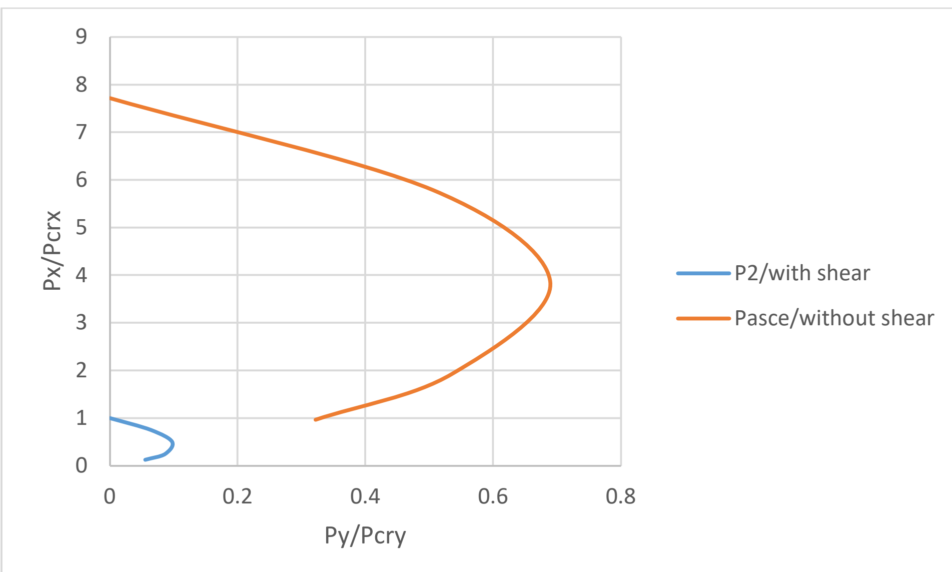

Figure 128. P_y vs P_x . Biaxial Bending , 6 in. x 6 in. x 3/8 in. Two Span.

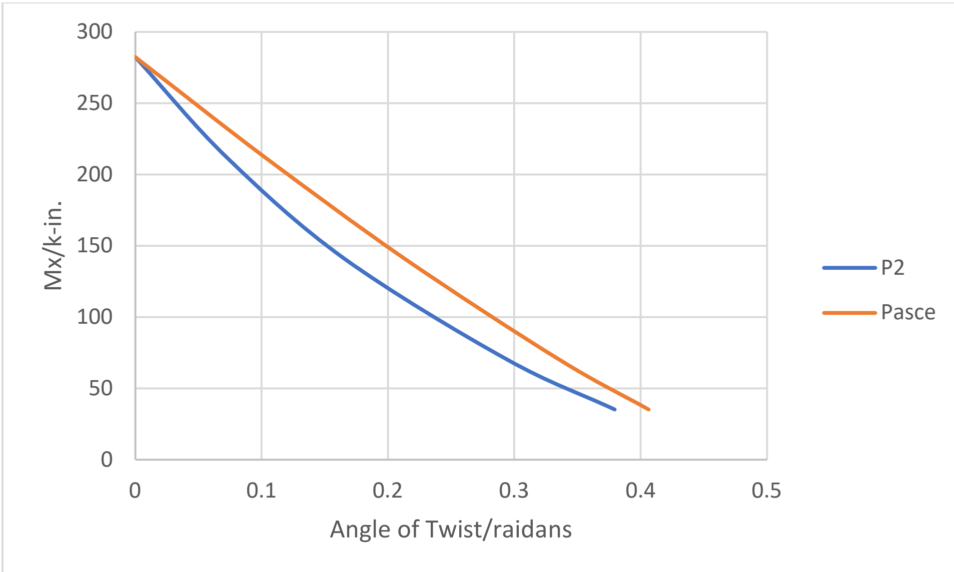

Figure 129. Moment vs Angle of Twist. Biaxial Bending. 6 in. x 6 in. x 3/8 in. Two Span

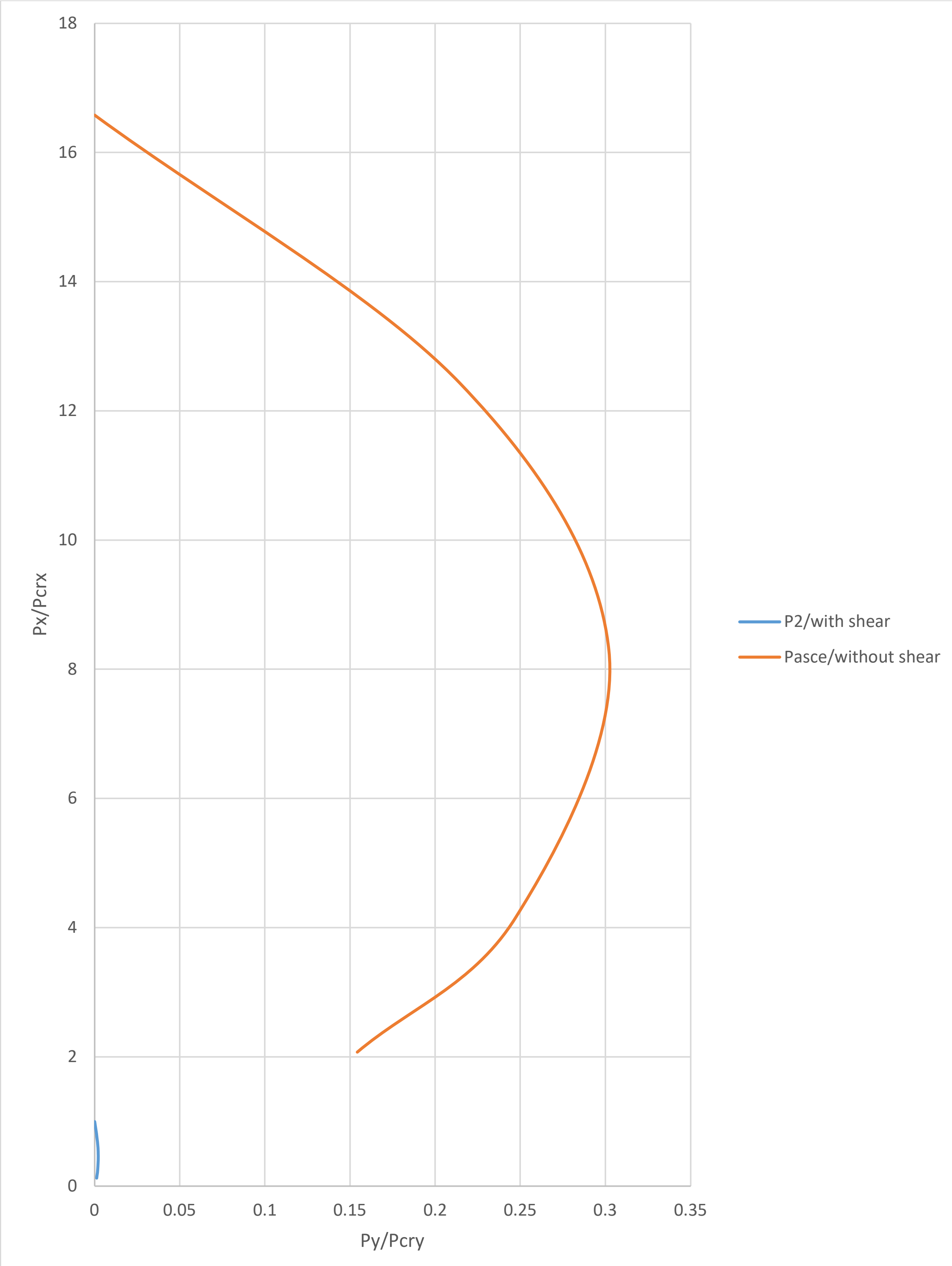

Figure 130. P_y vs P_x . Biaxial Bending, 8 in. x 8 in. x 3/8 in. Three Span.

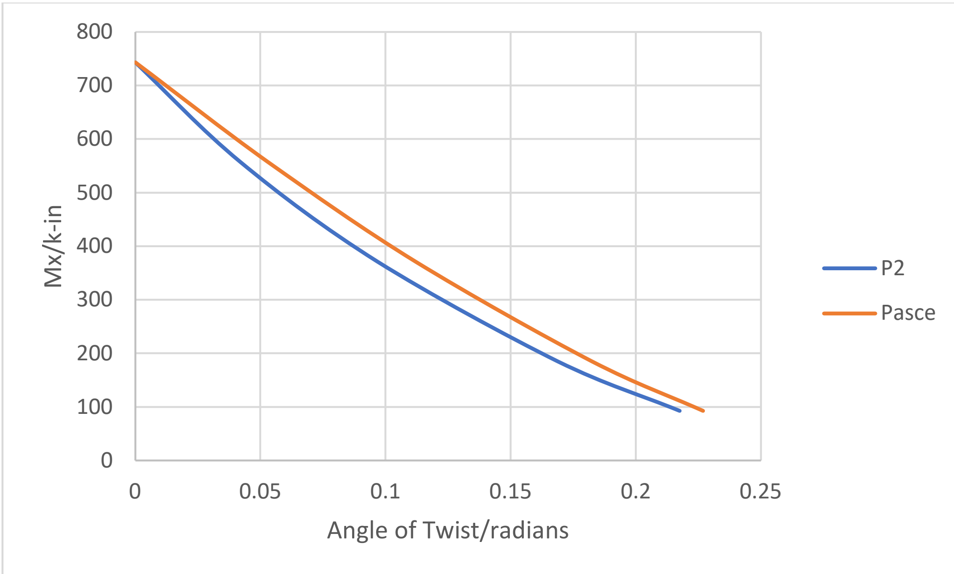

Figure 131. Moment vs Angle of Twist. Biaxial Bending. 8 in. x 8 in. x 3/8 in. Three Span

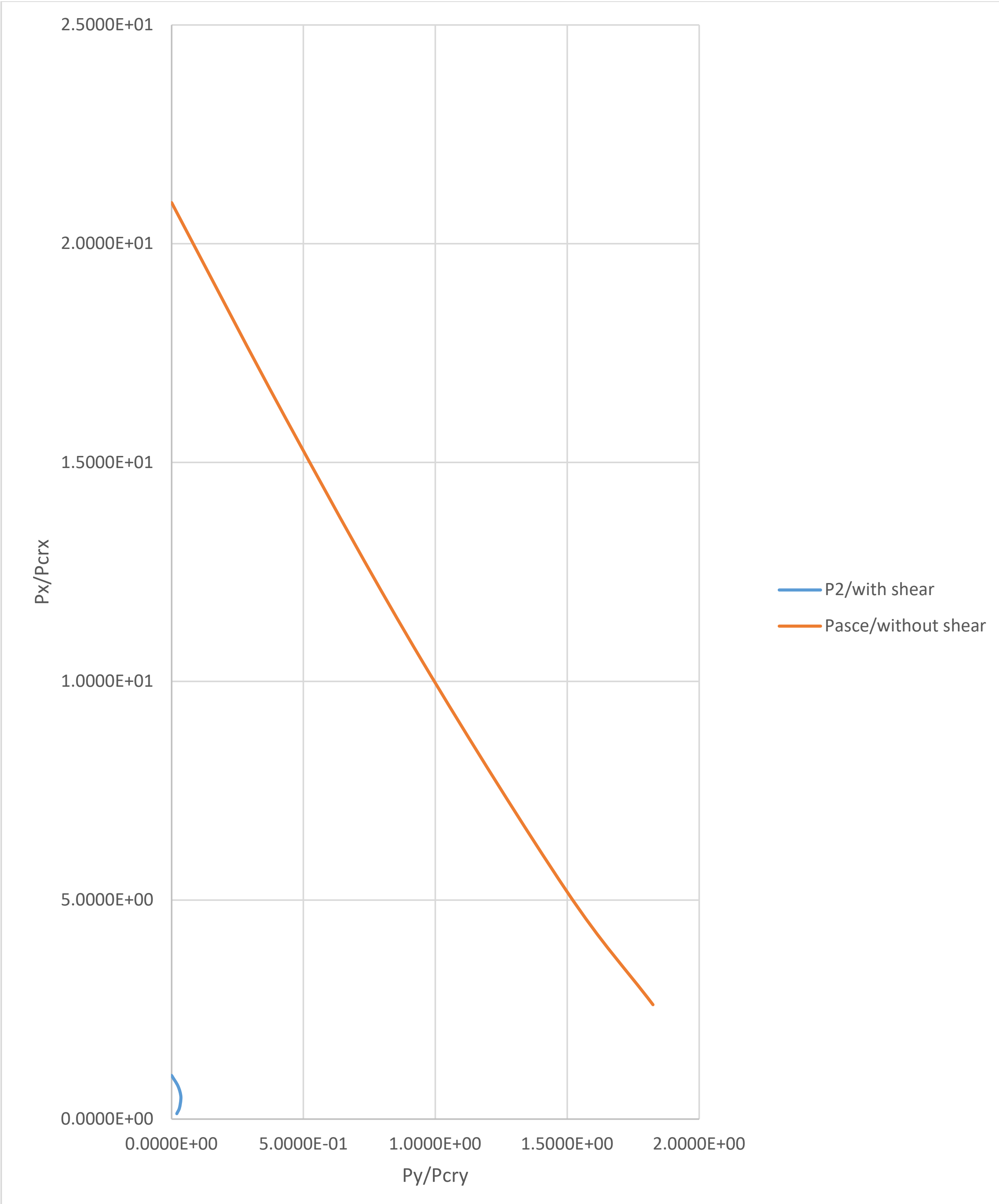

Figure 132. P_y vs P_x . Biaxial Bending , 12 in. x 12 in. x ½ in. Three Span.

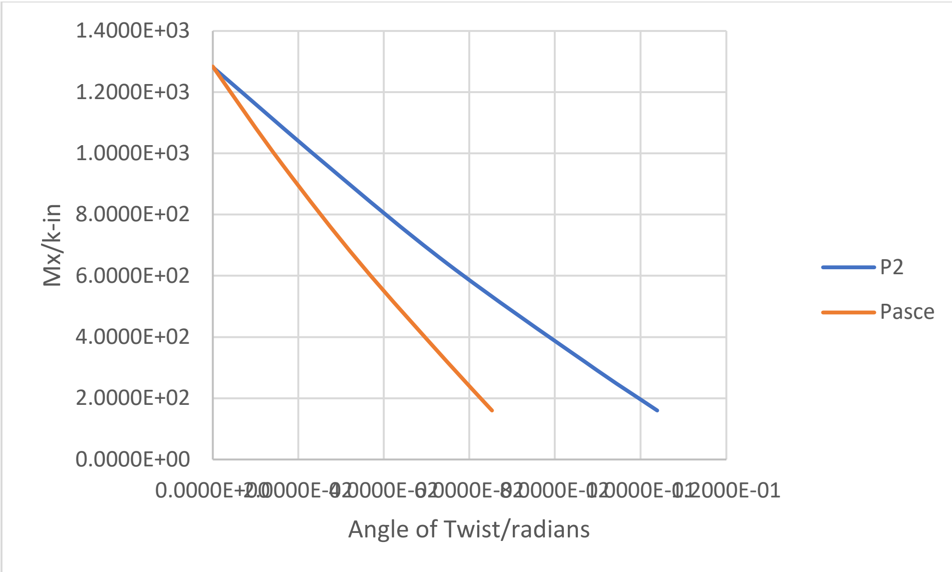

Figure 133. Moment vs Angle of Twist. Biaxial Bending. 12 in. x 12 in. x ½ in. Three Span

As evidenced by the magnitude of all the critical loads as determined by the ASCE values without shear moment, the applied loads in the y direction are dangerously high for each scenario. Moments for M_x and as such are misleading.

Values of applied loads with and without shear are shown in Table 61. Notice that although the moment M_x will be the same, the applied load without shear is 3 to 20 times higher than the applied load with shear for the problems shown in Figures 125a thru d. This is a very real and ever present danger that exists.

For the single span beam , buckling value of the applied load was determined to be 1.83 kips while the biaxial value was determined to be 2.05 kips. Both values are within 10% of the lab value of 1.88 kips for investigation 1. However, for the other scenarios where we increased the size of the beam thereby reducing their L/D ratios the beams fail biaxially and the buckling limits are of no significance. This is due to the slenderness ratio being much less than 20 and approaching that of a deep beam. For the 6 in. x 6 in. x 3/8 in. I beam and the 8 in. x 8 in. x 3/8 in. ; I beam thee buckling limits are 8.2 and 36 kips ; while the biaxial stresses are 2.67 and 4.27 kips, respectively. Investigation 9 includes a 4x4x1/4 three span biaxially loaded off center. As is the case for problem 1a of this chapter, theoretical buckling limit and the biaxial stress values of the moment M_x fall within 10% of the laboratory values for the same problem. However, the biaxial stress value is slightly lower. Biaxial load was less than 10% of the in-plane load.

Table 61. Applied Load at M_{xcr} and Max Normal Stress of 30ksi. P_{asce}/P_2

Beam Type	P_2 (kips,w/ shear)	P_{asce} (kips,w/o shear)	P_{asce}/P_2
Single Span, 4 in. x 4 in. x ¼ in.	2.045	6.48	3.17
Two Span, 6 in. x 6 in. x 3/8 in.	2.67	20.6	7.71
Three Span, 8 in. x 8 in. x 3/8 in.	4.27	70.8	16.58
Single Span, Off Ctr, 12 in. x 12 in. x 1/2 in.	3.29	68.9	20.94

Table 62. Bending and Warping Stresses at 12.5% M_{xcr} and Max Normal Stress of 30 ksi.

Beam Type (in.)	$\sigma_{xbending}$ (M_xc/I_x)	$\sigma_{ybending}$ (M_yc/I_y)	σ_w ($Ew_n\,\phi''$)	σ_w/σ_{total} (σ_w/30.0 ksi)
Single Span, 4 x 4 x ¼	.0007993 x 3000 x 2.0 = 4.8 ksi	-.0005696x 3000 x 2.0 = 3.4 ksi	.001956 x 3000 x 3.75 = 22.0 ksi	.728
Two Span, 6 x 6 x 3/8	3.9 ksi	2.8 ksi	23.4 ksi	.777
Three Span, 8 x 8 x 3/8	3.7 ksi	2.5 ksi	24.1 ksi	.795
Single Span, Off Ctr, 12 x 12 x1/2	3.8 ksi	.6 ksi	25.8 ksi	.854

CHAPTER 6

CONCLUSIONS AND FUTURE RESEARCH

6.1 Conclusions

The following conclusions are drawn based on the present study of GFRP beams:

1. The theoretically predicted behavior of beams is in good agreement with that observed experimentally.

2. Inclusion of shear deformation effects resulted in significantly different lateral-torsional buckling loads compared to those found using ASCE - LRFD Prestandard.

3. The lateral-torsional buckling formula in the ASCE- LRFD Prestandard is found to be up to 20% on the unconservative side as compared with the experimental results.

4. The degree of unconservativesness in the buckling load estimates when ASCE - LRFD Prestandard increases with a decrease in beam slenderness when compared with predicted values based on the theoretical analysis presented , and is found to be over 100% is some cases.

5. For biaxially bent beams , the induced warping normal stresses are found to be in the range from moderate to very high in comparison with the primary bending stresses with warping stresses accounting for over 75% of the total maximum stress.

6. The proposed lateral-torsional buckling formula accounting for the shear deformation effects is in good agreement with the experimental results.

Based on the findings presented in this dissertation , it is concluded that the current ASCE-LRFD Prestandard can result in unconservative results in practical applications for lateral-torsional buckling and biaxial flexure of GFRP beams.

6.2 Future Research

Additional experimental study is needed in the future on deep GFRP beams susceptible to lateral-torsional buckling. Experiments also need to be conducted on biaxially bent beams with a variety of load types and boundary conditions including both large induced warping effects and shear deformations.

REFERENCES

1. Galambos, T., Structural Analysis and Design, Prentice-Hall Unc., 1997, 371 pages.

2. Load and Resistance Design Specification(LRFD), AISC, Chicago, IL. 2007

3. Timoshenko, S., Strength of Materials, Volume I, D. Von Nostrand Co. Inc., New York, 3rd Edition, April 1955, 442 pages.

4. Timoshenko, S., Strength of Materials, Volume I, D. Von Nostrand Co. Inc., New York, 3rd Edition, April 1956, 572 pages.

5. Reddy, J.N., Introduction to Finite Element Method, McGraw Hill, Inc. , 3rd Edition 2005, 784 pages.

6. Wang, C. W. , Reddy, J. N., and Lee, K.H., Shear Deformable Beams and Plates, Elselvier, 2002, 312 pages.

7. Chen, W. and Atsuta,T., Theory of Beam Columns, Volume I, J. Ross Publishing/McGraw Hill, New York, 1976, 513 pages.

8. Torsional Analysis of Steel Members, AISC, Chicago, IL., 1983.

9. Sirjani, M., Bondi, S.B., and Razzaq, Z., “Flexural-Torsional Response of FRP I-Section Members”, International Journal of Mechanics, Issue One, Volume 6, 2012

10. Sirjani, M., Bondi, S.B., and Razzaq, Z.,”Combined Bending with Induced or Applied Torsion of FRP I-Section Beams”, Recent Researched in Geography, Geology, Energy, and Biomedicine, 2012

11. Razzaq, Z. and Prabhakaran, R., “Load and Resistance Factor Design Approach for Reinforced-Plastic Channel Beam Buckling”, Elsevier, Great Britain, 1996.

12. Sirjani, M. , and Razzaq, Z. “Stability of FRP Beams under Three Point Loading and LRFD Approach”, Journal of Re-inforced Plastis and Composites, Vol. 24, No. 18, 2005.

13. Pre-standard for Load and Resistance Facot Design of Pultruded Fiber Re-inforced Polymer Structures, ASCE, Reston, VA., 2010

14. Knoroski, J., “The Behaviour og FRP I-Beams Subject to Biaxial Bending Using Finite Difference”, ODU, Norfolk, Va. 23529, 2015

15. Peck, T., “The Behaviour and Strength of Three Span FRP Beams Under A Midspan Point Load”, ODU, Norfolk, Va. 23529, 2015

16. Matthews, J.H. and Fink, K.D., Numerical Methods Using MATLAB, 4th Edition, Prentice-Hall Inc., New Jersey

17. Hibbler, R.C, Structural Analysis, Prentice-Hall, 1997, 729 pages

18. Weaver, J.W. and Johnston, P.R. Structural Dynamics by Finite Elements, Prentice-Hall, 1987, 591 pages

19. Timoshenko, S., Theory of Elasticity, McGraw-Hill, 1970, 567 pages

20. Timoshenko, S., Theory of Plates and Shells, McGraw-Hill, 1959

21. Timoshenko, S. and Gere, Mechanics of Materials, McGraw-Hill, 1996

22. Razzaq and Galambos, Biaxial Bending of Beams With or Without Torsion , Nov., 1979, Vol 105, No. 11. Journal of Structural Engineering, Oct 1986

23. Salvadori, M., Why Buildings Stand up: The Strength of Architecture. Published 1980

VITA

Waverly G Hampton

Old Dominion University

College of Engineering, Department of Civil/Environmental Engineering

135 Kaufmann Hall, Norfolk, Virginia 23529

Doctor of Philosophy May 2020

Major or Concentration: Civil Engineering /Structural Engineering

GPA: 3.96 for PhD. 3.7 Graduate Overall

Relevant Courses: Finite Elements, Plates, Optimization

Old Dominion University, Norfolk, VA

M. C. E December 1999

Major or Concentration: Civil Engineering/ Structural and Geotechnical Engineering

Relevant Courses: Advanced Soils, Partial Differentials